DOE/ID-10665(98)

1997 Performance Testing of Multi-Metal Continuous Emissions Monitors

Published September 1998

Prepared for:

U.S. Environmental Protection Agency
National Risk Management Research Laboratory
and
U.S. Department of Energy
Office of Environmental Management
Office of Science and Technology

Prepared by:

Sky +
7000 Thornhill Drive
Oakland, CA 94611

with
Ames Laboratory, Idaho National Engineering and Environmental Laboratory,
Savannah River Technical Center, and
EPA National Risk Management Research Laboratory

DISCLAIMER

ABSTRACT

Five prototype and two commercially available multi-metals continuous emissions monitors (CEMs) were tested in September 1997 at the Rotary Kiln Incinerator Simulator facility at the EPA National Risk Management Research Laboratory, Research Triangle Park, North Carolina. The two commercial CEM instruments were the Inductively Coupled Plasma - Atomic Emission Spectrometry (ICP-AES) system offered for sale by Thermo Jarrell Ash, and the X-Ray Fluorescence system offered for sale by Cooper Environmental Services in Portland, OR. The five prototype CEMs were: another ICP-AES system tested using two different spectrometers (mono and hi-resolution) from Diagnostic Instrumentation and Analytical Laboratory (DIAL) at Mississippi State University; two Laser Induced Breakdown Spectrometry—Atomic Emission Spectroscopy (LIBS) systems, one from DIAL and one from Sandia National Laboratories; a Microwave-Induced Plasma Spectroscopy (MIPS) system from Massachusetts Institute of Technology (MIT); and a Spark-Induced Breakdown Spectroscopy (SIBS) system from Physical Sciences, Inc. In addition, one participant, Laser Diagnostics, demonstrated a new data analysis approach, post-processing some spectroscopy data from the Sandia LIBS instrument to independently calculate metal concentrations.

The seven CEMs were tested side by side in a long section of duct following the secondary combustion chamber of the RKIS. Two different concentrations of six toxic metals were introduced into the incinerator—approximately 15 and 75 μg/dscm of arsenic, beryllium, cadmium, chromium, lead, and mercury (We also tested for antimony but we are not reporting on it here because EPA recently dropped antimony from the list of metals addressed by the draft MACT rule). These concentrations were chosen to be close to emission standards in the draft MACT rule and the estimated Method Detection Limit (MDL) required of a CEM for regulatory compliance purposes.

Results from this test show that no CEMs currently meet the performance specifications in the EPA draft MACT rule for hazardous waste incinerators. Only one of the CEMs tested was able to measure all six metals at the concentrations tested. Even so, the relative accuracy of this CEM varied between 35% and 100%, not 20% or less as required in the EPA performance specification. As a result, we conclude that no CEM is ready for long-term performance validation for compliance monitoring applications. Because sampling and measuring Hg is a recurring problem for multi-metal CEMs as well as Hg CEMs, we recommend that developers participate in a 1998 DOE-sponsored workshop to solve these and other common CEM measurement issues.

Real-time data from this test indicate that one-minute updates to hourly averages may be more frequent than is necessary to track incinerator and air pollution control system performance. In addition, the good performance observed for the only batch CEM tested, i.e., the HEST+XRF combination, suggests that a batch CEM may have important advantages compared with a continuous analyzer. The Performance Specification in the draft MACT rule accommodates batch CEMs. We also used the test results to evaluate which performance specifications in the draft MACT rule are achievable and to provide

recommendations for those that are currently unachievable. Realistic, achievable performance specifications (for parameters such as relative accuracy and up-time availability) will accelerate the availability, acceptance, and use of multi-metal CEMs, thus supporting EPA goals for compliance assurance.

EXECUTIVE SUMMARY

Introduction and Test Objectives

In theory, multi-metal Continuous Emission Monitors (CEMs) offer a better way to control pollutants and monitor compliance with emission regulations. Draft EPA regulations provide incentives to use multi-metal CEMs to reduce waste feed characterization and to reduce dependence on operating parameters for compliance verification. However, multi-metal CEM techniques are more complex than the O_2, CO, SO_x, and NO_x. CEMs that are already commercially available. Technical risks and small market sizes are serious impediments to commercial development of multi-metal CEMs. Of the technical risks, performance verification is one of the most important.

This report describes the third in a series of multi-metal CEM performance tests conducted jointly by EPA and DOE. This test was conducted during September 1997 at the Rotary Kiln Incinerator Simulator facility at the EPA National Risk Management Research Laboratory, Research Triangle Park, North Carolina.

This test was designed to measure the performance of multi-metal CEMs for regulatory compliance applications. As such, the test focused on six metals currently slated for regulation in the draft EPA MACT rule (EPA, 1996): arsenic, beryllium, cadmium, chromium, lead, and mercury (Antimony was dropped from the draft MACT rule during 1997). Assuming the MACT rule will be promulgated largely as drafted, the most important performance issue is whether the multi-metal CEMs can quantitatively measure all six metals at concentrations near the emission limits. In this test we measured Relative Accuracy at two metal concentration levels that were near the emission limits to address this question. Relative Accuracy is a quantitative measure of agreement between measurement results obtained by a multi-metal CEM under test and those obtained by the EPA Reference Method (RM) during measurement periods when both the CEM and RM were employed. In the draft performance specification for multi-metal CEMs (EPA, 1996b), EPA has proposed that instruments that can measure a metal with Relative Accuracy of 20% of less at concentrations near the emission limit provide acceptable quantitative measurement capability.

The performance specification does not prescribe the Method Detection Limit (MDL). However, to evaluate the CEMs at this stage of development, it is useful to use MDL as a way to assess improvements needed in the instrument. In general, to be quantitative at the emission limit (or the emission standard), an instrument needs an MDL equal to one-tenth the emission limit. In this test we evaluate CEM measurements at two metal concentration levels—one near the emission limit and one below the emission limit. CEM measurements at concentrations near the emission limit are useful to compare against the EPA Relative Accuracy performance specification. CEM measurements at concentrations below the emission limit can indicate if the CEM MDL is adequate.

CEM data scatter, the variation of CEM measurement results over time intervals equal to or less than typical RM measurement periods, is another important issue. The meaning of these variations is not clear because the actual second-to-second and minute-to-minute variations in trace metals concentrations in the process are not known, and no simple "metals calibration gas" exists to compare the instruments' real-time readings to a known source. To quantify the variation of the multi-metal CEM results, we calculate the standard deviation of the data points during each RM measurement period. Because the instruments in this test all measured the same test stream during common test periods, the observed standard deviation values indicate which multi-metal CEMs operated with more or less instrumental variation than other multi-metal CEMs. Clearly, very large variations will limit the usefulness of real-time data for process control.

The results of this test show which elements of the draft EPA performance specification for multi-metal CEMs are currently achievable and provide a technical basis for recommendations concerning those that are not currently achievable. Realistic, achievable performance specifications (for parameters such as relative accuracy and up-time availability) are expected to accelerate the availability, acceptance, and use of multi-metal CEMs, thus supporting EPA goals for compliance assurance.

The test results also provide a technical basis for decisions concerning extended duration performance testing of multi-metal CEMs.

Multi-metal CEMs Tested

Nine CEM technologies were tested. These included the six complete multi-metal CEM systems listed in the upper rows of Table ES-1. One of these, the Navy/TJA ICP-AES system, is commercially available, although with limited field experience. The other five CEMs are prototypes under development by research laboratories. The other three technologies that were tested are potential components of a CEM system. These were: (1) the Hazardous Element Sampling Train (HEST) combined with off-site X-Ray Fluorescence analysis (commercially available, although also with limited field experience), (2) a High Resolution Interferometric Spectrometer (HiRIS), tested here with the DIAL air ICP unit, and (3) new software under development by Laser Diagnostics, LLC, which was used in this test to post-process some spectroscopic data from the Sandia LIBS instrument to provide independently calculated metal concentrations. Table ES-1 identifies the technologies, the developing organizations, and the development sponsors.

Test procedures

The CEMs were tested side by side along a long duct following the secondary combustion chamber of the RKIS. Two different concentrations of six toxic metals were introduced into the incinerator—approximately 15 and 75 μg/dscm of arsenic, beryllium, cadmium, chromium, lead, and mercury. We did not address antimony because EPA had recently removed it from the list of metals proposed to be regulated under the draft MACT rule. These

Table ES-1. Summary of multi-metal CEM technologies, organizations, and sponsors.

CEM Technology	Developing Organization	Abbreviation Used	Sponsoring Organization
Inductively Coupled Plasma—Atomic Emission Spectrometry (ICP-AES)	U.S. Department of Defense (DoD) Naval Air Warfare Center	Navy/TJA ICP	U.S. Army Demilitarization Technology Office Commercially available through Thermo Jarrell Ash
Inductively Coupled Plasma—Atomic Emission Spectroscopy (ICP-AES)	Diagnostic Instrumentation and Analytical Laboratory (DIAL) at Mississippi State University	DIAL ICP	U.S. Department of Energy Characterization, Monitoring, and Sensor Technology Crosscutting Program (DOE CMST-CP)
Laser Induced Breakdown Spectrometry—Atomic Emission Spectroscopy (LIBS)	Diagnostic Instrumentation and Analytical Laboratory (DIAL) at Mississippi State University	DIAL LIBS	U.S. Department of Energy Characterization, Monitoring, and Sensor Technology Crosscutting Program (DOE CMST-CP)
Laser Induced Breakdown Spectrometry—Atomic Emission Spectroscopy (LIBS)	Sandia National Laboratories, Livermore, CA	Sandia LIBS	DOE CMST-CP and the U.S. Army Demilitarization Technology Office
Spark-Induced Breakdown Spectroscopy	Physical Sciences Inc.	PSI SIBS	U.S. Department of Energy, FETC
Microwave Induced Breakdown Spectroscopy	Massachusetts Institute of Technology	MIT MIPS	U.S. Department of Energy Mixed Waste Focus Area
Hazardous Element Sampling Train (HEST) + X-Ray Fluorescence	Private. Cooper Environmental Services, Inc.	HEST+XRF	Private. Cooper Environmental Services, Inc. Commercially available through CES, Inc.
High Resolution Interferometric Spectrometer	Ames Laboratory U.S. DOE, Iowa State University	HiRIS	U.S. Department of Energy Characterization, Monitoring, and Sensor Technology Crosscutting Program (DOE CMST-CP)
Self-Calibration Technique for LIBS	Laser Diagnostics, LLC	Laser Diagnostics	U.S. Department of Energy Characterization, Monitoring, and Sensor Technology Crosscutting Program (DOE CMST-CP)

concentrations were chosen to be close to emission standards in the draft MACT rule and the estimated Method Detection Limits (MDL) required of a multi-metal CEM for regulatory compliance purposes.

The test procedures focused mainly on collecting data for relative accuracy calculations. The RA values are considered to be reliably estimated when at least nine independent data pairs are used for each calculation (a data pair being an EPA Reference Method measurement and the average of the individual CEM measurement results obtained during the time period when the sampling for the Reference Method was performed). This test collected EPA Reference Method samples simultaneously at two locations in the duct, one upstream of all the CEMs and one just upstream of the sampling points for the final three multi-metal CEMs. This test included ten such RM measurement periods for each of the two different metal concentrations, for a total of forty Reference Method samples.

The metals were introduced into the flue gas by atomizing aqueous metal solutions directly into the flame of the secondary combustion chamber of the incinerator. Flyash particles containing metals and other elements were also injected into the transition duct between the kiln and SCC to simulate actual flue gas conditions. No hazardous or other waste was fed into the incinerator. EPA Reference Method samples were drawn at two locations in the duct, one upstream of all the multi-metal CEMs and one just upstream of the final three downstream CEMs.

Test Results

Results from this test show that no CEMs currently meet the performance specifications in the EPA draft MACT rule for hazardous waste incinerators. Only one of the CEMs tested was able to measure all six metals at concentrations tested. Even so, the relative accuracy of this CEM varied between 35% and 100%, not 20% or less as required in the EPA performance specification. Based on these results, we conclude that no CEM is ready for long-term performance validation for use in compliance monitoring applications. Since sampling and measuring mercury is a consistent problem for multi-metal CEMs as well as dedicated mercury CEMs, we recommend that developers of the leading technologies participate in a 1998 DOE-sponsored workshop to address these and other common CEM measurement issues.

Real-time data from this test indicate that one-minute updates to hourly averages may be more frequent than is necessary to track incinerator and air pollution control system performance.

The good performance observed for the only batch CEM tested, i.e., the HEST+XRF combination, suggests that a batch CEM may have important advantages compared with a continuous analyzer. The Performance Specification in the draft MACT rule accommodates batch CEMs.

We also used the test results to evaluate which performance specifications in the draft MACT rule are achievable and to provide recommendations for those that are currently unachievable. Realistic, achievable performance specifications

(for parameters such as relative accuracy and up-time availability) will accelerate the availability, acceptance, and use of multi-metal CEMs, thus supporting EPA goals for compliance assurance.

Conclusions

This test provided performance data that will be used to assess the current state of the art in multi-metal CEMs. This data, and the analyses presented in this report, support the following conclusions:

- No multi-metal CEM met the EPA Performance Specification in the Draft MACT rule, which requires measuring all 6 metals (at concentrations near the emission standard) with Relative Accuracy less than or equal to 20%.

- Based upon demonstrated capability to measure all six MACT metals at or near the concentrations tested here, with RA close to 20%, none of the multi-metal CEMs tested here appear ready for long-term testing.

- The Navy/TJA ICP system can measure all 6 metals, with RA between 35% and 100%.

- The HEST+XRF combination, although it does not analyze in real-time, and the DIAL ICP can likely be adapted to measure all six metals.

- This test did not show that Relative Accuracies $\leq$20% are achievable with current technology.

- The *in situ* LIBS and SIBS configurations tested here used optical fiber to transmit atomic emission from the point of excitation to the spectrometric measurement equipment. Because of that, the LIBS and SIBS systems were not able to take advantage of some of the strongest atomic emission lines for As and Hg. In addition, for the wavelengths transmitted by the optical fiber, those instruments suffered from insufficient spectral resolution and spectral interference that precluded simultaneous measurement of As and Cd at detection limits required for compliance monitoring. However, the LIBS and SIBS systems could be adapted to measure extracted and/or concentrated sample material, either in a manner similar to the XRF analyzing the sample collected by the HEST, or in real time using some other sample extraction and/or concentration means.

- Additional testing with Hg would be useful to isolate the cause of the discrepancies between the RM results and the CEM results.

- For reliable comparison of the detection capabilities of different multi-metal CEMs, a single common method must be used for

estimation of Method Detection Limits (MDLs). The developers that participated in this test did not use a single common method.

- Short term variations of the multi-metal CEM results were significant and were considerably different for the different CEMS. How much variation is caused by real variations in the flue gas and how much is due to the CEMs should be addressed in future tests. The CEM data variations and data averaging times are important if the data are to be used for real-time process control or compliance.

- Short term variations in the CEM results are greatly reduced if real-time data points are averaged over several minutes, instead of seconds. Additional field data and experience are needed to determine how real-time data should be used for process control and compliance assurance. The current draft MACT rule performance specification requires 1-minute updates to one-hour rolling averages. Based on data from this test, a 1-minute update would probably not provide useful information. A two to five minute update would be more useful.

- "Batch" monitoring techniques that pre-concentrate samples for subsequent analysis, as in the HEST+XRF system, for example, may be more capable and less expensive to operate and maintain than a real-time CEM.

- It may be possible to improve relative accuracies by performing instrument calibrations in the field at stack conditions. Field calibration is not straightforward for a multi-metal CEM because calibration standards are not readily available. In this test, only one of the CEMs (the MIT MIPS system) performed a calibration at stack conditions. The Navy/TJA ICP system routinely performs field calibrations, but not at stack conditions.

If a new multi-metal CEM calibration procedure were developed, it could spawn a new validation procedure that would allow assessment of RA without using EPA Reference Method 29. This would reduce the uncertainty in RA assessments caused by RM uncertainties and might help establish a more achievable RA performance requirement.

ACKNOWLEDGMENTS

This work was jointly sponsored and executed by the U. S. Department of Energy (DOE) and the U. S. Environmental Protection Agency (EPA). The DOE sponsorship was through the Characterization, Monitoring, and Sensor Technology Crosscutting Program (CMST-CP) and the Mixed Waste Focus Area (MWFA), both of the Office of Science and Technology (OST), Office of Environmental Management. The EPA sponsorship involved the National Risk Management Research Laboratory (NRMRL), Air Pollution Prevention and Control Division (APPCD), Research Triangle Park (RTP), North Carolina, and the National Exposure Research Laboratory (NERL), Air Measurements Division, RTP.

This is the third DOE/EPA performance test of multi-metal CEMs. The second test was conducted in April 1996 at the same EPA facility. The first test was in August 1995 at the EPA Incineration Research Facility (IRF) in Jefferson, Arkansas. We thank all the engineers, scientists, and managers who contributed to these efforts.

CONTENTS

FIGURES

TABLES

ACRONYMS

AES	Atomic Emission Spectroscopy
ALARA	As low as reasonably achievable, a principle of exposure minimization
alpm	actual liters per minute
APPCD	Air Pollution Prevention and Control Division of the EPA NRMRL
ASME	The American Society of Mechanical Engineers
BIFs	Boilers and industrial furnaces
CAA	Clean Air Act
CBD	The *Commerce Business Daily*
CD	Calibration drift
CEM	Continuous emissions monitor
cfm	Cubic feet per minute
CFR	The Code of Federal Regulations
CMST-CP	The Characterization, Monitoring, and Sensor Technology Crosscutting Program, within the U.S. DOE EM Office of Science and Technology
CVAAS	Cold vapor atomic absorption spectroscopy
DIAL	Diagnostic Instrumentation and Analysis Laboratory, at Mississippi State University, Starkville, Mississippi
DL	Detection limit
DOE	The U. S. Department of Energy
DRE	Destruction and removal efficiency
dscf	dry standard cubic foot or dry standard cubic feet
dscm	dry standard cubic meter
EM	The U. S. Department of Energy Office of Environmental Management
EPA	The U. S. Environmental Protection Agency
FR	The Federal Register
GFAAS	Graphite furnace atomic absorption spectroscopy
HAP	Hazardous air pollutant
HAZWOPER	Hazardous Waste Operations and Emergency Response
HEST	Hazardous element sampling train
ICP-AES	Inductively coupled plasma - atomic emission spectrometry
ICP-MS	Inductively coupled plasma - mass spectrometry
IFRF	International Flame Research Foundation
IRF	The EPA Incineration Research Facility in Jefferson, Arkansas
LIBS	Laser-induced breakdown spectrometry
LVM	Low volatility metals
LWAK	Lightweight aggregate kiln
MDL	Method detection limit
MS	Matrix spike, a spiked sample used to evaluate analytical method recovery
MS	Mass spectrometry

MSD	Matrix spike duplicate, a duplicate MS sample
MWFA	The Mixed Waste Focus Area, within the U. S. DOE EM Office of Science and Technology
NERL	The EPA National Exposure Research Laboratory
NIST	National Institute for Standards and Technology
NPT	Nominal pipe thread
NRMRL	The EPA National Risk Management Research Laboratory
OAQPS	The EPA Office of Air Quality Planning and Standards
OST	The EM Office of Science and Technology
OSW	The EPA Office of Solid Waste
POHC	Principal organic hazardous constituent
PS	Performance specification
QA	Quality assurance
QAO	Quality assurance objective
QAPP	Quality assurance project plan
QC	Quality control
RA	Relative accuracy
RATA	Relative accuracy test audit
RCRA	The Resource Conservation and Recovery Act
RKIS	Rotary kiln incinerator simulator
RM	Reference method
RPD	Relative percent difference
RSD	Relative standard deviation
RTP	Research Triangle Park, North Carolina
SNL	Sandia National Laboratories
SRM	Standard reference material
SVM	Semi-volatile metals
SVOC	Semi-volatile organic compound
THC	Total hydrocarbon
TJA	The Thermo Jarrell Ash Corporation
VOC	Volatile organic compound
XRF	X-ray fluorescence
ZD	Zero drift

1997 Performance Testing of Multi-Metal Continuous Emissions Monitors

1. INTRODUCTION

This report summarizes the results of side-by-side testing of continuous emissions monitor (CEM) technologies for real-time measurements of concentrations of toxic metals in flue gas emissions from hazardous waste treatment and combustion devices. Multi-metal CEMs are important to provide assurance that the combustion process is operating properly, and within regulatory compliance standards. CEMs can also predict changes in operating conditions that are required to maintain operation within compliance.

The hazardous waste thermal treatment community needs real-time monitoring of particulate matter, organic compounds, and metals in stack emissions. Current monitoring procedures involve manual sample collection over an extended period of time, and then sample analysis later. Several developers have produced multi-metal CEMs for real-time monitoring of hazardous trace metal emissions. This project tested the performance of seven such CEM systems. This report compares CEM results with results from simultaneous flue gas sampling using conventional EPA Reference Method (RM) sampling trains and analytical procedures.

1.1 Background

The impetus for developing CEMs for trace metals in flue gas emissions arose with the promulgation of regulations governing the destruction of hazardous wastes in boilers and industrial furnaces in 1991 (EPA, 1996c). These rules, extended to hazardous waste incinerators during permit revisions and re-authorizations under the omnibus authority granted permit writers within the Resource Recovery and Conservation Act, limit the emissions of several trace metals from waste combustion devices. At the time these rules were promulgated, the ultimate desire was to require continuous monitoring of the emissions of the regulated metals. However, at the time, no metal CEMs existed. Therefore, compliance with the standard had to be shown during the trial burn. Subsequent continuous compliance with the emission standards is ensured by limiting the feedrate of each regulated metal to the waste combustor and constraining facility operation to conditions within the range of those previously tested during the trial burn. The metal feedrate limitation, in turn, requires the operator to have detailed knowledge of the metal concentrations in wastes being fed to the process. In practice, this requires extensive waste feed characterization to determine the quantities of regulated metals in the waste.

Recently, EPA announced a proposed rule under the title, "Revised Standards for Hazardous Waste Combustors" (EPA, 1996). The proposed rule would promulgate revised emission standards reflecting the performance of Maximum Achievable Control Technologies (MACT) as specified by the Clean Air Act and would clearly establish CEMs as the preferred[a] method for compliance monitoring.

Under the proposed MACT rule, the application of continuous emissions monitoring for HCl, Cl_2, Hg, semi-volatile metals (SVM), and low volatile metals (LVM) can replace feedstream analysis for those

---

a. The top tier of the compliance monitoring hierarchy is the use of a continuous emissions monitor for that HAP or standard. In the absence of a CEM, the second tier is the use of a CEM for a surrogate of that HAP or standard and, when necessary, setting some operating limits to account for the limitations of using surrogates. Lacking a CEMS for either, EPA sets appropriate feedstream and operating parameter limits to ensure compliance and requires periodic testing of the source.

constituents and can eliminate consideration of those waste constituents during required comprehensive and confirmatory tests. This is especially important in the case of mixed waste, because of ALARA concerns, i.e., a commitment to keep radioactive exposure to personnel as low as reasonably achievable, and because both the feedstream analysis and the testing, the latter comparable to the RCRA trial burn, are high cost activities. At this time, only Particulate Matter CEMs will be required in the MACT rule.

CEMs can provide several benefits for waste treatment. By providing more complete and timely information on emissions, they can enable better control for safe and compliant operation of treatment facilities, provide documentation of such operation, and help provide greater assurance of the quality of the final waste forms. These benefits address important public concerns regarding the siting and operation of incinerators or other thermal treatment equipment. Consequently, quality CEMs could help reopen the door to public acceptance of such facilities. However, most multi-metal CEMs are not yet commercially available.

This test was sponsored jointly by the Department of Energy (DOE) and the Environmental Protection Agency (EPA). The DOE sponsorship was through the Characterization, Monitoring, and Sensor Technology Crosscutting Program (CMST-CP) and the Mixed Waste Focus Area (MWFA), both of the Office of Science and Technology (OST), Office of Environmental Management. The EPA sponsorship involved the National Risk Management Research Laboratory (NRMRL), Air Pollution Prevention and Control Division (APPCD), Research Triangle Park (RTP), North Carolina, and the National Exposure Research Laboratory (NERL), Air Measurements Division, RTP.

The testing described in this report builds upon previous DOE/EPA testing of metal and organic compound CEMs conducted in August 1995 at the EPA Incineration Research Facility (IRF) in Jefferson, Arkansas (Ghorishi et al, 1997) and the 1996 multi-metal CEMs test conducted at the Rotary Kiln Incinerator Simulator facility at the EPA National Risk Management Research Laboratory, Research Triangle Park, North Carolina (Haas et al, 1997). The tests described here owe much to the planning and lessons learned from these test programs.

1.2 Technologies Tested

Nine CEM technologies were tested. These included the six complete multi-metal CEM systems listed in the upper rows of Table 1. One of these, the Navy/TJA ICP-AES system, is commercially available, although with limited field experience. The other five CEMs are prototypes under development by research laboratories. The other three technologies that were tested are potential components of a CEM system. These were: (1) the Hazardous Element Sampling Train (HEST) combined with off-site X-Ray Fluorescence analysis (commercially available, although also with limited field experience), (2) a High Resolution Interferometric Spectrometer (HiRIS), tested here with the DIAL air ICP unit, and (3) new software under development by Laser Diagnostics, LLC, which was used in this test to post-process some spectroscopic data from the Sandia LIBS instrument, to provide independently calculated metal concentrations. Table 1 identifies the technologies, the developing organizations, and the development sponsors.

The DIAL ICP HiRIS uses the same DIAL ICP and sampling interface, but with a different spectrometer. This new spectrometer design combines high resolution with compact, light weight (it weighs only 10 kg), which makes it attractive for at-stack monitoring.

The HEST+XRF system was the only batch CEM tested. It includes the Cooper Environmental Services (CES) hazardous element sampling train (HEST), which is used to collect sample material on a rotating filter, and an off-site XRF analysis system (in San Francisco), which was used to analyze the.

Table 1-1. Summary of multi-metal CEM technologies, organizations, and sponsors.

CEM Technology	Developing Organization	Abbreviation Used	Sponsoring Organization
Inductively Coupled Plasma—Atomic Emission Spectrometry (ICP-AES)	U.S. Department of Defense (DoD) Naval Air Warfare Center	Navy/TJA ICP	U.S. Army Demilitarization Technology Office Commercially available through Thermo Jarrell Ash
Inductively Coupled Plasma—Atomic Emission Spectroscopy (ICP-AES)	Diagnostic Instrumentation and Analytical Laboratory (DIAL) at Mississippi State University	DIAL ICP	U. S. Department of Energy Characterization, Monitoring, and Sensor Technology Crosscutting Program (DOE CMST-CP)
Laser Induced Breakdown Spectrometry—Atomic Emission Spectroscopy (LIBS)	Diagnostic Instrumentation and Analytical Laboratory (DIAL) at Mississippi State University	DIAL LIBS	U. S. Department of Energy Characterization, Monitoring, and Sensor Technology Crosscutting Program (DOE CMST-CP)
Laser Induced Breakdown Spectrometry—Atomic Emission Spectroscopy (LIBS)	Sandia National Laboratories, Livermore, CA	Sandia LIBS	DOE CMST-CP and the U.S. Army Demilitarization Technology Office
Spark-Induced Breakdown Spectroscopy	Physical Sciences Inc.	PSI SIBS	U.S. Department of Energy, FETC
Microwave Induced Breakdown Spectroscopy	Massachusetts Institute of Technology	MIT MIPS	U. S. Department of Energy Mixed Waste Focus Area
Hazardous Element Sampling Train (HEST) + X-Ray Fluorescence	Private. Cooper Environmental Services, Inc.	HEST+XRF	Private. Cooper Environmental Services, Inc. Commercially available through CES, Inc.
High Resolution Interferometric Spectrometer	Ames Laboratory U.S. DOE, Iowa State University	HiRIS	U. S. Department of Energy Characterization, Monitoring, and Sensor Technology Crosscutting Program (DOE CMST-CP)
Self-Calibration Technique for LIBS	Laser Diagnostics, LLC	Laser Diagnostics	U. S. Department of Energy Characterization, Monitoring, and Sensor Technology Crosscutting Program (DOE CMST-CP)

filters collected during the test. The CES HEST+XRF approach is unique in that it was developed solely with private (non-government) funding

The ninth participant, Laser Diagnostics, LLC, tested only data analysis software, post-processing some spectroscopic data from the Sandia LIBS instrument, to independently determine metal concentrations.

1.3 Test Objectives

This test was designed to measure the performance of multi-metal CEMs for regulatory compliance applications. We refer to such CEMs as "compliance CEMs," to distinguish them from process control and "stakeholder assurance" CEMs, which may have less rigorous quantitative requirements. The test focused on the six metals currently slated for regulation in the draft EPA MACT rule: arsenic, beryllium, cadmium, chromium, lead, and mercury (EPA dropped antimony from the draft MACT rule during 1997).

Assuming the MACT rule will be promulgated largely as drafted, the most important performance issue is whether the multi-metal CEMs can quantitatively measure all six metals at concentrations near the emission limits. To address this issue, we measured Relative Accuracy at two metal concentration levels that were near the emission limits.

Relative Accuracy is a quantitative measure of agreement between measurement results obtained by a multi-metal CEM under test and those obtained by the EPA Reference Method (RM) during measurement periods when both the CEM and RM were employed. The draft EPA performance specification for a multi-metal CEM (EPA, 1996b) requires Relative Accuracy of 20% or less at concentrations at or slightly above the emission standard (a.k.a. the emission limit). The performance specification does not prescribe the Method Detection Limit (MDL). However, the MDL can be used for preliminary assessment of whether or not an instrument can provide quantitative results at the emission limit. In general, to be quantitative at the emission limit an instrument needs an MDL that is equal to or less than one-tenth the emission limit.

CEM measurements at concentrations at or slightly above the emission limit are useful to compare against the EPA Relative Accuracy performance specification. CEM measurements at concentrations below the emission limit can indicate if the CEM MDLs are adequate.

The variation of CEM measurement results over relatively short time intervals, i.e., times equal to or less than the typical RM measurement periods, is another important issue. The meaning of these variations is not obvious because the actual second-to-second and minute-to-minute variations in the trace metals concentrations in the stream being measured are not known and no simple "metals calibration gas" exists to compare the real-time multi-metal CEM readings to a known source. To quantify the variation of the multi-metal CEM results, we calculate the standard deviation of the data points during each RM measurement period. Because the instruments in this test all measured the same test stream during common test periods, the observed standard deviation values indicate which multi-metal CEMs operated with more or less instrumental variation than other multi-metal CEMs. Clearly, very large variations will limit the usefulness of real-time data for process control.

We also used the test results to evaluate which performance specifications in the draft MACT rule are achievable and to provide recommendations for those that are currently unachievable. Realistic, achievable performance specifications for parameters such as relative accuracy and "up-time availability" will accelerate the availability, acceptance, and use of multi-metal CEMs, thus supporting EPA goals for compliance assurance.

Finally, we also wanted to identify which CEM technologies are ready for long-term performance testing by EPA. Successful long-term testing is required before use as a regulatory compliance monitor.

2. TEST FACILITY, PROCEDURES, AND CONDITIONS

All tests were conducted using a simulated flue gas stream produced by the Rotary Kiln Incinerator Simulator (RKIS) at the U. S. EPA Environmental Research Center, Research Triangle Park, North Carolina. The test facility and test procedure are identical to that described in the 1996 multi-metal CEM test report (Haas et al, 1997). The exceptions are the test layout, and the Reference Method (RM) sampling procedure. The RM sampling procedures were modified to eliminate sample nozzle traversing across the duct. Section 2.1 describes the new test layout, which includes the 45 feet of new exhaust ductwork added to accommodate the seven CEMs.

2.1 Rotary Kiln Incinerator Simulator Test Layout

A schematic diagram of the RKIS, indicating the locations of key process condition measurement points and the locations of the RM sampling points and test CEMs, is provided in Figure 2-1.

The RKIS consists of a primary combustion chamber, a transition section, and a fired afterburner in the secondary combustion chamber (SCC). Typical firing rates are 29 to 88 kW (0.1 to 0.3 MBtu/h) to each of the kiln and the SCC. A more complete listing of the design characteristics of the RKIS is provided in the 1996 multi-metal CEM test report (Haas et al, 1997). For all tests, both the kiln and the SCC were fired with natural gas. No waste or simulated waste was fed to the kiln.

Combustion flue gases exiting the SCC were cooled rapidly to approximately 538°C (1000°F) as they passed through the water-jacketed duct section immediately downstream of the SCC. Further cooling, to approximately 232°C (450°F), was achieved by adding air via an air dilution damper just downstream of the water-jacketed section. The locations of the ports, and their uses, are indicated by the labels (*RM, DIAL LIBS, SNL LIBS, and Navy/TJA)* in the upper portion of Figure 2-1.

The duct containing the RM sampling and CEM test access ports is a 20.4 m (67-ft) long run of 8-inch, Schedule 10, 304 stainless steel, insulated pipe. It runs just below the ceiling of the two-story, high-bay test area that contains the RKIS on the ground level and the SCC on the second floor.

The RM sampling and CEM test access ports are configured as shown in Figure 2-1. Each set provides access for isokinetic flue gas sampling via a 4-inch port opposite a 3-inch NPT port and a second 3-inch NPT diameter port at right angles to the other two.

The flue gas at the sampling locations had a temperature of approximately 230°C (450°F) and a moisture content between 4.5 and 7.9 percent by volume as measured by EPA Method 0060. Additional detail concerning the test conditions is provided in Section 2.4. There was a temperature drop of approximately 28°C (50°F) between the first and last CEM sampling ports.

2.2 Test Procedure

The CEMs were tested side by side along a long duct following the secondary combustion chamber of the RKIS. Two different concentrations of six toxic metals were introduced into the incinerator—approximately 15 and 75 μg/dscm of arsenic, beryllium, cadmium, chromium, lead, and mercury. We did not address antimony because EPA had recently removed it from the list of metals proposed to be regulated under the draft MACT rule. These concentrations were chosen to be close to the emission standards in the draft MACT rule.

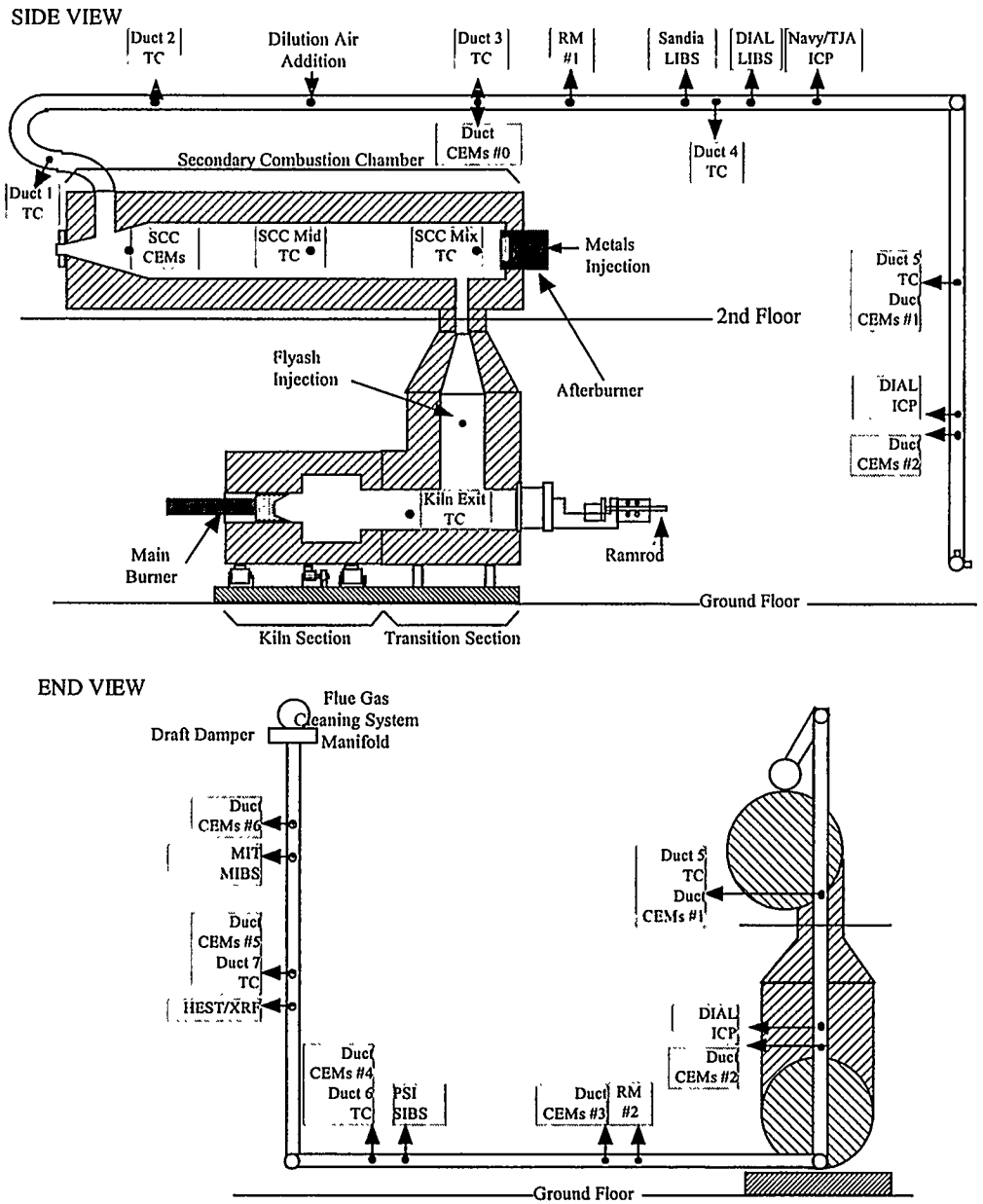

Figure 2-1. Schematic diagram of the RKIS (side view above, top view below).

The test procedures focused mainly on collecting data for relative accuracy calculations. The RA values are considered to be reliably estimated when at least nine independent data pairs are used for each calculation (a data pair being an EPA Reference Method measurement and the average of the individual CEM measurement results obtained during the time period when the sampling for the Reference Method was performed). This test collected EPA Reference Method samples simultaneously at two locations in the duct, one upstream of all the CEMs and one just upstream of the sampling points for the final three multi-metal CEMs. This test included ten such RM measurement periods for each of the two different metal concentrations, for a total of forty Reference Method samples.

The metals were introduced into the flue gas by atomizing aqueous metal solutions directly into the flame of the secondary combustion chamber of the incinerator, producing specific metal concentrations in the duct. Flyash particles containing metals and other elements were also injected into the transition duct between the kiln and SCC to simulate actual flue gas conditions. No hazardous or other waste was fed into the incinerator.

2.3 Reference Method Sampling and Analysis Procedures

The RM for trace metals (including mercury) in these tests is draft SW-846 Method 0060, Determination of Metals in Stack Emissions (EPA, 1994). The details of this method are described there and special adaptations of the method are described in the 1996 multi-metal CEM test report (Haas et al, 1997).

2.4 Facility Data

The flue gas test conditions as recorded by the test facility instruments are shown in Table 2-1.

Table 2-1. Facility data during multi-metal CEM test.

Date	RM #	Duct O2 (%)	Duct CO2 (%)	Duct CO (ppm)	Duct NO (ppm)	SCC O2 (%)	SCC CO2 (%)	SCC CO (ppm)	SCC NO (ppm)	Duct CO2 (%)[a]	Duct H2O (%)[a]	Kiln Exit (F)	SCC Mix (F)	SCC Exit (F)	Duct 1 (F)	Duct 2 (F)	Duct 3 (F)	Duct 4 (F)	Duct 5 (F)	Duct 6 (F)	Duct 7 (F)
9/22/97	1	17.2	3.6	0.5	153.1	13.4	4.8	9.3	276.2	2.4	6.3	1354.8	1083.7	1234.0	950.1	785.2	463.1	446.0	413.0	396.1	392.2
9/22/97	2	17.2	3.6	0.8	151.1	13.3	4.7	11.0	265.8	2.4	6.2	1374.4	1112.2	1248.5	954.1	784.9	465.2	448.6	414.0	396.1	394.2
9/22/97	3	17.1	3.6	20.6	158.3	13.3	4.7	11.6	284.0	2.4	6.1	1384.4	1123.9	1258.5	959.8	789.8	468.4	451.6	417.2	399.9	397.8
9/22/97	4	17.1	3.5	39.0	161.4	13.3	4.8	11.9	293.9	2.4	6.1	1395.0	1130.4	1270.2	965.7	794.4	471.3	454.6	420.8	402.7	400.8
9/22/97	5	17.0	3.6	45.0	167.5	13.2	4.8	12.4	304.2	2.4	6.2	1406.2	1138.9	1280.1	972.4	798.2	476.9	460.0	425.4	406.5	404.9
9/23/97	1	17.1	3.3	12.6	200.5	13.6	4.5	8.0	265.6	2.3	6.3	1353.2	1080.1	1226.4	947.7	786.5	469.4	452.0	418.9	403.3	397.6
9/23/97	2	17.1	3.3	12.2	222.3	13.6	4.5	7.5	297.5	2.3	6.4	1363.8	1094.0	1235.3	954.2	790.5	470.3	454.8	421.7	403.7	400.2
9/23/97	3	17.1	3.2	12.5	222.5	13.4	4.6	6.3	304.4	2.3	6.6	1385.4	1113.5	1250.0	940.8	777.9	471.8	455.3	421.3	403.2	399.5
9/23/97	4	17.1	3.1	16.4	226.8	13.3	4.6	5.4	316.2	2.3	6.6	1400.8	1127.1	1261.4	943.7	776.2	471.7	456.0	421.4	405.3	401.9
9/23/97	5	17.1	3.1	22.1	227.7	13.3	4.6	5.4	320.3	2.3	6.7	1410.2	1135.2	1268.9	949.1	780.7	475.0	458.5	423.6	411.9	402.8
9/24/97	1	17.0	3.2	11.8	163.3	13.4	4.5	6.2	299.3	2.4	6.4	1391.6	1122.4	1268.9	949.5	780.2	475.1	456.3	420.1	404.0	399.5
9/24/97	2	17.0	3.2	9.6	171.3	13.4	4.6	7.0	307.4	2.4	6.4	1402.3	1135.7	1281.4	956.0	785.3	476.6	458.9	422.6	406.4	401.8
9/24/97	3	17.0	3.2	14.6	181.0	13.3	4.6	5.6	323.5	2.4	6.5	1409.2	1142.6	1288.6	960.2	787.9	478.9	461.2	423.5	407.7	403.1
9/24/97	4	17.0	3.2	26.8	178.7	13.3	4.6	6.2	318.3	2.4	6.5	1415.8	1149.6	1296.3	964.5	791.5	479.9	462.0	426.2	409.8	404.7
9/24/97	5	16.9	3.2	35.0	184.0	13.2	4.6	6.7	327.0	2.4	6.5	1422.5	1155.7	1300.6	966.7	792.7	486.3	464.0	426.8	410.0	405.7
9/25/97	1	16.9	5.5	14.8	162.5	13.2	4.7	7.2	321.4	2.4	6.5	1389.9	1075.7	1248.3	933.0	768.4	467.5	450.7	414.5	399.7	393.1
9/25/97	2	16.9	5.3	10.5	170.6	13.2	4.6	6.6	338.0	2.4	6.5	1407.5	1092.3	1262.7	941.8	775.4	472.4	454.6	418.1	403.7	396.9
9/25/97	3	16.9	4.1	23.8	174.2	13.2	4.6	6.3	351.8	2.4	6.6	1423.4	1111.1	1278.5	950.0	781.5	475.8	458.6	422.8	407.9	401.0
9/25/97	4	16.8	4.0	37.7	169.9	13.2	4.6	6.4	344.3	2.4	6.6	1433.8	1121.7	1286.2	954.4	785.2	477.6	460.1	423.7	409.8	402.7
9/25/97	5	16.8	4.4	42.1	169.7	13.1	4.6	7.6	346.8	2.4	6.6	1444.2	1133.1	1295.1	960.8	789.3	481.6	464.2	427.1	412.6	405.3

a. as measured by the Perkin Elmer MCS 100 Multi-component Emission Monitoring System.

3. 1997 TEST RESULTS AND DISCUSSION

3.1 Continuous Sampling/Continuous Monitoring Results

All the multi-metal CEMs sampled the flue gas continuously. The two LIBS systems (DIAL and Sandia) and the PSI SIBS system measured *in situ*, i.e., directly in the flue gas. The other CEM systems extracted sample gas and then analyzed that gas.

Most of the CEM systems tested did not use equipment [spectrometers or photo-multiplier tubes (PMTs)] that was capable of continuous and simultaneous real-time monitoring of all six MACT metals. The Sandia LIBS system used only one (time-gated) spectrometer, making measurements in four different spectral windows sequentially to monitor the six metals of interest. As a consequence, none of the six elements was monitored more than 25% of the time. This limitation could have been avoided by using a dedicated spectrometer for each spectral window, as was done in the DIAL LIBS system.

The HEST+XRF system used XRF analysis equipment located in San Francisco. The filter paper from the test was analyzed after the test but before the RM results were released. The QA procedures were carefully followed and documented to ensure that the same analysis technique was used as would be employed if the XRF hardware were collocated with the sampling system.

Several other CEM systems did not provide real-time analytical results. The DIAL LIBS and the DIAL ICP/Mono post-processed their real-time data, including changing calibration factors. Brief, somewhat incomplete discussions of these data analysis procedures are included in the respective developers' reports located in the appendices of this report.

The other CEMs (Navy/TJA ICP, Sandia LIBS, MIT MIPS, and PSI SIBS) analyzed data in real-time and provided real-time analytical results during the test.

Table 3-1 summarizes the sampling characteristics, data-analysis times, and other pertinent information for 8 of the 9 technologies tested. Similar information is not included for Laser Diagnostics because it is not applicable to such software-only technology. Previous CEM test reports used parameters such as "duty cycle" to describe the percent of gas stream monitored. Instead, here we compare volume of stack gas sampled, sample frequency, and data-analysis time. Although the values of these parameters differ considerably from system to system (e.g., some analyze 100% of the stack gas sampled, some only 1%), the differences are not considered highly important because the real-time CEMs provide new measurement results so frequently (seconds) compared with the times (minutes) over which significant and measurable changes occur within the RKIS and flue gas duct. The latter changes are referred to as the characteristic times for the RKIS.

Table 3-1. Summary of sample and data analysis times for each technology (N/A = not available).

Technology	Sampling Method	Sample and Analysis Time and Volume Sampled	Other Features/Comments
Navy/TJA ICP	Extractive sample through 75-foot, heated sample line	2 to 3 second sample of stack gas (approximately 0.001 acm [1 liter]) analyzed every 90 to 100 seconds.	Argon-based plasma. Current size of ICP and AES equipment requires placement on ground level, necessitating long sample line.

Table 3-1. (continued).

Technology	Sampling Method	Sample and Analysis Time and Volume Sampled	Other Features/Comments
HEST+XRF	Extractive sample through short sample line, 1.2 cm diameter, onto filter.	Continuous sample collected at 1.4 alpm through moving filter paper. Filter paper analyzed off-site on XRF, providing concentration measurements at 6.5 minute intervals.	Future systems will use on-site XRF system, with analysis times less than one hour for each filter sample collected over 1 to 2 days. Later applications will likely go to weekly filter analysis. One XRF system can be shared by several sample probes, making this economical for multi-stack applications.
DIAL ICP Mono	Extractive sample through short sample line	Not available.	Current configuration uses air as carrier gas.
HiRIS	Same as DIAL ICP Mono	Same sample time as DIAL ICP Mono. Analysis time not available.	—
DIAL LIBS	*In situ* measurement.	10 Hz laser pulses; averaging over 20 seconds (200 pulses). Approximate sample volume per pulse 0.5 cm^3. Analysis time for each spectrum <0.5 seconds. Spectrum and estimated metal conc. displayed in near real-time during test. Data post-processed at end of test day and "corrected" using undefined scaling factor based on on-site calibration, accounting for fluctuations in laser power and optical attenuation.	Future systems improvements are aimed at automating on-site calibration, correcting for changes in laser power. The LIBS probe will be re-designed to prevent optics damage in the hot/humid test environments.
Sandia LIBS	*In situ* measurement.	5 Hz laser pulses; averaging over 2 minutes (600 pulses). Data analysis 1 second. Using only one spectrometer to measure all elements over broad spectral range. Requires scanning four different spectral windows during test, resulting in only 5 to 8 2-min. avg. data points for each element during each one-hour test.	Unique "conditional analysis" used to isolate single-pulse data containing metals, thereby increasing sensitivity. Data availability only 25% due to scanning 4 spectral windows. Can be overcome using additional spectrometers. Hardware failure caused calibration error, discovered after test. Results are factor of 1.3 to 2.6 too high.
PSI SIBS	*In situ* measurement	1 Hz spark rate, averaging over 60 sec. Dedicated PMTs to detect Pb and Cr. Data analyzed and reported at 1-minute time intervals.	Hardware was configured to monitor Pb and Cr only.
MIT MIPS	Extractive sample continuously flowing through short (normally 0.3 m) sample line into plasma.	Continuous sampling, data analysis time near instantaneous (5 data points per second). Average data over < 1 second to 1 minute intervals.	Sample line increased to 1.5 m long for this test to allow for scaffold movement. Estimate method detection limits about 3 $\mu g/m^3$ for 1 minute averaging time, and about 1 $\mu g/m^3$ for 10-minute averaging.

3.2 Reference Method (RM) Test Results

3.2.1 Upstream versus Downstream Measurement Locations

Simultaneous Reference Method (RM) measurements were performed for two locations in the duct. The first RM sampling location was upstream of all the multi-metal CEMs; the second was just upstream of the sampling points for the final three multi-metal CEMs, the PSI SIBS, the HEST, and the MIT MIPS. The two RM sampling locations were used to test whether there was any significant change in metals concentrations (due to deposition or air in-leakage) between the first and last multi-metal CEMs. Fixed gas CEMs located at various points along the sampling duct were used to verify that no air in-leakage occurred at the multi-metal CEM or RM sampling points. As expected, there was some variability in the results from the two RM sampling locations.

A statistical analysis was performed on the RM results: (1) to determine if there was a statistically significant difference between the upstream and downstream RM results; (2) to establish which concentration values to use for the metal concentrations along the duct; and (3) to calculate the standard deviation of the RM results for each metal. As documented in Appendix A, the results from this analysis showed that, at the 95% confidence level, there was no statistically significant difference between the upstream and downstream RM results. Therefore, we used the arithmetic average of the upstream and downstream Reference Method data to compare against CEM data in the Relative Accuracy calculations described in Section 3.3.4. RM data from two of the 40 RM sampling trains were not analyzed because of sampling or handling errors. For those two, the upstream or downstream value was used in place of the average. To quantify the effect of using the average of the reference method results, we also compared Relative Accuracies calculated using upstream, downstream, and average Reference Method data. The results of those calculations are presented in Section 3.3.6.

Table 3-2 shows the average of the upstream and downstream RM measurements and the standard deviation for each metal. Those data are also plotted in Figure 3-1. The plot shows more variation than expected during the first day of testing (RM #1 through RM #5). Two of the five concentration measurements from that day were approximately 50% lower than the others. The CEM data presented in Section 3.3.5 show that this behavior was verified by four of the six CEMs making measurements the first day. Based on these results, we believe the variations observed during this first test day were caused by facility fluctuations, not errors in reference method measurements.

3.2.2 Reference Method Measurement Results Compared with Target Concentrations

The target concentrations for the high and low concentration tests were 75 and 15 μg/dscm, respectively, for all the metals. Even with the variations of facility conditions that occurred on Test Day #1, the average concentrations for the high concentration of all metals except mercury (average of RM #1 through RM #10) were within 17% of the target concentration (between 62 and 78 μg/dscm). The low concentrations averaged within 80% of the target concentration (between 20 and 27 μg/dscm) for RM #11 through RM #20 (again, except for mercury).

The RM results for mercury are puzzling. As in the 1996 test, we question both the RM data and the CEM data (for the two CEMs that reported mercury). The RM sample handling and analytical procedures are especially critical for mercury. The target mercury concentrations were 75 and 15 μg/dscm. The average RM results were 182 and 38 μg/dscm, respectively, which are 142% and 153% of the respective target concentrations.

Table 3-2. Average of Reference Method (RM) results (µg/dscm) for upstream and downstream RM sampling locations and the means and standard deviations of those average values for the high concentration tests (RM #1 through RM #10) and the low concentration tests RM #11 through RM #20).

RM Measurement Number	As	Be	Cd	Cr	Hg	Pb
1	88	82	82	72	180	93
2	53	43	50	45	177	52
3	72	61	69	64	200	75
4	65	54	61	56	141	67
5	41	33	38	40	152	42
6	82	74	79	69	174	94
7	85	75	81	72	194	95
8	82	70	80	72	193	93
9	82	68	79	71	201	92
10	68	59	67	63	206	79
Avg. #1–10 ± Std. Dev.	72 ± 15	62 ± 15	69 ± 14	62± 11	182 ± 20	78 ± 18
11	27	19	23	29	38	28
12	23	16	18	25	39	23
13	21	15	16	22	30	20
14	26	19	20	28	29	26
15	27	19	22	31	45	28
16	28	22	24	27	36	31
17	29	23	24	28	41	29
18	30	24	25	30	36	32
19	28	21	23	29	44	30
20	23	17	19	24	41	24
Avg. #11-20± Std. Dev.	26 ± 3	20 ± 3	21 ± 3	27 ± 3	38 ± 5	27 ± 4

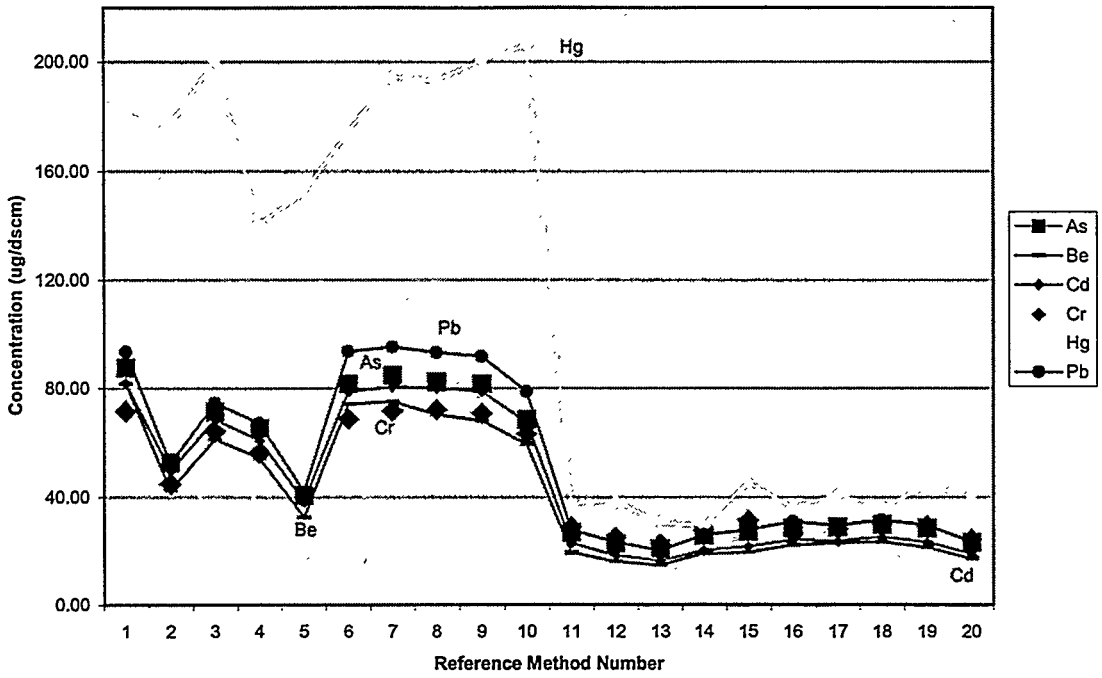

Figure 3-1. Average of Upstream and Downstream RM concentrations for each RM measurement period.

Based on the results of the 1996 multi-metal CEM test, we estimate that only about 20% of the injected mercury gets to the flue gas sampling locations, compared with about 33% of the other metals. Apparently, the remainder drops out of the gas stream or is captured by the wall materials of the secondary combustion chamber and the flue gas duct.. According to the RM results of this 1997 CEM test, more than 60% of the injected mercury made its way to the sampling locations, whereas the remaining metals still came in at about 33%. The RKIS staff speculates that the permanganate fraction might have been low last year, resulting in low Hg numbers. The poor matrix spike recoveries from the permanganate fractions in the 1996 tests support this hypothesis. During these 1997 tests, fresh permanganate was used. In Section 3.3.5, we compare trends in average CEM Hg results to trends in RM Hg results to try to understand this issue more fully.

The test was not completely "blind." That is, the CEM developers knew the target concentrations of the metals on each test day, but they did not know the RM results until after they had turned in their CEM data. In Section 3.3.5, we show the trends of the RM and average CEM results to examine whether the CEMs tracked the RM measurements and target concentrations. In general, we see most of the CEM results track the general trends in the RM results, so it seems unlikely the developers "corrected" their results to be closer to the target concentrations

3.3 Multi-metal CEM results

3.3.1 Method Detection Limit Requirements for CEMs

To be useful for compliance monitoring (the application of primary interest to the test sponsors), a multi-metal CEM must be capable of quantitative measurements of all six MACT rule elements at the emission limit concentrations or lower. Because concentrations equal to 10 times the Method Detection

Limit (MDL) (EPA, 1996d) are usually considered the least concentrations for which quantitative measurements can be performed, the MDL for each metal of concern must be equal to or less than one-tenth the emission limit for that metal. The MDL is defined as the concentration for which the method yields a signal-to-noise ratio of 3 to 1.

Based on the latest emission standards in the draft MACT rule, we estimate the required MDLs to be between 2 and 5 μg/dscm, as shown in Table 3-3. We also estimate the concentration at which the Relative Accuracy (RA) should be tested (essentially the draft emission standard for that one metal). This estimate will be used in Section 3.3.4 when we discuss Relative Accuracy.

No tests were conducted with metal concentrations as low as the estimated MDL requirements for MACT rule compliance monitoring. However, based on the results of the measurements at low (about 20 to 30 μg/dscm) and high (60 to 80 μg/dscm) concentrations, we can draw conclusions about which CEMs do NOT satisfy those MDL requirements. Since the MDLs are approximately one-tenth the lowest concentration that can be measured quantitatively, we can conclude that if a CEM could not detect the high concentrations of metals in this test, its MDLs are at least a factor of 20 to 40 too high.

3.3.2 CEM Measurement Capabilities

Table 3-4 summarizes the CEM measurement capabilities for the metals of concern during both the high and low concentration tests. The Navy/TJA ICP system is the only CEM that measured all six metals during this test. The DIAL ICP Mono system performed well, considering this was its first field test. Its performance was close to that of the Navy/TJA ICP, except that the DIAL system did not measure arsenic. The ability of the DIAL ICP system to detect and measure arsenic could probably be improved, but we do not see now how such an improved system would have advantages over the present Navy/TJA ICP system, which has already been shown to nearly meet the draft EPA PS.

The HEST+XRF combination, although not demonstrated as a real-time CEM in this test, was able to measure five of the six metals of concern. The HEST+XRF was not able to measure beryllium because of the physical characteristics of XRF. However, this is not a damning limitation because beryllium could be measured *in situ* using a simple LIBS system in combination with the HEST+XRF system.

Table 3-3. Volatility groups and metals, draft emission standards, suggested RA test concentrations, and estimated method detection limit (MDL) requirements for compliance monitoring applications of multi-metal CEMs.

Volatility Group (metals)	Draft Emission Standard[a] (μg/dscm)	Suggested Ra Test Concentration[b] (μg/dscm)	Estimated Mdl Requirement[c] (μg/dscm)
High Volatility Hg	40	40	4
Semi-volatile Cd and Pb	100	50	5
Low-volatility As, Be, and Cr	55	18	2

a. The draft emission standard applies to the sum of the concentrations of the metals in a volatility group.

b. The suggested RA test concentration for each metal is equal to the draft emission standard divided by the number of metals in the volatility group.

c. The estimated MDL requirement for each metal is equal to one-tenth the suggested RA test concentration for that metal.

Table 3-4. Average RM and CEM measurement results during 10 high concentration and 10 low concentration tests (μg/dscm).

Concentration[a]	Avg. RM Result	Navy/TJA ICP	HEST + XRF	DIAL ICP Mono	DIAL ICP HiRIS	DIAL LIBS	Sandia LIBS	PSI SIBS	MIT MIPS	Laser Diagn.
High (Target 75 μg/dscm)										
As (32 to 90 μg/dscm)	**72**	40	59	—	—	—	—	—	—	—
Be (26 to 83 μg/dscm)	**62**	47		44	16	47	163	—	56	6
Cr (34 to 78 μg/dscm)	**62**	33	43	38	—	68	196	125	52	14
Cd (31 to 86 μg/dscm)	**69**	44	70	53	65	92	270	—	—	1
Pb (34 to 101 μg/dscm)	**78**	38	58	76	—	110	—	25	80	—
Hg (104 to 226 μg/dscm)	**182**	23	111	146	—	—	—	—	—	—
Low (Target 15 μg/dscm)										
As (16 to 33 μg/dscm)	**26**	14	19		—	—	—	—	—	—
Be (11 to 26 μg/dscm)	**20**	14		13	10	16	85	—	21	6
Cr (17 to 33 μg/dscm)	**27**	15	17	9	—	29	70	58	18	18
Cd (13 to 28 μg/dscm)	**21**	11	27	8	—	31	77	—	—	0
Pb (15 to 35 μg/dscm)	**27**	12	17	20	—	33	—	9	19	—
Hg (25 to 53 μg/dscm)	**38**	11	18	16	—	—	—	—	—	—

a. The concentrations in parentheses indicate the range of metal concentrations in the gas stream as measured by the RM.

The DIAL ICP HiRIS measured Be and Cd in the high concentration tests, and only Be in the low concentration tests.

Laser Diagnostics used its proprietary software to process spectrometric data from the Sandia LIBS instrument. Consequently, the Laser Diagnostics MDLs cannot be better than the Sandia MDLs. For the high concentration test, Laser Diagnostics reported cadmium at 1 μg/dscm. This is well below the Sandia MDL for Cd, and therefore should more properly be reported as a non-detect. The Laser Diagnostics results for Be, reported at 6 μg/dscm for both the high and low concentration tests, are also likely less than the Sandia MDL for Be, and are therefore not meaningful. The same observation is also applicable to the Laser Diagnostics relative accuracies presented in Table 3-6.

Both LIBS systems measured Cd, but neither was able to measure As, even during the high concentration tests. Resolution may be a problem, but mostly it appears neither system had sufficient detection power for As. The other CEM techniques did not measure between two and four of the six metals, even at concentrations near 75 μg/dscm. For the two LIBS systems, the inability to measure As resulted in part from a spectrometer resolution limitation, a near coincidence between the strongest arsenic and cadmium emission lines that are amenable to fiber optic transmission. The ICP systems don't use optical fiber and avoid this interference by using a vacuum spectrometer to measure in the UV. We are not aware of any inexpensive remedies for the *in situ* techniques that use optical fiber to transmit the emission signal. Therefore, this may be an important limitation for *in situ* LIBS.

The PSI SIBS system was configured to measure Cr and Pb only. Because the PSI system relies on fiber optic cables to transmit the emission signals, and because of the near coincidence of the As and Cd emission lines that are amenable to fiber optic transmission, it will be subject to the same spectral interference for the As and Cd emission as discussed immediately above. As discussed in Section 3.3.3, both the PSI and DIAL LIBS developers believe they can overcome this problem by using very short lengths of UV-transmissive fiber (transmissive for wavelengths as low as190 nm).

Even with a fiber transmissive to 190 nm, measurement of mercury and arsenic will continue to be an issue. Compared with other elements, mercury and arsenic have weak atomic emission lines. Mercury has a weak ionic emission line at 194.2 nm, but it is not known if the SIBS system excites this spectrum. The neutral mercury emission line at 184 nm is unattainable with fiber optics. Arsenic has a line at 193.8 nm and another at 189 nm. Standard handbooks show the arsenic line at 189 nm is a factor of 100 less detectable than the cadmium emission line at 226 nm. Such basic characteristics of the atomic emission spectra of the elements limit the ability of all atomic emission spectroscopy techniques to measure mercury and arsenic at low concentrations.

At best, using a very short UV-transmissive fiber optic, a perfectly tuned system might be able to measure arsenic and mercury at concentrations 50 times higher than cadmium. Given current detection limits of 1 to 10 μg/dscm for cadmium, this means that these fiber-optic based systems will not be able to detect less than 50 to 500 μg/dscm of arsenic and mercury. Referring back to Table 3-3, which shows required MDL for arsenic and cadmium as 2 and 4 μg/dscm, respectively, it appears unlikely that systems using optical fibers will be able to satisfy MDL requirements.

The data from these tests, combined with the above discussion on the relative strengths of atomic emission lines, lead us to believe that the *in situ* LIBS and SIBS techniques will not be capable of measuring As and Hg at the low concentrations that are of concern for MACT rule compliance monitoring. In Chapter 4, however, we present some possibilities for improving the MDLs of the LIBS and SIBS systems.

3.3.3 Estimated Method Detection Limits

Table 3-5 summarizes the developers' estimates of method detection limits for each of the six test metals, based on field test results and laboratory data. Using the definition of method detection limits (EPA, 1996b), quantitative measurements can be made at concentrations equal to or greater than 10 times the MDL.

All developers do not use the same method to estimate MDLs. Hence, some caution is required when comparing MDLs reported by different persons.

No MDL estimates are available for the LIBS self-calibration procedure tested by Laser Diagnostics. The MDL depends upon the analysis method as well as on the instrumentation. Therefore, although Laser Diagnostics used spectroscopic data obtained with the Sandia LIBS instrument, we do not know if Laser Diagnostics achieved better or worse estimated MDLs than the Sandia LIBS instrument and method.

The detection limits quoted for the HEST+XRF method assume dilution air is used to cool the sample gas stream. If the sample gas is already at or below 300°C, these detection limits could be divided by at least a factor of two.

According to the developers, the following improvements can improve or have already improved detection capability since this test.

Table 3-5. Developers' estimates of method detection limits (μg/dscm). Not all MDLs have been demonstrated in combustion flue gas. Hg and As, in particular, need validation, and some are inconsistent with these test results. (N/A = Not Available, Not Applic. = Not Applicable)

Metal CEM Technology	As	Be	Cr	Cd	Pb	Hg
Navy/TJA ICP	8	0.1	0.5	0.25	2.5	10
HEST+XRF[a]	0.06 (0.2)	Not Applic.	0.2 (0.5)	0.6 (2.0)	0.2 (0.5)	0.2 (0.4)
DIAL ICP Mono and HiRIS	N/A[b]	0.6	1.5	4.5	6	21
DIAL LIBS[c]	130	0.3	1	8	14	140
Sandia LIBS[d]	400	2	5	5	20	80
PSI SIBS	N/A	N/A	15	N/A	15	N/A
MIT MIPS[e]	N/A	3 or 1	3 or 1	N/A	3 or 1	N/A
Laser Diagnostics	Not Applic.	Not Applic.	Not Applic.	Not Applic.	Not Applic.	Not Applic.

a. CES provided two detection limit estimates. The first number is for a one-hour sample; the second is for a 6.5-minute sample

b. The laboratory detection limit for As is approximately 50 μg/dscm. However this value has not been verified in the field.

c. The DIAL LIBS MDL estimates provided in μg/acm in Appendix E of this report were converted to μg/dscm using the approximate temperature and moisture observed in this test (conversion factor of 1.7).

d. The Sandia MDL estimates for As, Pb, and Hg, are based on new experiments conducted after the September 1997 EPA/DOE test.

e. For Be, Cr, and Pb, the MIT MIPS detection limit is estimated at 3 μg/dscm for 1 minute integration time, or 1 μg/dscm for a 10 minute integration time.

The PSI developers believe that, because their SIBS system provides high discharge energies with resulting strong signal-to-noise, and based on preliminary laboratory testing for other metals, future prototypes will be able to measure As, Cd, Be, and Hg at required MDLs. They believe they can overcome the fiber optic limitations by using UV-transmissive materials and minimizing cable lengths to access atomic emission lines in the 190–250 nm range. They would also evaluate using an extractive sample to eliminate fiber optics, although they recognize the advantages of *in situ* measurements.

In the case of the MIT MIPS, the technology is still under development. The MIPS prototype uses two spectrometers, one commercial and one fabricated at MIT. The commercial spectrometer was used with an intensified diode array detector and was dedicated to beryllium measurement. The second spectrometer used two linear CCD array detectors, one dedicated to monitoring Cr, and the other dedicated to Pb. A personal computer was dedicated to each of these spectrometers for data acquisition and real-time display of the atomic emission signals. The developer is confident he can improve the ability to detect As, Cd, and Hg by increasing the plasma residence time of these metals and by improving the spectrometer.

Other suggestions from the developers are included in Table 3-6.

3.3.4 Relative Accuracy Comparisons

Table 3-7 summarizes the relative accuracy of the multi-metal CEMs. The relative accuracy is calculated according to the equations in Appendix I of this report.

Based on the results and discussion in Section 3.3.2, only the ICP and HEST+XRF systems, at this stage of development, can measure all six metals at the required concentration levels (assuming the HEST+XRF system is adapted to measure beryllium). Therefore, although we report relative accuracy for the other CEMs, extended discussion of those "other" relative accuracies is not relevant. The purpose of the RA comparison and this discussion is to speculate on the likelihood that the other CEM technologies can be improved to measure all six metals.

Referring back to Table 3-3, which estimates the concentration at which Relative Accuracy should be measured, we first evaluate which relative accuracy calculations are relevant to the EPA requirements. These concentrations are compared with average RM measurements, shown again in the second column of Table 3-7, and a notation is made in the third column whether this series of tests is at concentrations meeting relative accuracy requirements (i.e., is the average RM concentration greater than the emission limit?). We see that all relative accuracies are relevant except the Cd and Pb tests at low concentrations. Consequently, the low concentration Cd and Pb RA values are presented in parentheses.

Referring to Table 3-5 and examining the relative accuracy of the ICP and XRF systems, we see only one case (Pb at high concentrations as measured by DIAL ICP mono) where relative accuracy is 20% or less. From this, we deduce that current technology cannot achieve relative accuracies less than 20%.

Evaluation of relative accuracy results requires some caution. Referring back to Table 3-4, we see that for the high concentration tests, the average mercury RM result was 182 µg/dscm, while the Navy/TJA ICP, the HEST+XRF, and the DIAL ICP Mono measured 23, 111, and 146 µg/dscm, respectively. The corresponding relative accuracies were 96%, 53%, and 43%, however, giving the impression of roughly comparable performance, even though the HEST+XRF and DIAL ICP results were much closer to the RM result than the Navy/TJA ICP result. The reason is that relative accuracy depends on the number of data pairs employed in the calculation, and the HEST+XRF system did not collect data during the first day of testing. Therefore, although the HEST+XRF average measurement was very good,

Table 3-6. Developers' suggestions for improving method detection limits and authors' prognosis for meeting required MDLs.

CEM Technology	Suggested Improvement(s)	Prognosis for meeting MDL Requirements
Navy/TJA ICP	MDL satisfactory, except perhaps for Hg.	Good. All problems identified post-test contribute to signal loss. Reasonable to assume that the MDL for Hg will be improved.
HEST+XRF	Except for Be, the MDLs are satisfactory. Improved flow control, increased filter exposure area, installation of a continuous particulate matter sampler.	Good. Authors believe it will be relatively easy to add existing technology (LIBS) to accomplish the Be measurements.
DIAL ICP Mono and HiRIS	Change to axial viewing of plasma.	Good, based on Navy/TJA ICP performance.
DIAL LIBS	Optimize the experimental parameters for detecting As and Hg. A high-resolution spectrometer, a short UV optical fiber with optics developed by CVI Laser Corp. in collaboration with DIAL will also be used to improve the MDL of As and Hg.	Not sure it will solve MDL problem. See discussion in text above.
Sandia LIBS	New experiments for Pb at 405.98nm with very long delay times, similar to DIAL LIBS, markedly improved Pb MDL. Hg detection also significantly improved using extremely long delay.	Alternate emission lines and long delay times alone are not likely to solve As MDL problem. Estimated Hg and Pb MDLs have not been verified in the field. The authors believe LIBS will have to pre-concentrate the analytes (perhaps using extractive sampling) to meet required As and Hg MDLs.
PSI SIBS	Future prototypes will address additional metals and reduce MDLs by using UV-transmissive fiber optics, improved light collection, and increased spark frequency.	Not likely to meet MDL for Hg and As with this approach.
MIT MIPS	Improve MDL for As, Cd, and Hg by increasing the plasma residence time of these metals, along with spectrometer improvements	Open question
Laser Diagnostics	Use higher resolution spectrometer to increase S/N. Use long delay times for metals with low ionization potential and no ion emission (such as lead).	Not demonstrated to be quantitative.

Table 3-7. Relative Accuracy of each multi-metal CEM at high and low concentrations. Column 2 lists the average of the concentrations measured by the Reference Method (RM). Column 3 indicates whether the test concentration was greater than the draft EPA MACT emission limit as listed in Table 3-3. The low concentration for Cd and Pb was less than the emission limit and therefore the corresponding RA results were not appropriately determined (as indicated by parentheses).

Metal (Range of CEM Measured Concentration)	Avg. RM	Avg. RM > Emission Limit	Navy/TJA ICP	HEST +XRF	DIAL ICP Mono	DIAL ICP HiRIS	DIAL LIBS	Sandia LIBS	PSI SIBS	MIT MIPS	Laser Diagn.
High (Target 75 µg/dscm)											
As (32 to 90 µg/dscm)	72	Yes	57%	31%	—	—	—	—	—	—	—
Be (26 to 83 µg/dscm)	62	Yes	36%	—	38%	92%	49%	176%	—	N/A[a]	128%
Cr (34 to 78 µg/dscm)	62	Yes	56%	43%	64%	—	42%	253%	151%	39%	101%
Cd (31 to 86 µg/dscm)	69	Yes	49%	22%	40%	84%	67%	341%	—	—	ND
Pb (34 to 101 µg/dscm)	78	Yes	64%	47%	19%	—	66%	—	89%	28%	—
Hg (104 to 226 µg/dscm)	182	Yes	96%	53%	43%	—	—	—	—	—	—
Low (Target 15 µg/dscm)											
As (16 to 33 µg/dscm)	26	Yes	81%	39%	—	—	—	—	—	—	—
Be (11 to 26 µg/dscm)	20	Yes	51%	—	46%	55%	37%	367%	—	37%	91%
Cr (17 to 33 µg/dscm)	27	Yes	76%	46%	76%	—	19%	196%	163%	98%	65%
Cd (13 to 28 µg/dscm)	21	**No**	(86%)	(55%)	(84%)	—	(78%)	(290%)	—	—	(112%)
Pb (15 to 35 µg/dscm)	27	**No**	(103%)	(48%)	(45%)	—	(37%)	—	(82%)	(50%)	—
Hg (25 to 53 µg/dscm)	38	Close	94%	66%	96%	—	—	—	—	—	—

a. There was only one CEM and RM measurement pair in this data set. Relative accuracy is not defined for only one measurement pair.

the RA suffered because it was based on only 5 data pairs. The HEST+XRF relative accuracy would likely have been improved by about 20% if it had been based on 10 data pairs instead of 5. The RA for the DIAL Mono system included 8 data pairs out of the 10 that were potentially available.

Although RA values for the HEST+XRF system were mostly less than 50%, the HEST+XRF concentration results seemed to be biased low. Although the CES staff cannot confirm the causes of these differences, they believe it is due to uncertainties in the dilution ratio that was used. The HEST required dilution of the stack gas to reduce the temperature to accommodate the filters. The flow meter to quantify this dilution factor was damaged in the field, and they had to use a flow meter that measured close to its maximum scale value. Laboratory calibrations of this second flow meter after the test showed non-reproducible results. Small differences in this calibration would have a large effect on the dilution factor and could explain the low bias.

The DIAL ICP HiRIS produced relative accuracy results for only two of the metals at high concentrations: Be and Cd, with RA of 94% and 84%. At low concentration, only Be was measured, with a RA of 55%.

The DIAL LIBS relative accuracy appears as good as and in some cases better than, the ICP. However, since LIBS did not measure arsenic and mercury, it is unlikely that it will be used in the near future as a multi-metal CEM. The same is true for the Sandia LIBS.

The PSI SIBS produced an 80 to 90% relative accuracy for lead, somewhat higher than most of the other CEMs.

The MIT MIPS system showed good relative accuracy for the two metals that were measured: 28% to 98%. However, this technology did not demonstrate capability for monitoring the other metals.

The Sandia LIBS system showed the poorest relative accuracy of all the instruments tested. After the test, the Sandia team discovered a hardware failure that caused a calibration error, offsetting their results by a factor of approximately 2.6 for Cd, 1.8 for Cr, and 1.3 for Be. In addition, Sandia uses a single spectrometer to monitor all 4 spectral windows required to measure multi-metals. The spectrometer grating takes 1 to 2 minutes to move; hence, each spectral area is scanned only once during a one-hour reference method measurement. Thus, in addition to only 25% data availability, data is only taken once during the time period. If the flue gas concentrations were fluctuating, the Sandia system would have little chance to correctly measure the average concentrations.

The Laser Diagnostics analysis of the 10 RM data sets (RM #1 through RM #5 and RM #16 through RM #20) from the Sandia LIBS instrument yielded better relative accuracy results than Sandia reported. But, except for chromium at low concentrations, with a relative accuracy of 65%, the Laser Diagnostics relative accuracy results were much worse than provided by the other techniques, raising questions regarding the usefulness of this approach. Note that the high-concentrations for Be and Cd calculated by Laser Diagnostics were close to zero (6 and 1 μg/dscm respectively). Although these relative accuracies are about 100%, which doesn't seem too bad compared with other data, the measurements are a factor of 10 to 50 lower than the RM. The Laser Diagnostics final report describes what they believe to be the reason for this low bias.

The developers' suggestions for improving RA and the authors' prognosis regarding the likely success of those actions for meeting the RA requirement are included in Table 3-8.

Table 3-8. Developers' suggestions for improving RA and authors' prognosis for meeting required RA.

System	Suggested Improvement(s)	Prognosis for Meeting RA
Navy/TJA ICP	RA improved by QA/QC on hardware, e.g., solenoid valve seals in sample loop, and precise adjustment of pressure equalization in sample loop. RA also improved by changing CN interference correction.	Good. All problems identified post-test contribute to signal loss. Reasonable to assume that RA will be improved.
HEST+XRF	RA good: 22% to 53% at high concentrations.	Good. Might already be good enough.
DIAL ICP Mono & HiRIS	Change to axial viewing of plasma.	Good, based on Navy/TJA ICP performance.
DIAL LIBS	RA will be improved by improving the current on-site calibration methods and also by including a routine in data analysis to reject poor quality data.	Secondary issue until MDL demonstrated.
Sandia LIBS	N/A	Secondary issue until MDL demonstrated.
PSI SIBS	RA can be improved with an in-situ calibration method.	Secondary issue until MDL demonstrated.
MIT MIPS	N/A	Secondary issue until MDL demonstrated.
Laser Diagnostics	Use spectrometer designed to measure out to 750 nm. Acquire nitrogen spectra simultaneous (or nearly so) to metal spectra acquisition.	Not sure it will be quantitative.

3.3.5 Trends in Average CEM Data compared with RM Trends

The RM and average CEM data were examined as a function of time to determine if the CEM results tracked the RM results. Figure 3-2 shows average chromium concentrations measured by the CEMs and the RM for each of the first 10 RM test periods (Day #1 and #2 of testing). Also, during the first day of testing, the RM results showed more variation than expected (RM #1 through RM #5). Figure 3-2 shows that none of the CEMs tracked the RM results, although the Navy/TJA, HEST+XRF, and the DIAL ICP Mono were close. The Sandia and PSI systems both measured too high for most of the tests, but showed similar trends for RM #7 through RM #10. As discussed in Section 3.3.4, the Sandia results were too high because of a hardware failure that made the SNL calibration incorrect by a factor of 1.8 for Cr and between 1.3 and 2.6 for the other metals. The behavior of the RM results obtained during the first two days of testing, i.e., considerable variation during Day #1 and less variation during Day #2, was confirmed by some of the CEMs. Of the five RM data points from Day #1, two data points were approximately 50% lower concentration than the others. This behavior was verified by four of the six CEMs that made measurements the first day, leading us to believe that the facility conditions actually changed this much during Day #1.

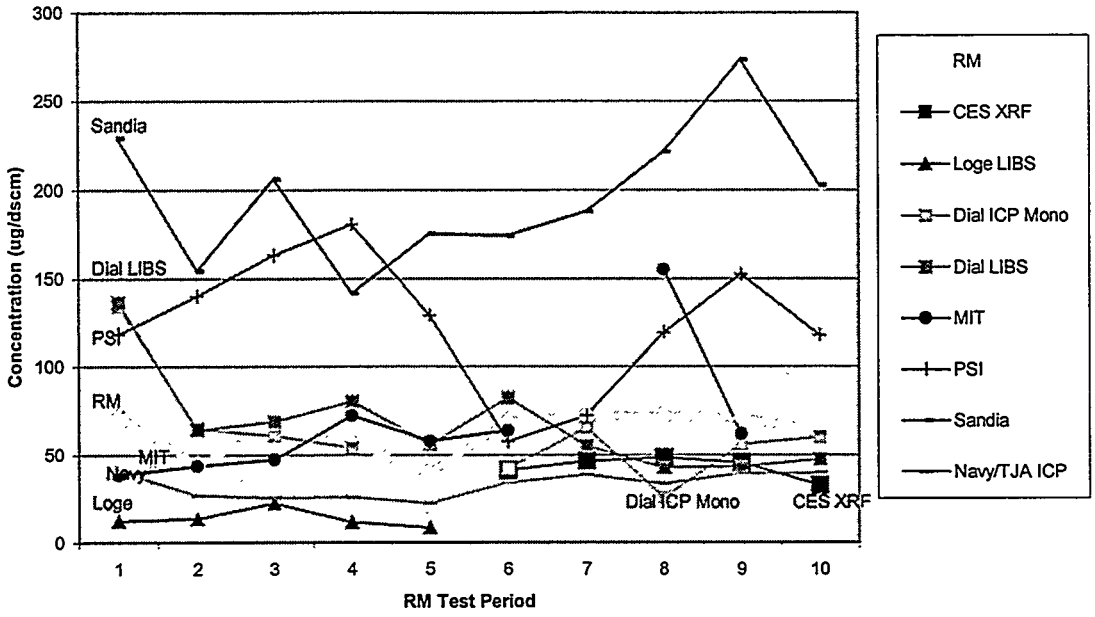

Figure 3-2. Average Cr concentrations vs. RM time periods, comparing trends in average CEM data to trends in RM data.

We can use the CEM data to help resolve questions surrounding mercury RM measurements. Figure 3-3 shows average mercury CEM results versus RM time period compared with (average) RM measurements. Only three CEMs (Navy/TJA ICP, HEST+XRF, and DIAL ICP Mono) reported mercury results. Of these, the HEST+XRF system did not report results on Day 1 (RM #1 through RM #5), and the DIAL ICP/Mono did not report results for RM #3 and RM #6.

Figure 3-3 shows trends in the Hg results for the first 10 RM measurement periods. Mercury is especially important because its high volatility makes it more difficult to capture in flue gas cleaning systems than the other regulated metals. Because of its volatility, it is also more challenging to extract and measure accurately. This is seen by looking at the Navy/TJA ICP mercury results. That system measured about 35 μg/dscm on average whereas the reference method measured about 180 μg/dscm. The relative accuracy of the Navy/TJA for these RMs is 96%. In addition, average Navy/TJA results were nearly constant from one RM time period to another, whereas the RM results varied considerably, from 145 μg/dscm to 205 μg/dscm.

The HEST+XRF mercury results shown in Figure 3-3 are also quite constant from one RM measurement period to another, although results are only available for RM #6 through RM #10, which in fact is more constant than RM #1 through RM #5. The HEST+XRF results were much more satisfactory than the Navy/TJA ICP results, averaging about 110 μg/dscm for RM #6 through RM #10. This produced a RA of 53%, where the RA calculation penalizes for only five data pairs instead of 10.

Finally, as seen in Figure 3-3, the DIAL ICP Mono mercury results varied considerably, both above and below the RM results. Oddly enough, even with the variability observed for these average CEM measurements, the DIAL ICP Mono result matched the RM result exactly during RM #10. The RA of the DIAL ICP Mono is 43%, where the RA calculation levies a small penalty for 8 instead of 10 data pairs.

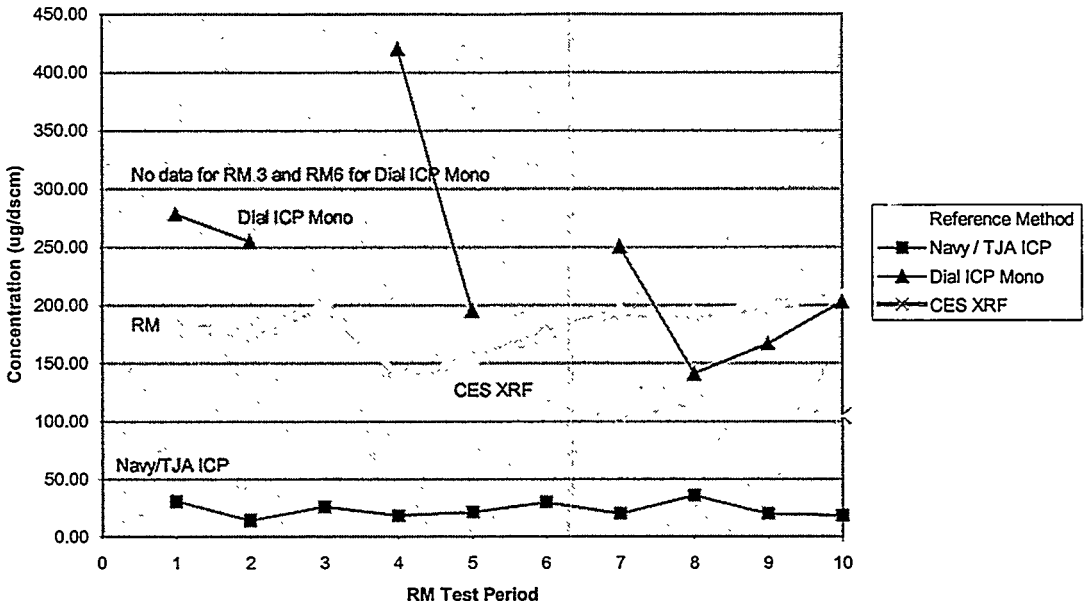

Figure 3-3. Average Hg concentrations vs. RM measurement periods, comparing trends in average CEM data to trends in RM data.

Two of the three CEMs reported higher Hg concentrations on test Days #1 and #2 than they did for the other metals. This is consistent with the RM results. However, none of the CEMs reported the same Hg concentrations as the RMs, nor did their Day #1 mercury results track Day #1 RM results for mercury. Based on these results, additional testing with Hg would be useful to isolate the cause of the differences between the RM results and the CEM results. Such testing would also quantify the best Hg CEM performance and thus help EPA develop new regulations for Hg compliance monitoring.

3.3.6 Effect on Relative Accuracy of Using Average vs. Up/Downstream Reference Method Measurements

The seven systems tested required a 40-foot-long duct to accommodate all the sample probes with adequate spacing to reduce the chances for interference. Because the duct was so long, two separate RM measurements were made, one upstream of all the multi-metal CEMs, and one downstream, just before the last three multi-metal CEMs.

The question then arose as to which CEMs should be assigned to which RM measurement. As discussed in Section 3.2.1 of this report, a statistical analysis showed no significant difference (at the 95% confidence level) between upstream and downstream RM results. Therefore, all RA calculations in this report were performed using the *average* of the upstream and downstream RM results.

To quantify how this decision affected the RAs, we also calculated RA for each CEM and each metal using the upstream RM results and the downstream RM results. How much the RA values calculated using upstream and downstream RM results differed, in percent, from the RA values that were obtained when calculated using the average of the upstream and downstream RM results is shown in Table 3-9. Most of the differences are in the range of 1 to 3%. A few differences were 5% or greater, however, such small differences had no impact on the major conclusions of this report. Those conclusions concerned which CEMs measured all 6 metals and demonstrated RA <20%. Note that the cases where the effect was largest were those where the RA was large (e.g., 9% effect for a PSI SIBS RA of 151%).

Table 3-9. Effect of using upstream or downstream Reference Method measurements on relative accuracy calculations. Results expressed as absolute value of increase (+) or decrease (-) in relative accuracy using Upstream/Downstream reference method data.

Concentration	Navy/TJA ICP	HEST +XRF	DIAL ICP Mono	DIAL ICP HiRIS	DIAL LIBS	Sandia LIBS	PSI SIBS	MIT MIPS	Laser Diagn.
High (Target 75 µg/dscm)									
As (32 to 90 µg/dscm)	-1%/+2%	-1%/+2%	—	—	—	—	—	—	—
Be (26 to 83 µg/dscm)	-2%/+1%	—	-1%/+2%	-3%/+3%	-2%/+3%	-8%/+8%		N/A[a]	-4%/+4%
Cr (34 to 78 µg/dscm)	-3%/+4%	-3%/+3%	-4%/+5%	—	-3%/+2%	-8%/+8%	-9%/+9%	-2%/+3%	-5%/+6%
Cd (31 to 86 µg/dscm)	-2%/+1%	-1%/0%	0%/0%	-6%/+6%	-2%/+3%	-9%/+9%	—	—	-3%/+3%
Pb (34 to 101 µg/dscm)	-2%/+4%	-2%/+3%	0%/0%	—	-2%/+2%	—	-3%/+2%	-1%/+1%	—
Hg (104 to 226 µg/dscm)	-2%/+2%	0%/0%	—	—	—	—	—	—	—
Low (Target 15 µg/dscm)									
As (16 to 33 µg/dscm)	-3%/+2%	-1%/+2%	—	—	—	—	—	—	—
Be (11 to 26 µg/dscm)	-2%/+1%	—	-1%/+1%	-1%/+2%	-1%/+1%	-9%/+9%	—	-1%/+1%	-1%/+1%
Cr (17 to 33 µg/dscm)	-3%/+2%	-1%/+2%	-3%/+2%	—	0%/+1%	-7%/+7%	-6%/+6%	-3%/+3%	-1%/+2%
Cd (13 to 28 µg/dscm)	-3%/+2%	-1%/+2%	+2%/+8%	—	-2%/+2%	-9%/+9%	—	—	-3%/+2%
Pb (15 to 35 µg/dscm)	-3%/+2%	-1%/+1%	-1%/+2%	—	-1%/+1%	—	-2%/+2%	-1%/+1%	—
Hg (25 to 53 µg/dscm)	-3%/+2%	-1%/+3%	—	—	—	—	—	—	—

a. The MIT MIPS system provided Be CEM measurements for only one RM measurement period. Relative accuracy is not defined for only a single pair of CEM and RM data points.

3.3.7 Variability of CEM Results (Ability to Produce Data Useful for Real-Time Compliance Monitoring)

So far, we have examined relative accuracy, which compares only *average* CEM results to the results of Reference Method measurements. It is also useful to appreciate the discrete nature of the CEM measurements. Each relative accuracy comparison represents the average of tens or hundreds of data points. When the CEM data are plotted as concentration versus time, we can see how the discrete data points vary during the averaging time.

Even though data variability is not addressed in the draft EPA MACT rule CEM performance specifications, it will be important if CEM measurement results are to be used for establishing regulatory compliance or for process control. Because of the lack of methods to characterize short term variations in metal concentrations in the duct or stack, we do not know how much of the variation displayed by the CEM results is due to the instrument versus how much is characteristic of the gas stream being measured. Figure 3-4 shows real-time chromium concentration results for 6 of the 7 CEMs tested,[b] as a function of time, for the first test day. To equitably compare the variability of the results from the different CEMs, we adopted 90-seconds as a standard data averaging and reporting period and re-averaged the individual data points from each of the CEMs to periods of that length.

Figure 3-4 shows the variability is considerably different for each instrument. In addition to reporting concentrations several times larger than the results of the reference method measurements, the

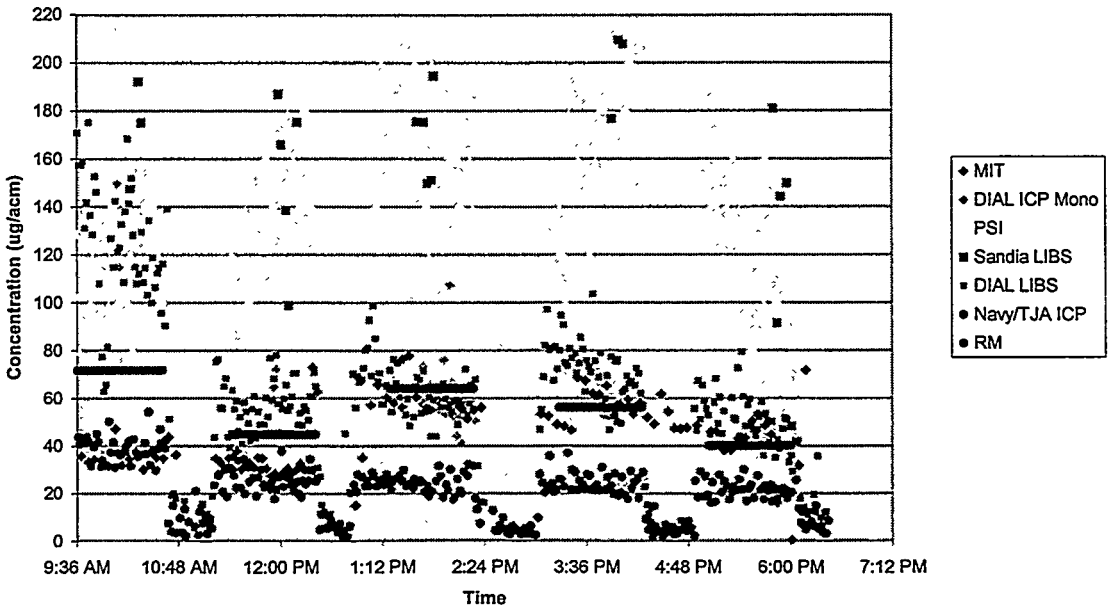

Figure 3-4A. 9-22-98. Real-time chromium concentrations for 6 of 7 CEMs tested as function of time during first day of testing, compared with RM results (blue bars). For comparison, all CEM data were converted to dry standard cubic meters, and averaged over 60 to 90 second time intervals.

b. The DIAL ICP HiRIS CEM did not report data for Cr. Laser Diagnostics simply treated the SNL real-time data in an alternative manner, so the variation of the Laser Diagnostics results was the same as that of the SNL results.

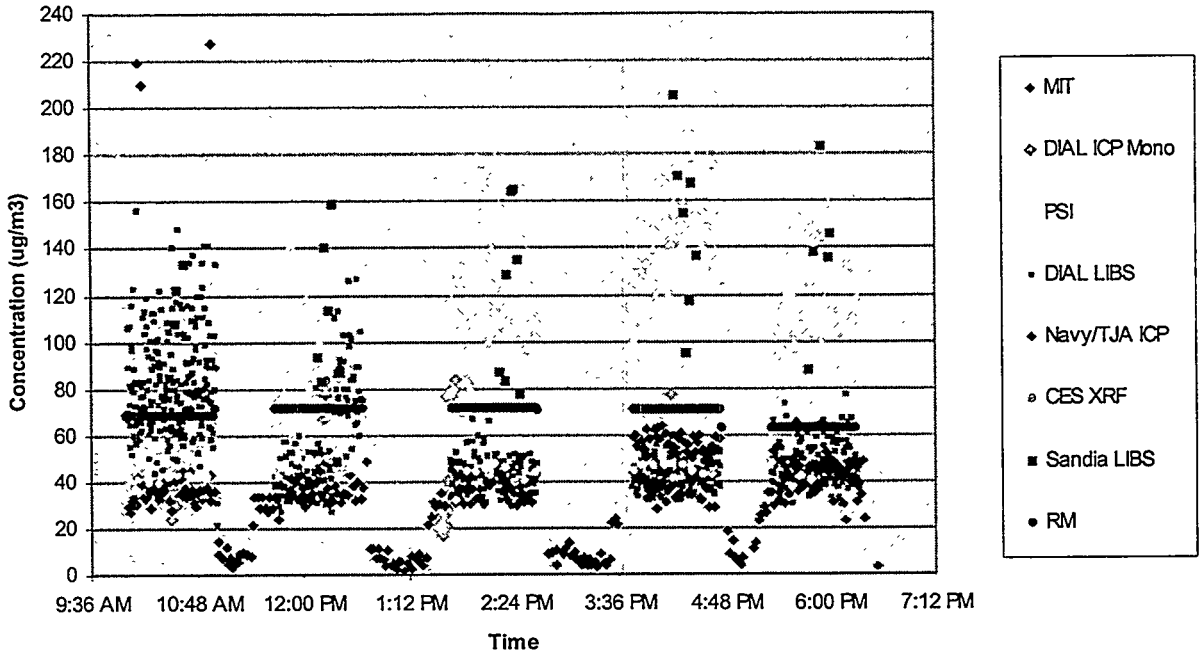

Figure 3-4B. 9-23-98. Real-time chromium concentrations for 6 of 7 CEMs tested as function of time during second day of testing, compared with RM results (blue bars). For comparison, all CEM data were converted to dry standard cubic meters, and averaged over 60 to 90 second time intervals.

Sandia LIBS and PSI SIBS systems showed the most variability in real-time data. The Dial LIBS results also had a more variability than those of the other CEMs. The Navy/TJA, Dial ICP, and MIT MIPS results had the smallest real-time variability.

The standard deviation of the real-time data during each RM measurement period provides a measure of variability. Figure 3-5 shows standard deviations for CEM data taken on the first test day, September 22 (RM #1 through RM #5). The average of the standard deviations for the CEM data acquired during those RM measurement periods is shown as an error bar on the average concentration for each CEM. The yellow line in Figure 3-5 is the average concentration measured from the five RM measurements made that day.

As can be seen from Figures 3-5 and 3-6, 90-second-averaged data from the CEMs would likely not be very useful for process control or compliance—assuming catastrophic events such as baghouse failure are monitored using other rapid-response instruments such as pressure gauges. It appears that the characteristic time for changes in emissions in this incinerator is longer than the 90-second averaging time, perhaps on the order of many minutes. Future data from PM and multi-metal CEMs should be able to substantiate this hypothesis.

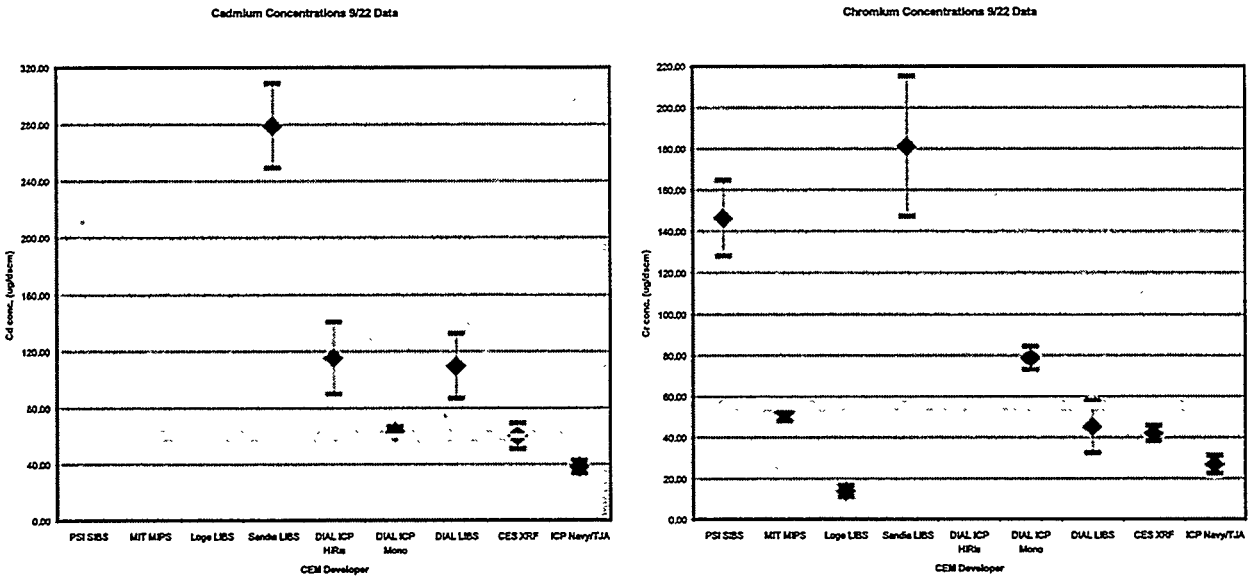

Figure 3-5A. Average cadmium and chromium concentrations measured by each of the CEMs, compared with the average of five reference method measurements taken on Test Day #1. Error bars on the CEM data points indicate average of the standard deviations of the CEM results during each of the reference method time periods.

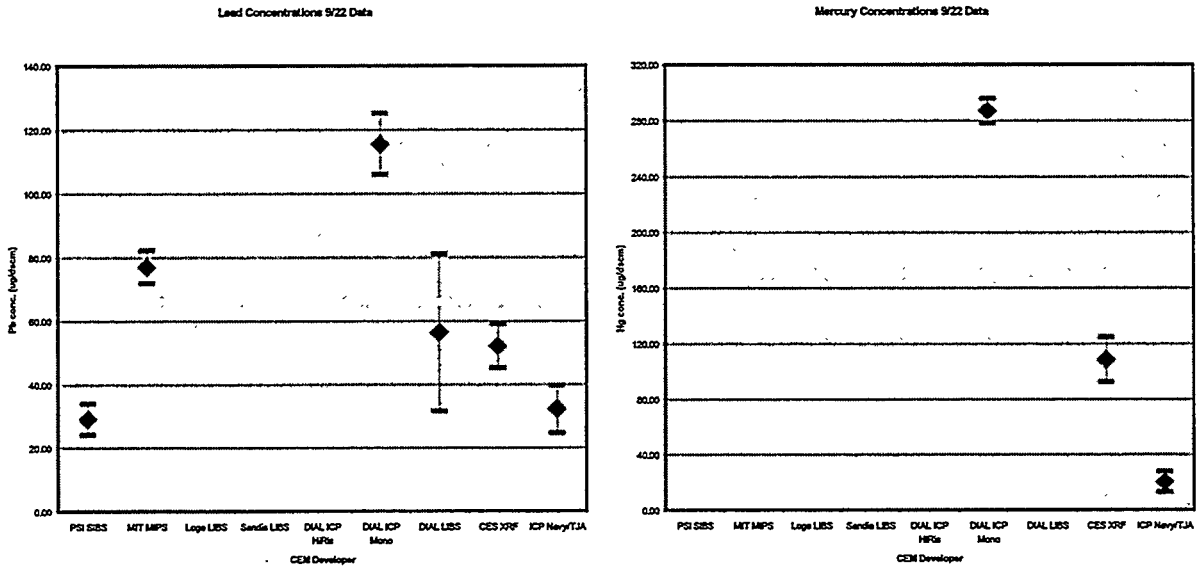

Figure 3-5B. Average lead and mercury concentrations measured by each of the CEMs, compared with the average of five reference method measurements taken on Test Day #1. Error bars on the CEM data points indicate average of the standard deviations of the CEM results during each of the reference method time periods.

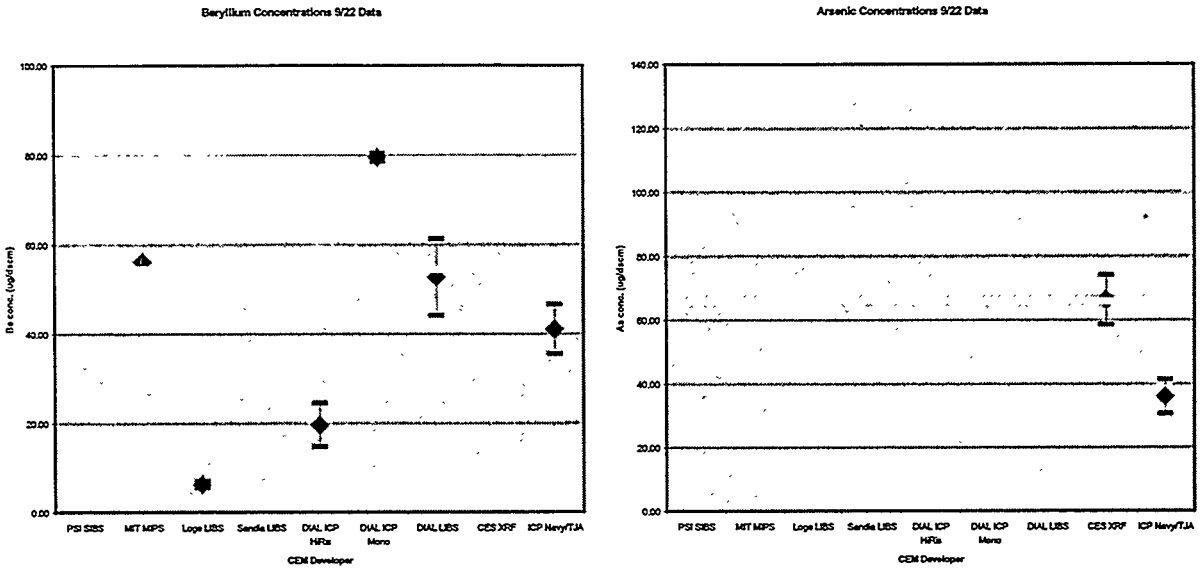

Figure 3-5C. Average arsenic and beryllium concentrations measured by each of the CEMs, compared with the average of five reference method measurements taken on Test Day #1. Error bars on the CEM data points indicate average of the standard deviations of the CEM results during each of the reference method time periods.

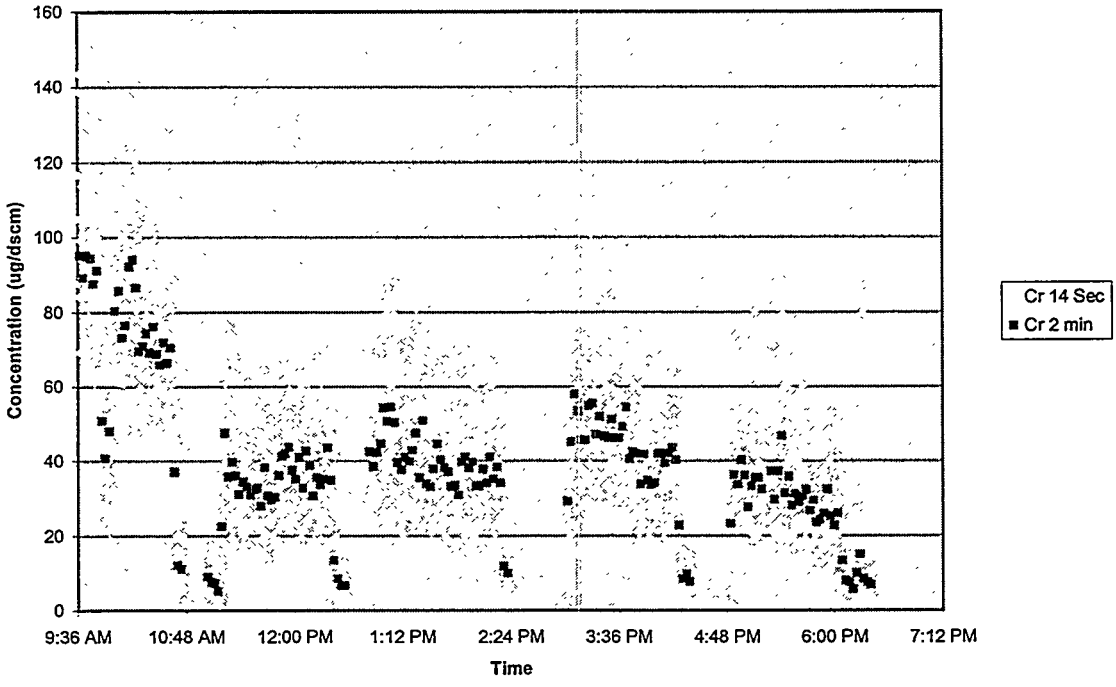

Figure 3-6. Chromium concentration as measured by Dial LIBS, data as provided to the Test Committee the day after the test (approximately 14 seconds per data point)(yellow data points) and same data re-averaged to 2 minutes (red data points).

We also evaluated the effect of time averaging on the variability of the CEM data. Figure 3-6 shows DIAL LIBS data as provided to the Test Committee the day after the test (averaged over approximately 14 seconds per data point), and the same data re-averaged to 2-minute time periods. This figure shows that data variability is greatly reduced if real-time CEM data points are averaged over several minutes, instead of seconds. Data averaging times are very important if the data are to be used for real-time process control or compliance assurance.

We conclude two things from our consideration of the variability of the CEM results. First, only a certain (so far undefined) amount of variability can be tolerated if the data are to be used for process control or compliance assurance. Second, since data variability decreases with longer averaging times, more field data is needed to determine how real-time data should be used for process control or compliance assurance. The current draft MACT rule performance specification requires 1-minute updates to one-hour rolling averages. Based on data from this test, a 1-minute update would probably not provide useful information. A two- or five-minute update would be more useful.

3.3.8 Other Metals Detected

Several of the CEM technologies reported measurement results for additional metals beyond the six MACT rule metals that were the focus of this test. The technologies and additional metals reported are shown in Table 3-10. No assessment of accuracy was performed for these additional metals.

Table 3-10. Additional metals reported by CEMs during this test.

CEM Technology	Other Metals Reported (not quantified)
Navy/TJA ICP	Ag, Ba, Co, Mn, Ni, Sb, Se, Tl
CES HEST+XRF	Ti, Fe, Ni, Cu, Zn, Se, Sr, Y, Ag, Sn, Sb
DIAL LIBS	Fe, Si, Ca, Mn
Sandia LIBS	Sb, Fe, Si, Y

4. CONCLUSIONS AND RECOMMENDATIONS

This test provided performance data that will be used to assess the current state of the art in multi-metal CEMs. This data, and the analyses presented in this report, support the following conclusions and recommendations:

- No multi-metal CEM tested here met the EPA Performance Specification in the Draft MACT rule, which requires measuring all 6 metals (at concentrations near the emission standard) with Relative Accuracy ≤20%.

- Based upon demonstrated capability to measure all six MACT metals at or near the concentrations tested here, with RA close to 20%, none of the multi-metal CEMs tested here appear ready for long-term testing.

- The Navy/TJA ICP system can measure all 6 metals, with RA between 35% and 100%.

- The CES HEST+XRF combination, although it did not analyze in real-time, and the DIAL ICP system most likely can be adapted to measure all six metals. The measured RAs for these systems were between 20% and 95%. The measurement problems that were encountered would likely not have occurred if a routine validation procedure had been employed. This is planned for future prototypes.

- This test did not show that Relative Accuracies ≤20% are achievable with current technology. Realistic, achievable performance specifications for parameters such as relative accuracy and "up-time availability" will accelerate the availability, acceptance, and use of CEMs, thus supporting EPA goals for compliance assurance.

- The *in situ* LIBS and SIBS configurations tested here used optical fiber to transmit atomic emission from the point of excitation to the spectrometric measurement equipment. Because of that, the LIBS and SIBS systems were not able to take advantage of some of the strongest atomic emission lines for As and Hg. In addition, for the wavelengths transmitted by the optical fiber, those instruments suffered from insufficient spectral resolution and spectral interference that precluded simultaneous measurement of As and Cd at detection limits required for compliance monitoring. However, the LIBS and SIBS systems could be adapted to measure extracted and/or concentrated sample material, either in a manner similar to the XRF analyzing the sample collected by the HEST, or in real-time using some other sample extraction and/or concentration means.

- Additional testing with Hg would be useful to identify the cause of the discrepancies between the RM results and the CEM results. Such testing would also quantify the best Hg CEM performance. This would help EPA establish new regulations for Hg compliance monitoring. Because sampling and measuring Hg is a recurring problem for multi-metal CEMs as well as Hg CEMs, we recommend that developers participate in a 1998 DOE-sponsored workshop to solve these and other common CEM measurement issues.

- For reliable comparison of the detection capabilities of different multi-metal CEMs, a single common method must be used for estimation of Method Detection Limits (MDLs). The developers that participated in this test did not use a single common method.

- Short term variations of the multi-metal CEM results were significant. How much variation is caused by real variations in the flue gas and how much is due to the CEMs should be addressed in future tests. The characteristic times of flue gas variations should also be compared with the characteristic times of the CEM data acquisition and analysis systems.

- The short term data variations were considerably different for the different CEMS. In addition to producing results that differed most from the RM results, the Sandia LIBS and PSI SIBS systems had the largest data variations. The DIAL LIBS system had moderate variations; the Navy/TJA ICP, DIAL ICP, and MIT MIPS systems had the smallest data variations.

- Short term variations in the CEM results are greatly reduced if real-time data points are averaged over several minutes, instead of seconds. The CEM data variations and data averaging times are important if the data are to be used for real-time process control or compliance. Additional field data and experience are needed to determine how real-time data should be used for process control and compliance assurance. The current draft MACT rule performance specification requires 1-minute updates to one-hour rolling averages. Based on data from this test, a 1-minute update would probably not provide useful information. A two to five minute update would be more useful.

- "Batch" monitoring techniques that pre-concentrate sample material for subsequent analysis, as in the CES HEST+XRF system, for example, may be more capable and less expensive to operate and maintain than a real-time CEM. Another form of pre-concentrating CEM could sample continuously onto a mechanically advanced filter paper tape; the contents of the tape could be analyzed periodically or continuously with time resolutions of 5 to 10 minutes.

- Historically, interference problems have surfaced during CEM field testing. This was true in this test as well. The measurement environment was much more challenging to the CEMs (due to real combustion flue gas and the simultaneous presence of all the metals) than the controlled laboratory experiments. Interferences should be evaluated in laboratory experiments early in the development cycle of any new CEM technology.

- It may be possible to improve relative accuracies by performing instrument calibrations in the field at stack conditions. Field calibration is not straightforward for a multi-metal CEM because calibration standards are not readily available. In this test, only one of the CEMs (the MIT MIPS system) performed a calibration at stack conditions. The Navy/TJA ICP system routinely performs field calibrations, but not at stack conditions.

- If a new multi-metal CEM calibration procedure were developed, it could spawn a new validation procedure that would allow assessment of RA without using EPA Reference Method 29. This would reduce the uncertainty in RA assessments caused by RM uncertainties and might help establish a more achievable RA performance requirement.

5. REFERENCES

EPA (U.S. Environmental Protection Agency), 1994. "Test Methods for Evaluating Solid Waste: Physical/Chemical Methods," EPA SW-846, Method 0060 "Determination of Metals in Stack Emissions," 3rd edition, Revision 2, September 1994.

EPA (U.S. Environmental Protection Agency), 1996. Proposed Rule "Hazardous Waste Combustors; Maximum Achievable Control Technologies Performance Standards," in Federal Register, Volume 61, pp. 17353–17536, April 19, 1996.

EPA (U.S. Environmental Protection Agency), 1996b. Revised Standards for Hazardous Waste Combustors, Performance Specification 10—Specifications and test procedures for multi-metals continuous monitoring systems in stationary sources. 61 FR 17499–17502, April 19, 1996.

EPA (U.S. Environmental Protection Agency), 1996c. "Standards for the Management of Specific Hazardous Wastes and Specific Types of Hazardous Waste Management Facilities,—Hazardous Waste Burned in Boilers and Industrial Furnaces," 40 CFR 266, Subpart H, U.S. Government Printing Office, Washington, DC, July 1996.

EPA (U.S. Environmental Protection Agency), 1996d. "Test Methods for Evaluating Solid Waste Physical/Chemical Methods," SW-846, 3rd edition, Update III, Chapter One, Quality Control, Page 1–25, December 1996.

Ghorishi, S. B., W. E. Wentworth, Jr., C. G. Goldman, and L. R. Waterland, "Testing the Performance of Real-Time Incinerator Emission Monitors," EPA-600/R-97-024 (NTIS PB97-142871), National Risk Management Research Laboratory, U.S. EPA, Cincinnati, Ohio, March 1997.

Haas, W. J. Jr., N. B. French, C. H. Brown, D. B. Burns, P. M. Lemieux, S. J. Priebe, J. V. Ryan, and L. R. Waterland, 1997, "Performance Testing of Multi-Metal Continuous Emissions Monitors," U.S. Department of Energy Research and Development Report # IS-5128, Ames Laboratory, Iowa State University, Ames, IA, November 1997.

Appendix A

Statistical Analysis of Upstream/Downstream Reference Method Data

WESTINGHOUSE SAVANNAH RIVER COMPANY
Savannah River Technology Center

SRT-SCS-97041
(Rev. 1)

January 6, 1998

To: D. B. Burns, 773-42A

From: S. P. Harris, 773-42A

CC: R. C. Tuckfield, 773-42A
E. P. Shine, 773-42A

Statistical Analysis of Combustion Emissions Using the SRM(U)

E.P. Shine, Technical Reviewer — 1-8-98 Date

R.C. Tuckfield, Manager(SCS) — 1/8/98 Date

Summary

An error in variables approach reveals that the down stream and up stream samples for combustion gases are essentially the same using the standard reference method(SRM) of analysis for trace metals(As, Be, Cd, Cr, Hg, Pb, Sb, Y).

The differences between down stream and up stream samples *did not* prove to be statistically significant at the 95% level. Therefore, no bias correction is warranted for these elements. However, the results for Fe seem problematic.

The percent standard error among the elements for the first two days(High Level) ranges between 4.2% to 8.9% and ranges between 3.3% to 5.3% for the last two days(Low Level).

The discrete SRM data will be used to calibrate and verify continuous monitors that were also run during the sampling campaign.

Data

The SRM method involves manual sampling and analysis methods using a sample of waste gas pulled through a filter followed by laboratory analysis of the substance in question. Gas samples have been collected at both up stream and down stream sampling locations for elemental analysis using the SRM for analysis of combustion gases. The up stream and down stream analysis results have been supplied in a time matched format for statistical analysis. The data were supplied to the Statistical Consulting Section(SCS) as the time matched pairs in an Excel spreadsheet format(Appendix 1). The differences between the up stream and down stream data, by time, are shown in Appendix 2 while the averages are shown in Appendix 3.

The samples have been analyzed for the following elements As, Be, Cd, Cr, Fe, Hg, Pb, Sb and Y. Specifically, presented for statistical analysis were four days of data with five samples analyzed each day using the SRM for both up-stream and down stream flows. The first two days were targeted at a high level(80 μg) for the combustion elements, excluding Fe, Hg and Y, and the final two days were targeted at a low level(20 μg). The result was 20 time matched SRM pairs (10 at each level) that essentially cover the measurement range of the continuous emission monitors(CEM's).

Statistical Analysis

The data have been statistically analyzed for bias. In particular, statistical analysis would reveal if a bias correction must be applied down stream because of sampling and measurement bias. This possibly could result from different calibrations or flows resulting from the accumulation of metal-containing particulates on the duct walls.

Traditional linear regression methods using least squares, as documented in the report by ENTEC Cremer & Warner(1994), although appropriate for a wealth of applications, are not valid for this particular comparison. Both up stream and down stream monitoring procedures using the SRM have equal variance. In particular, one cannot be considered as a standard with negligible variance, for comparison with the other. Thus, an error in variables approach must be used.

One error in variables approach that is well founded and accepted is that from Mandel.[1] Consider the familiar straight line model:

[1] Mandel, J.(1984). *Fitting Straight Lines When Both Variables are Subject to Error*. Journal of Quality Technology, Vol. 16, No. 1, January 1984.

$y_i = \alpha + \beta x_i$ where i=1 to N

where y_i is the measured up stream concentration for a particular element and x_i is the measured down steam concentration. The run number is designated as i and N=20. The α and β are unknown constants to be estimated from the data.

The usual assumptions underlying the least squares fitting procedure are

1. The x values have no error.
2. The y values are subject to errors having zero mean and constant standard deviation. Also, assumed is that the errors are uncorrelated.

In practice, the usual textbook procedure is applied even when the assumptions are not strictly fulfilled. Many users feel that this is appropriate when the errors in x are small relative to the errors in y. However, for this combustion gas flow experiment, the error variance in the up stream data is expected to be the same as the error variance in the down stream data since the SRM is applied at both ends.

We assume, for the Mandel model, that the ratio of variance for the errors in x(σ_δ^2) to that of y(σ_ε^2) is unity. Also, we assume that the errors between x and y are uncorrelated,

$\lambda = \sigma_\varepsilon^2/\sigma_\delta^2 = 1$ and $\rho=0$.

Mandel shows that the conditions for applicability of ordinary least squares are $\phi = |\beta| / \sqrt{\lambda} << 1$ and also that $\rho=0$. Strict applicability of OLS requires that both $\phi= 0$ and $\rho=0$.

The Mandel procedure has been implemented by SCS in a Microsoft Excel, Ver. 7, spreadsheet. The methodology has been checked against the data in Mandel(1984) for accuracy.

The results for the combustion data test are given in Table 1. Most of the slope estimates, when compared to their standard errors, are not different from unity. The slope for Fe is significant(t=Estimate/Std. Error $\cong$ 2.0) using a one tailed test with 95% confidence. A one-tailed test was applied because we wanted to test the hypothesis that there was no difference in gas particulate flow versus the alternative that the particulate flow was less down stream than up stream.

The least squares estimates, for all elements, are also presented for thoroughness. The predicted mean values, and their standard errors, for the Mandel model are also shown in Table 1. The fit of the Mandel model to the SRM data is shown in Plot 1.

Box-and-Whisker Plots for the average of the up stream and down stream data are shown in Plot 2. Each Box-and-Whisker plot displays the minimum and maximum values, the 25th and 75th percentiles. The box is aligned vertically and encloses the interquartile range(the 25th to 75th percentile). The upper part of the box represents the 75th percentile while the lower part represents the 25th percentile. The median(50th percentile) is at the midpoint of the box. Extreme points, indicated by small boxes, □'s, or +'s, are shown extending from the box.

The next stage of analysis considers:

$y_i = \alpha + x_i$ where i=1 to N, and α is a constant to be estimated,

More specifically

$\delta = y_i - x_i = \alpha$, i=1 to N.

The mean differences, δ's, paired within time & day, are shown in Table 3. In addition, the standard errors are given and also the resulting 95% confidence limits. None of the differences are significantly different from zero. However, the data for Fe seems biased as previously determined. The combined data across all four days were examined and also the data for the first two days considered separately from the last two days. Box-and-Whisker Plots for the differences are shown in Plot 3. The first two days, run at high levels, seem to have greater variability than the last two days that were run at low levels.

The percentage differences between up stream and down stream were also calculated(Table 3) with the same conclusions obtained. The average percent difference was within 3% for all elements except for Cr(7%) and Sb(7%) using all four days of data combined. However, these differences *did not* prove to be statistically significant at the 95% level. Box-and-Whisker Plots for the relative differences are shown in Plot 4. Day 1(High Level) seems to have higher relative differences than days 2, 3, or 4.

The Pearson correlation coefficients for average of the up stream and down stream data are shown in Table 4. In Table 4, we see that As, Be, Cd, Cr, Hg, Pb, Sb are all highly correlated($r \geq 0.88$) and yield similar results.

From Tables 1, 2, & 3, we can conclude that the combustion data, excluding Fe, need not be bias-corrected due to monitor position within the stack. Essentially, the same combustion gases are present up stream and down stream as measured by the SRM.

Day-to-day variability was not consistently significant for the elements within the High and Low level data sets. Therefore sample summary statistics, rather than

statistics based on variance components, are presented for the elemental means(Table 5). The percent standard error among the elements for the first two days(High Level) ranges between 4.2% to 8.9% and ranges between 3.3% to 5.3% for the last two days(Low Level).

SUMMARY of TABLES, PLOTS & APPENDICES

Table 1

Statistical Regression Data for Bias Correction

y= Alpha + Beta x

x: Down Stream Data(μg)
y: Up Stream Data(μg)

Element		Mandel(*)		Least Squares		Mandel Predicted Values					
		Beta	Alpha	Beta	Alpha	x=20	x=80	x=40	x=200	x=500	x=3000
As	Estimate	1.110	-1.735	1.001	3.261	20.47	87.10				
	Std. Error	0.117	5.986	0.111	5.693	7.4	10.1				
Be	Estimate	1.106	-1.114	1.018	2.181	21.00	87.33				
	Std. Error	0.104	4.453	0.099	4.371	8.0	8.9				
Cd	Estimate	1.109	-1.591	1.020	2.117	20.58	87.10				
	Std. Error	0.105	5.032	0.100	4.836	8.7	9.3				
Cr	Estimate	1.220	-4.187	1.027	3.700	20.21	100.82				
	Std. Error	0.160	7.076	0.145	6.457	11.3	10.0				
Fe	Estimate	0.528	1100.3	0.107	1980.1	-	-			1364	2684
	Std. Error	0.270	580.4	0.223	482.4					535	403
Hg	Estimate	1.037	1.068	0.988	6.172	-	-	42.56	208.5		
	Std. Error	0.077	9.700	0.075	9.499			18.9	19.7		
Pb	Estimate	1.093	-1.489	0.999	3.077	20.4	85.92				
	Std. Error	0.107	5.993	0.102	5.746	10.2	10.2				
Sb	Estimate	1.054	1.886	0.953	6.254	22.97	86.23				
	Std. Error	0.112	5.437	0.107	5.190	8.7	9.3				
Y	Estimate	0.993	7.728	0.862	26.01	-	87.16				
	Std. Error	0.129	18.940	0.120	17.76		21.4				

(*) J. Mandel(1984). *Fitting Straight Lines When Both Variables are Subject to Error.* Journal of Quality Technology, Vol. 16, No. 1, January 1984. (λ=1, ρ=0)

Table 2

Statistical Summary for Up Stream - Down Stream Data

Day 1, 2, 3 & 4, High & Low Combined, N=19

95.0 percent confidence intervals

	Mean	Stnd. error	Lower limit	Upper limit
AsDIF	3.28809	2.57059	-2.11253	8.68871
BeDIF	2.87574	2.17941	-1.70303	7.45452
CdDIF	2.93777	2.36722	-2.03557	7.91112
CrDIF	4.82094	2.49223	-0.41506	10.0569
FeDIF	114.362	173.815	-250.81	479.533
HgDIF	4.90036	5.31366	-6.26326	16.064
PbDIF	3.04509	2.72186	-2.67333	8.76351
SbDIF	4.22365	2.37402	-0.763994	9.21129
YDIF	6.72541	6.03308	-5.94965	19.4005

Day 1 & 2, High Level, N= 9

95.0 percent confidence intervals

	Mean	Stnd. error	Lower limit	Upper limit
AsDIF	5.16176	5.11135	-6.62508	16.9486
BeDIF	4.90427	4.37693	-5.18899	14.9975
CdDIF	4.94639	4.79968	-6.12173	16.0145
CrDIF	8.04929	4.83267	-3.09489	19.1935
FeDIF	2.85333	214.116	-490.899	496.606
HgDIF	8.52678	11.1968	-17.2932	34.3468
PbDIF	5.04019	5.41855	-7.45503	17.5354
SbDIF	5.85593	4.92766	-5.5073	17.2192
YDIF	6.79597	7.30601	-10.0518	23.6437

Day 3 & 4, Low Level, N=10

95.0 percent confidence intervals

	Mean	Stnd. error	Lower limit	Upper limit
AsDIF	1.60179	1.88211	-2.65584	5.85942
BeDIF	1.05007	1.39336	-2.10193	4.20207
CdDIF	1.13002	1.44844	-2.14658	4.40662
CrDIF	1.91543	1.71427	-1.96253	5.79339
FeDIF	214.719	275.254	-407.951	837.389
HgDIF	1.63658	2.12112	-3.16173	6.43489
PbDIF	1.2495	1.97674	-3.2222	5.7212
SbDIF	2.75459	1.2186	-0.00207246	5.51125
YDIF	6.6619	9.77801	-15.4575	28.7813

Table 3

Statistical Summary for 100(Up Stream - Down Stream)/(Up Stream) Data

Day 1, 2, 3 & 4, High & Low Combined, N=19

95.0 percent confidence intervals

	Mean	Stnd. error	Lower limit	Upper limit
AsP	2.85045	5.96154	-9.6743	15.3752
BeP	2.82501	6.02615	-9.8355	15.4855
CdP	2.7324	5.53679	-8.89999	14.3648
CrP	6.66743	5.25811	-4.37946	17.7143
FeP	-2.26367	11.0054	-25.3853	20.8579
HgP	2.43314	4.2064	-6.4042	11.2705
PbP	1.82514	6.13977	-11.0741	14.7244
SbP	7.3801	4.87152	-2.85461	17.6148
YP	2.64541	5.0947	-8.05819	13.349

Day 1 & 2, High Level, N= 9

95.0 percent confidence intervals

	Mean	Stnd. error	Lower limit	Upper limit
AsP	2.88773	8.9106	-17.6602	23.4356
BeP	3.4407	9.2588	-17.9102	24.7916
CdP	3.16939	8.4855	-16.3983	22.737
CrP	9.11362	8.21233	-9.82408	28.0513
FeP	-3.29226	12.0488	-31.0769	24.4924
HgP	3.47897	6.34743	-11.1583	18.1162
PbP	2.45776	8.77494	-17.7773	22.6929
SbP	5.10287	9.3168	-16.3818	26.5875
YP	2.90352	8.97114	-17.784	23.5911

Day 3 & 4, Low Level, N=10

95.0 percent confidence intervals

	Mean	Stnd. error	Lower limit	Upper limit
AsP	2.8169	8.45768	-16.3158	21.9496
BeP	2.27089	8.32724	-16.5667	21.1085
CdP	2.33911	7.67162	-15.0153	19.6936
CrP	4.46587	7.06897	-11.5253	20.457
FeP	-1.33794	18.5449	-43.2896	40.6137
HgP	1.49189	5.89887	-11.8523	14.8361
PbP	1.25579	9.03173	-19.1755	21.687
SbP	9.42961	4.44444	-0.624436	19.4836
YP	2.41311	5.85107	-10.823	15.6492

Table 4

Pearson Correlations for the Average of Upstream & Downstream Data

Day 1, 2, 3, 4, High & Low Combined, N=19

Element	As	Be	Cd	Cr	Fe	Hg	Pb	Sb	Y
As	1	0.9975	0.9990	0.9956	0.2923	0.9290	0.9964	0.9890	-0.6277
Be	0.9975	1	0.9953	0.9907	0.3028	0.9151	0.9950	0.9947	-0.6041
Cd	0.9990	0.9953	1	0.9964	0.2740	0.9410	0.9966	0.9848	-0.6483
Cr	0.9956	0.9907	0.9964	1	0.3099	0.9376	0.9945	0.9788	-0.6372
Fe	0.2923	0.3028	0.2740	0.3099	1	0.0208	0.3276	0.3425	0.4411
Hg	0.9290	0.9151	0.9410	0.9376	0.0208	1	0.9191	0.8846	-0.8096
Pb	0.9964	0.9950	0.9966	0.9945	0.3276	0.9191	1	0.9893	-0.6017
Sb	0.9890	0.9947	0.9848	0.9788	0.3425	0.8846	0.9893	1	-0.5504
Y	-0.6277	-0.6041	-0.6483	-0.6372	0.4411	-0.8096	-0.6017	-0.5504	1

1 rows not used due to missing values.

Table 5

Summary Statistics by Level

Y: Average of Up Stream & Down Stream Data

Day 1 & 2, High Level, N=9

	Mean (µg/dscm)	Standard Error (µg/dscm)	Percent Standard Error
As	70.46	5.26	7.5%
Be	61.02	5.33	8.7%
Cd	67.27	5.07	7.5%
Cr	61.26	3.96	6.5%
Fe	2117.8	168.0	7.9%
Hg	180.6	7.54	4.2%
Pb	76.57	6.50	8.5%
Sb	65.85	5.85	8.9%
Y	98.69	7.80	7.9%

Day 3 & 4, Low Level, N=10

	Mean (µg/dscm)	Standard Error (µg/dscm)	Percent Standard Error
As	26.12	0.96	3.7%
Be	19.60	0.93	4.8%
Cd	21.42	0.90	4.2%
Cr	27.32	0.89	3.3%
Fe	2171.1	115.9	5.3%
Hg	37.84	1.64	4.3%
Pb	26.99	1.17	4.3%
Sb	26.58	1.21	4.5%
Y	182.0	8.38	4.6%

Plot 1

Mandel Straight Line Fit

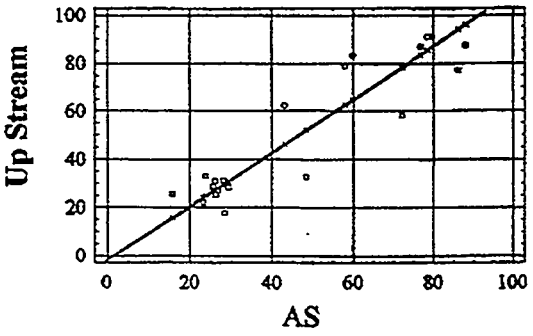

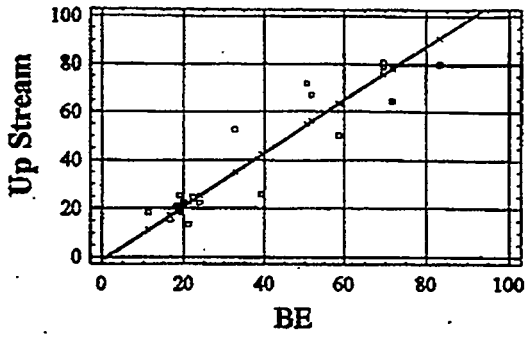

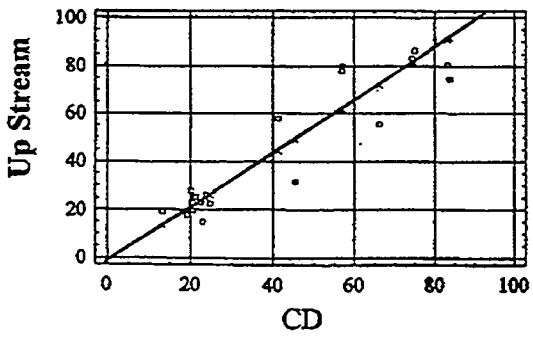

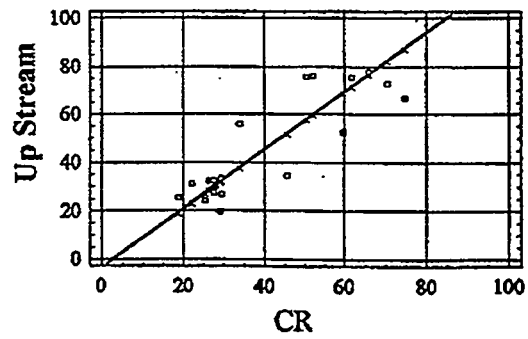

Plot 1
(Continued)
Mandel Straight Line Fit

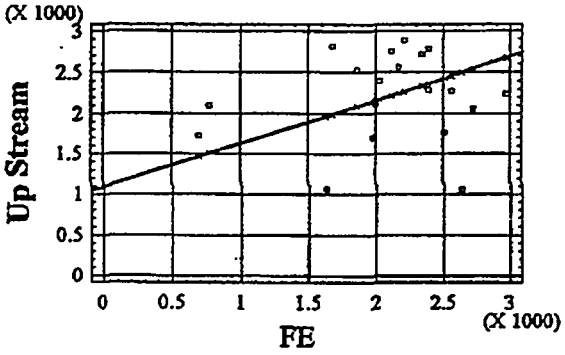

Down Stream

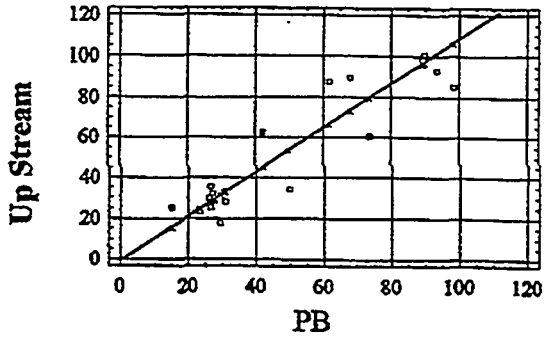

Down Stream

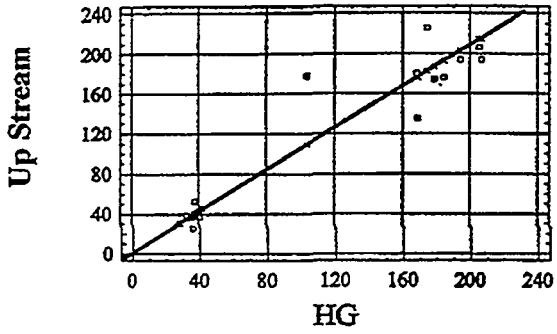

Down Stream

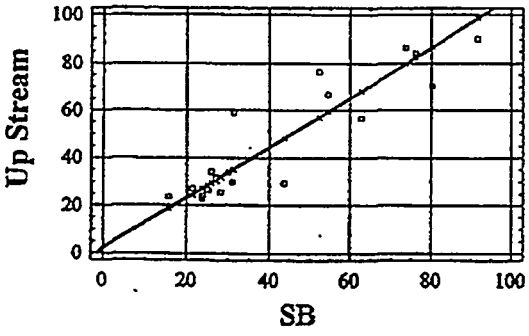

Down Stream

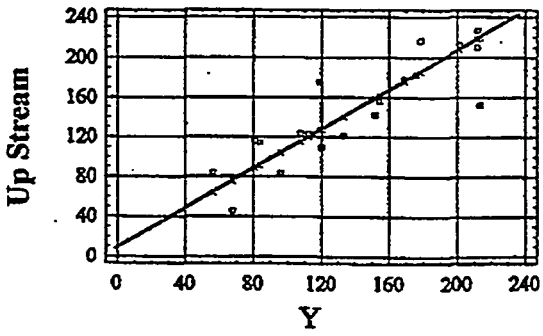

Down Stream

Plot 2

Average of Up Stream & Down Stream By Level & Day

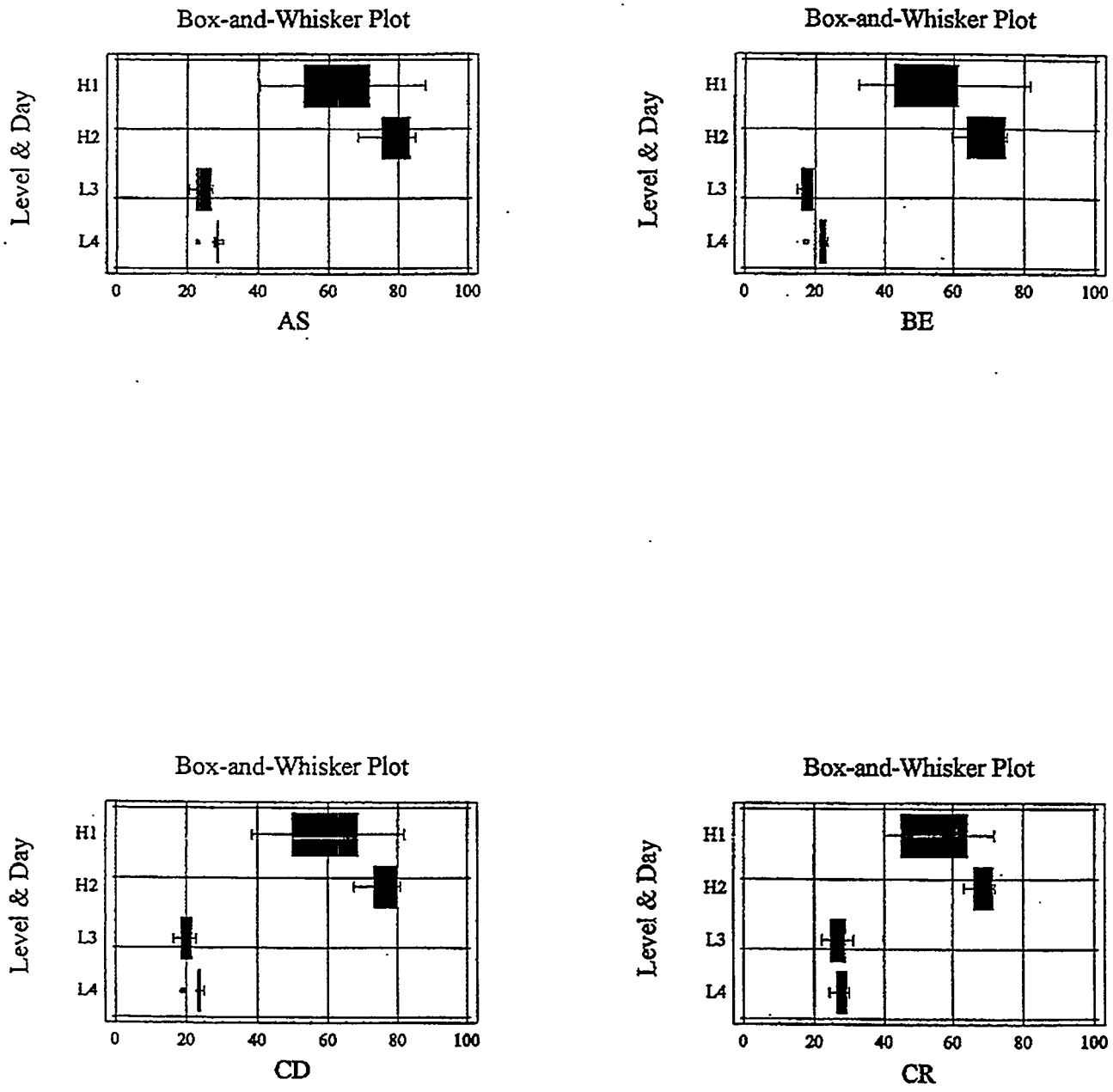

Plot 2
(Continued)
Average of Up Stream & Down Stream By Level & Day

Box-and-Whisker Plot

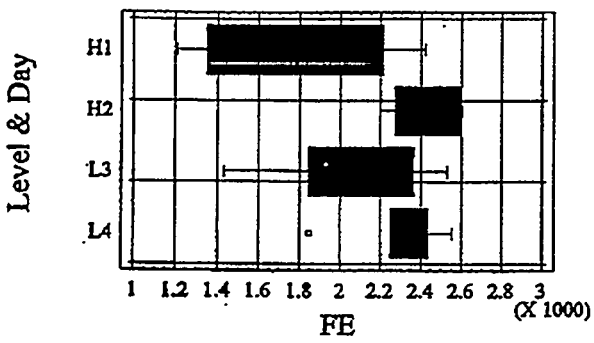

Box-and-Whisker Plot

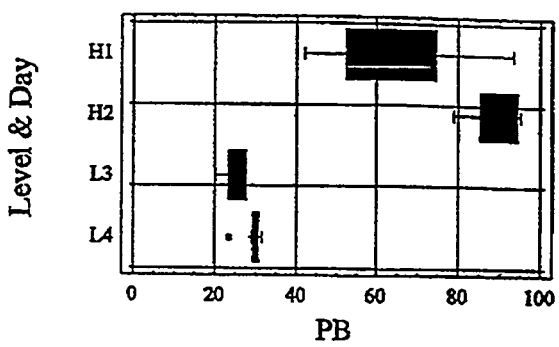

Box-and-Whisker Plot

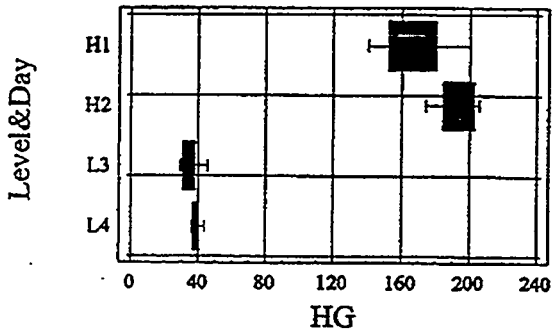

Box-and-Whisker Plot

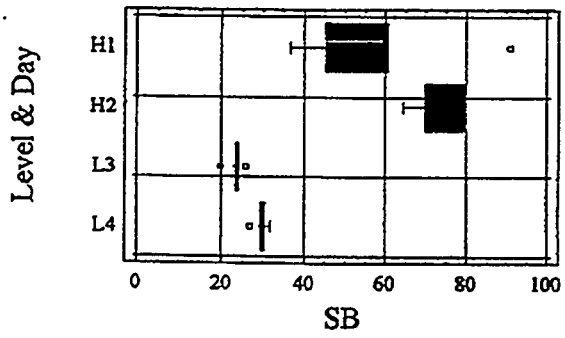

Box-and-Whisker Plot

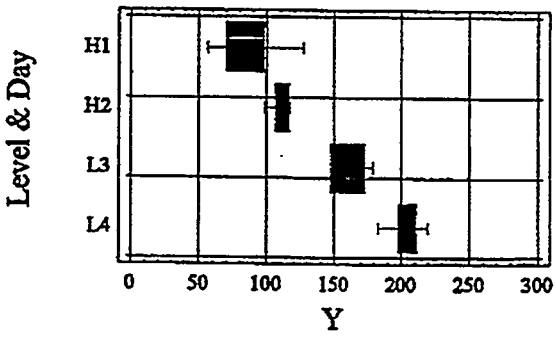

Plot 3

Up Stream - Down Stream Data

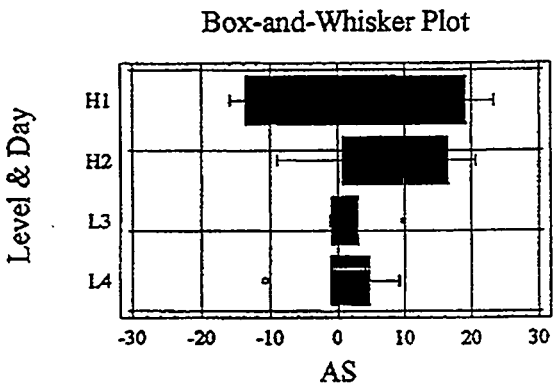

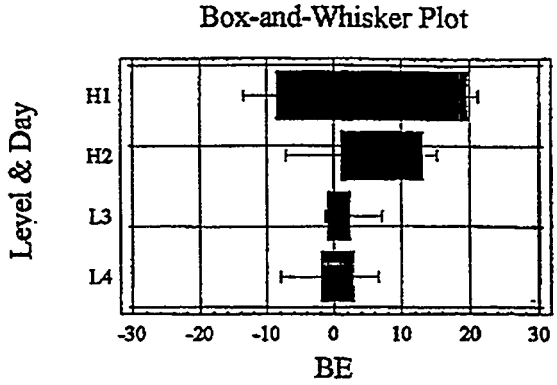

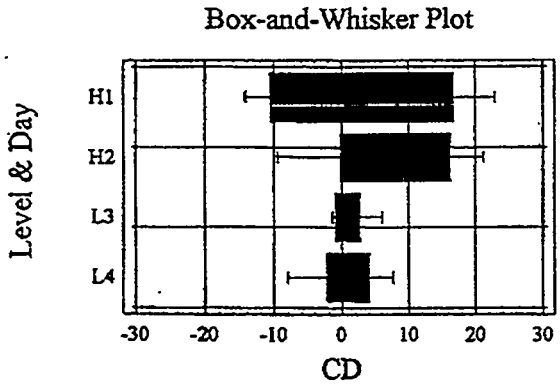

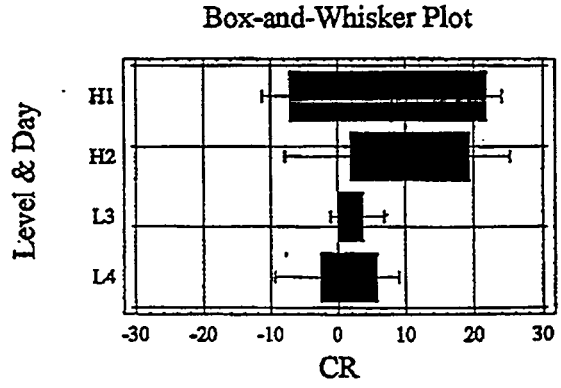

Plot 3
(Continued)
Up Stream - Down Stream Data

Box-and-Whisker Plot

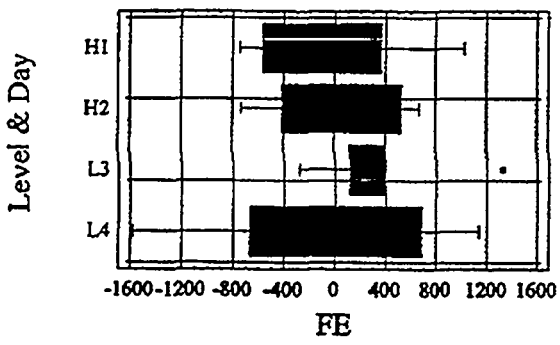

Box-and-Whisker Plot

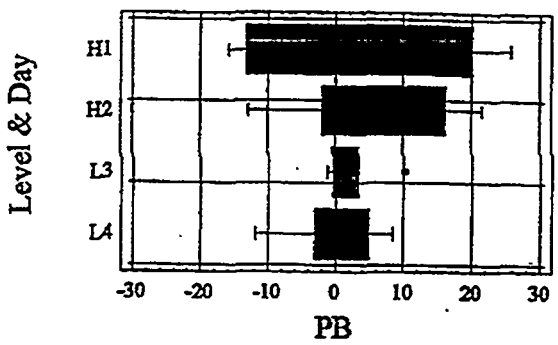

Box-and-Whisker Plot

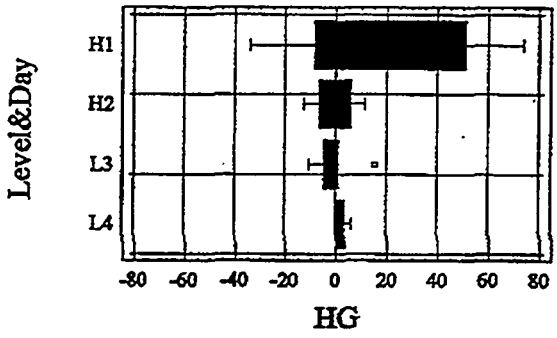

Box-and-Whisker Plot

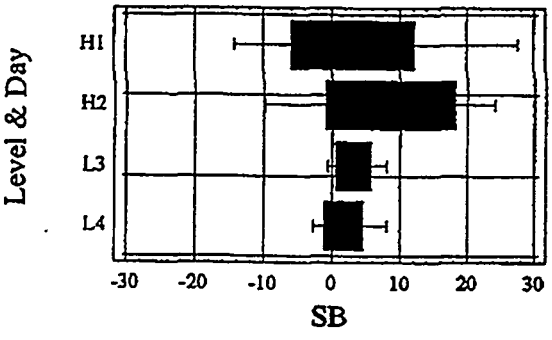

Box-and-Whisker Plot

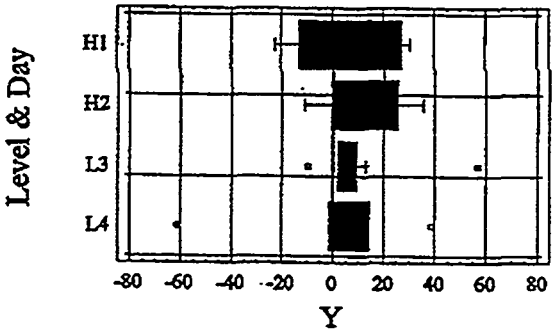

Plot 4

100(Up Stream - Down Stream)/(Up Stream)

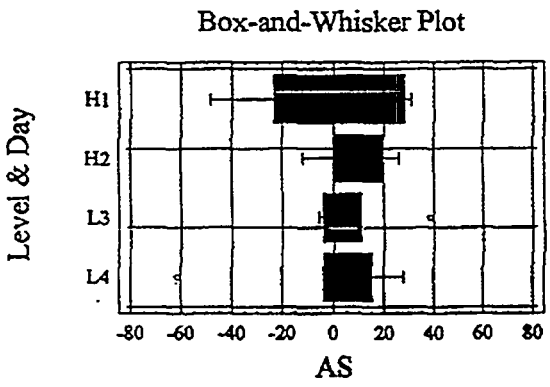

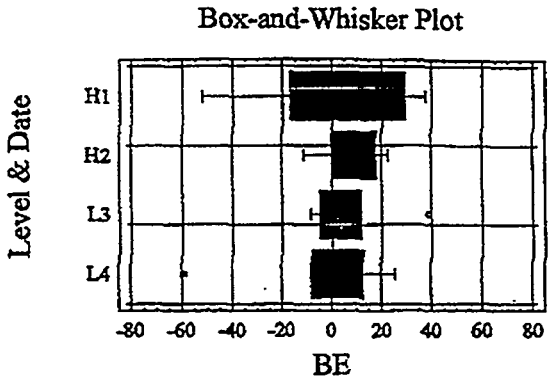

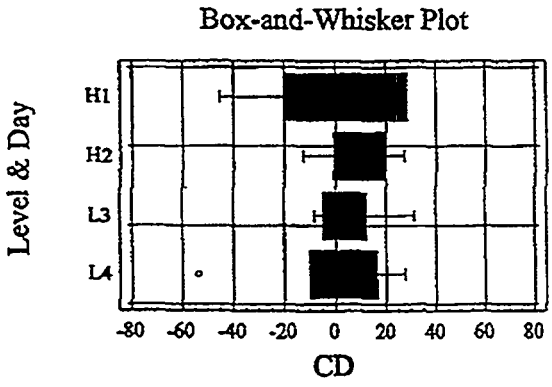

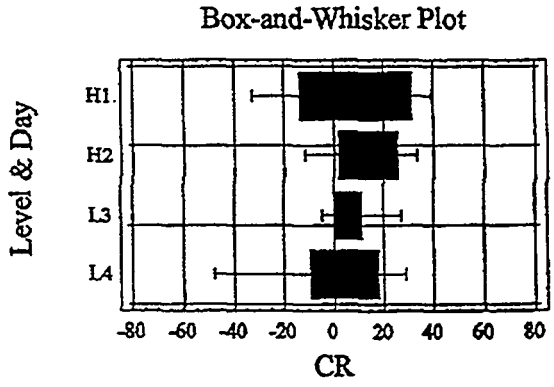

Plot 4
(Continued)
100(Up Stream - Down Stream)/(Up Stream)

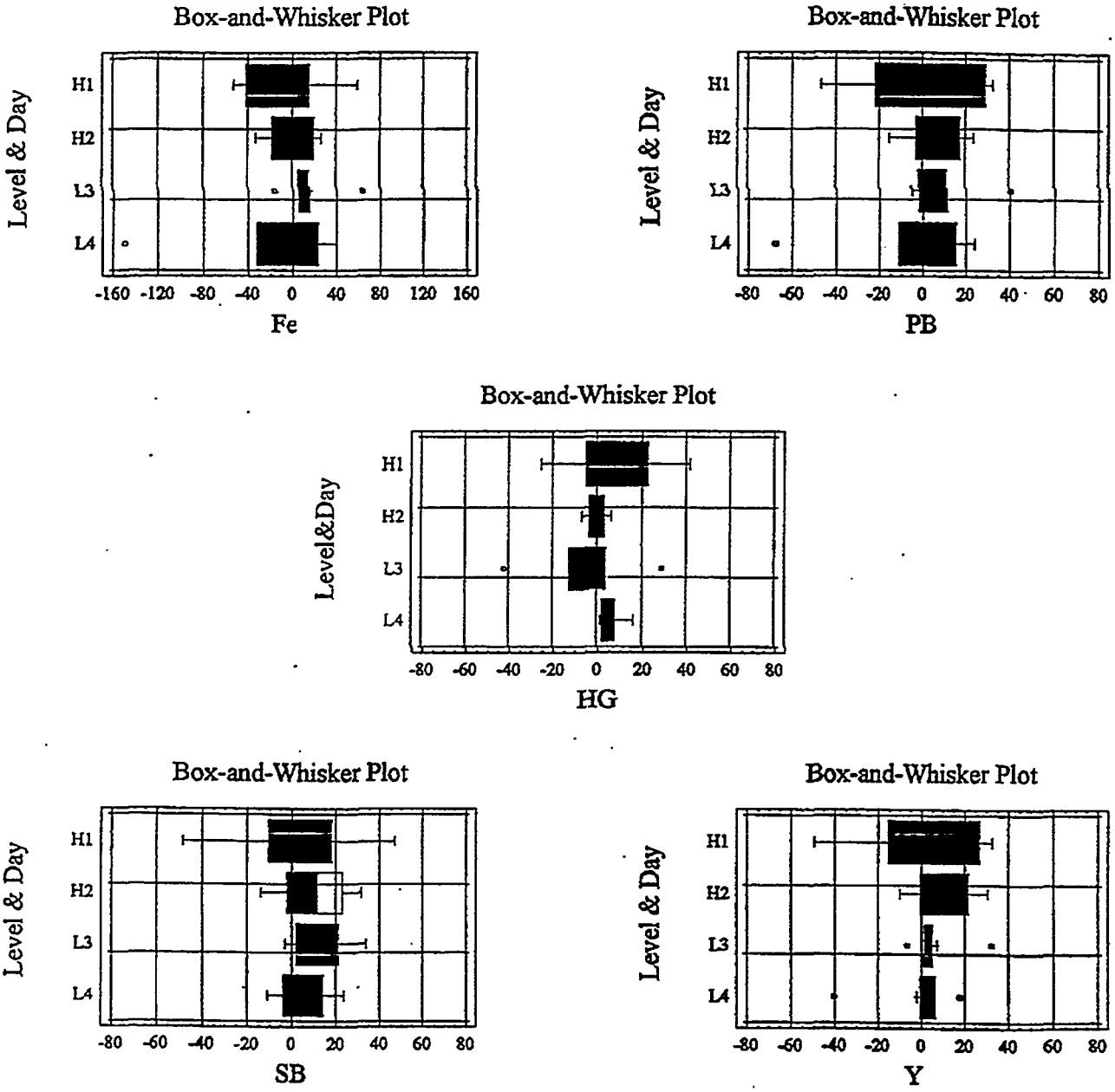

APPENDIX 1

DOWN STREAM DATA(µg/ dscm)

SEQ	DATE	Run	ID	As	Be	Cd	Cr	Fe	Hg	Pb	Sb	Y
1	1	1	High	88.06	83.23	83.23	70.57	2563.3	184.76	93.49	91.68	133.29
2	1	2	High	43.11	32.77	41.19	33.97	697.5	178.04	42.09	31.39	56.34
3	1	3	High	59.83	50.62	57.11	52.16	2027.2	174.79	61.80	54.51	83.44
4	1	4	High	72.06	58.52	66.20	59.75	2513.2	103.58	73.81	62.68	96.07
5	1	5	High	48.48	39.27	45.52	45.58	1630.3	169.07	49.94	43.76	67.88
6	2	1	High	76.69	69.56	74.32	61.83	2390.0	168.65	89.18	73.72	107.61
7	2	2	High	78.48	69.56	74.91	65.99	2390.0	194.60	89.77	76.10	112.37
8	2	3	High									
9	2	4	High	86.25	71.77	83.84	74.79	2973.5	206.92	98.31	80.22	120.02
10	2	5	High	57.97	51.82	56.90	50.51	1862.7	205.52	68.06	52.24	80.60
11	3	1	Low	26.71	18.96	22.44	28.02	2168.6	37.32	27.54	23.74	154.33
12	3	2	Low	23.25	16.65	19.14	25.39	1987.6	40.80	23.49	21.35	151.79
13	3	3	Low	15.79	11.26	13.29	18.70	767.7	35.68	15.12	15.75	118.93
14	3	4	Low	26.20	19.31	20.65	27.54	2001.6	28.58	26.60	23.80	169.03
15	3	5	Low	25.56	18.24	20.27	29.41	2342.2	37.61	26.15	25.03	175.94
16	4	1	Low	23.84	18.93	20.18	22.13	1679.0	32.77	26.65	25.94	178.42
17	4	2	Low	29.31	23.99	24.70	29.46	2727.6	40.22	30.95	31.07	211.80
18	4	3	Low	27.96	22.26	23.74	27.49	2210.1	36.14	30.65	30.03	201.09
19	4	4	Low	26.10	19.85	21.19	26.38	2114.8	41.84	27.04	27.04	212.26
20	4	5	Low	28.42	21.31	22.99	29.08	2638.6	39.27	29.47	28.26	213.51

UP STREAM DATA(µg/ dscm)

SEQ	DATE	Run	ID	As	Be	Cd	Cr	Fe	Hg	Pb	Sb	Y
1	1	1	High	87.22	80.00	80.56	72.78	2277.8	176.08	93.33	90.00	121.11
2	1	2	High	62.36	52.46	57.99	55.80	1723.2	174.14	62.36	59.08	83.70
3	1	3	High	83.18	71.83	80.03	76.24	2400.8	226.08	87.59	66.79	114.05
4	1	4	High	58.32	50.00	55.62	52.54	1765.7	177.66	60.48	56.70	83.15
5	1	5	High	32.66	25.81	31.33	34.34	1064.7	134.95	34.06	29.49	45.37
6	2	1	High	86.75	78.89	83.38	75.52	2785.0	180.16	98.26	86.19	123.53
7	2	2	High	90.96	80.60	86.36	77.72	2291.3	194.19	100.75	84.05	122.63
8	2	3	High	82.33	70.33	80.05	72.04	2704.4	193.13	93.20	97.77	111.49
9	2	4	High	77.28	64.59	74.39	66.90	2237.6	194.09	85.35	70.36	109.00
10	2	5	High	78.66	67.09	78.08	75.77	2527.5	206.33	89.65	76.34	116.25
11	3	1	Low	26.80	19.71	23.16	29.68	2562.5	38.03	28.13	23.05	156.18
12	3	2	Low	21.98	15.35	17.65	24.28	1704.4	36.29	23.04	27.11	142.16
13	3	3	Low	25.61	18.46	19.38	25.65	2094.8	25.13	25.27	23.81	175.84
14	3	4	Low	25.17	18.39	19.65	27.65	2117.3	29.80	25.32	24.30	178.22
15	3	5	Low	28.70	20.72	23.12	33.20	2721.2	52.96	29.51	26.60	182.61
16	4	1	Low	33.07	25.51	27.90	31.14	2815.6	39.20	35.08	34.00	217.13
17	4	2	Low	28.20	22.16	22.45	26.89	2058.9	41.09	27.83	29.91	210.37
18	4	3	Low	31.12	24.75	26.27	32.37	2896.1	36.70	32.37	33.66	212.28
19	4	4	Low	30.87	22.82	25.33	32.22	2757.6	45.47	32.03	31.62	226.68
20	4	5	Low	17.63	13.38	14.96	19.66	1056.4	41.91	17.56	25.49	152.26

APPENDIX 2

Up Stream - Down Stream DATA(µg/ dscm)

SEQ	DATE	RUN	ID	As	Be	Cd	Cr	Fe	Hg	Pb	Sb	Y
1	1	1	High	-0.84	-3.23	-2.68	2.21	-285.6	-8.68	-0.15	-1.68	-12.18
2	1	2	High	19.25	19.69	16.80	21.82	1025.7	-4.91	20.27	27.69	27.35
3	1	3	High	23.35	21.22	22.92	24.08	373.6	51.29	25.78	12.28	30.62
4	1	4	High	-13.74	-8.52	-10.58	-7.22	-747.5	74.09	-13.34	-5.99	-12.92
5	1	5	High	-15.82	-13.46	-14.19	-11.24	-565.6	-34.12	-15.88	-14.27	-22.51
6	2	1	High	10.05	9.33	9.06	13.69	394.9	11.50	9.08	12.47	15.92
7	2	2	High	12.48	11.04	11.45	11.73	-98.7	-0.41	10.97	7.95	10.26
8	2	3	High									
9	2	4	High	-8.97	-7.18	-9.44	-7.89	-735.9	-12.83	-12.96	-9.86	-11.03
10	2	5	High	20.69	15.27	21.18	25.26	664.8	0.81	21.59	24.11	35.66
11	3	1	Low	0.09	0.76	0.72	1.66	394.0	0.71	0.58	-0.70	1.85
12	3	2	Low	-1.27	-1.31	-1.49	-1.10	-283.2	-4.51	-0.45	5.76	-9.63
13	3	3	Low	9.82	7.21	6.10	6.95	1327.1	-10.54	10.15	8.06	56.91
14	3	4	Low	-1.03	-0.91	-1.00	0.11	115.7	1.22	-1.27	0.50	9.19
15	3	5	Low	3.13	2.48	2.85	3.79	379.0	15.35	3.36	1.57	6.67
16	4	1	Low	9.23	6.58	7.72	9.01	1136.6	6.43	8.44	8.06	38.71
17	4	2	Low	-1.11	-1.84	-2.24	-2.57	-668.7	0.87	-3.12	-1.15	-1.43
18	4	3	Low	3.16	2.50	2.53	4.88	686.1	0.56	1.72	3.63	11.19
19	4	4	Low	4.77	2.97	4.14	5.85	642.8	3.63	4.99	4.58	14.41
20	4	5	Low	-10.78	-7.93	-8.03	-9.42	-1582.2	2.65	-11.91	-2.77	-61.25

100(Up Stream - Down Stream)/(Up Stream)

SEQ	DATE	RUN	ID	As	Be	Cd	Cr	Fe	Hg	Pb	Sb	Y
1	1	1	High	-1.0	-4.0	-3.3	3.0	-12.5	-4.9	-0.2	-1.9	-10.1
2	1	2	High	30.9	37.5	29.0	39.1	59.5	-2.8	32.5	46.9	32.7
3	1	3	High	28.1	29.5	28.6	31.6	15.6	22.7	29.4	18.4	26.8
4	1	4	High	-23.6	-17.0	-19.0	-13.7	-42.3	41.7	-22.1	-10.6	-15.5
5	1	5	High	-48.4	-52.2	-45.3	-32.7	-53.1	-25.3	-46.6	-48.4	-49.6
6	2	1	High	11.6	11.8	10.9	18.1	14.2	6.4	9.2	14.5	12.9
7	2	2	High	13.7	13.7	13.3	15.1	-4.3	-0.2	10.9	9.5	8.4
8	2	3	High									
9	2	4	High	-11.6	-11.1	-12.7	-11.8	-32.9	-6.6	-15.2	-14.0	-10.1
10	2	5	High	26.3	22.8	27.1	33.3	26.3	0.4	24.1	31.6	30.7
11	3	1	Low	0.3	3.8	3.1	5.6	15.4	1.9	2.1	-3.0	1.2
12	3	2	Low	-5.8	-8.5	-8.4	-4.5	-16.6	-12.4	-1.9	21.2	-6.8
13	3	3	Low	38.3	39.0	31.4	27.1	63.4	-42.0	40.2	33.9	32.4
14	3	4	Low	-4.1	-5.0	-5.1	0.4	5.5	4.1	-5.0	2.0	5.2
15	3	5	Low	10.9	12.0	12.3	11.4	13.9	29.0	11.4	5.9	3.7
16	4	1	Low	27.9	25.8	27.7	28.9	40.4	16.4	24.1	23.7	17.8
17	4	2	Low	-3.9	-8.3	-10.0	-9.6	-32.5	2.1	-11.2	-3.9	-0.7
18	4	3	Low	10.2	10.1	9.6	15.1	23.7	1.5	5.3	10.8	5.3
19	4	4	Low	15.5	13.0	16.3	18.1	23.3	8.0	15.6	14.5	6.4
20	4	5	Low	-61.2	-59.2	-53.7	-47.9	-149.8	6.3	-67.9	-10.9	-40.2

APPENDIX 3

Up Stream & Down Stream Average(μg/ dscm)

SEQ	DATE	RUN	ID	As	Be	Cd	Cr	Fe	Hg	Pb	Sb	Y
1	1	1	High	87.64	81.62	81.89	71.67	2420.6	180.42	93.41	90.84	127.20
2	1	2	High	52.74	42.62	49.59	44.89	1210.4	176.59	52.23	45.24	70.02
3	1	3	High	71.50	61.23	68.57	64.20	2214.0	200.44	74.70	60.65	98.74
4	1	4	High	65.19	54.26	60.91	56.15	2139.4	140.62	67.14	59.69	89.61
5	1	5	High	40.57	32.54	38.42	39.96	1347.5	152.01	42.00	36.62	56.63
6	2	1	High	81.72	74.22	78.85	68.68	2587.5	174.40	93.72	79.95	115.57
7	2	2	High	84.72	75.08	80.63	71.86	2340.7	194.40	95.26	80.08	117.50
8	2	3	High									
9	2	4	High	81.76	68.18	79.12	70.84	2605.5	200.50	91.83	75.29	114.51
10	2	5	High	68.31	59.46	67.49	63.14	2195.1	205.93	78.85	64.29	98.42
11	3	1	Low	26.76	19.33	22.80	28.85	2365.6	37.67	27.83	23.40	155.26
12	3	2	Low	22.62	16.00	18.39	24.84	1846.0	38.54	23.26	24.23	146.97
13	3	3	Low	20.70	14.86	16.33	22.17	1431.3	30.41	20.19	19.78	147.39
14	3	4	Low	25.69	18.85	20.15	27.59	2059.4	29.19	25.96	24.05	173.63
15	3	5	Low	27.13	19.48	21.69	31.30	2531.7	45.29	27.83	25.81	179.27
16	4	1	Low	28.46	22.22	24.04	26.63	2247.3	35.98	30.86	29.97	197.78
17	4	2	Low	28.75	23.07	23.58	28.18	2393.3	40.66	29.39	30.49	211.09
18	4	3	Low	29.54	23.51	25.01	29.93	2553.1	36.42	31.51	31.84	206.69
19	4	4	Low	28.49	21.33	23.26	29.30	2436.2	43.66	29.54	29.33	219.47
20	4	5	Low	23.02	17.35	18.98	24.37	1847.5	40.59	23.51	26.87	182.88

Appendix B

Developer Report
Diagnostic Instrumentation and Analysis Laboratory (DIAL)
Air ICP-AES System

Final Report

Fieldable Air ICP-AES System

Multi-metal Continuous Emission Monitor Demonstration
EPA National Risk Management Laboratory,
Research Triangle Park, NC.
September 1997.

Principal Investigator: Dr. George P. Miller

Co-Investigators: Dr. Z. Zhu, Mr. W. Okhuysen.

Affiliation:

Diagnostic Instrumentation & Analysis Laboratory,
College of Engineering
Mississippi State University
Mississippi State, MS 39762

Tel: 601-325-7631, FAX: 601-325-8465, email: miller@dial.msstate.edu

Collaborator: Dr. David P. Baldwin
Ames Laboratory, USDOE
9 Spedding Hall
Ames, IA 50011

TABLE OF CONTENTS

FIGURES

TABLES

TECHNOLOGY DESCRIPTION

Increasing regulatory demands requiring significant reductions in the emission of hazardous air pollutants have led to the need for techniques capable of providing real-time monitoring, at the stack, of toxic metals in combustion gas streams. These waste streams range from coal-fired boilers, municipal waste combustors to plasma vitrification systems used for the remediation of low level radioactive waste. This lack of a fieldable continuous emission metal monitor (CEM) has been recognized as a significant gap in the available technology. The system described below has been designed to fill this gap.

Over the last twenty years the use of argon ICP-AES for the measurement of trace elements in solution has matured into a standard analytical technique. However, unlike the laboratory ICP, it is essential for a CEM that the system be hardened sufficiently to handle the problems of a real-world environment. These problems include the ability to readily tolerant the introduction of a variety of molecular gas matrices, significant variations in moisture and particle loading as well as the thermal, vibrational and clogging problems found outside the laboratory. The system described in this report has taken the standard laboratory ICP-AES and modified it into a form capable of accurately measuring the real-time concentration of metals in exhaust stacks.

While our use of the latest technology has provides the ability to operate as either an argon or as an air-ICP system, it is our opinion that the air plasma holds the greatest promise as an on-line CEM.. Each option has its advantages and disadvantages. The argon based system has a higher ionization energy to excite the sample but does not tolerant molecular gases very well (resulting in reduced sample volume). The air-ICP provides significant reduction in operating costs, together with its increased tolerance of particle loading and reduced susceptibility to changes in moisture content (due to more efficient heat transfer from an air plasma to the sample) in the exhaust stream. The air plasma readily tolerates molecular gases (allowing increased sampling volume). On the other hand, it requires higher rf powers and the maximum available ionization energy is reduced.

The air-ICP plasma results in a totally different spectrum from the line spectrum seen in an argon ICP. The emission spectrum includes molecular bands (e.g. OH, CN, NO, N_2^+) in the wavelength regions of interest (200-350 nm). These increased interferences place a more stringent requirement on both the resolution of the detection system and the software used to analysis the data. We have developed two separate approaches to address these problems. A unique chemometric software package to handle the analysis and a collaboration with Ames National Laboratory to reduce the size of the detection system (HiRIS) while increasing the resolution. In the main body of this report we will concentrate on the monochromator based system. The HiRIS system and the experimental results obtained using it are discussed separately in Appendix A.

The remaining hardware required to complete the system consists of providing an isokinetic sampling interface between the ICP and the exhaust duct. The extractive sampling techniques used introduces the sample stream into a controlled environment where matrix effects are minimized and the plasma properties are stabilized. Any matrix effects that remain are dealt with through the use of internal standards and/or standard addition methods via the isokinetic sampling apparatus. These are options that are impossible for in-stack methods.

Summary of Technology Development History and Sponsorship

Although the ICP has reached the status of a mature analytical laboratory instrument its application as an on-line continuous emission monitor for exhaust stacks is much more recent. Meyer and Thompson first evaluated the air-ICP as a modification to the standard argon system in 1985.[2] Due to the lack of advantages over the argon ICP for liquid samples the technique remained neglected. The use of an argon ICP to analysis molecular offgas stream was reported by Seltzer starting in 1994.[3,4] The problems associated with analyzing molecular gases using an argon ICP attracted renewed interest in the air-ICP. Baldwin et. al revisited the technology in 1995 with very promising results.[5] Research on developing the fieldable air-ICP system, described within this report, was begun in 1996 and is funded under DOE Grant DE-F602-93CH-10575.[6]

Equipment

Our development program includes, intentionally, a large research component. As previously mentioned, ICP-AES is widely regarded as a mature technology. This view is generally valid for the analysis of liquid samples in the laboratory, however, the application of ICP-AES to the analysis of molecular gases has only very recently begun to attract attention and the optimum solution has yet to be determined.

DIAL's ICP system is capable of operating on either argon or air. However, due to the air-ICP system's inherent advantages with respect to handling molecular gases, we decided to concentrate solely on the air-ICP system as a metals CEM. One major advantage of the instrument described herein is the substantial reduction achieved in the size of the components. This allows us to interface the instrument directly at the stack, which significantly simplifies the calibration problem and eliminates the difficulties associated with the use of long heated sample lines. This instrument has moved the ICP from being an analytical laboratory system to a fieldable instrument capable of providing continuous real-time data for both regulatory compliance and process control.

Instrumentation

For this test, the ICP system incorporates a novel 3.5 kW solid-state 27.12 MHz rf generator with the load coil modified for air-plasma operation. This is coupled to a detection system with the offgas sample being extracted from the duct and introduced into the air-ICP via an isokinetic sampling system. Figure 1 is a schematic diagram of the Air-ICP continuous emission monitor and Table 1 lists the system specifications.

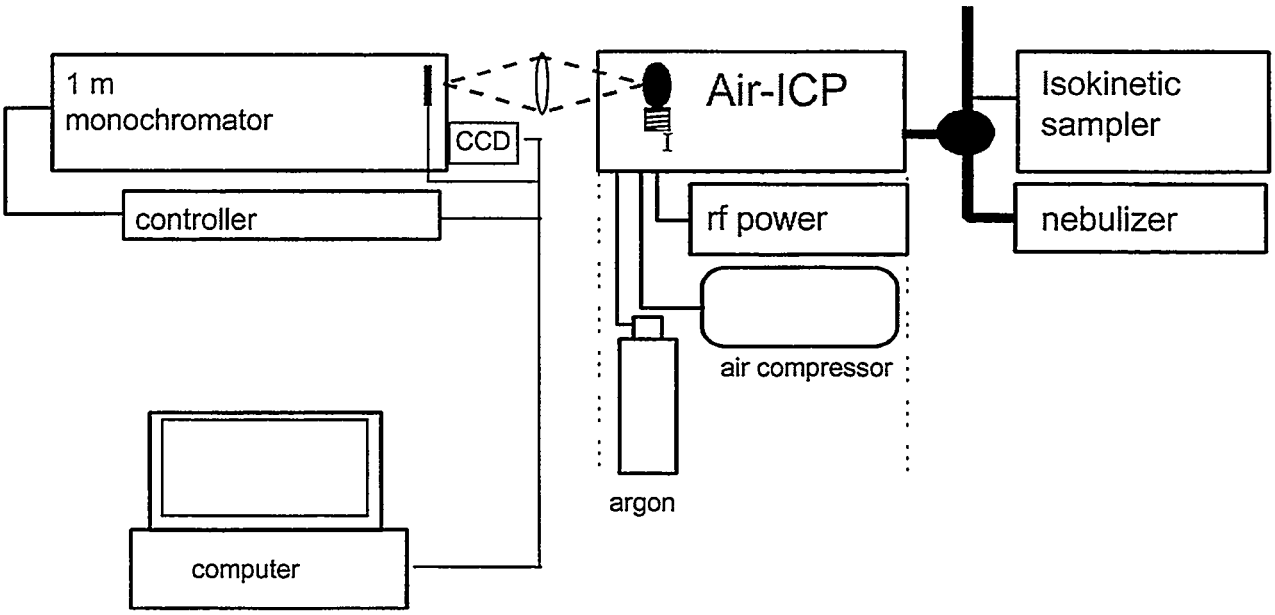

Figure 1. Air-ICP schematic diagram.

Table 1. Specifications of a Fieldable Air-ICP.

ICP, 27.12 MHz solid-state rf generator and matching unit (SEREN I3500)
RF output power 3.5 kW into 50 ohms
output impedance 50 ohms
input power 185-250, 50/60 Hz, single phase, 35 amps
Dimensions, 14" H × 19" W × 21" D. Weight approx. 57 kgs
Ultrasonic nebulizer, CETAC U-5000AT
Air compressor, small bottle compressed Argon
1 m SPEX, Model 1704 monochromator with a Spectrum One CCD detector
HiRIS Detection System
Isokinetic Sampler

For complete air operation, the ICP is started using argon and progressively switched over to air. The only modifications required to achieve a successful transition are increased gas flowrates (to prevent torch failure) and the replacement of the load coil, the number of turns being increased from 3.2 to 4.7. To eliminate the added expense and complications arising from using bottled compressed air, a small air compressor is used to supply the gas. Calibration in both cases is performed using a Cetac (Model U-5000AT) ultrasonic nebulizer.

The detection system is the eyes of the instrument, collecting the data necessary to analysis the offgas constituents. At present, the fieldable air-ICP uses a 1 m SPEX monochromator, Model 1704, and CCD detector. This remains the largest single component of the system. It provides amply resolution but operates sequentially and is relatively large. It, nevertheless, provides the ideal platform for identifying and characterizing the spectral emissions and possible interferences arising from unidentified components

making up exhaust gas emissions. To provide simultaneous metal concentration measurements, this monochromator could be replaced by a polychromator.

In addition, it was decided to use this demonstration to perform an evaluation of a novel spectrometer design. UV-HiRIS, a fiber-optic interferometer, developed for this project by Dr. David Baldwin, Ames National Laboratory. This instrument is compact, thermally and vibrationally stable. It uses a combination of an acousto-optic tunable filter and a Fabry-Perot interferometer to provide the resolution of a 1.5 m monochromator into a 10 kg package. A full description of this instrument is included in Appendix A. The successful combination of the solid-state air-ICP and the HiRIS spectrometer would represent a large step forward in instrument development and would reduce the overall size and weight of the complete air-ICP package substantially (from original ~1000 kg, present 250 kg, to ~150 kg) while improving the resolution and thereby the detection limits.

Isokinetic Sampling System

To correctly measure the concentration of metals present within an exhaust gas stream it is necessary to introduce a sample from the exhaust gas stream into the ICP under isokinetic conditions. Therefore, a sampling system has been designed to extract such a sample from a gas stream and introduce it into the air-ICP for analysis. The system operates by filling a loop with sample gas and then pushing this sample with air into the ICP. The robustness of the air plasma permits an optimum sample flowrate into the ICP of 1.14 sl/min., approximately three times more than tolerated by an argon ICP.

The sampling system for the Air-ICP consists of three components:

1. A heated Pyrex probe (max. gas temp = 650 C) housed in a 1 inch outside diameter stainless steel sheath. This is a standard Graseby stack sampler probe with a 2 ft effective length (longer lengths are available to accommodate large ducts or if traverses across a duct are desirable).

2. A heated sample unit containing the sample loop together with the pumps, condensor, flowmeter, flow controller, and other instrumentation required to perform isokinetic sampling.

3. A S-type pitot tube and stack thermocouple are inserted at an adjacent port to measuring duct flow velocity and stack gas temperature. These items are located according to EPA Method 2C—*Determination of Stack Gas Velocity and Volumetric Flow Rate in Small Ducts (Standard Pitot Tube).*

Calibration

An important concern with any CEM is the question of calibration. In this instance, instrument calibration follows a modified standard ICP calibration procedure.[1] An ultrasonic nebulizer is used to provide metal-containing aerosols at known concentration ($\mu g/m^3$). This concentration is determined from

$$C_A = \frac{C_s u \varepsilon}{F}$$

where C_A is the aerosol concentration ($\times 10^3$ $\mu g/m^3$), C_s is the standard solution concentration ($\mu g/g_{solv}$), u is the solution uptake to the ultrasonic nebulizer, F is air flow rate to the ICP, and μ is nebulizer efficiency. The efficiency of the nebulizer was determined both in the laboratory and again on-site prior

to the test. (A rf transducer in the ultrasonic nebulizer failed in the middle of the test and this experiment was repeated to measure any change in efficiency). For the initial instrument calibration, the metal aerosol is mixed with ambient air. Instrument response was checked against standard calibration curves prepared previously.

However, in the field, the presence of flyash as well as variations in loading and exhaust gas composition allow the possibility of substantial matrix effects significantly impacting the results of any real-world analysis. This variation in composition between laboratory air and the exhaust gas composition renders any direct comparison of the laboratory air calibrations to the instrument offgas response highly suspect. To circumvent this problem, we have developed a novel technique whereby the calibration standards are mixed with the exhaust offgas at the entrance to the sampling loop while maintaining isokinetic conditions. This ensures (as near as possible) that the standard and offgas sample are matrix-matched. To achieve this the standard metal aerosol from the ultrasonic nebulizer is mixed in the isokinetic sampling system with exhaust gases (for this demonstration 1 part aerosol to 3 parts offgas was used). Throughout the demonstration, zero, calibration and quality assurance (QA) checks were performed prior to the start of the day's runs and between reference metals with fly-ash running. The system has the additional capability to spike the offgas sample during long periods of continuous metal emission. This allows recalibration and QA checks to be performed on-line under actual operating conditions.

To further improve the sensitivity of the instrument, a novel chemometric software package has been developed which by modeling background spectrum (at the spectra regions of interest) effectively reduces the background noise and thus improves the instrument sensitivity. To apply this method accurately, data from the spectral regions of interest was collected during the shakedown period prior to the test. In addition, as the instrument presently employs a sequential detection system, wavelength calibration is essential. A chemometric-based software package was developed to check and, if necessary, correct wavelength calibration. This software checks the wavelength position with respect to the pixel position on the CCD every time the wavelength setting is changed as well as periodically checking for instrument drift.

Installation Procedure

Installation involved unloading from DIAL's Mobile Laboratory, and placing the ICP adjacent to the sample port (Photograph 1). This was followed by the installation of the isokinetic sampling system into the port. As can be seen in Photograph 2, the complete isokinetic sampling system was supported from the port. Electric and cooling connections were made. At this stage, with the exception of having an ICP exhaust available, the system was ready for operation. The time taken to this point was approximately 2 hours after unloading had begun. It effectively took the rest of the day before the EPA facility had provided us with a suitable exhaust outlet. Therefore, it was not until the next day during the time scheduled for preliminary metal tests that we could begin our calibration and alignment checks. This delay, which was beyond our control, resulted in us being unable to complete our preliminary modeling and prevented the submission of the daily results for As and Sb.

In a typical test sequence, the sampling probe is first inserted and the port leak-checked. Power is turned on to heat the isokinetic sampling system and ultrasonic nebulizer to the required temperature and allow them to equilibrate. The ICP system is then started and, when equilibrated (~15 mins.), zero checked. Once fly-ash is started, standards are introduced via ultrasonic nebulizer (and isokinetic sampling system) and the instrument calibration is confirmed and QA checks made.

Due to the integration of our sampling and calibration methods, metal concentrations are determined in wscm and moisture correction is required to convert to the more standard dscm. As the air-ICP is stationed immediately adjacent to the sample port with the isokinetic sampling system mounted

directly on to the port, sample transverse time is negligible. The sample is isokinetically collected. This consists of flushing the sample loop with sample for 18 seconds (3 × loop volume) and then introducing the sample into the ICP, equilibrating, and measuring the emission intensity (12 seconds). Wavelength calibration is performed following each wavelength change. In between RM runs and at the completion of the day's run, zero and QA checks are performed. Data analysis was then completed.

Results

Detection Limits

The toxic metals species of concern to EPA and DOE include: As, Be, Cd, Cr, Hg, Sb, Pb. The detection limit, as defined by IUPAC, is the concentration required to produce a net line intensity equivalent to three time the standard deviation of the background signal (for a full definition see ref. 1). While this definition does have some uses e.g. optimizing operating conditions of a single instrument, the measurement obtained are unrealistically low for practical analysis in either the laboratory or the field.

Of these metals, the instrument detection limits presently obtainable by the air-ICP for As and Sb are presently not good enough to make realistic measurements at either the high (nominally 75 $\mu g/m^3$) or low (15 $\mu g/m^3$) concentration levels used during the demonstration. It was possible, for example, to tell when Sb metal was turned off and on but the levels were below 5 times the instrument detection limit so an accurate measurement can not be made. The same is true for mercury at the low concentration level.

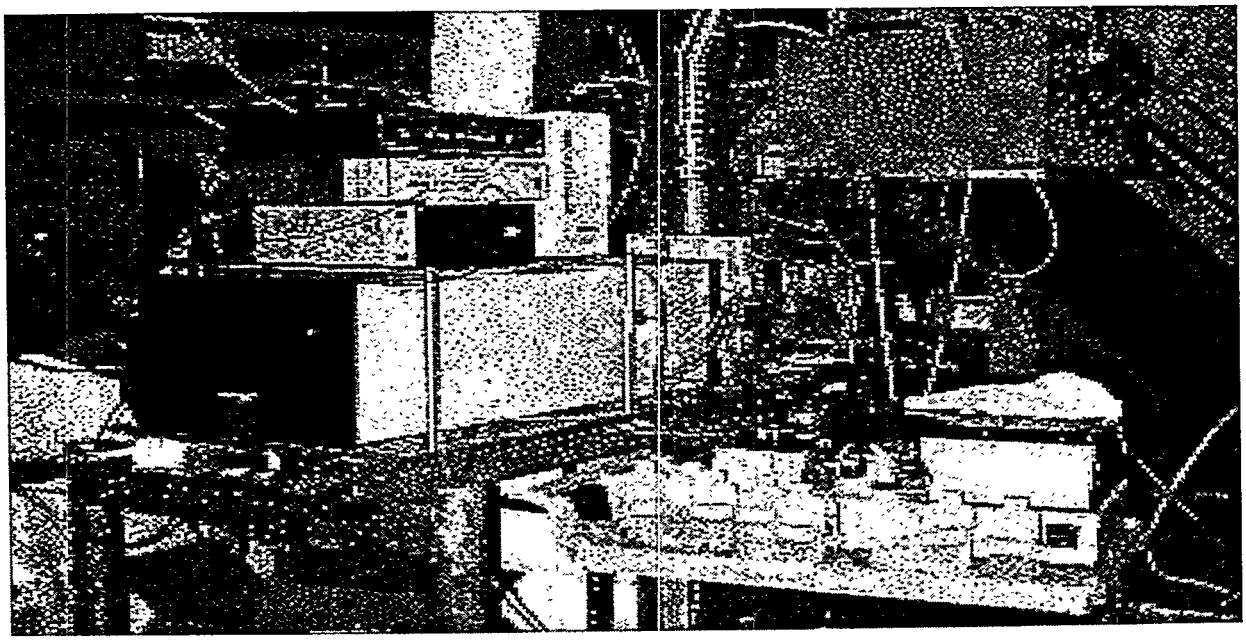

Photograph 1: Air-ICP System

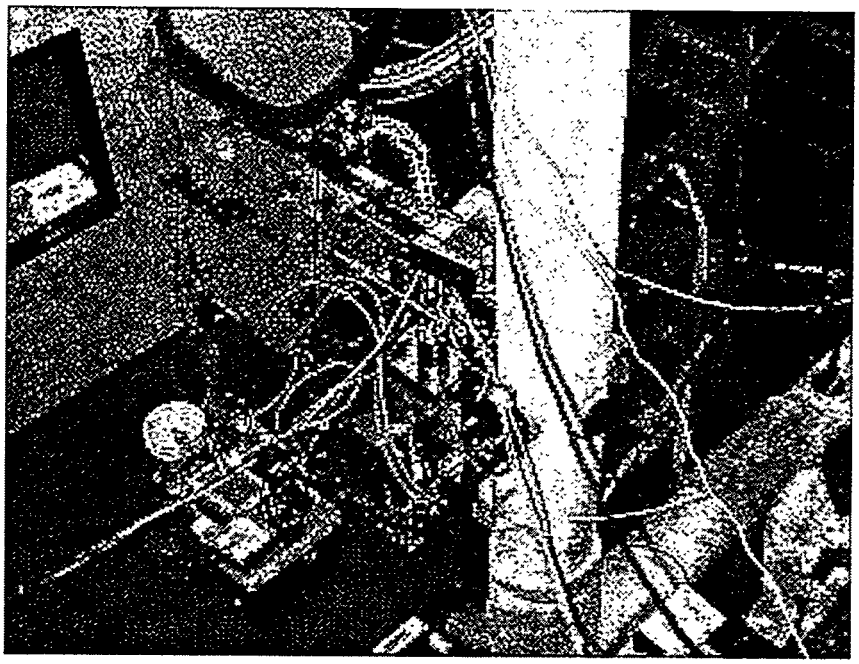

Photograph 2: An overhead view shows the isokinetic sampling system mounted into the duct port directly adjacent to the Air-ICP.

As can be clearly seen in Table 2, the detection limits obtained during the test are in some cases significantly higher than achieved in the laboratory. While it is well known that the background signal can vary both randomly and systematically between recalibration with a 50% change in detection limits per hour (between calibration checks) being accepted as the norm in the laboratory.[1] Another effect, especially with respect to insitu continuous emission monitors, is spectral interferences. Molecular offgas streams can contain concomitant elements which give rise to spectral interference in the form of background enhancement or line overlap. At low concentrations, this can be the main determinant of the detection limit. However, a special case of interference effects likely to be encountered in incinerators is the presence of the metals from background due to residues present on the walls of the furnace and duct. For elements with higher sensitivity, e.g. Be and Cr, this is probably the dominant cause of the higher apparent detection limits listed in Column 3 of Table 2. For the less sensitive elements, such as mercury, this background does not have any significant impact. These results clearly demonstrate that while instrument detection limits are the lowest concentration that can be detected, to obtain realistic measurements in the field the limit of quantitative determination (LQD), set at 10 times the instrument detection limit must be used. This is the **practical detection limit** and is more suitable for real-world analysis than the instrument detection limit given above. However it must be noted that the facility detection limit , determined by the background levels normally present in the exhaust gas stream without the addition of metals, may well restrict the sensitivity that is actually achievable.

Transient Behavior

The real-time behavior of metals once they are introduced into a furnace or incinerator are of interest. If this behavior can be accurately monitored then the process can be optimized thereby minimizing the offgas emissions. For example, with the addition of a substantial amount of new ducting for this demonstration, the hysteresis of the furnace was of interest to EPA. With this in mind, we monitored the change in metal concentrations as the metal introduction was turned off and on. We found that the metal concentration dropped rapidly when switched off. The reverse being equally true when the metal was reintroduced, with the signal reaching equilibrium within 5 minutes. This clear cut behavior was repeated for all the metals we checked. These results serve to demonstrate the potential of this instrument to process control applications.

Table 2. Detection limits for the air-ICP for various metals under both ideal laboratory conditions and in the field, specifically the EPA facility in NC.

Metal	Instrument Detection Limits (μg/scm)	Detection Limits in The Field at DOE/EPA Test (μg/scm)
As	47	—
Be	0.07	0.6
Cd	2.5	4.5
Co	0.6	
Cr	0.25	1.5
Hg	20	21
Mg	0.05	—
Ni	0.4	—
Pb	0.9	6
Sb	55	60
Sr	0.003	

[**Note:** Table 2 lists the detection limits obtainable for this instrument operating in air-mode, side viewing. Improved instrument detection limits may be attainable using axial viewing. This will be attempted using the air-ICP in the near-future. If successful improvements in detection limits of an order of magnitude better than those given in Table 2 are expected.]

Metal Concentrations and Relative Accuracy

The DOE/EPA demonstration was the first opportunity to check the accuracy and quality of the data provided by the air-ICP and, as noted earlier, a number of computational errors were identified during post-test analysis. Figure 2 and Table 4 present both our corrected data (for both moisture and computation errors) and the RM results. The relative errors with respect to the EPA Method 29 are given in Table 3. The reference method was employed at two separate ports, one upstream of the CEMs and one halfway along the length of the ducting. As can be seen from Table 4, three of the five metals are within 30% for the high concentration level. None are within that range at the low concentration level.

At this point, we must note that our group, amongst others,[6] has raised concerns about the accuracy of EPA Method 29, especially at the low concentration level. We feel that without the determination of the error in the RM measurement (at both the upper and lower ports) using Dual- and Quad-trains, calculation of relative accuracy of the individual CEMs with respect to EPA RM 29 are of limited scientific value at this level.

In addition, the apparent variability in the metal concentration during the runs means that since the ICP measurements are not continuous, the concentration in the duct over the interval of the ICP measurements may be either significantly higher or lower than the average as expressed by the Reference Method.

Recommendations for Program Improvement

1. The CEM committee is already aware of our concerns regarding the accuracy of EPA Method 29 at these low concentration levels and the appropriateness of using a sample method to evaluate real-time techniques. There is a need for a full and open evaluation of EPA Reference Method 29's suitability for evaluating continuous emission monitors.

2. Access to a well-characterized and calibrated facility for long-term testing. The EPA facility personnel did an excellent job supporting the demonstration but the need to extensively modify the exhaust ducting in a very short time frame to accommodate the developers coupled with 1) raises questions with respect to system characterization and calibration. There is the need to develop a system that allows individual CEM testing on less expensive, well calibrated systems.

3. Double blind testing. A more accurate evaluation of the both the CEMs and the reference method would be provided with the use of a double blind test.

4. The requirement to present data overnight without allowing the developers to confirm, correct and submit final data prior to the release of RM results was premature. Further, any conclusions based on this data without making such allowances will underestimate the potential of CEMs not yet at the field deployment stage.

5. Additional funding is required to provide the long-term testing, under real-world conditions, before any multi-metal CEM will be able to meet EPA requirements. Tests such as this one at Raleigh are invaluable to the development of these instruments. However, the cost and the very limited funding available for such research will make further progress very difficult.

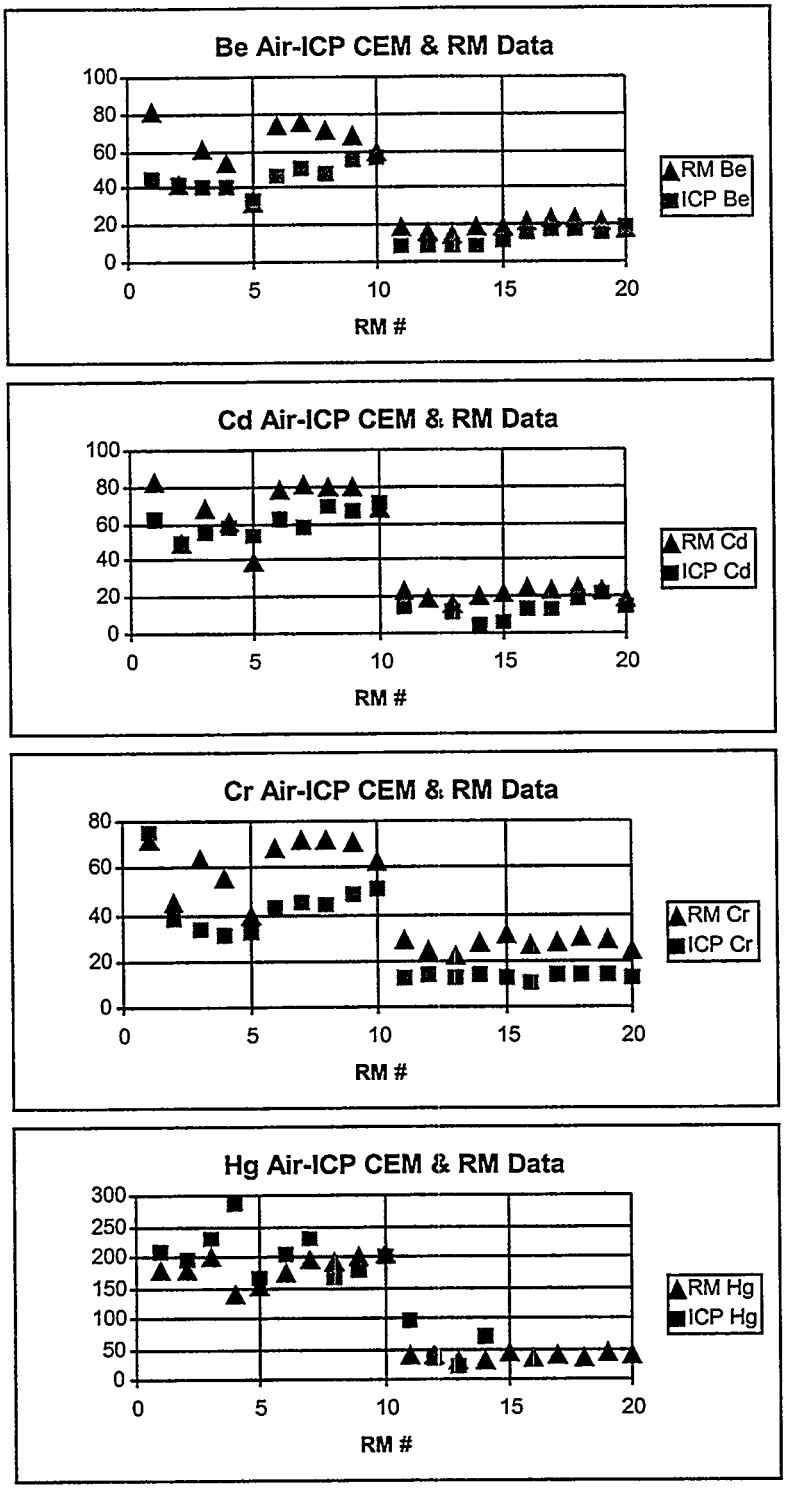

Figure 2. A comparison of average metal concentrations obtained by EPA RM 29 and the air-ICP for each RM run.

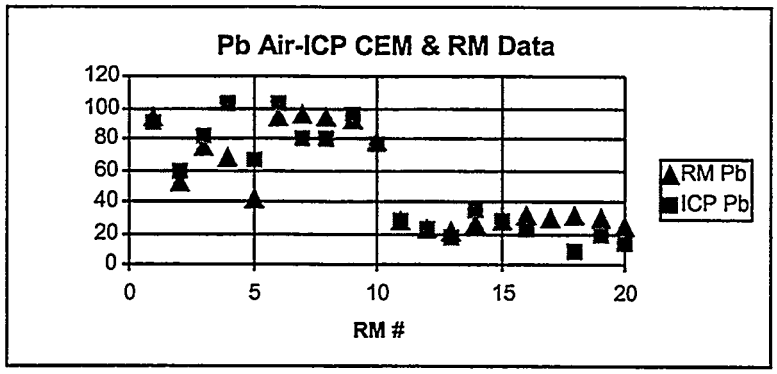

Figure 2. (continued).

Note: These are the corrected results, analyzed after the demonstration was completed.

Table 3. Average Metal Concentrations (µg/dscm) obtained using the air-ICP during each Reference Method Run.

Average CEM Concentrations at Dry Standard Condition (µg/dscm)							
	Time						
RM#	Start	Stop	Be	Cd	Cr	Hg	Pb
1	936	1037	45.50	63.00	75.20	208.80	89.60
2	1125	1225	41.40	49.40	38.30	193.80	58.70
3	1317	1417	41.10	55.40	33.90	231.30	81.10
4	1515	1615	40.70	57.40	31.10	288.10	102.00
5	1702	1802	33.40	53.60	31.90	167.20	65.50
6	1001	1101	46.70	62.20	42.60	202.30	101.80
7	1140	1240	50.20	57.70	45.70	232.40	79.70
8	1340	1440	47.60	69.60	44.00	164.30	79.80
9	1545	1645	54.90	66.70	48.60	179.40	95.10
10	1720	1820	56.00	71.50	50.50	201.90	76.00
11	940	1110	9.10	14.30	12.40	94.70	28.00
12	1145	1315	8.10		13.70	35.20	22.70
13	1345	1515	9.20	11.20	12.60	23.90	17.30
14	1540	1710	8.50	4.70	14.20	68.10	34.00
15	1735	1842	12.10	6.00	12.20	—	28.40
16	920	1050	16.40	13.10	10.10	—	22.70
17	1120	1250	17.90	13.40	13.40	—	—
18	1345	1515	16.80	19.50	13.90	—	9.50

Table 3. (continued).

Average CEM Concentrations at Dry Standard Condition (μg/dscm)							
	Time						
RM#	Start	Stop	Be	Cd	Cr	Hg	Pb
19	1535	1705	16.50	21.80	13.50	—	19.90
20	1730	1900	18.50	15.10	12.70	—	14.00

Table 4. Relative accuracy of DIAL Air-ICP data.

Relative Accuracy, using the Average Upstream EPA RM 29 Measurement					
	Be	Cd	Cr	Hg	Pb
RM 1 to 10	40%	26%	40%	13%	21%
RM 11 to 20	43%	46%	59%	67%	42%

Relative Accuracy, using the Average Downstream EPA RM 29 Measurement					
	Be	Cd	Cr	Hg	Pb
RM 1 to 10	44%	27%	47%	13%	22%
RM 11 to 20	45%	47%	63%	60%	45%

Technology Strengths and Weaknesses

The preeminence of the ICP-AES for trace analysis in solution is unchallenged. The inherent strengths of this technology carries over into this new application e.g., linear range of 7 orders of magnitude, reduced matrix effects, etc. For the air-ICP, we have the ability to handle high loading of particles and moisture, increased sample volume, while reducing operating costs. The reduction in component size eliminates the need for long sample lines and the approach taken with respect to instrument interfacing solves the calibration problem. The present design does not provide simultaneous multi-metal detection but does provide the ideal instrument to evaluate unknown offgas stream with respect to possible interferences and matrix effects. With the identification of these, the use of a purged (or vacuum) polychromator, modified to handle the real-world environment, would solve the multi-metal problem and increase the system sensitivity to allow the measurement of As and Sb down to the levels used in this test.

The promise inherent in UV-HiRIS, due to circumstances beyond our control, was not able to be demonstrated fully in this test. This was due, in part, to the lack of opportunity to interleave the HiRIS system into the basic operating parameters [due to manufacturer delays, HiRIS arrived at DIAL only 3 weeks prior to the test (and damaged)]. This instrument is compact, thermally and vibrationally stable. If the successful combination of the solid-state air-ICP and the HiRIS spectrometer could be achieved this would represent a large step forward in instrument development and will reduce the overall size and weight of the complete air-ICP package substantially.

The one over-riding difficulty in solving the above problems is in obtaining funding support for equipment upgrades and to cover the man-power costs associated with the long-term testing required.

Lessons Learned

This was our first field trip and, as we expected, provided an important shakedown opportunity. We learnt an enormous amount in almost every area. These lessons ranged from the need to automate data collection and analysis as much as possible, to keeping things simple and uncomplicated. With respect to the second item, we were perhaps too ambitious to attempt to use two separate detection systems simultaneously. It quickly became apparent that this required considerably more preparation than was available to us before this test. However, these experiments did provide the first opportunity to test HiRIS with the air-ICP.

We had no major problems with the hardware. The solid-state rf generator proved reliable under extreme conditions. The sequential monochromator-based system while it has advantages in characterizing the unknown composition of an exhaust gas stream, especially where the possibility of spectral interferences exists, has obvious limitations in terms of providing simultaneous metal measurements. Nevertheless, the results presented above clearly demonstrate the potential that ICP technology holds for fulfilling the need for multi-metal continuous emission monitor. The fact that we ran the entire period and had no major hardware problems together with the results presented above clearly demonstrate the promise of this technique.

With respect to the demonstration format, the evaluation of the relative accuracy of the instrument based on the initial (overnight) raw data placed us at a disadvantage to those developers who had taken part in the last year's demonstration test. While appropriate for field-ready instrumentation, this decision does not allow the full potential of previously untested technology to be evaluated. This situation was further complicated by publication of the RM results before the developers had the opportunity to submit a corrected data set to the committee.

None of the technologies represented at Raleigh are novel. Rather, they are previously known techniques facing a new application. Of these technologies, the ICP has the most successful record and would appear, in our opinion, to be the most suitable candidate for an on-line CEM. While some equipment costs will be involved, the major requirement to the successful development of an ICP-based multi-metal CEM is the ability to develop a long-term real-world testing program. Provided funding is available, the Technology Development and Verification Center, presently being instituted here at Mississippi State University, could provide the support infrastructure necessary to perform this work.

Attachment A: HiRIS

Technology Description

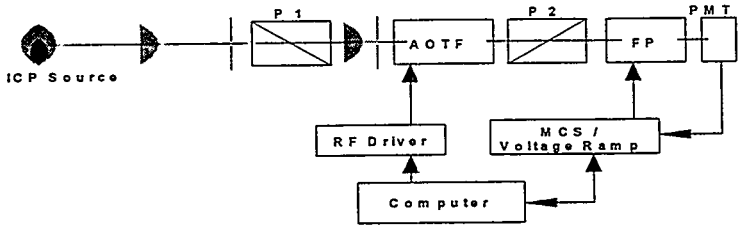

Figure A-1. Schematic diagram of HiRIS.

Air-plasma ICPAES is a sensitive, real time technique for analysis of elemental contaminants in air samples that are introduced into the plasma. Sensitivities to a number of regulated elements have been demonstrated to be nearly as good as those for conventional (argon plasma) ICPAES and sufficient to meet the requirements of proposed EPA rules. Extension of this technique to lower detection limits in complex sample matrices and resolution of analytical lines from the complex emission background in the air plasma may be obtained by improving the spectral resolution of the detection system. Normally this is accomplished by using a higher resolution spectrometer with a longer pathlength. However, the demands of a portable or field-deployable system make the size, weight, and requirements for stability of a long pathlength spectrometer unreasonable. An alternative technique uses a high throughput, short pathlength spectrometric device, an acousto-optic tunable filter (AOTF), as a pre-disperser and a high resolution Fabry-Perot (FP) interferometer to obtain similar or higher resolution spectra with higher sensitivities in a compact package. We have developed high resolution interferometric spectrometer (HiRIS) systems in the past for measuring isotopic abundances and resolving isobaric interferences in actinides. These systems are operated in the blue (395–430 nm) where the emission lines of the actinides are strongest. One of these HiRIS systems will be utilized in FY98 work for monitoring alpha-emitting actinides in stack gases. For monitoring heavy metals, we developed a UV wavelength device consisting of a quartz AOTF and a bulk-optics FP interferometer, to resolve the emission lines of heavy metal contaminants.

AOTF technology involves the use of a birefringent crystalline material in which acoustic waves, induced by an external radio-frequency (rf) source, are used to separate a particular wavelength of light from an incident multiwavelength beam. Typical bandwidths for visible and ultraviolet wavelengths are less than 1 nm (constant frequency bandwidth of 20–40 cm^{-1}). The selected wavelength is continuously tunable by scanning the applied rf frequency. The applied frequency may be changed in a period of ms, allowing selection of emission features over the entire range of the device very rapidly, with no moving parts. Efficiencies are quite good, >85% for most visible wavelengths and ~50% for much of the UV range. For the quartz AOTF, the applied rf frequency causes rotation of the polarization of the selected wavelength; this wavelength is isolated using a pair of crossed polarizers (P1 and P2).

The bulk-optics FP interferometer utilized in this project is a plane parallel device that works on the principle of constructive and destructive interference of light between two coated mirrors. Light that is selected by the AOTF is introduced into the FP; a voltage applied to the FP changes the spacing of the cavity mirrors, thereby scanning the interferometer to produce a high resolution spectrum. Commercially available bulk-optics FP devices are typically capable of finesse (ratio of bandwidth to spacing of consecutive transmission orders) of up to 100. For an AOTF bandwidth of 1 nm, the resolution of the

combined AOTF-FP system is 0.01 nm, without multiple orders being transmitted. This resolution is higher than that of most commercial ICPAES spectrometers. However, during FY98, the resolution of the UV HiRIS can be improved. The quartz AOTF was specified to have a ~1 nm bandpass, but the device that was delivered has a bandpass of ~0.1 nm. By matching the free spectral range (spacing between consecutive orders) of the FP to the AOTF bandpass, an instrumental resolution of ~0.002 nm may be obtained. This improvement in resolution should enable lower detection limits to be attained using the HiRIS.

The development of HiRIS systems based on AOTF and FP technologies was initially sponsored by CMST-CP during FY94, which resulted in the development of a compact, portable spectrometer having the capability of resolving isotope emission lines of actinide elements such as uranium. In following years, support from ANL-West and DIAL for development of this system for potential use in glovebox ICPAES and air ICP emission monitoring applications have been received. The current HiRIS system, developed as a CEM for RCRA metals, was funded by CMST-CP beginning in February, 1997. Optical components of this HiRIS were assembled in June and July, and the system was transferred to DIAL in August, prior to the RTP test.

Equipment

The HiRIS spectrometer and three electronics components (AOTF driver, FP controller, and multichannel scaler) were mounted next to DIAL's 1-m monochromator. Optical emission from the air ICP was detected by the HiRIS system, with computer control of the optical, electronic, and detection systems of the HiRIS. The operational requirements for the HiRIS are 110 VAC power, a nitrogen gas purge (~1 L/m) of the spectrometer to prevent moisture condensation on the optical components inside the HiRIS, and water cooling of the AOTF (provided by DIAL's water recirculator for the air ICP system). The operational requirements and characteristics of DIAL's sampling system and air ICP system have been described above.

Procedures

Calibration of the HiRIS spectrometer was performed as described above for the DIAL 1-m monochromator system by measuring optical emission from the air ICP for solution standards introduced as aerosols, using an ultrasonic nebulizer. The emission intensities for a blank and two or three solution standards were measured and used to construct calibration curves of intensity vs. concentration. Since a calibrated solution delivery rate, nebulizer efficiency, and air flow rate to the ICP were used, the solution concentrations were converted directly to aerosol concentrations. Wavelength calibration of the HiRIS was performed by monitoring the optical emission for the solution standards introduced into the air ICP, using a software peaking algorithm to locate the peaks of analyte emission lines. Metal concentrations in the gas stream were determined by injecting the gas sample from the sampling loop into the air ICP, measuring the optical emission signal, and determining the aerosol concentration from the calibration curve. No calibration check procedure or quality assurance procedures, other than the initial calibration procedures, were used. During the RTP test, the concentration for one element at a time, usually beryllium, was determined at 30-second time intervals.

Results

During the RTP test, metal concentrations for beryllium and cadmium were measured using the HiRIS. The 3σ limits of detection for these two elements are 1.2 μg/acm for Be and 43μg/acm for Cd. Concentrations for the other five metals were not measured because the detection limits for these metals are greater than the aerosol concentrations used during the test. Metal concentrations were measured at 30-second time intervals; this is the frequency of the sampling probe system. The response time for the

HiRIS, under the conditions used during the test, is approximately 8 seconds. A plot of Be concentrations measured using the HiRIS throughout one day, September 23, is shown in Figure A-2. The Be and Cd concentrations measured throughout the RTP test period are listed in Table A-1.

Discussion

The Be concentrations measured using the HiRIS show less than a factor of two difference between the "high" concentration runs (September 22 and 23) and the "low" metals runs (September 24 and 25), with values of less than 20 μg/acm for the first two days and approximately 10 μg/acm for the last two days of the test. However, the difference in concentration between the high and low metals runs was expected to be a factor of 5 (75 and 15 μg/acm, respectively). The fluctuation (relative standard deviation) in the measured Be concentrations was approximately 20% during a particular metals run. While some fraction of the fluctuation is undoubtedly due to measurement errors and uncertainties, a contribution from fluctuations in the RTP source (variation in metals feed rates and emissions rates) is likely. The fluctuation in the Cd concentrations measured September 22 was larger, approximately 40% rsd. Since the measured Cd concentrations, approximately 60 μg/acm, are near the Cd-HiRIS detection limit, this larger fluctuation is not unexpected. The 1s fluctuation in the instrument background should account for at least half of the 40% rsd.

The HiRIS provides a compact, portable spectrometer system that is easily deployed in on-line process monitoring applications. During the RTP test, the need for nitrogen gas purging of the HiRIS was determined; water condensation on the optical components occurred during part of the first week, preventing transmission of ultraviolet light and, therefore, normal operation. Due to the limited amount of time available for development of this HiRIS and unexpected limitations in some of the components, the performance of this prototype HiRIS was compromised. Light scattering by the quartz AOTF causes an elevated, nonspecific background signal that limited the detection capabilities of the system. As a result, only Be and Cd could be monitored during the RTP test. Correction of this problem may require replacement of the AOTF. The mirror coatings of the FP have a wavelength range of approximately 220–240 nm. Since chromium and mercury have no strong emission lines in this wavelength range, detection of these two elements is not possible with the current HiRIS. A second FP interferometer having different mirror coatings would be required for detection of these two metals at the required limits. Finally, the current scanning FP interferometer and PMT detector system is not optimal for multielement CEM applications using the current pulsed sampling system. The use of the PMT results in sequential, not simultaneous, detection of metals. The use of a scanning FP requires that the "correct" voltage be applied to pass the desired analytical wavelength; drift and temperature fluctuations require a voltage peaking routine to be used prior to each measurement, thereby limiting the overall measurement response time to approximately 8 seconds per element. In FY98, a HiRIS consisting of a fixed FP interferometer and an array detector will be developed. This system will eliminate the need for spectral peaking and allow simultaneous measurement of peak and background signals. This system will be more reliable and should improve data collection times to several elements per second.

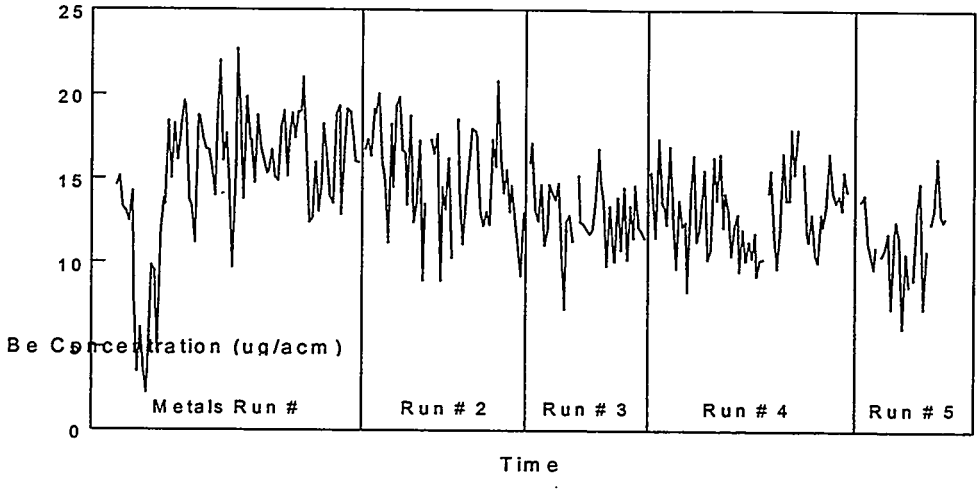

Figure A-2. Beryllium monitoring using the HiRIS on 9/23/97.

Table A-1. Average Dial ICP Hiris CEM concentrations, corrected for T, moisture (µg/dscm).

	Time		Concentrations (µg/dscm)		
RM#	Start	Stop	As	Be	Cd
1	936	1037		33.99	116.66
2	1125	1225		35.22	
3UP	1309	1409		32.61	107.94
4	1515	1615		25.38	94.11
5	1702	1802		23.09	
6	1001	1101		26.50	
7	1140	1240		26.59	
8	1340	1440		22.72	
9	1545	1645		23.03	
10	1720	1820		20.07	
11	940	1110		16.86	
12	1145	1315		14.30	
13	1345	1515		12.24	
14	1540	1710		13.51	
15	1735	1842		13.14	
16	920	1050		21.94	
17	1120	1250		20.23	
18	1345	1515		18.72	
19	1535	1705		20.51	
20	1730	1900		18.38	

REFERENCES

1. Inductively Coupled Plasmas in Analytical Atomic Spectrometry, 2nd Ed. Edited by A. Montaser & D. W. Golightly. VCH Publishers, Inc (1992).

2. G. A. Meyer and M. D. Thompson, Spectrochim. Acta 40B, 195 (1985).

3. M. D. Seltzer and R. B. Green. Proc. Control & Quality, 6, 37 (1994).

4. M. D. Seltzer. Proc. Control & Quality, 7, 71, (1995).

5. D. P. Baldwin, D. S. Zamzow, and A. P. D'Silva. J. Air & Waste Manage. Assoc. 45, 789 (1995).

6. H. G. Rigo and A. J. Chandler, Quantitation limits for Reference Methods 23, 26, and 29. JWM. In Press.

Appendix C

Developer Report
Massachusetts Institute of Technology (MIT)
Microwave Plasma CEM

Microwave-Plasma Continuous Emissions Monitor

Paul P. Woskov, Kamal Haddidi, Paul Thomas, Karyn Green, and Guadalupe Flores
Plasma Science and Fusion Center
Massachusetts Institute of Technology

CONTENTS

FIGURES

TABLES

TECHNOLOGY DESCRIPTION

The microwave-plasma continuous emissions monitor (MP-CEM) uses microwave power at the household oven frequency of 2.45 GHz to sustain a plasma in a flowing sample of the exhaust stack gas for atomic-emission-spectroscopy (AES) of entrained metals. The plasma hardware is mounted onto the exhaust stack and an undiluted sample of the exhaust gas at stack flow velocity is continuously directed into the plasma chamber by a short sample line. The continuous volume of stack gas sampled is equivalent to that sampled by EPA Method-29 but through a shorter sample line. Near *in situ* installation of the microwave-plasma minimizes metals and particulate losses while at the same time provides access to the plasma for real-time calibration. Another advantage of having the plasma just outside the stack rather than inside is that the plasma parameters and size can be optimized for maximum sensitivity. This aspect of the MP-CEM technology is still under development.

The major elements of the MP-CEM and their configuration are illustrated in Figure 1. A short sample line directs a fraction of the stack gas to the microwave plasma. The sample line has a branch just outside the stack that is connected to a calibration system which periodically adds a known metal concentration to provide a real-time span calibration. The microwave plasma volatilizes all particulates, breaks up species into their elemental components, and excites atomic emission. A suction pump system establishes an isokinetic draw of the stack gases into the plasma and returns these gases back to the stack down stream from the sample line. Optics collect the plasma emission light by a longitudinal view down the axis of the plasma column and focus this light onto fiber optics for transmission to a spectrometer system. The spectrometer system resolves the atomic emission spectra for detection. Computers identify the relevant metal transitions and record and display these signal levels in real-time. The strength of the signal levels are proportional to the metals concentrations in the plasma.

DEVELOPMENT HISTORY

Initial laboratory tests of an air microwave-plasma for metals detection were carried out at the Massachusetts Institute of Technology (MIT) in 1993. This work was supported by the Office of Science and Technology, Department of Energy (DOE) as part of a project to develop graphite electrode DC plasma arc technology for the treatment of mixed DOE wastes. MIT worked with Pacific Northwest

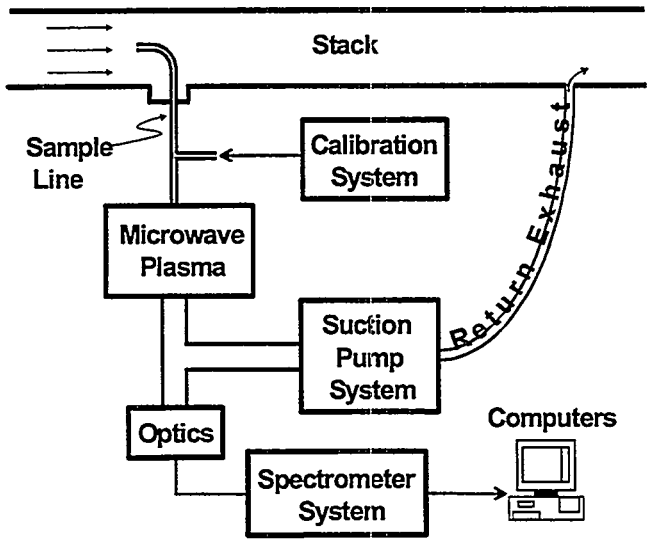

Figure 1. Block diagram of the microwave-plasma continuous emissions monitor.

National Laboratory (PNNL) on this furnace technology for which a number of advanced diagnostic sensors were needed including for heavy metals emissions. The initial 1993 experiments demonstrated robust plasma operation in air and high sensitivity to mercury vapor with a threshold detection limit of approximately 3 $\mu g/m^3$ in slow nitrogen and air gas flows.[1]

In the following two years more extensive laboratory testing was carried out, as well as installation of a microwave plasma inside the exhaust duct of the Mark II pilot scale plasma arc furnace at MIT. Continued laboratory testing confirmed the robust nature of the microwave-plasma including with gas flows having large particulate and water loadings. High-sensitivity ranging from 0.04 to 3 $\mu g/m^3$ was demonstrated for 10 of the Resource Conservation and Recovery Act (RCRA) metals when directly inserted as solids into the plasma.[2] Laboratory tests at PNNL also demonstrated an initial detection limit of approximately 17 $\mu g/m^3$ for plutonium.[3] Following the successful laboratory tests an all refractory material constructed microwave-plasma device was installed into the Mark II arc furnace exhaust duct where temperatures reached 664°C (1227°F). It operated continuously for 49 hours providing qualitative measurements of chromium, manganese, and iron with 0.5 second time resolution.[2] Some preliminary qualitative testing was also carried out in a radioactive furnace environment at PNNL.

In the past year the emphasis of the development activity has been shifted to calibrated quantitative measurements and to improve metals sensitivity in fast aerosol flows. After some initial work with dry powder feeding, a pneumatic nebulizer was configured for real-time injection of calibrated aerosol samples during operation of the MP-CEM on a furnace stack. The present test at the EPA National Risk Management Laboratory represents the first time that the MP-CEM technology has attempted a quantitative measurement on a furnace. This work is currently supported by the Mixed Waste Focus Area, Office of Science and Technology, DOE.

EQUIPMENT

Sample Probe

The sample probe used for the EPA test was a 35 cm long, 6 mm internal diameter fused quartz tube with a 50 mm radiused, 90° bend which intercepted the gas flow in the center of the stack and directed it out the side port. Being just a bare quartz tube it was brought out of the stack trough a standard 5/16 inch vacuum feed through on the port flange.

The original design for interfacing this probe to the plasma was to use a ball and socket joint to connect it to the 19 cm long, 6 mm i.d. tee quartz tube going into the plasma chamber. The ball and socket joint would allow some motion between the stack and the microwave plasma hardware without breaking the sample probe. The total sample line length from the center of the stack to the plasma chamber in this case would have been approximately 57 cm. However, because of the precarious positioning of the plasma hardware on a swaying scaffolding 14 feet above ground level, much larger motions between the microwave plasma hardware and stack than previously anticipated were observed. This necessitated the replacement of the ball joint section with a 1 m long flexible loop of 5/16 inch diameter Teflon tubing. The total sample line length was thus increased to 151 cm for the EPA test even though the plasma hardware itself was only about 30 cm away from the stack port.

The continuous gas volume delivered to the plasma chamber by this sample probe corresponded to 13 liters per minute for an isokinetic sampled gas velocity of 26 ft/sec.

Calibration System

The real-time span calibration system was connected to the quartz tube tee between the sample probe and plasma chamber. The major elements of the calibration system are shown in Figure 2. A spray chamber with a Meinhard nebulizer was connected to the 7.5 cm long branch tube of the tee. A weak nitric acid standard solution prepared by Alfa Aesar containing 200 µg/ml of each metal being

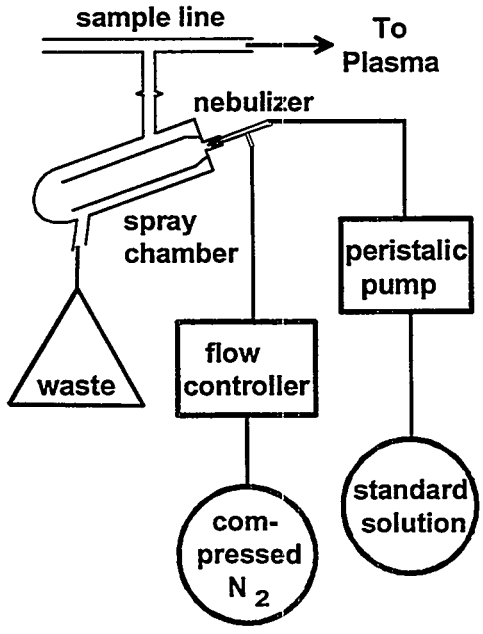

Figure 2. Calibration system.

quantitatively monitored was delivered by a Masterflex C/L peristalic pump to the liquid input of the nebulizer. The pressurized nitrogen gas flow to the nebulizer was controlled by an MKS Instruments flow controller at a rate of 1 liter per minute. The resulting liquid feed rate into the nebulizer was 1.12 ml/min. Since the nebulizer efficiency for small aerosol droplets that get aspirated into the sample line is very low most of the standard solution liquid is collected in a waste flask. The tubing connection to the waste flask must be air tight because it is part of the stack vacuum.

Microwave Plasma

The microwave-plasma system is illustrated in Figure 3. The microwave power source was an ASTeX Model AX 2050 2.45 GHz Microwave Generator which was operated at a nominal forward power of 1.5 kW. A waveguide circulator protected the magnetron source from reflected power by deflecting reflected microwaves into a water cooled dump. During the EPA testing nominal reflected power was approximately 100 Watts. A triple stub waveguide tuner was used to match the waveguide impedance between the microwave source and plasma. The waveguide size was standard WR-284 (3.0" × 1.5" outside dimensions) which is normally used for the next higher frequency band, but in our application this smaller waveguide size increased the microwave power density for improved plasma robustness. A window at the output of the triple stub tuner served as a vacuum seal to the stack and kept the circulator and magnetron clean.

The waveguide section in which the plasma is sustained is tapered in a constant impedance manner to 3.0" × 0.75" to further increase the microwave power density. A 25.4 mm i.d. boron nitride tube penetrates through the center of the wider waveguide walls one quarter wavelength back from the shorted end of the waveguide. The plasma is sustained inside this boron nitride tube. The gas input side of the boron nitride tube is capped with a 5/16" vacuum feed through for the sample line. The sample line enters into the center of the boron nitride tube and terminates about 100 mm back from the base of the waveguide. Swirl gas is also injected at the entry location of the sample line to keep the plasma centered. A high voltage spark near the base of the waveguide is used to start the plasma. The plasma generally extends approximately 100 mm or more toward the optics and exhaust. For the EPA testing the plasma was orientated horizontally.

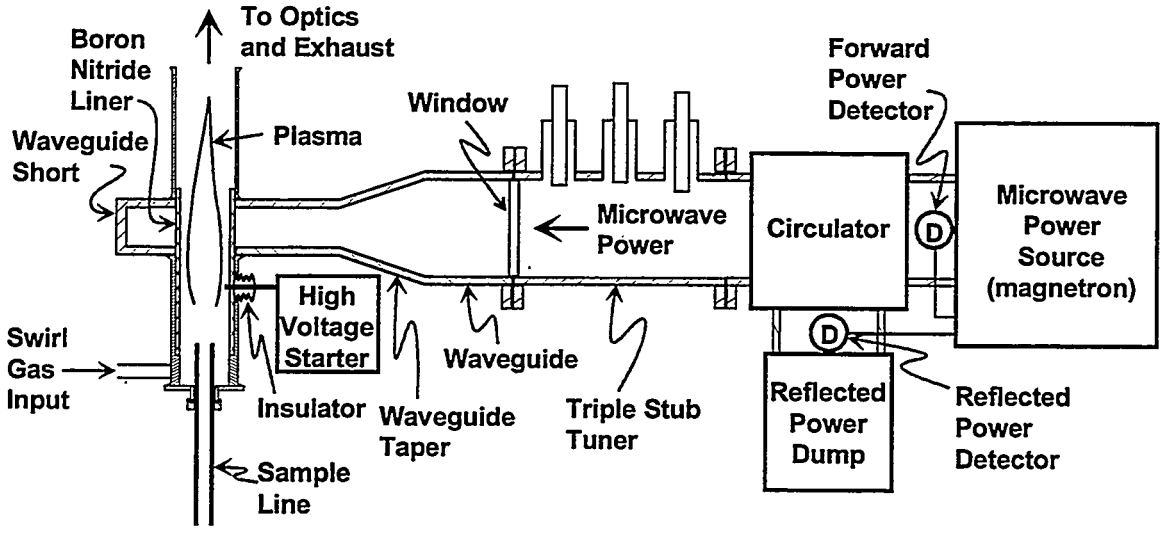

Figure 3. Microwave plasma hardware.

Suction Pump System

The suction pump system was comprised of a heat exchanger, small particle filters, an electrical pump, a valve for adjusting suction, and a flowmeter. Figure 4 illustrates the configuration of these components. The gases from the plasma first passed through a water cooled heat exchanger to reduce the gas temperature down to the operating range of the pump. A small particle filter, Wilkerson Model E16-03-000B C97, was used in line between the heat exchanger and pump to further protect the pump from contamination. The pump was a Cole-Parmer model GX-07055-04 rotary valve oil pump. Two additional filters, of the same type as used at the pump input, were used at the output to filter out pump oil. The plasma gases were returned to the stack through a flowmeter, an Omega Model FL-1501A Rotameter. A bypass valve between the pump input and output was used to adjust suction while letting the pump operate under a constant load.

Optics

The plasma light collection optics used fused quartz for the window, focusing lens, and fiber optics to allow transmission of UV light. A window first sealed the stack and plasma vacuum envelope with a view down the longitudinal axis of the plasma. A small gas jet continuously blew clean air onto the inside surface of the window to prevent deposition of fly ash. The focusing lens immediately outside the window had an F-number of 2. The focused light was bifurcated by a first surface aluminum mirror inserted into the beam such that half the light was reflected to one fiber and the other half was transmitted to a second fiber. Each fiber was a single 1 mm diameter strand. The fiber cable lengths were 2 and 3 meters.

Spectrometer System

Two grating spectrometers were used to perform the AES for the EPA test, located on the scaffold shelving immediately below the microwave-plasma hardware. One spectrometer was a commercial unit, an Instruments SA Model THR-640, 0.64 m Czerny-Turner spectrometer with a 2400 groove/mm grating. It was used with a Princeton Instruments Model IRY-512W intensified 512 element diode detector array. The spectrometer spectral resolution was about 0.03 nm in the UV with the input slit adjusted to a minimum value of approximately 10 μm. This spectrometer was set to observe the 234.9 nm Be transition.

The second spectrometer was an in house built unit using a 3600 groove/mm grating with two linear 2048 element CCD array detectors from StellarNet, Inc. for coverage of two separate spectral

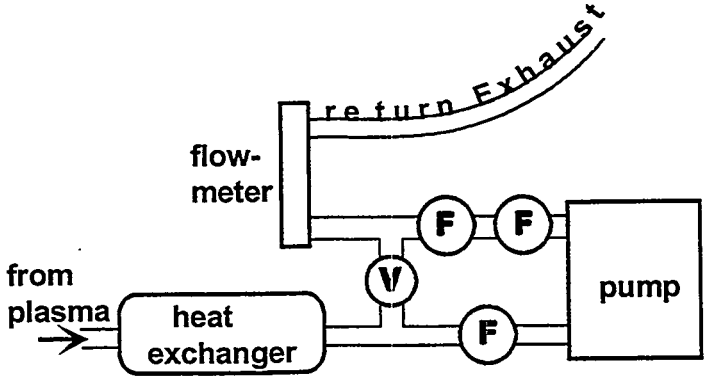

Figure 4. Exhaust system, V: valve, F: filter.

bands. The two bands were fixed to monitor chromium at 359.349 nm and lead at 405.787 nm. The spectral resolution was estimated at about 0.05 nm with a 50 μm fixed slit. Iron was also observed in these bands but did not interfere with the chromium and lead lines used for quantitative measurements.

A PC computer was dedicated to each spectrometer to record and display atomic emission signals in real-time. Data was recorded 2 times a second with the Princeton Instruments detector and approximately 5 times a second with the StellarNet detectors.

Operational Requirements

The operational requirements for electrical power, cooling water, and gas supplies for the microwave-plasma continuous emissions monitor are given in Table 1.

PROCEDURES

Calibration Procedures

Nebulizer Calibration

The nebulizer transport efficiency of the standard solution analyte to the sample line output inside the microwave-plasma chamber is the key parameter which must be known to achieve a precise calibration of the MP-CEM. This parameter was not definitely determined prior the present EPA test and is the subject of continuing research. However, upper and lower limits were established in the laboratory which combined with the initial observation of the furnace metals feed during shakedown testing in the week prior to the reference measurements allowed the selection of a value which proved accurate in the subsequent testing.

A number of different approaches to determine the nebulizer transport efficiency were attempted in the laboratory prior to the EPA test. The first and simplest was to compare the collected waste liquid volume to that which was aspirated from the uptake reservoir. The assumption here is that all the analyte corresponding to the solution volume that is missing in the collected waste is injected into the plasma. This assumption has been shown not to be accurate.[4] Not all the analyte corresponding to the missing solution volume finds its way to the plasma, so this method can only establish an upper limit to the

Table 1. Operational requirements.

Requirement	For	Value
Electrical Power	Microwave source	408 V, 3 phase, 10 A
	Suction pump	115 V, 1 phase, 2.2 A
	Calibration system	115 V, 1 phase, 1 A
	Spectrometers/computers	115 V, 1 phase, 5 A
Water	Heat exchanger	2 gal/min.
Clean Air	Plasma swirl flow	14 l/min.
	Optics window	14 l/min.
Nitrogen Gas	Calibration system	1 l/min.

nebulizer transport efficiency. Averaging six trials we determined an upper limit for the nebulizer transport efficiency of 5.3 ± 1.2% by this approach.

The method generally recommended for establishing the transport efficiency of a nebulizer is to install a filter in the output of the plasma chamber, with the plasma off, and collect all the aerosol aspirated through the system. The filter is then analyzed for the analyte making it directly through the system. In our attempts to implement this approach we found that the filter obstructs the pump suction to such a degree that gas flows through the system could not be established anywhere near the operating values. Therefore we had to abandon this nebulizer calibration approach.

The third nebulizer calibration method which we attempted, and which we believe will eventually lead to a definitive calibration, was to use the light emission from a directly inserted sample mass. A small droplet of the standard solution was micropipetted onto the tip of an alumina rod, allowed to dry, and then inserted near the base of the plasma flame. The resulting light signal was integrated as all the sample mass was volatilized. Next, the feed time of the nebulizer to produce the same integrated signal was determined. Taking the ratio of the directly inserted mass to the nebulizer uptake analyte mass needed to produce the same emission signal gives the mass transport efficiency of the nebulizer to the point of volatilization of the rod inserted sample.

The advantage of this approach is that the entire MP-CEM system is operating exactly as it would for stack measurements except for an alumina rod that is inserted up the center of the quartz tee or through one of the high-voltage starting wire holes. The perturbation of inserting a blank rod was readily determined to be small and easily corrected for.

The main difficulty with this approach is that the inserted rod must be much closer to the plasma flame than the end of the sample line to completely volatilize the solid sample. The nebulizer transport efficiency determined by this approach, therefore is a lower limit because there are additional aerosol transport losses between the end of the sample line and the point of volatilization of the directly inserted mass. Also when the sample rod is almost in the plasma, direct insertion has the additional advantage of a longer plasma residence time for the stationary sample.

Using a 5% nitric acid solution with a 200 μg/ml lead concentration and 2 μl droplets on the alumina rod we determined the nebulizer mass transport efficiency to be: 0.035 ± 0.008% with the point of volatilization 6 mm upstream from the waveguide wall; 0.14 ± 0.06%, 16 mm from the waveguide; and 0.35 ± 0.08%, 25 mm from the waveguide. The plasma heat radiation was not sufficient to completely volatilize the lead sample more than 25 mm away from the waveguide. The sample line output was about 100 mm upstream from the waveguide. As expected the mass transport efficiency of the nebulizer relative to rod insertion increases as the point of rod volatilization approaches the location of the sample line gas flow output. On going research will use lower melting point metals and/or a heated filament to launch a known sample mass at the same location as the end of the sample line to definitely calibrate the nebulizer efficiency for quantitative CEM measurements.

Therefore, at the time the MP-CEM equipment was shipped to the EPA test site we were only able to established the mass transport efficiency of the calibration nebulizer to be between the limits of 0.35 % and 5.3 %. We were also aware of past determinations of the transport efficiency of this type of Meinhard nebulizer to be between 0.5 and 1.5 %.[4]

Field Calibration

The required calibration in the field must to be in terms of a concentration (μg/m^3). Therefore in addition to the nebulizer mass transport into the sample line the volume of gas into which the calibrated

mass is injected must be known. To accomplish this the flowmeter in the suction pump system was calibrated in terms of the actual sample line flow. A Matheson Model 605 flowmeter with a stainless steel ball was attached to the quartz tee input where the sample line would be connect and laboratory air was drawn through it. The Matheson flowmeter readings were record as the suction system valve was adjusted. The MP-CEM was operating as it would be for stack measurements for this sample line flow calibration. The results are plotted in Figure 5. The vertical axis corresponds to the Matheson flowmeter reading in terms of air flow at standard temperature and pressure (the approximate condition for this calibration) and the horizontal axis corresponds to the output flowmeter reading. The measurements were made for two different swirl flow settings covering the range of actual operation during the EPA reference measurements. To establish isokinetic sampling the sample line had to be set at an actual flow of approximately 13 l/min.

The initial field observations of the EPA furnace stack metals feed was used to determine the calibration nebulizer mass transport efficiency. The data for lead on the afternoon of September 19th the week before the reference measurements is shown in Figure 6. The point at which the aerosol metals feed to the furnace was turned off is marked near the middle of the plot. The dashed line through the signal level after the metals feed is turned off denotes the zero metals baseline. The signal level before the metals are turned off corresponds to the concentration of lead present in the stack except for a one and a half minute period near 14 minutes into the data set when the calibration nebulizer was turned on. It was stated at the time that the stack lead concentration was in the range of 20 - 30 μg/acm. The nebulizer

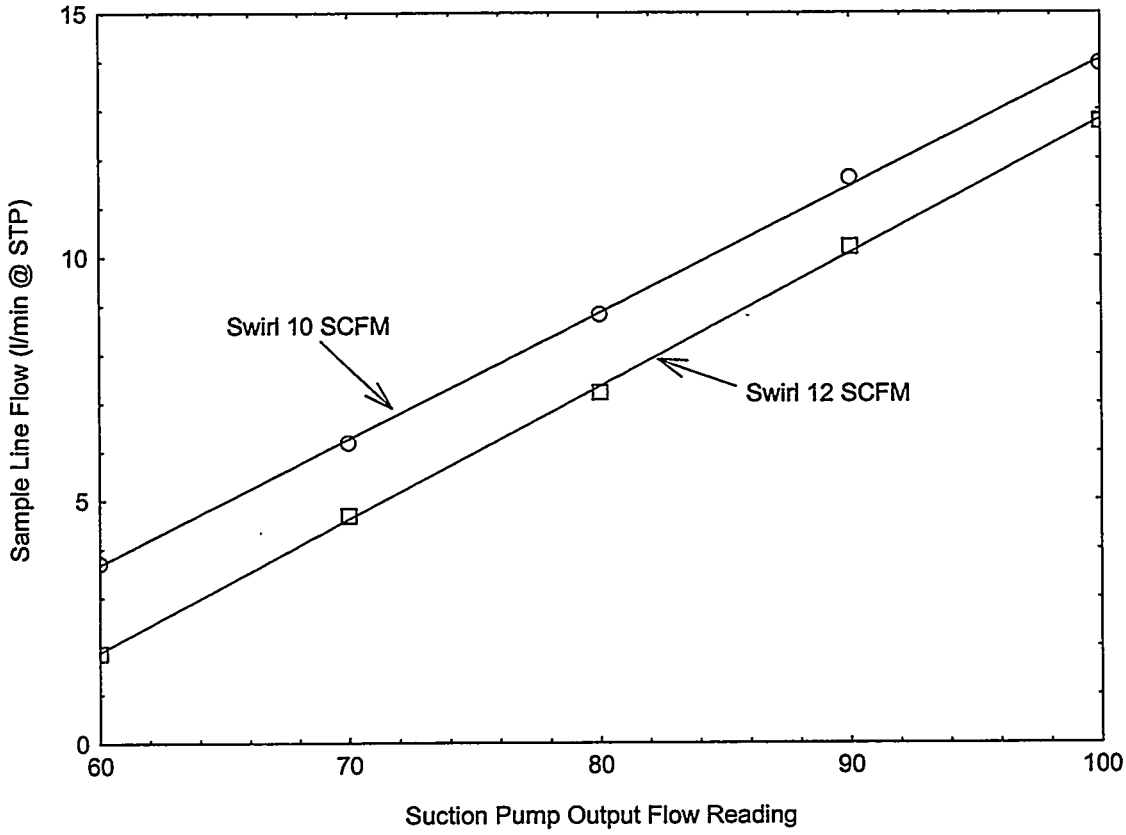

Figure 5. Calibration of suction pump system flowmeter for sample line flow.

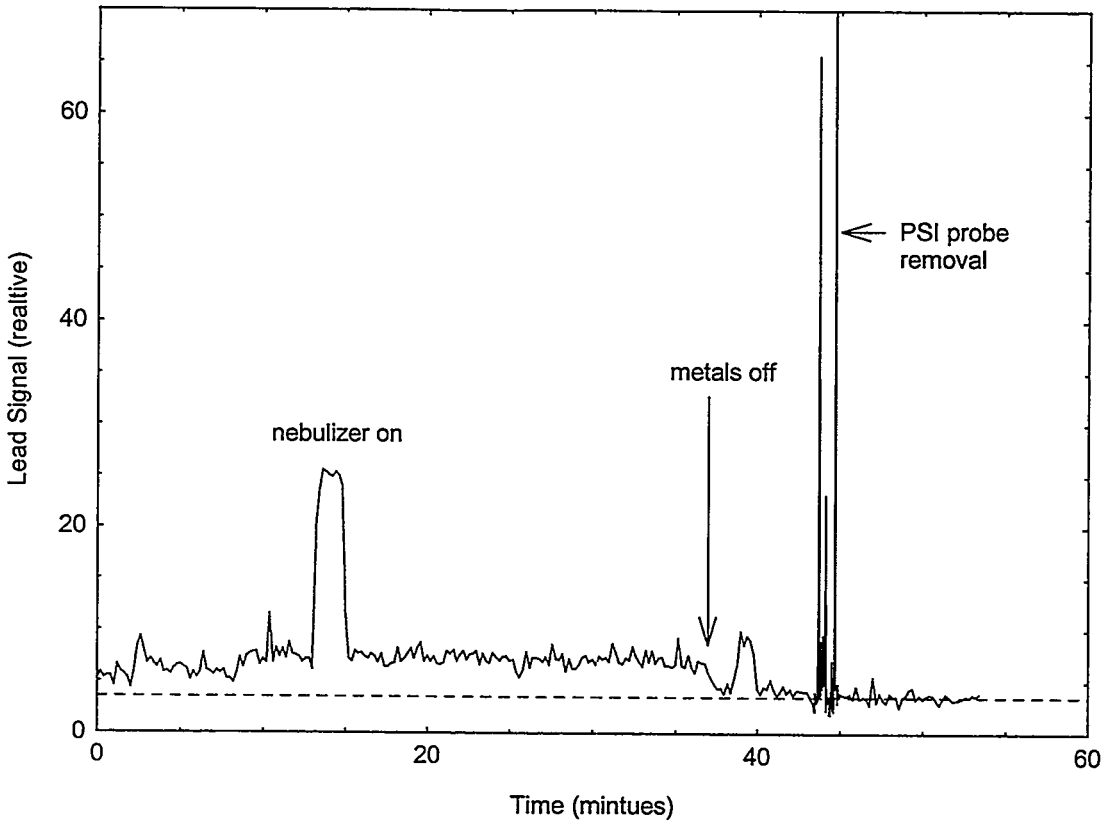

Figure 6. Initial lead signal data during shakedown testing on the afternoon of Sept. 19th.

mass transport efficiency would need to be 0.50% with the above determined sample line gas volume flow to be consistent with this data. This number was also consistent with the laboratory limits and adopted for all subsequent measurements in the following week. The nebulizer transport efficiency is actually somewhat higher if the gas volume flow is corrected for temperature.

Additional features in the metals signals first noted during the shakedown testing were large transients whenever hardware changes were made to the stack. In particular the PSI probe, which was installed at the being of each day's testing and removed at the end of each day, generated signal saturating metals concentrations every time it was removed as shown in Figure 6. This probe was a large aluminum tube inserted halfway into the stack, a cold finger which occluded approximately 20% of the stack cross-section just up stream of the MP-CEM. A small fraction of the metals deposited onto this probe during a day's testing were blow off each time it was removed. Another stack flange opening event further up stream form the PSI probe produced the bump in the signal at 39 minutes just after the metals were turned off. The time resolution for the data in Figure 6 is 12 seconds except for the PSI transients where it is 2.4 seconds.

Wavelength Calibration

The spectrometer detector array pixels corresponding to the metals transitions being monitored were determined by turning on the calibration nebulizer and taking a spectrum for each spectrometer band. Each metal being monitored was present in the standard solution and the desired metals transitions were readily evident when the nebulizer was turned on. The computers were programmed to record and display the detector pixels representing the desired metals. The wavelength calibration was checked at

the being of each day's testing and occasionally during the day. Some pixel drift was noted. For the in house constructed spectrometer this drift was not significant and would not preclude continuous emissions measurements through out the test period if left uncorrected. However, we did optimize the pixel setting if a change was noted. For the ISA spectrometer the wavelength drift was more significant and required correction during the course of a day's testing.

It should be noted that the calibration method for the MP-CEM system automatically corrects for any signal degradation due to wavelength drift away from optimum as long as the drift is not large enough to completely kill the signal.

Procedure for Determination of Metals Concentrations

The procedure for the determination of the metals concentrations is easily understood by referring to Figure 6. For each of the 10 high concentration tests and 10 low concentration tests a data set similar to Fig 6 was recorded showing the metals signal with the metals feed on, metals feed off, and a nebulizer span signal. The fly ash contribution which was continually on throughout the data sets could be distinguished as brief transients at the raw data time resolution of 0.2 seconds and eliminated from the zero and span level determinations. The metals concentration is simply the height of the signal above zero as calibrated by the nebulizer span, 92 μg/acm.

Typical Daily Test Sequence

The typical daily test sequence is outlined in the flow diagram in Figure 7. A typical test day would begin about an hour before the stack metals feed is started with the turn on of the MP-CEM system. The cooling water and suction pump are started first, followed by the start up of the microwave-plasma with the high-voltage spark, and finally the swirl and window gas flows are turned on. Once plasma light emission is established background spectra are stored for automatic subtraction from subsequent emission measurements. The emission wavelengths are checked next by briefly turning on the nebulizer. The data acquisition detector pixel numbers are adjusted in the software if necessary. The data acquisition is then started to record the metals signals, preferably before the stack metals feed is started to get an initial zero level check.

After the reference measurements and metals feed are stopped, the MP-CEM data acquisition continues to acquire a zero level followed by a calibration span check by turning on the nebulizer for one to two minutes. Once the zero and span data are acquired, data recording is stopped. If there is another test, the test sequence starts again with the storing of new background spectra. If the test day is over, then the MP-CEM system is shut down.

The flow diagram is typical with variations during the one week test period. It was not necessary to check the wavelength between every test, particularly late in the day when equipment drifts were negligible. Also the calibration nebulizer was turned on more often than once during some of the tests to get addition span calibration data. One of the advantages of this calibration method is that it can be turned on whenever and as often desired to maintain confidence in the measurements.

RESULTS

Performance

The detection limit for metals in an analytical plasma is generally defined as three times the standard deviation of the signal noise fluctuations. The standard deviation for a given data set is a

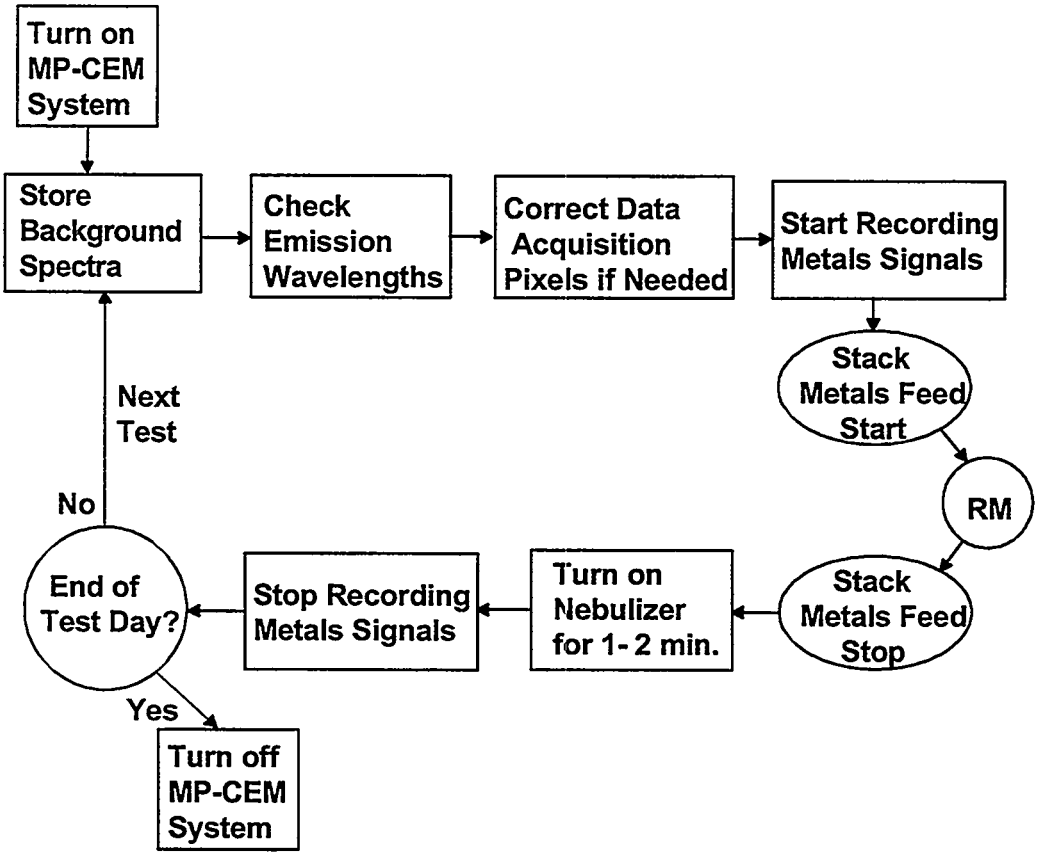

Figure 7. Typical daily sequence flow diagram.

measure of how precisely a root mean square (rms) value can be assigned to that data set. For thermal or white noise the standard deviation varies as the inverse square root of the signal integration time. Incoherent plasma light emission is inherently a thermal process. Therefore, detection limit and response time are related to each other. The lower the detection limit, the longer will be the response time.

The detection limit and its relation to the response time were evaluated for the data taken during the EPA test. Figure 8 shows the analysis of the signal fluctuations for the three metals monitored by the MP-CEM. For chromium and lead 3.5 minute record lengths of approximately 1000 points each were evaluated for a detection period when the signal level was relatively flat with fly ash on but no metals feed. For beryllium a 5 minute time period of 600 points was evaluated with both fly ash and metals feed. Each of the data sets was filtered with a number of different integration times which covered the range from 0.2 seconds to 1 minute for Cr and Pb, and 0.5 seconds to 1 minute for Be. For each integration time the standard deviation of the resulting data set was calculated and plotted in Figure 8. The minimum integration time in each data set corresponds to the raw data time resolution. The straight line on the log-log plot is the best fit to all the data points of a square root function as expected for white noise. There is good agreement for a white noise relationship between the standard deviation and response time and no evidence of a 1/F noise limit out to the maximum one minute integration time considered here. Taking three times the standard deviation as the detection limit, the present MP-CEM results show that for a response time of 0.2 seconds the detection limit is approximately 50 $\mu g/m^3$, at one minute it decreases to approximately 3 $\mu g/m^3$, and is projected to be 1 $\mu g/m^3$ for a time response of approximately 10 minutes.

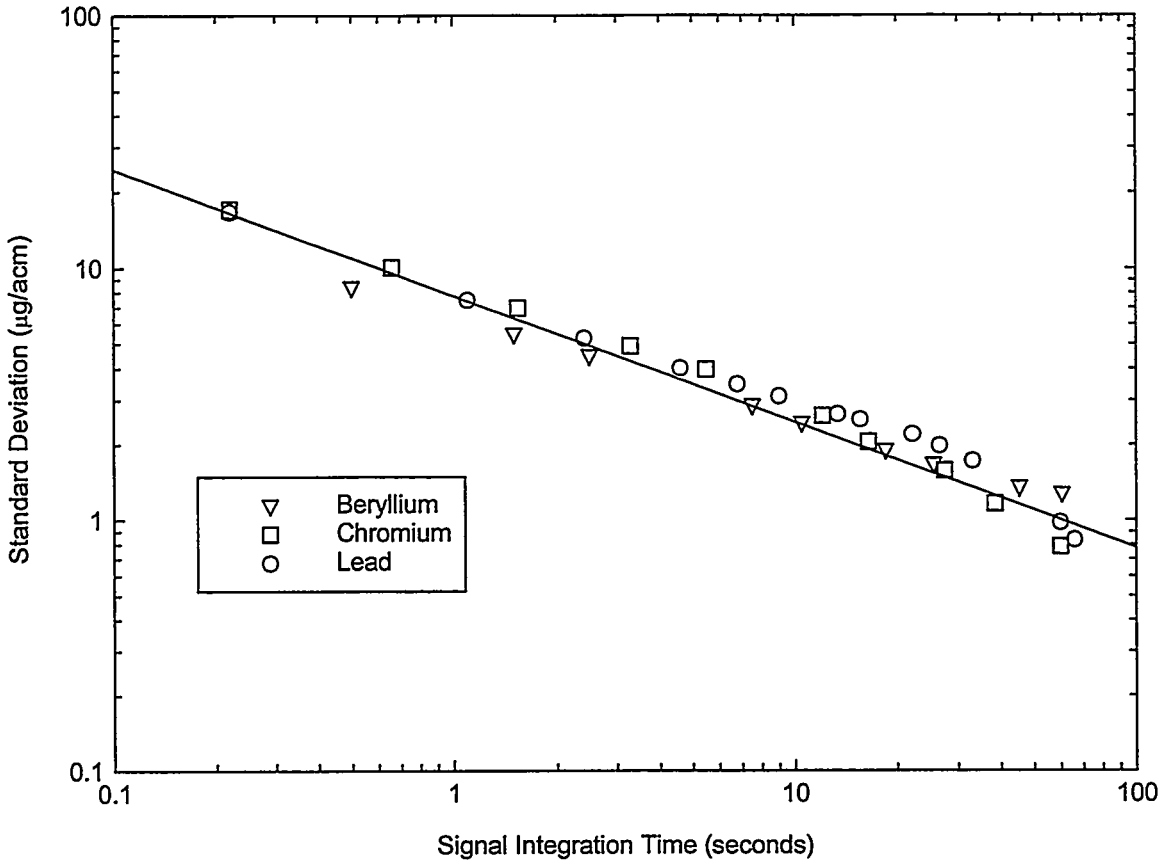

Figure 8. The relationship between detection limit (3x vertical axis) and response time.

Measurements

Data was collected for lead, chromium, and beryllium. Figure 9 shows 3.5 minute long samples of raw data for lead and chromium at the beginning of the first reference measurement test on Monday morning September 22nd. The notable features in the raw data are the large signal spikes caused by individual fly ash particulates. The concentration scale extrapolated from the 92 µg/acm nebulizer level indicates transient concentrations due to lead particulates of the order of 1000 µg/acm and for chromium over 10000 µg/acm. The chemical composition of the particulates varied, some being composed of only lead, some of only chromium, and others with a combination of both lead and chromium. The fly ash contained much more chromium than lead. Similar data for beryllium did not reveal any beryllium fly ash particulates.

The raw data illustrates that the MP-CEM is a truly continuous monitor collecting signal for every particulate at every instant in the sample stream like the reference method. However, unlike the reference method it has a much shorter time resolution and is much more sensitive considering that only a ten minute sample time is needed to achieve a sensitivity of 1 µg/acm. The fly ash transients could be used to determine particulate sizes and number densities as demonstrated by the Japanese,[5] also with a microwave plasma, but for our purposes the raw signals were averaged for comparison to the reference method and the other CEMs.

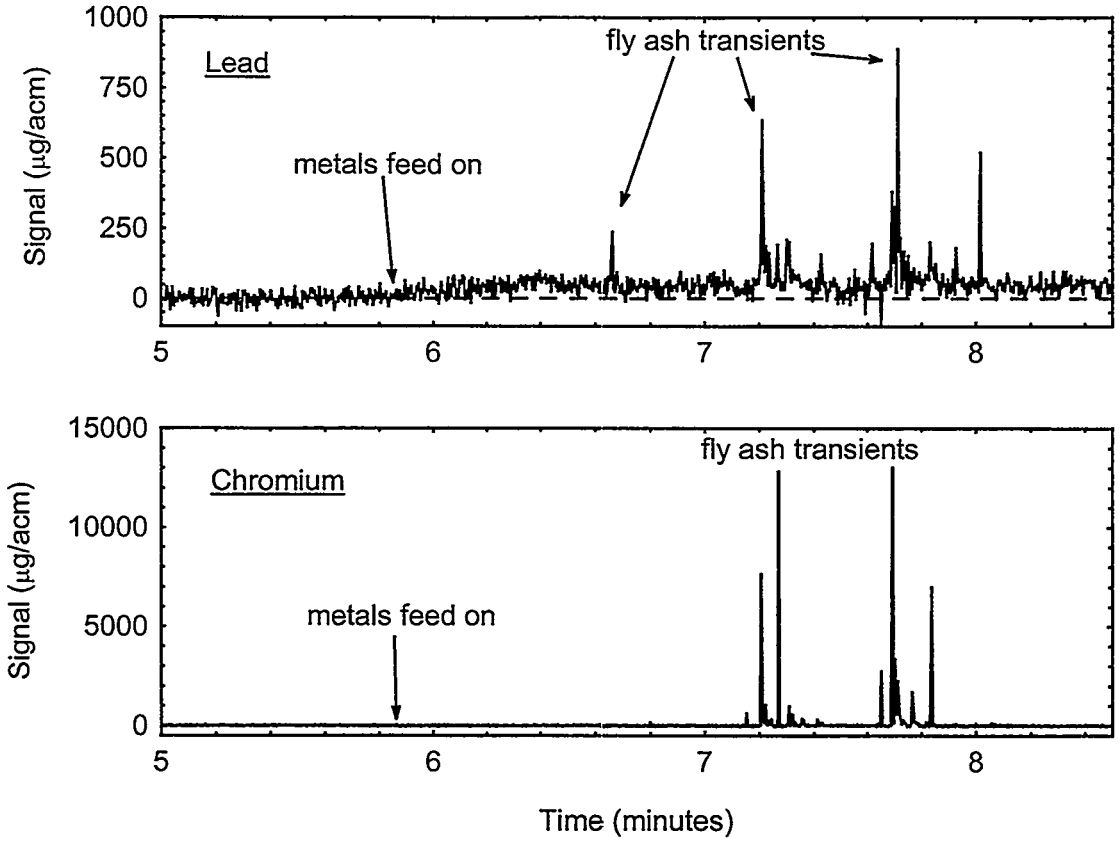

Figure 9. Raw data taken at beginning of the first reference method test Sept. 22nd.

Figure 10 shows the complete data records for Pb and Cr for the time period overlapping reference method test #1 after smoothing with a 1 minute time resolution. These plots are representative of all the tests. The turn on and turn off of the aerosol metals feed into the furnace is clearly evident by the stepped increase and decrease of the metals signals at the beginning and end of each record, at approximately 6 and 89 minutes, respectively in Figure 10. The calibration nebulizer signal, taken shortly after the 100 minute time in this case, is superimposed on the data plots at 94 to 96 minutes. The nebulizer establishes the vertical scale calibration as indicated by the top dashed line. The raw data shown in Figure 9 makes up only three to four points of the Figure 10 plots at the metals turn on time. The very large fly ash transients contribute very little to the integrated data because of their momentary nature. It is also evident from an examination of the data that the threshold detection limit plotted in Figure 8 realistically describes the detectable levels in the 0.2 second data of Figure 9 and the one minute data of Figure 10.

The data was further averaged over the reference measurement time period as indicated in Figure 10 to obtain a single number for comparison with the reference method. The results for all the tests are summarized in Table 2. The early development state of the MP-CEM system for real-time monitoring is evident by the number of missing entries. There was insufficient time prior to the EPA test to bring on line the other metals such as cadmium, mercury, arsenic, and antimony which were all observed in the laboratory, but needed more work to improve sensitivity in fast flowing aerosols. Also, comparatively little time has been devoted so far to the spectroscopy and data acquisition parts of the MP-CEM system. Consequently, a number of the data records of the metals that were monitored were

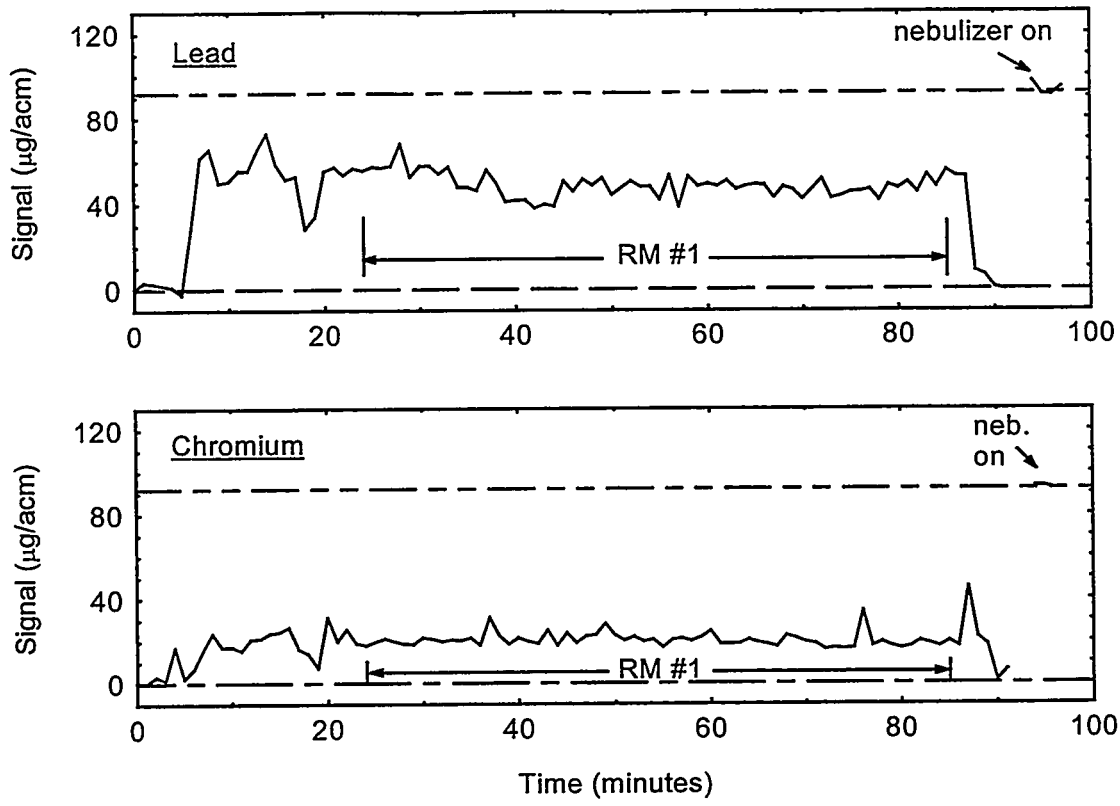

Figure 10. Data for first reference method test with one minute smoothing.

lost or incomplete due to software or detector array electronics problems as indicated in Table 2. However, the first field test of this technology can be considered successful for producing the results that it did.

DISCUSSION

Test Results

The primary goal of the EPA test was to evaluate the relative accuracy of CEM technologies to the EPA reference method (Method 29). In this respect the MP-CEM delivered one of the best performances of any CEM technology in a maiden field test. It portends well for easily meeting EPA's goal for relative accuracy as this technology matures.

Just how well the MP-CEM did is given by the analysis in Tables 3–5. The second column in each table lists the MP-CEM measurement converted to dry standard cubic meters, the third column the average of the two reference methods upstream of the MP-CEM, the fourth column the difference between the MP-CEM and RMs in (µg/dscm), and the last column the difference in per cent. A negative difference signifies that MP-CEM measurement is lower than the RM measurement. Of the 44 individual tests listed in those tables all except 2 agree within 50%. More than two thirds of the measurements for lead and beryllium are within 20% and many are within 10%. Only the results for chromium show a significant systematic offset to lower concentrations. This suggests that there may be a difference in the sack metals concentrations between the upstream RMs and the MP-CEM. If this is true then the agreement between the MP-CEM and EPA reference method may be much better than the present results indicate.

Table 2. MP-CEM measured averaged metal concentrations.

RM Number	Date	Time	Lead (µg/acm)	Chromium (µg/acm)	Beryllium (µg/acm)
1	22 Sept 97	9:36–10:37	43.3	20.2	SDL
2	22 Sept 97	11:25–2:25	43.8	31.1	SDL
3	22 Sept 97	13:17–4:17	36.7	25.9	SDL
4	22 Sept 97	15:15–16:15	39.6	25.8	33
5	22 Sept 97	17:02–18:02	44.3	27.7	SDL
6	23 Sept 97	10:01–11:01	35.2	21.4	SDL
7	23 Sept 97	11:40–12:40	SDL	SDL	SDL
8	23 Sept 97	13:40–14:40	54.5	28.0[a]	SDL
9	23 Sept 97	15:45–16:45	53.7	32.6	SDL
10	23 Sept 97	17:20–18:20	40.6	26.7	SDL
11	24 Sept 97	9:40–11:10	8.8	9.5[a]	7.7[a]
12	24 Sept 97	11:45–13:15	11.2	11.5[a]	—
13	24 Sept 97	13:45–15:15	11.1	7.4	8.5
14	24 Sept 97	15:40–17:10	9.0	6.4	9.1
15	24 Sept 97	17:35–18:42	12.8	12.2	9.4
16	25 Sept 97	9:20–10:50	13.1	DEM	13.9
17	25 Sept 97	11:20–12:50	14.9	DEM	16.3
18	25 Sept 97	13:45–15:15	14.7	DEM	13.3
19	25 Sept 97	15:35–17:05	15.1	11.0[a]	11.3
20	25 Sept 97	17:30–19:00	11.3	DEM	9.1

SDL: software data loss

DEM: detector electronics malfunction

a. Average extrapolated from partial data set.

There are a number of observations that suggest that the stack concentrations are different between the upstream location of the reference methods and the downstream location of the microwave-plasma. First, the ratio of lead to chromium is different. This is difficult to explain unless the stack concentration is different. The microwave plasma is calibrated by injection into the sample line of an aerosol of equal concentrations of metals of the same chemistry as those injected into the test furnace. The ratio of metals entering the sample probe are therefore very accurately measured and are independent of any uncertainty in the nebulizer transport efficiency or in the flowmeter calibration.

Table 3. Lead results.

RM Number	MP-CEM (μg/dscm)	Ref. Methods (μg/dscm)	Difference (μg/dscm)	% Difference
1	75.0	93.4	-18.4	-19.7
2	75.8	52.2	23.6	45.1
3	63.7	74.7	-11.0	-14.7
4	69.0	67.1	1.9	2.8
5	78.1	42.0	35.6	84.8
6	61.4	93.2	-31.8	-34.4
7	—	95.3	—	—
8	95.4	93.2	2.2	2.2
9	94.3	91.8	2.5	2.7
10	71.9	78.8	-6.9	-8.8
11	15.4	27.8	-12.4	-44.6
12	19.6	23.3	-3.7	-15.7
13	19.5	20.2	-0.7	-3.4
14	15.9	26.0	-10.1	-39.0
15	22.6	27.8	-5.2	-18.8
16	22.8	30.9	-8.1	-26.1
17	26.1	29.4	-3.3	-11.3
18	25.9	31.5	-5.6	-17.8
19	26.6	29.5	-2.9	-9.7
20	20.0	23.5	-3.5	-14.9

Second, if the difference between the MP-CEM and RM measurements (4th column of Tables 3-5) are plotted, as in Figures 11, a systematic behavior is evident. At the start of every test day and for every metal the concentration difference is greatest and lower metals for the MP-CEM than later in the day. This behavior is very reproducible and is indicated by arrows in Figure 11. There is nothing in the MP-CEM system that would vary in this way. The nebulizer transport efficiency is a constant with the standard solution flow and gas flow actively controlled. Any other system changes are automatically account for by the span signal. The most likely explanation for the systematic difference behavior is a hardware change in the stack between the RMs and microwave-plasma every morning which absorbs more of the metals in the morning, and as a loose deposition coating is built up absorbs less later in the day. Chromium, being the least volatile of the three metals would be loss more readily also account for the change in the ratio of chromium to lead.

Table 4. Chromium results.

RM Number	MP-CEM (µg/dscm)	Ref. Methods (µg/dscm)	Difference (µg/dscm)	% Difference
1	35.0	71.7	-36.7	-51.2
2	53.8	44.9	8.9	19.8
3	44.9	64.2	-19.3	-30.0
4	45.0	56.2	-11.2	-19.9
5	48.5	40.0	8.5	21.5
6	37.4	68.7	-31.3	-45.6
7	—	71.9	—	—
8	49.0	70.0	-21.0	-31.9
9	57.2	70.8	-13.8	-19.2
10	47.3	63.1	-15.8	-25.1
11	16.6	28.8	-12.2	-42.3
12	20.2	24.8	-4.6	-18.7
13	13.0	22.2	-9.2	-41.4
14	20.4	27.6	-7.2	-25.9
15	21.5	31.3	-10.0	-31.3
19	19.4	29.3	-9.9	-33.8

Table 5. Beryllium results.

RM Number	MP-CEM (µg/dscm)	Ref. Methods (µg/dscm)	Difference (µg/dscm)	% Difference
4	57.5	54.3	3.2	6.0
11	13.5	19.3	-5.8	-30.2
12	—	16.0	—	—
13	14.9	14.9	0	0
14	16.0	18.8	-2.8	-14.7
15	16.6	19.5	-2.9	-15.0
16	24.2	22.2	2.0	9.0
17	28.5	23.1	5.4	23.5
18	23.4	23.5	-0.1	-0.3
19	19.9	21.3	-1.4	-6.4
20	16.1	17.4	-1.3	-6.9

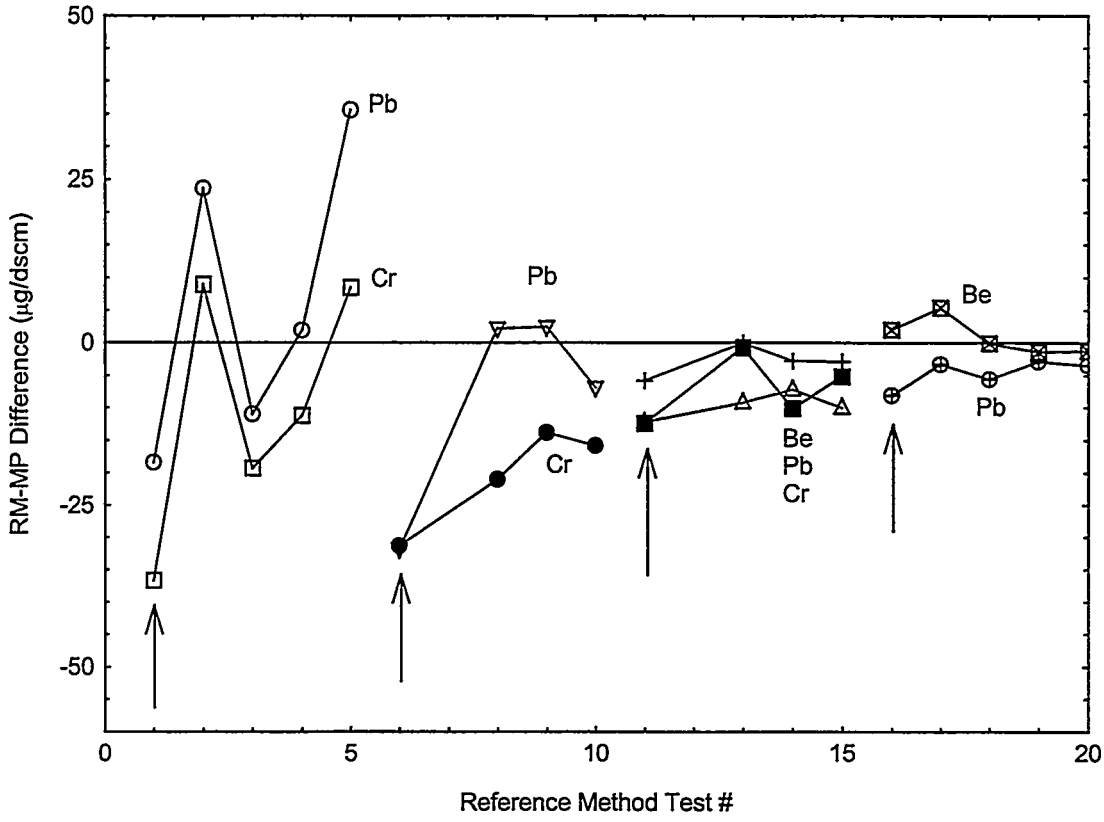

Figure 11. The difference between the reference method and microwave-plasma measurements. Arrows point to the first measurement each day.

Third, we observe very large saturating metals concentrations at end of every test day as documented in Figure 6 when the PSI probe is removed and the vacuum break blows off loose deposition off the probe into the stack. The most likely source of this deposition is the stack gas. The PSI probe was freshly reinstalled every morning between the RM locations and the MP-CEM.

The MP-CEM agreement with the reference method measurements is very close and a 10 to 20 % perturbation in the metals concentration between the RM locations and the microwave-plasma would have a significant effect on the present results. It is very likely that if a reference measurement was made right beside the MP-CEM, agreement would be within a few per cent. It could be further stated that if on installation of the MP-CEM system it was operated side by side with the reference method and the nebulizer and flowmeter calibration transferred from the reference measurement, then the MP-CEM would be accurate to the within a few percent for all subsequent monitoring. The measurements would also be directly traceable to the EPA standard, a necessary requirement for regulatory acceptance.

If this reasoning is correct then the present results represent a significant advance for the development of multimetals CEMs. They demonstrate for the first time that the EPA goals for accuracy can be achieved and they demonstrate a method by which they are achievable. However, there is a caveat to the calibration method as demonstrated. Only a span calibration was demonstrated. The zero calibration which is just as important for an accurate measurements was obtained as an artifact of the testing processes. The feed metals were always turned off between the RM tests allowing continual updating of the background spectra zero for metals emission signals. It is true the fly ash was on continuously, but because of the speed of MP-CEM system it was possible to look between the fly ash

particulates after the metals feed was turned off to determine the true zero level. In an actual furnace facility installation a CEM can not depend on having the metals turned off for a zero check, therefore a zero check method must be implemented in the CEM system. This should be a realizable development goal for future work.

Technology Strengths and Limitations

The microwave-plasma CEM has many strengths. It is flange mountable to the exhaust stack and samples a large, undiluted, isokinetic sample volume on which a large continuous plasma is sustained. It is truly continuous, sampling every particulate and at every instant of time in the sample stream just as the reference methods. It is capable of very fast time resolution and already meets EPA's current requirement for detection limit for Cr, Pb, and Be. The MP-CEM has the combined advantages of near *in situ* operation for sampling a truly representative volume of stack gas, with the advantage of being just out side of the stack to allow access for a calibration system and for better control of the plasma parameters for maximizing sensitivity. This unique configuration for the MP-CEM should eventually allow it to achieve a very high performance capability in both measurement accuracy and sensitivity to meet all of EPA's goals.

Another advantage of the MP-CEM is that it makes use of relatively inexpensive and reliable components. The magnetron microwave source technology is mass produced for home kitchen ovens. It is a very mature and reliable technology with long lifetimes between failures. The calibration system used an inexpensive pneumatic nebulizer and flow controllers that have a long history of successful use in laboratories. The in house spectrometer system made use of inexpensive CCD arrays costing ten times less that conventional laboratory grade systems. It is expected that once fully developed the MP-CEM system could be made very affordable to all users.

The main limitation of the MP-CEM technology is that it is still in an early state of development. The calibration system development is not complete. The performance of the calibration system needs to be better evaluated in the laboratory and a zero check method must to be incorporated into this subsystem. More work also remains to be done to improve sensitivity to fast aerosol flows of metals not monitored in the present test. In addition, spectrometer and data acquisition software improvements are needed. There are no fundamental limitations at present to the MP-CEM technology and it is expected that all of EPA goals for all the RCRA metals will eventually be achieved.

ACKNOWLEDGMENTS

The support of Mixed Waste Focus Area, Office of Science and Technology, U. S. Department of Energy for the development of this technology is gratefully acknowledged.

REFERENCES

1. P. P. Woskov, D. R. Cohn, D. Y. Rhee, C. H. Titus, J. K. Whittle, and J. E. Surma, Diagnostics for a Waste Remediation Plasma Arc Furnace, Proc. 6th Int. Sym. on Laser-Aided Plasma Diagnostics, Bar Harbor, ME, pp.260–266, and MIT Plasma Science and Fusion Center Report PFC/JA-93-28, October 1993.

2. P. P. Woskov, D. Y. Rhee, P. Thomas, D. R. Cohn, J. E. Surma, and C. H. Titus, Microwave Plasma Continuous Emissions Monitor for Trace Metals in Furnace Exhaust, Rev. Sci. Instrum., Vol. 67, pp. 3700–3707, 1996.

3. D. Y. Rhee, K. Gervais, J. E. Surma, and P. P. Woskov, Detection of Plutonium with the Microwave Plasma Continuous Emissions Monitor, 6 pages, MIT Plasma Science and Fusion Center Report PFC/RR-95-11, 1995.

4. D. D. Smith and R. F. Browner, Measurement of Aerosol Transport Efficiency in Atomic Spectrometry, Analytical Chemistry, Vol. 54, pp. 533–537, 1982.

5. H. Takahara, K. Asano, M. Iwasaki, Y. Takamatsu, Y. Tanibata, and T. Suzuki. "Particle Analyzer System", Conference Proceedings 1994, IEEE Instrumentation and Measurement Technology Conference, IEEE Cat. No. 94CH3424-9, p. 833, 1994. JWM. In Press.

Appendix D

Developer Report
Physical Sciences, Inc.
Spark Induced Breakdown Plasma CEM

A Spark-Induced Breakdown Spectroscopy Based Continuous Emissions Monitor for Lead and Chromium

Amy J. R. Hunter, Mark E. Fraser
and
Joseph R. Morency, Constance L. Senior, Thomai Panagiotou, and Steven J. Davis

Physical Sciences Inc.
20 New England Business Center
Andover, Massachusetts 01810

CONTENTS

FIGURES

TABLES

Appendix D

Developer Report Physical Sciences, Inc. Spark Induced Breakdown Plasma CEM

1. TECHNOLOGY DESCRIPTION

The Physical Sciences Inc. (PSI) spark-induced breakdown spectroscopy (SIBS) continuous emissions monitor is based on the vaporization of airborne particulate material and subsequent excitation of the metals by an electric spark. Following this excitation, the emitted radiation is passed through optical fibers to two radiometers, one for the measurement of chromium and another for lead. Each of these units contains dual photomultiplier tubes and on- and off-line interference filters to perform wavelength selection and background subtraction. The radiometers are used to monitor the intensity of the persistent atomic lines and to quantify the amount of each of the metals present. This scheme is presented as a block diagram in Figure 1. This methodology is simple, inexpensive and rugged. PSI has applied for a patent on the SIBS technology.

2. SUMMARY OF TECHNOLOGY DEVELOPMENT HISTORY AND SPONSORSHIP

The integration of the four elements of our system, spark power supply, spark probe, radiometer detection, and computer data acquisition and display, was accomplished on internal PSI funding beginning in June, 1997.The tasks were as follows: design and build the probe, integrate the system components and test in PSI's entrained flow reactor, test for interferences, and measure and optimize the sensitivity for lead and chromium. A portion of the travel and shipping costs for the EPA/RTP test was paid by DoE.

The genesis of SIBS as an analytical technique began with a Navy SBIR Phase I program. The use of spark-induced breakdown spectroscopy (SIBS) has been further developed in part by DoE-FETC under a two-phase program (currently under review for the third phase). To aid decontamination and decommissioning activities, we have examined the use of this technology to monitor As, Sb, Cr, Cd, Hg, Be, Pb in addition to three radionuclides, ^{238}U, ^{232}Th and Tc (a surrogate was tested). The portions of this program that have benefitted the CEM test are use of the spark power supply and knowledge of the relevant wavelengths to measure Cr and Pb.

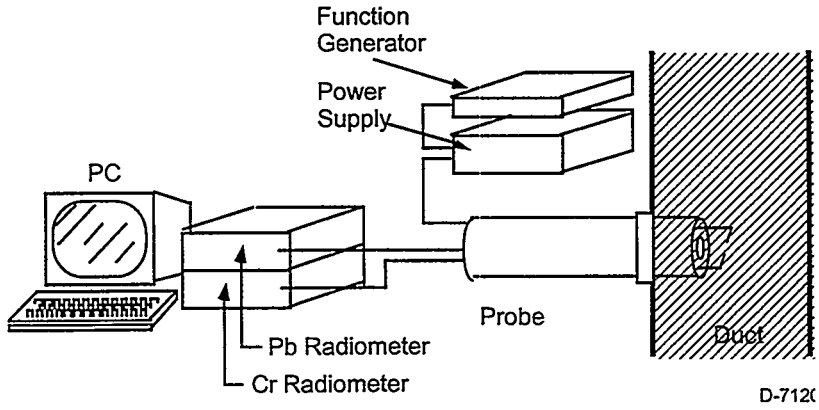

Figure 1. Block diagram of SIBS CEM test instrument.

Appendix D

Developer Report
Physical Sciences, Inc.
Spark Induced Breakdown Plasma CEM

A Spark-Induced Breakdown Spectroscopy Based Continuous Emissions Monitor for Lead and Chromium

Amy J. R. Hunter, Mark E. Fraser
and
Joseph R. Morency, Constance L. Senior, Thomai Panagiotou, and Steven J. Davis

Physical Sciences Inc.
20 New England Business Center
Andover, Massachusetts 01810

CONTENTS

FIGURES

TABLES

Appendix D

Developer Report Physical Sciences, Inc. Spark Induced Breakdown Plasma CEM

1. TECHNOLOGY DESCRIPTION

The Physical Sciences Inc. (PSI) spark-induced breakdown spectroscopy (SIBS) continuous emissions monitor is based on the vaporization of airborne particulate material and subsequent excitation of the metals by an electric spark. Following this excitation, the emitted radiation is passed through optical fibers to two radiometers, one for the measurement of chromium and another for lead. Each of these units contains dual photomultiplier tubes and on- and off-line interference filters to perform wavelength selection and background subtraction. The radiometers are used to monitor the intensity of the persistent atomic lines and to quantify the amount of each of the metals present. This scheme is presented as a block diagram in Figure 1. This methodology is simple, inexpensive and rugged. PSI has applied for a patent on the SIBS technology.

2. SUMMARY OF TECHNOLOGY DEVELOPMENT HISTORY AND SPONSORSHIP

The integration of the four elements of our system, spark power supply, spark probe, radiometer detection, and computer data acquisition and display, was accomplished on internal PSI funding beginning in June, 1997.The tasks were as follows: design and build the probe, integrate the system components and test in PSI's entrained flow reactor, test for interferences, and measure and optimize the sensitivity for lead and chromium. A portion of the travel and shipping costs for the EPA/RTP test was paid by DoE.

The genesis of SIBS as an analytical technique began with a Navy SBIR Phase I program. The use of spark-induced breakdown spectroscopy (SIBS) has been further developed in part by DoE-FETC under a two-phase program (currently under review for the third phase). To aid decontamination and decommissioning activities, we have examined the use of this technology to monitor As, Sb, Cr, Cd, Hg, Be, Pb in addition to three radionuclides, ^{238}U, ^{232}Th and Tc (a surrogate was tested). The portions of this program that have benefitted the CEM test are use of the spark power supply and knowledge of the relevant wavelengths to measure Cr and Pb.

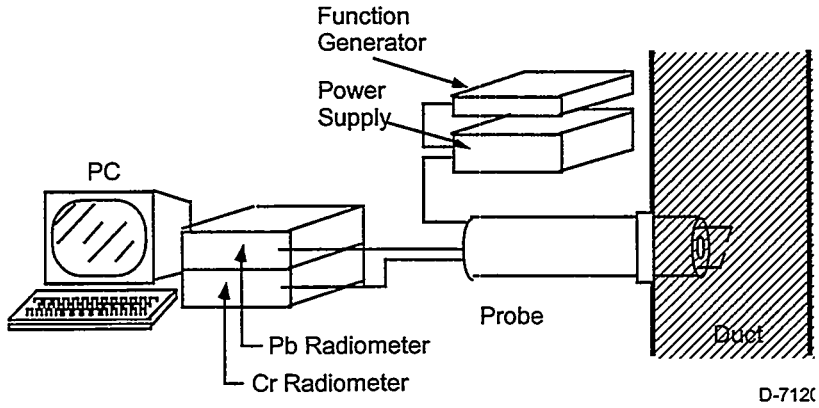

Figure 1. Block diagram of SIBS CEM test instrument.

Another DoE sponsored program has contributed to our success at the EPA/RTP CEM test. This program developed the radiometer and data acquisition and display systems as part of a process control technology for optimizing laser-based coatings removal. The technology has been funded under the SBIR program and is currently in Phase II.

3. EQUIPMENT DESCRIPTION

3.1 PSI Equipment

For the EPA/RTP test, PSI transported our SIBS CEM system (composed of probe, spark power supply, radiometer, and data acquisition and display) plus an optical multichannel analyzer. The SIBS CEM system was designed to measure lead and chromium. The OMA was used as a spectral survey probe to examine possible interferences and to identify promising wavelengths to monitor other elements.

3.2 PSI SIBS CEM

3.2.1 Subsystem A: Sampling Probe and Observation Ports

The probe is a tube that houses optical fibers and high voltage leads and supports the electrodes at the centerline of the duct. A photo of the unit is shown in Figure 2. The probe is entirely enclosed, with a quartz window on the front plate to collect the emission from the discharge. It is air cooled to protect the fibers and the insulative outer sheathing on the high voltage wires. Because of the large surface area of the tube within the flow, 2.5 to 3 cfm of shop air was needed to maintain the required temperature inside the probe (<60 C). The probe is 2 ft long, 3 in. in diameter and weighs less than 5 lb.

The probe was designed to fit into a 4-in. NTP cap outfitted with a vacuum fitting to seal around the body of the probe. The ports at 90 and 180 deg with respect to the probe port were used to install quartz viewing windows to enable visual alignment of the probe so that the electrodes were perpendicular to the flow and that the spark would occur at the centerline of the duct.

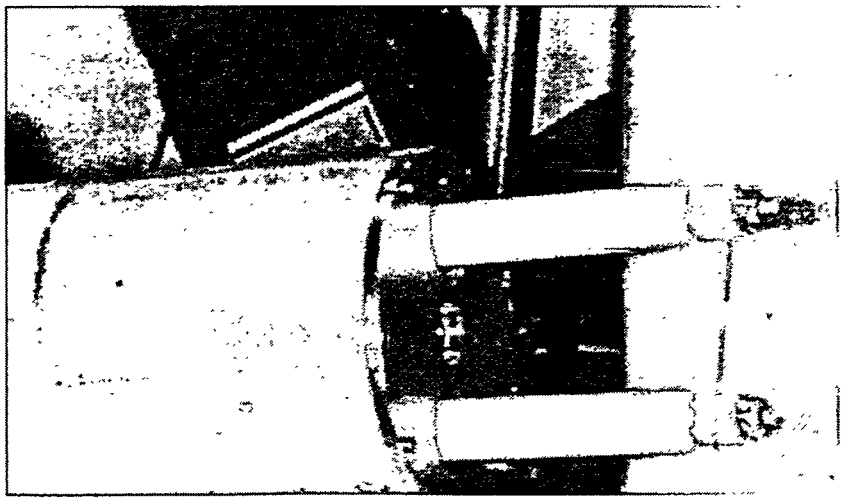

Figure 2. Photograph of SIBS CEM probe showing front face.

The electrodes are two rods at a fixed gap. The electrodes are set perpendicular to the flow of gas though the gap such that the flow through the gap is unrestricted. The pulsed discharge at the gap results in a large volume filling spark (several cubic millimeters) of nearly spherical shape.

3.2.2 Subsystem B: Spark Power Supply

The power supply is housed in a box with dimensions of 13 × 15 × 16 in., and weighs approximately 25 lb. This unit requires 120 V/60 Hz line voltage. The timing of the power supply is controlled by a function generator, which can drive the power supply from about 0.5 Hz to over 10 Hz. The function generator was nearly always used at a repetition rate of 1 Hz, as this was the rate used in the calibration arrangement.

3.2.3 Subsystem C: Radiometer Detection

The emission from the metals in the spark is passed to the radiometer with optical fibers, and detection of the persistent atomic features is accomplished by narrow-bandwidth interference filters and miniature photomultiplier tubes. The strategy behind the radiometer is to accumulate the signal associated with the atomic line with one filter and to subtract any background signal with a nearby filter that has no atomic feature inside its bandwidth. This unit requires only 120 V/60 Hz line current.

Subsystem D: Data Acquisition and Display

The analog signals output by the radiometer are input into a computer with a 1.2-MHz A/D data acquisition board. The temporal traces are evaluated by PSI-developed routines employing LabWindows CVI® software. The on-line and off-line temporal traces are subtracted and integrated.

An example of the screen performing this function is shown in Figure 3. For the testing at RTP, we used collected signal from a temporal regime that mirrored the conditions of the laboratory calibration and testing at PSI.

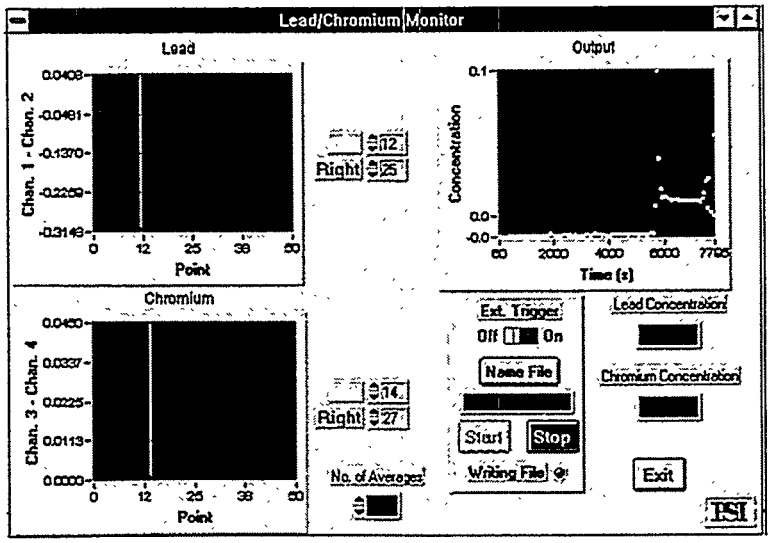

Figure 3. Data temporal control and acquisition screen.

3.3 Optical Multichannel Analyzer System

A complete OMA system composed of a spectrometer, multichannel analyzer array, and data acquisition board, software and computer was also employed at the test. We used this system for semi-quantitative analysis and broad spectral surveys as a supplemental diagnostic.

Input to the OMA used two spare optical fibers from the probe. The data from this system were not used to quantify lead or chromium, so are not included in this report.

3.4 Optical Alignment

We lacked the time and resources to develop an *in-situ*, field calibration source for our CEM. In the laboratory, however, we determined that precise, reproducible optical alignment was the key to maximizing signal and obtaining reliable calibrations.

We therefore developed a method to return the system in the field to the geometry under which it was calibrated in the laboratory. This was performed by imaging a small, battery-operated (two AA batteries) diode laser (at 670 nm) through the collection fibers onto a flat surface a fixed distance in front of the probe. The image was then compared to an image obtained with the calibrated, optimized configuration.

4. PROCEDURES

4.1 Calibration Procedures

The entire unit was calibrated in the laboratory at PSI prior to shipment to the RTP facility. The calibration unit has at its heart a Berglund-Liu style droplet generator for the production of a monodisperse liquid aerosol. Solutions of metal salts dissolved in water are fed through the unit and used to create a metal-containing aerosol. This wet aerosol is then passed through a drying column held above 100 C to remove the water. This apparatus has been gravimetrically calibrated with known amounts of lead nitrate, and has a throughput efficiency to the spark chamber near 90%.

This aerosol generator was interfaced to the probe and the probe calibrated with several known concentrations each of lead and chromium. Each metal calibration generated a calibration factor, which was input to the operating program to convert the raw voltages into concentrations. The two metals were not calibrated simultaneously due to solubility incompatibilities of the salt solutions.

We performed extensive tests in the laboratory with this aerosol calibration source and a multispectral detector (Princeton Instruments OMA) to ascertain interference-free operation within the bandwidths of the filters under the conditions likely to be encountered during the RTP tests.

4.2 Optical Alignment

After calibration in the lab with the aerosol generator, a projection of the diode laser through the optical fibers was made at a short distance from the electrodes of the laser beam. The pattern of the electrodes in their optimized configuration was inscribed on a small piece of plexiglas and used to return the probe to the calibrated state. During the test, it was necessary to perform this task twice, both times after the electrodes had been mechanically misaligned during either insertion into or removal from the test duct. Since this brief check was a simple one, we performed it each morning of the test to assure that the electrode geometry was correct before we started.

4.3 Zero Check

Each morning during the test, immediately following power-up, we tested the gas stream within the duct before the addition of either flyash or metals. This enabled a system comparison to those conditions under which a zero calibration was performed. This check showed no change from the calibration conditions in that it was not necessary to change the PMT voltages to obtain similar curves from the on- and off-line filter channels.

4.4 Procedure for Metals Determinations

Real-time determinations of the concentrations in the gas stream are performed by creating sparks *in situ* and allowing the software to compare the observed intensities at certain set conditions to those obtained during calibration. In particular, this is accomplished by the Lab Windows CVI-based software in a short set of steps upon receipt of the data. The first step is the subtraction of the off-line PMT intensity (the spectral background at a wavelength similar to the atomic emission being used to quantify the metal) from the on-line PMT intensity (the intensity at the wavelength of the atomic feature of interest). These voltages are then integrated and written to a file in strip chart fashion. After the tests, the voltages were input into QuattroPro where backgrounds were determined, and the calibration constant was then applied. The finished files of date, time and concentrations were then copied and given to EPA/DoE personnel.

4.5 Typical Daily Test Sequence

1. Insertion of the probe in the duct: Following the removal of the 4-in. NPT cap, the sleeve for the probe was inserted. Immediately thereafter, the cooling air was turned on, and the probe put into the duct.

2. Alignment of the probe in the duct: The probe was visually aligned at the centerline of the duct and perpendicular to the flow using a flashlight and the two window ports positioned 90 deg and 180 deg to the probe.

3. Begin pulsed discharges.

4. Bring up data acquisition (DAQ) and reduction program and turn on radiometers.

5. Adjust PMT voltages to calibrated state.

6. Ascertain zero levels and other program variables.

7. Turn on data save feature.

8. Monitor temperature of probe throughout run.

9. At end of day, end file save.

10. Turn off radiometers, exit DAQ program.

11. Terminate discharges.

12. Wait for okay to open ports.

13. Remove probe from duct, place on floor away from items likely to melt/combust.

14. Remove probe sleeve and replace 4-in. NPT cap.

5. RESULTS

5.1 Performance Figures of Merit

In the laboratory calibrations, both lead and chromium exhibited 3 detection limits of 9 ppbw which correspond to ~10 μg/acm for the CEM test conditions. Although we were not able to calibrate under the exact CEM test conditions, measurements of the signal to noise with ash during the pre-test conditions indicate nearly a factor-of-two improvement for lead and a corresponding degradation for chromium relative to laboratory calibration.

The PSI SIBS technology has an inherently fast response time. With sufficient analyte signal, detection is possible on each spark. In our current configuration we operate with a spark rate of 1 Hz with 60 s averaging to improve signal-to-noise. (Operation at higher spark rates with corresponding lower averaging periods is possible but has not yet been explored.) Under these conditions, we expect a response time (to a short-lived pulse) of about 1 to 2 min for the SIBS unit. The CEM data directly afford a measurement of the instrument response time. During the test we observed several chromium concentration events which rose and decayed rapidly. These appeared to be short-lived pressure fluctuations entraining ash from the walls probably propagating at or near the average flow velocity. Examination of our chromium data shows the full rise and decay times for these events to be 4 to 6 min. Thus, the measured response time is 2 to 3 min.

5.2 CEM Test Data

The PSI SIBS detector was operational for the full duration of all reference method tests. During these periods we collected and analyzed data for both lead and chromium. Sample plots for these two elements are shown in Figures 4 and 5. The data in Figure 4 were taken on the first day during the third high concentration run. The upper plot shows the Cr results and the lower plot the Pb data. Our average chromium results for this period were 96.0 ± 13.2 μg/acm and the average lead results were 22.7 ±4.3 μg/acm (one standard deviation). It is important to note that these standard deviations are representative of variability about the actual flow and not indicative of noise levels. Figure 5 shows the data from the fourth low concentration run on the third day. The plot shows one large and a second smaller high concentration spike. Several of the data files contain such spikes. The spikes appear only in the chromium data and we believe they correspond to duct operations causing pressure pulses and particle entrainment. The large particle pulse which must be high in chromium then causes a short-lived, but substantially elevated chromium signal. The measured chromium average concentration in Figure 5 was 38.6 ± 15.6 μg/acm and that for lead was 5.2 ± 4.2 μg/acm (also one standard deviation).

A summary of our data for the entire test, with one standard deviation, is presented in Table 1. The standard deviations are well in excess of the signal to noise of the data. The high value of the standard deviations for some RM tests is attributed to large changes in metals concentrations from process upsets (such as the Cr spikes noted previously).

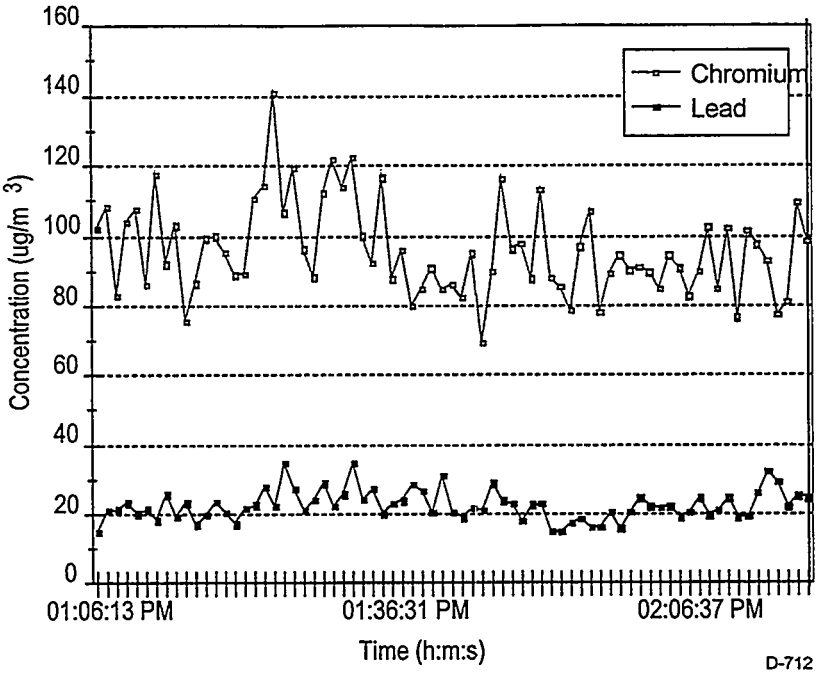

Figure 4. Typical Pb and Cr data: high concentration, first day.

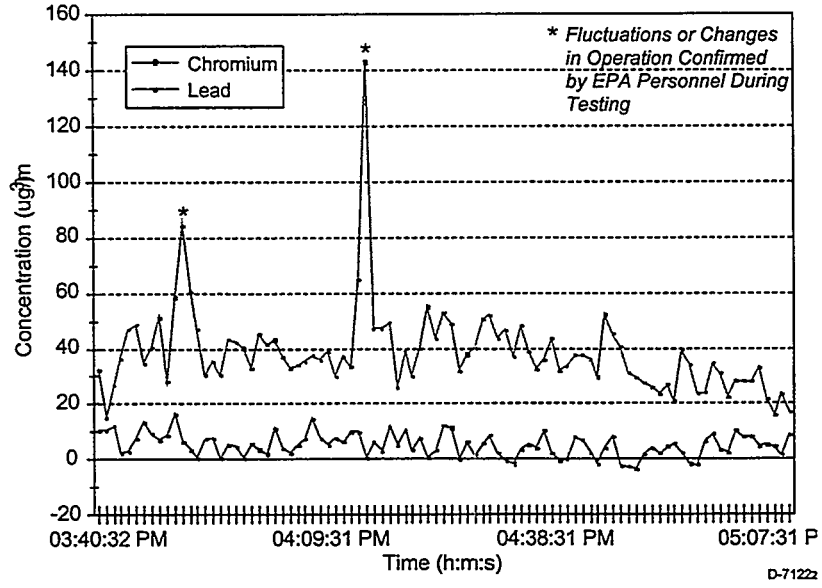

Figure 5. Typical Pb and Cr data: low-level concentration on third day.

Table 1. Metal concentration measurement results for (low | medium | high) test concentrations.

Reference Method	Average Concentration (µg/acm) with Standard Deviation (Note: **Not** corrected for temperature, pressure, or O_2)	
Measurement Period Date and Time	Cr Concentration and Time Period(s) Data Collected	Pb Concentration and Time Period(s) Data Collected
22 Sept 97—1D 0936–1936	70.7 ± 12.6	18 ± 3.3
22 Sept 97—2D 1125–1225	82.6 ± 14.5	16.1 ± 2.9
22 Sept 97—3D 1317–1417	96.0 ± 13.2	22.7 ± 4.3
22 Sept 97—4D 1515–1615	106 ± 27	13.6 ± 5.3
22 Sept 97—5D 1702–1802	75.7 ± 25.1	15.1 ± 9.2
23 Sept 97—1D 1001–1101	33.8 ± 11.1	9.48 ± 4.9
23 Sept 97—2D 1140–1240	42.5 ± 12.3	6.16 ± 6.32
23 Sept 97—3D 1340–1440	68.7 ± 14.2	20.7 ± 6.7
23 Sept 97—4D 1545–1645	88.5 ± 13.8	12.4 ± 5.7
23 Sept 97—5D 1720–1820	67.3 ± 11.4	12.4 ± 5.4
24 Sept 97—1D 0940–1110	40.1 ± 11.5	5.99 ± 3.2
24 Sept 97—2D 1145–1315	24.9 ± 9.5	8.38 ± 5.8
24 Sept 97—3D 1345–1515	43.8 ± 23.3	3.63 ± 4.1
24 Sept 97—4D 1540–1710	38.6 ± 15.6	5.20 ± 4.2
24 Sept 97—5D 1735–1842	20.8 ± 12.4	9.9 ± 4.4
25 Sept 97—1D 0920–1050	49 ± 43	10 ± 13
25 Sept 97—2D 1120–1250	23.7 ± 10.6	5.0 ± 9.2
25 Sept 97—3D 1345–1515	28.5 ± 15	7.1 ±5.3
25 Sept 97—4D 1535–1705	46.5 ± 32	7.2 ±5.8
25 Sept 97—5D 1730–1900	18.6 ± 11.3	-2.9 ± 10.0

6. DISCUSSION

6.1 Comparison to RM Results

We have performed a comparison of our data against the RM data. The results indicate that our measured values typically exceeded the actual chromium values by a factor of two (i.e., we were a factor of two more sensitive to chromium than expected). We are presently trying to understand this observation. We know that the spark discharge was better behaved and more reproducible in the duct than in the laboratory. We plan to investigate whether the duct conditions produce an enhanced signal intensity in comparison to that from the lab aerosol calibrator. The observation of an enhanced chromium signal in the duct underscores the need for an *in-situ* calibration system. Such a system would introduce metals directly in the sampled environment (duct) to provide an unambiguous calibration. We believe that all CEM multi-metal techniques, whether in situ or extractive, will require such a calibration method to establish absolute accuracy.

The comparison of the RM results against our lead data indicate that we were typically a factor of three less sensitive to lead. Our OMA data show no apparent evidence of spectral interference and we have sufficient energy in our spark to make us relatively immune to quenching and speciation effects. We therefore feel that this sensitivity difference may also be due to the dissimilarity in conditions between calibration and measurement, or there may be additional effects contributed by the lead itself under the conditions of the test. In many cases, the lead levels measured by the reference method were below the intended levels. Many of the CEM testing groups (particularly the groups measuring *in situ*) were apparently experiencing difficulties in the measurement of lead. Lastly, we are aware that some developers have expressed concern regarding the absolute accuracy of RM 29 under these test conditions.

6.2 General Performance Characteristics

The probe was designed and built over the summer, and had only been briefly tested in our lab before the EPA/RTP test. This time frame also encompassed our extension of the technology to include chromium. Prior to the summer, the PSI SIBS technology had only been calibrated and field tested for lead in an ambient environment. We believe that a significant amount of progress has been made and we are optimistic that we can further extend the technology to the remaining suite of RCRA metals.

During the test, our station was placed in close proximity to the operations area. Thus, we had immediate access and knowledge of burner operation changes that affected metals concentrations. We found that our elevated chromium concentration events were well correlated to damper changes and other events that could cause elevated ash levels. In the majority of these events we were the first to notify Paul Lemieux of an event which he invariably confirmed. Thus, in a qualitative sense our technology has already demonstrated feedback control.

The PSI SIBS CEM acquired data for both lead and chromium, the only metals we targeted, for all RM test periods. The data do show some discrepancies against the absolute RM values but such differences are typical for the first field test of a new technology. The absolute calibration and performance of the instrument will be improved such that the correlation to the RM data will be improved in the future.

Direct comparison of our data to the RM data is a subject requiring further discussion. We have already pointed out that the standard deviation of our data reflect the variability of the duct operational conditions rather than the inherent noise in our system. The question therefore arises as to how the integrating RM data can be accurately compared to the CEM data which reflect these periodic

fluctuations. We hope that further discussions with the CEM test organizers will lead to a better understanding of these systematic uncertainties.

The biggest strengths of our system are low cost and simplicity. Our entire system can fit on a tabletop or in a 19-in. rack, and the total component cost is very low (< $20K). Ours is probably the only technology tested that could be marketed at a cost affordable to the power industry. This is an important consideration because excessive CEM cost may cause prolonged resistance of the industry to the anticipated regulations. Simplicity is another important consideration. To be successful in the power industry, at a cement kiln, or similar application the technology must be readily operable by existing staff. The PSI SIBS technology offers such simplicity.

The biggest limitations presently are the absence of an *in-situ* calibration method and the need to extend the technology to the rest of the RCRA metals. We are working to solve both of these issues. Extension to the rest of the metals will depend, in part, upon finding reasonable wavelengths. Our preference has been to operate in the visible to minimize expense and to be able to use simple bandpass filters. Moving to the UV and to additional elements may require shorter fiber optics and the use of an optical multichannel analyzer. If the latter is required we will find the least expensive vendor and automate the analysis.

7. RECOMMENDATIONS

In addition to resolving the *in-situ* calibration and metals extension issues noted above, there are several other technology improvements we will be pursuing. These include: redesign of the probe to better dissipate the heat from the duct, improved light collection for better sensitivity, and modifications to the data display software for easier operator interaction.

We are performing this work and are seeking further government funding to accomplish these tasks in a suitable time frame. Commercial sources are also being sought. Our success depends, in part, on receiving these funds.

8. ACKNOWLEDGMENTS

Amy Hunter and Mark Fraser of PSI would like to thank Paul Lemieux and the Acurex crew for all their support. We would also like to thank Bill Haas, Steve Priebe, Nina French and Dan Burns for inviting us to attend the test. Lastly, we'd like to thank Physical Sciences Inc. for sponsoring the upgrades that made our entry to the test such a success.

Appendix E

Developer Report
Naval Air Warfare Center Weapons Division
TraceAIR Multimetals CEM

TraceAIR Multimetals Continuous Emissions Monitor Report and Test Results

E.P.A. Research Center
Rotary Kiln Incinerator Simulator
Research Triangle Park, NC
September 22-25, 1997

Michael D. Seltzer, Ph.D.
Naval Air Warfare Center Weapons Division
China Lake, CA 93555

in collaboration with

U.S. Army Armaments Research, Development and Engineering Center
Picatinny Arsenal, NJ 07806-5000

CONTENTS

FIGURES

TABLES

Appendix E

Developer Report
Naval Air Warfare Center Weapons Division
TraceAIR Multimetals CEM

TECHNOLOGY DESCRIPTION

The TraceAIR multimetals continuous emissions monitor[1] continuously extracts a stream of sample air from a combustor exhaust stack under strictly isokinetic conditions. Automatic isokinetic extraction is achieved by monitoring such parameters as stack gas velocity, temperature, and pressure, using these parameters to calculate the appropriate volumetric sampling rate for 100 percent isokinetic conditions, and adjusting the sampling rate accordingly using a computer-actuated mass flow controller. The sample air stream is pneumatically transported through a heated transfer line to the elemental analyzer. Periodic introduction of aliquots of extracted air, into an inductively coupled argon plasma, enables elemental analysis of entrained particulate matter and metal vapors using classic atomic emission spectrometry. Particulate matter entering the hot argon plasma is instantaneously vaporized and excited resulting in the emission of characteristic wavelengths of light. A direct reader polychromator permits simultaneous detection of up to 61 individual emission wavelengths. Detection methodology features blank subtraction, on-line correction for spectral interferences arising from plasma emissions from both atomic and molecular species in the sample air stream,[2] and automatic correction of metal concentrations to dry, standard conditions. A diluent oxygen analyzer, positioned at the end of the sampling system, permits automatic normalization of metal concentrations to 7 percent oxygen. The TraceAIR system is entirely automated with the exception of calibration and QA/QC procedures, and is capable of autonomous operation. The TraceAIR system, as presently configured, provides measurement results at 1–2 minute intervals depending on user-selected display and data processing options. Activation of a data limit check function enables automatic alarms or triggering of automatic waste feed cutoff. Figure 1 is a schematic drawing of the TraceAIR system, showing all major components.

TECHNOLOGY DEVELOPMENT HISTORY AND SPONSORSHIP

The TraceAIR Multimetals CEM was developed at the Naval Air Warfare Center Weapons Division, China Lake, CA as a result of a 3 year effort sponsored by the Army Demil Technology Office through the U.S. Army Armaments Research, Development, and Engineering Center, Picatinny Arsenal, NJ. Development of the TraceAIR system was greatly facilitated by a Cooperative Research and Development Agreement established between the Navy and Thermo Jarrell Ash Corporation (TJA), Franklin, MA. A license agreement has recently been signed that will enable commercial production and marketing of the TraceAIR technology by TJA.

EQUIPMENT DESCRIPTION

Sampling System

A heated, stainless steel Method 5 sampling probe is mounted securely using a locking and sealing flange. To accommodate the recent text conditions, a 3/8" diameter isokinetic sampling nozzle was positioned at the stack centerline with the nozzle opening oriented to directly intercept the flow of stack gas. An S-type pitot tube assembly and a type-K thermocouple are mounted on the end of the probe adjacent to the sampling nozzle. The sampling probe is connected to the elemental analyzer using a

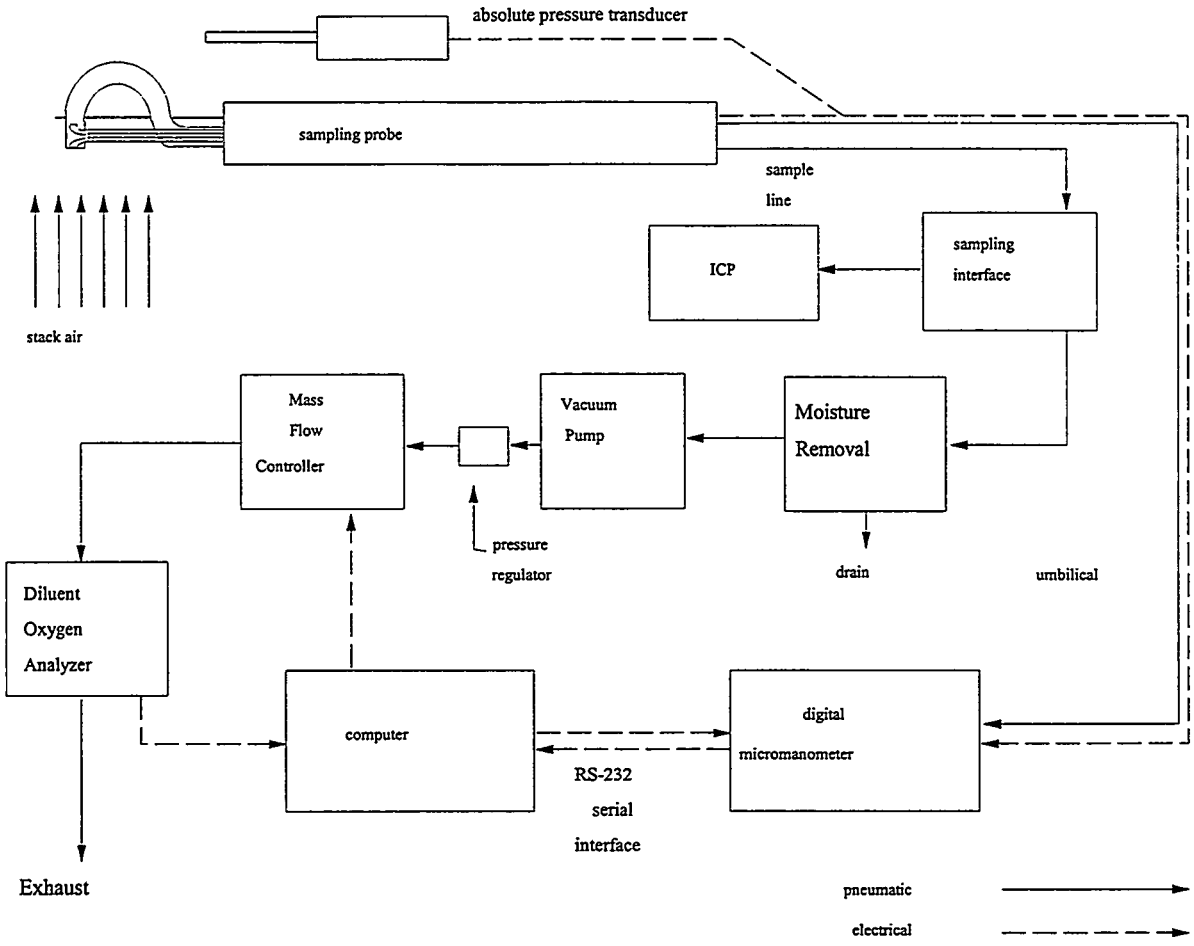

Figure 1. Schematic of TraceAIR multimetals CEM system.

heated transfer line thermostatted to maintain a sample gas temperature above dew point. A standard umbilical is used to provide pneumatic and electrical connections for the pitot tubes and thermocouple, respectively. A digital micromanometer is used to measure differential pressure from which stack gas velocity is derived. A serial interface permits data transfer between the micromanometer and the computer controller. The stack gas velocity, temperature, and pressure is used to periodically calculate the volumetric extraction rate required to achieve 100 percent isokinetic conditions. The computer provides a setpoint voltage through a digital to analog converter to adjust a mass flow controller which throttles the flow rate of the extracted air.

A vacuum pump is used to draw stack gas through the sampling probe, heated transfer line, and sampling interface (described below and in ref. 1). A diluent oxygen analyzer, positioned at the exhaust end of the sampling circuit in accordance with EPA PS-10, Performance Specifications for Multimetals CEMs, to accounts for deliberate or inadvertent dilution of the sample gas, and normalization of metal concentrations to 7 percent oxygen. The voltage output of the oxygen analyzer is interfaced to the computer controller through an analog to digital converter. A type-T thermocouple and signal conditioner are used to measure the temperature of the sample air resident in the sampling interface. A sampling interface is used to accommodate the mismatch in flow rates required for isokinetic extraction (high, variable) and plasma sample injection (low, constant). Extracted stack gas enters the interface inlet port, traverses the length of a sample loop or sample reservoir, end exits the interface through the vacuum

pump, mass flow controller, and to exhaust, such that at any instant, a representative portion of sample air is resident in the sample loop. Meanwhile, a clean air at constant flow is introduced into the argon plasma and serves as a measurement blank. Upon computer command (or manually), a series of solenoid valves are energized causing the flow of extracted stack gas to bypass the sample loop and be diverted to exhaust. Simultaneously, the constant flow of clean air is diverted to the upstream end of the sample loop to pneumatically displace the resident stack gas sample from the loop and into the argon plasma.

Calibration Apparatus

Calibration aerosols are generated from aqueous solutions using a commercially-available ultrasonic nebulizer with an integrated desolvation system. Dry, metal-containing aerosols exit the nebulizer unit and are further diluted within an ambient air stream to a final concentration expressed in micrograms per cubic meter. Typically, a blank plus three standard metal concentrations are used to establish a linear calibration curve. Correlation coefficients of 0.999 or greater are routinely achieved in the field. The calibration apparatus has been standardized in the laboratory using a process that involves the analysis of N.I.S.T. Standard Reference Materials.

Elemental Analyzer

The TraceAIR system employs an inductively coupled argon plasma (ICAP) spectrometer as an elemental analyzer. The ICAP is traditionally used for the elemental analysis of liquid samples such as wastewater. Hardware and methodology were developed to facilitate injection of sample air into the argon plasma. The argon plasma was chosen over molecular gas sustained plasmas because of the 14+ eV excitation provided by argon. Consequently, the argon plasma is capable of exciting the most sensitive atomic and ionic lines of the hazardous air pollutant metals. The plasma is sustained using a fused silica plasma torch positioned within a helical induction coil powered by a1.35 kW crystal-controlled RF generator at 27 Mhz.

Operational Requirements

The TraceAIR system requires a 4-wire electrical hookup capable of supplying 208 V, 1Φ at a minimum of 80 A. Argon gas is supplied from a liquid argon dewar. The TraceAIR trailer must be located with reasonable proximity to the sampling point such that a heated transfer line of 125-foot maximum length can be used.

PROCEDURES

Calibration

The TraceAIR system is calibrated in the field using the apparatus described above. A 1.1 LPM air carrier flow is used to transport the generated aerosols to a concentric mixing device mounted at the inlet port of the sampling interface. The aerosols are intimately mixed with ambient air to achieve a total flow rate of 15.0 SLPM, controlled by a mass flow controller. By introducing aqueous solutions containing 0, 5, 10, and 20 μg/mL into the calibration apparatus, aerosol concentrations of 0, 115, 230, and 460 $\mu g/m^3$ are obtained. These aerosols are introduced in sequence and the resulting atomic emission intensities are obtained. A linear relationship between aerosol concentration and emission intensity is then automatically calculated for each element using the linear least squares method. Following calibration, preparations are made to account, and correct for, spectral interferences arising from the plasma emissions of both atomic and molecular species present in the stack gas sample.

Prior to actual monitoring, an initial calibration verification is carried out in which metal aerosols of known concentration are introduced into the elemental analyzer and measurements are made. The measured concentration values are compared against those stored in a QC table and agreement to within 15 percent is required for successful operation. A zero check procedure involves the introduction of clean, reference air and the measurement of metal concentrations. Successful operation requires the measured values to be less than the absolute value of 2 percent of the calibrated span value.

Wavelength calibration of the vacuum spectrometer is achieved at the time of installation by introducing metals into the ICAP and conducting wavelength scans of short duration over the individual emission peaks. Those channels showing emission peaks offset from their center wavelength must undergo fine tuning, by means of an adjustable refractor plate. Pumping down to the 10 micro-Torr operating pressure thermally isolates the spectrometer and henceforth, channel drift is greatly minimized. During monitoring, the spectrometer undergoes an automatic profiling procedure approximately once each half-hour. This procedure measures the deviation of a representative plasma background emission line from a reference value and the spectrometer alignment is then optically compensated during all ensuing measurements to minimize the effects of any ambient thermal instabilities.

Determination of Metal Concentrations

Aliquots of extracted sample air are periodically introduced into the ICAP. Each aliquot of sample air provides approximately 45 seconds of steady state sample introduction during which all optical measurements are made. Emission intensities are measured for each metal at both peak and background positions in the spectrum resulting in a net emission intensity directly representative of the absolute metal concentration in the sample air. The sample air stream injected into the ICAP is usually at some temperature and pressure other than what exists in the stack itself. The sample air stream injected into the ICAP is also not at dry, standard conditions, *i.e.,* 70°F and 29.92 inches of mercury. To correct the measured metal concentrations to dry, standard conditions, the temperature of the sample air is automatically measured using a thermocouple. The barometric pressure which defines the pressure of the injected air sample, is obtained from a reliable source, or it can be acquired from an appropriate transducer. An estimate of the moisture content of the sample air must also be known. These parameters are used to calculate a correction factor for the metal concentrations that is automatically applied during the conversion of raw concentration data to that in the proper format for reporting purposes. These calculations are performed by the CEM operating software and include such steps as blank subtraction and correction of spectral interferences.

The blank subtraction corrects for concentration offsets due to linear regression calculations in which non-zero intercepts are obtained. Spectral interference corrections on the other hand, are required to ensure accuracy in instances where concomitant metals or molecular species in the plasma emit light at the same wavelengths as the analyte metals.

Final results are displayed on the computer screen for a few seconds in tabular form followed by a display in which up to three elements are plotted as concentration *vs.* time to illustrate trends. Optionally, the final data is printed out along with parameters such as stack velocity, stack temperature and pressure, volumetric sampling rate, sample air temperature, and oxygen content. Optionally, the data can be acquired from external terminals using a modem or appropriate network hardware. All final data is written to a database for later retrieval and archiving.

Quality Assurance Procedures

The primary quality assurance procedure is instrument calibration in which a linear relationship is established between atomic emission intensity and metal concentration. Successful calibration of the TraceAIR system requires achieving a linear correlation coefficient of at least 0.995. Failure to achieve this level of linearity results in deletion or re-measurement of the offending standard. As described above, the field calibration method used by the TraceAIR system is directly traceable to previous laboratory standardization. Secondary QA procedures include the calibration drift checks and zero checks described above to assure the continuing validity of an original calibration. An additional QA procedure is conducted on-line and involves monitoring the magnesium ion/atom emission intensity ratio[3] as a means of documenting plasma robustness and reproducibility of sample air injection. The automated spectrometer profile procedure described above represents yet another QA procedure that helps ensure high precision by mitigating thermal spectrometer drift.

Typical Daily Test Sequence

Instrument warm-up (20–30 min.)
Calibration drift check
Zero check
Re-calibration (if required)
Determination and confirmation of interference correction coefficients
Initiate monitoring (monitoring is entirely automated)
Suspend monitoring
Calibration drift check
Zero check
Down load data for later inspection and reporting
Instrument shut-down

RESULTS

Performance Figures of Merit—Detection Limits

The TraceAIR Multimetals CEM detection limits listed in Table 1 represent values obtained by making 10 replicate measurements while introducing a *stack gas matrix* in the absence of metal concentrations. These detection limits are the concentrations that are equal to 3 times the standard deviation of the replicate baseline measurements. In principle, the detection limit is defined as that concentration of analyte resulting in a detectable signal equal in magnitude to 3 times the RMS value of the limiting noise, or a signal-to-noise ratio of 3, and can be conveniently approximated using the procedure described above. Since these measurements are made while introducing a true sample matrix, they can be considered to be method detection limits.

Estimated Response Time

The response time of a CEM, according to Method 301, is the time required to register 90 percent of the total signal in response to a step-change in analyte concentration. The extractive nature of the TraceAIR technique make necessary that the sample air transit the length of the heated transfer line between the stack and the elemental analyzer. However, this transit time is very short when compared to the measurement period (1–2 minutes). Consequently, the response time is only limited by the measurement period. Any step-change in stack metal concentration will be will be fully indicated within 1 full measurement period, or 1–2 minutes.

Table 1. TraceAIR CEM stack air detection limits *vs.* proposed MACT standards.

HAP Metal	Stack Air Detection Limit µg/dscm	Existing Incinerator µg/dscm	New Incinerator µg/dscm
As	8	210	60
Be	.1	210	60
Cd	.2	270	62
Cr	.5	210	60
Hg	5–10	50	50
Pb	2.5	270	62
Sb	7	210	60

DISCUSSION

Test Results

The TraceAIR multimetals CEM detected all of the spiked target metals during the recent tests at the EPA facility. In addition to the spiked target metals, the TraceAIR system easily detected metals associated with fly ash including the major constituents, Al, Fe; and several of the minor constituents, Mn, Ni, Mg. The TraceAIR system also demonstrated excellent precision and rapid response time. It was observed on the first two days of testing, during high-level spiking, that the metal concentrations detected by the TraceAIR system appeared to be lower than the intended target concentrations (75 µg/dscmDSCM). However, on the final two days of testing, good agreement with the target concentrations (15 µg/DSCM) was observed. General agreement in concentration between metals was evident.

The TraceAIR system underwent periodic zero checks and calibration drift checks, usually before monitoring was initiated and again at the end of each test day. All calibration drift checks passed with the exception of two in which a single metal failed to be within 15 percent of the calibrated value. In those cases, the values were within 20 percent of the calibrated value. The sampling system underwent a leak check prior to the tests to confirm the pneumatic integrity of the probe and transfer line. In addition, the oxygen and carbon dioxide concentrations determined by TraceAIR system hardware were in close agreement with facility CEM readings, providing additional confirmation of the absence of serious leaks.

With due respect to the data formatting requirements specified for this test, and the fact that the TraceAIR is an extractive system that automatically accounts for sample gas temperature and pressure, and reports metal concentrations accordingly, submission of metal concentrations expressed in *micrograms per actual cubic meter* was not feasible. The TraceAIR results, when corrected after-the-fact, for stack gas moisture content, are expressed in *micrograms per dry, standard cubic meter* and therefore are in a format that is amenable to direct comparison with Method 29 results. While real-time data is available from an on-line diluent oxygen analyzer for the purpose of automatically normalizing metal concentrations to 7 percent oxygen as is customarily done, oxygen data was acquired during the recent test for *archiving purposes only* and *no subsequent oxygen correction was made.* For the recent tests, the metal concentrations printed out and submitted on a daily basis, were corrected only for temperature and pressure; corrections for sample gas moisture content were reserved for a later time when accurate

determinations from the reference method sampling trains became available, The data tabulated below has been corrected for moisture content as well as temperature and pressure and is expressed in *micrograms per dry, standard cubic meter.*

CEM Test Program

The CEM test program provided a unique opportunity to evaluate the operation and performance of the prototype CEMs under highly-controlled conditions. Last year's test was particularly beneficial in elucidating a number of hardware and methodology features that needed refinement or re-design. This year's test will undoubtedly serve the same purpose. Future deployment of multimetals CEMs will be accomplished only as a result of iterative testing and refinement and the present CEM test program greatly facilitates that process. The amount of planning that preceded these test was evident in the relative ease with which the tests were conducted. The host facility and staff are to be commended for their superb efforts.

It is the opinion of the present investigator that during future tests, it would be advantageous to not interrupt metal spiking between reference method runs and to allow sufficient time for equilibration prior to the first run. While consideration must be given to conserving materials and limiting the total stack emissions of various metals over the course of the test, efforts to ensure the validity of the test results should take precedence. Some of the TraceAIR CEM data suggest that metal spiking levels were not consistently stabilized in time for the beginning of reference method runs. This was particularly evident for mercury, which was not entirely surprising given the peculiar transport behavior traditionally observed for mercury aerosols.

Technology Strengths and Weaknesses

The TraceAIR multimetals CEM has consistently demonstrated its robustness in operation and its compatibility with various stack gas environments. While analytical performance (sensitivity, accuracy, precision) is generally satisfactory, factors affecting data availability and long-term operation are under consideration. For example, on numerous occasions during the test, the plasma spontaneously extinguished, requiring manual re-ignition. The cause of plasma extinction, and a solution to the problem have been identified. Nevertheless, appropriate software and hardware modifications that will allow automatic re-ignition within 1 or 2 minutes of plasma extinction are under development. At the present time, operation of the TraceAIR system is entirely automated with the exception of calibration and QA/QC procedures and plasma re-ignition as described above. Successful automation of those functions will make the TraceAIR system a fully-integrated and fully-automated continuous emissions monitor.

Recommendations

Several technology refinements have been identified for the TraceAIR system, involving plasma torch design and spectrometer detection that promise to lower detection limits for most or all of the HAP metals. Most significant is the anticipated improvement in mercury sensitivity that will result from these improvements. The TraceAIR system presently detects mercury emission in the deep-UV at 184.950 nm using a first-order spectrometer position. It has been demonstrated that detection of this emission using a second-order spectrometer position allows a dramatic increase in emission throughput to the photodetector, due primarily to the proximity of the second-order line to the diffraction grating blaze wavelength. Given the anticipated improvement in mercury detection and the disappointing outcome of a recent high-visibility program aimed at evaluating commercial mercury CEMs, it is believed that the TraceAIR, with certain improvements, will be able to fulfill many of the present requirements for

continuous mercury monitoring and will be directly competitive with the existing, dedicated mercury analyzers.

Additional improvements in optical throughput achieved through more efficient purging of the optical path between the plasma and collection optics will further enhance mercury detection as well as that of other deep-UV lines such as As, 189.042 nm; Se 196.026 nm; and Tl 190.864 nm. Improvement in purging of the optical path will be achieved through the implementation of plasma torches with extended outer tubes which will also prevent the entrainment of ambient air and help minimize the effects of associated, deleterious effects.

References

1. Seltzer, M. D. and Meyer, G. A., *Environmental Science and Technology* **31** (1997) 2665.

2. Seltzer, M. D., unpublished work.

3. Mermet, J. M., *Analytica Chimica Acta* **250** (1991) 85.

Acknowledgments

The developer of the TraceAIR CEM wishes to acknowledge the sponsorship of the U.S. Army Demil Technology Office, Savanna, IL, and the U.S. Army Armaments Research, Development and Engineering Center, Picatinny Arsenal, NJ, and the generosity and technical support of Thermo Jarrell Ash Corporation, Franklin, MA.

Table 2. Tabulated test results.

	Micrograms per Dry, Standard Cubic Meter						
Date/Time	Arsenic	Beryllium	Cadmium	Chromium	Mercury	Lead	Antimony
9/22 09:36–10:37	55.8	62.6	49.6	40.9	30.9	45.9	54.3
9/22 11:25–12:25	32.8	40.0	38.4	27.0	14.3	31.6	28.2
9/22 13:09–14:09	33.1	39.5	38.9	25.5	26.2	31.1	25.6
9/22 15:15–16:15	36.3	41.9	41.1	26.0	18.3	32.1	31.0
9/22 17:02–18:02	32.9	34.0	33.9	22.6	21.6	26.6	28.4
9/23 10:01–11:01	44.6	52.2	45.7	38.6	33.4	44.0	49.0
9/23 11:40–12:40	37.7	53.6	47.4	38.5	20.0	43.8	48.3
9/23 13:40–14:40	40.2	51.0	47.6	37.7	40.0	42.4	56.1
9/23 15:45–16:45	45.8	53.3	51.8	39.6	20.0	47.9	46.5
9/23 17:20–18:20	46.5	52.7	51.6	39.5	18.3	48.3	46.1
9/24 09:40–11:10	15.2	12.9	13.4	16.2	13.7	12.1	20.5
9/24 11:45–13:15	11.6	12.0	11.3	15.3	8.20	10.9	17.2
9/24 13:45–15:15	14.1	13.3	11.5	15.9	7.27	10.2	28.9
9/24 14:30–17:10	5.6	13.2	11.7	16.4	26.5	11.9	31.2
9/24 17:35–18:42	16.1	13.1	11.3	17.4	13.5	13.3	31.3
9/25 09:20–11:00	13.4	14.0	9.55	12.8	7.94	11.8	9.37
9/25 11:20–12:50	13.8	15.4	9.47	13.1	7.50	11.9	11.2
9/25 13:45–15:15	15.2	15.6	9.93	13.6	8.40	11.7	7.10

9/25 15:35–17:05	15.2	14.4	9.34	13.7	7.65	11.7	9.80
9/25 17:30–19:00	15.8	14.0	8.66	14.2	6.94	11.2	13.5

Chromium 9/25/97

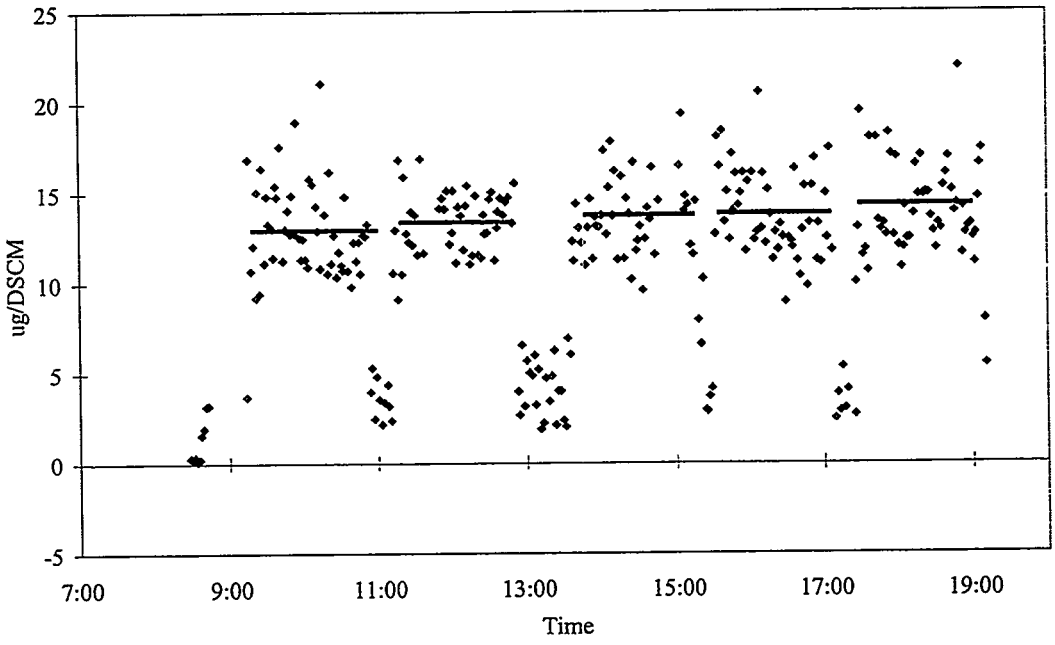

Arsenic 9/23/97

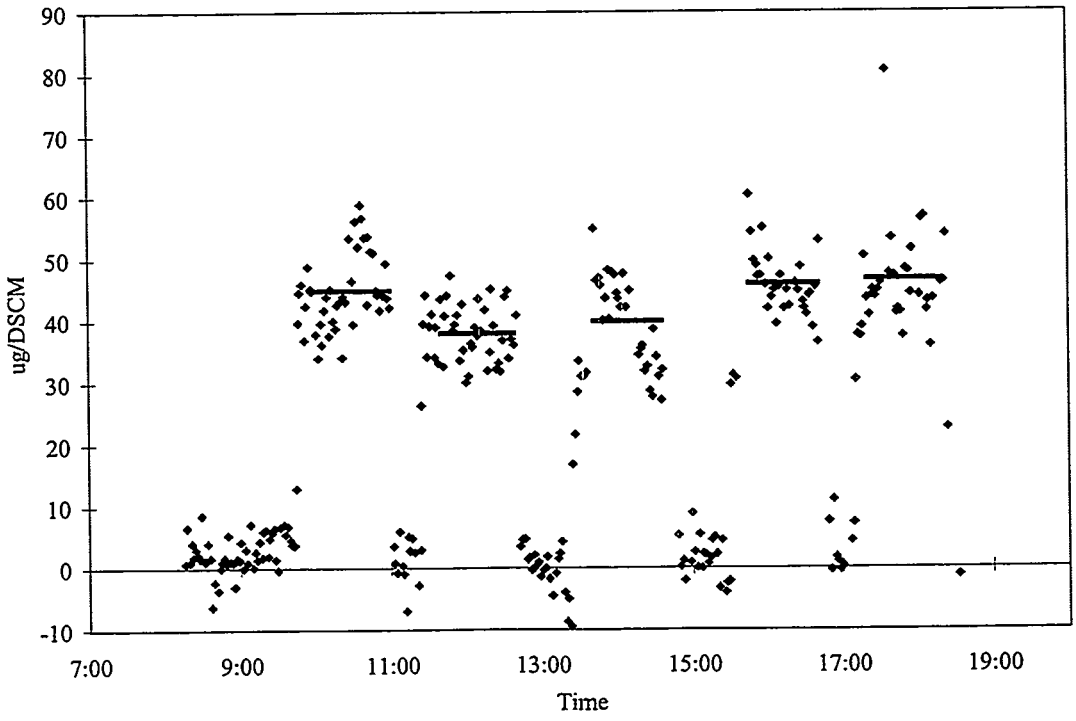

Figure 2. Plots of metal concentration *vs.* time. Solid lines denote average value over RM period.

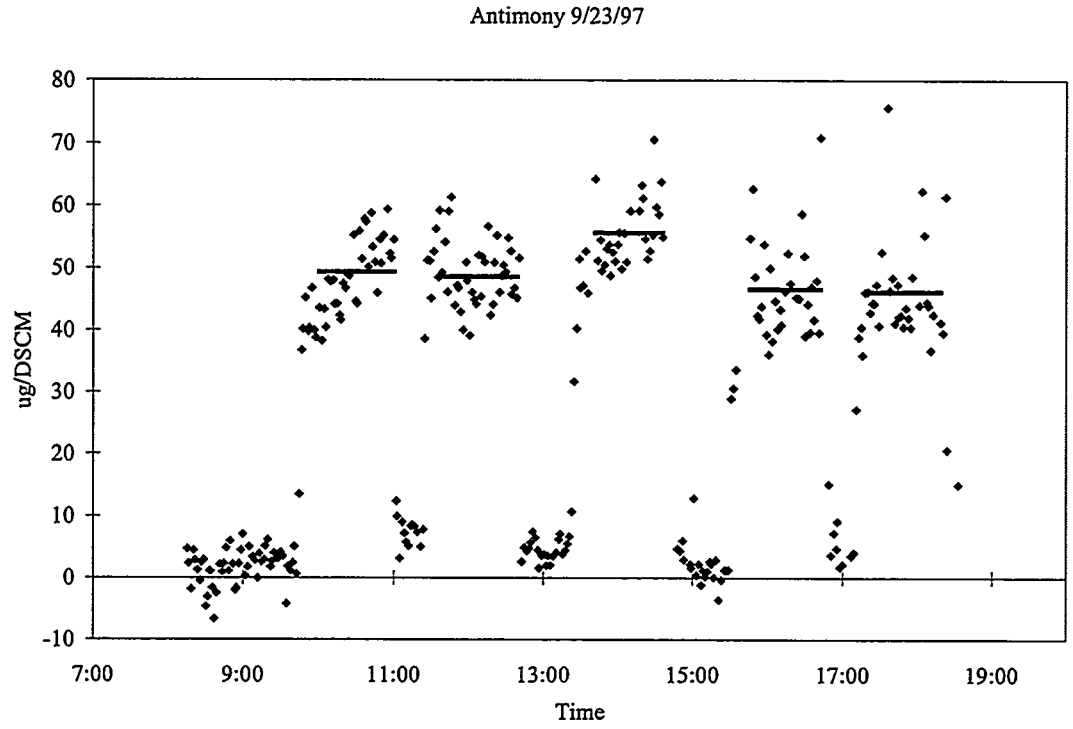

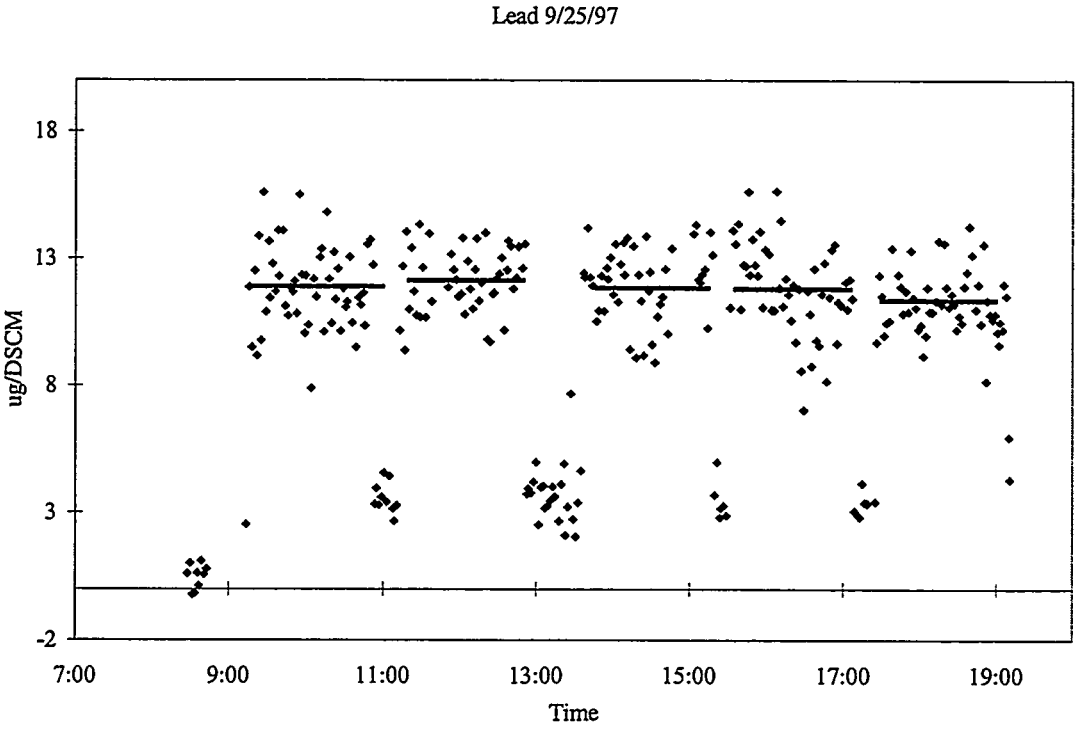

Figure 3. Plots of metal concentration *vs.* time. Solid lines denote average value over RM period.

Appendix F

Developer Report
Sandia National Laboratory
Laser Induced Breakdown Plasma System

Performance Testing of a Laser-Induced Breakdown Spectroscopy (LIBS) Based Continuous Metal Emissions Monitor at the US EPA Rotary Kiln Incinerator Simulator

D. W. Hahn, K. R. Hencken, H. A. Johnsen, and E. J. Walsh
Sandia National Laboratories
Livermore, CA 94551-0969

CONTENTS

FIGURES

TABLES

ABSTRACT

A program was initiated at Sandia National Laboratories to develop and demonstrate an advanced continuous emissions monitor that will provide real-time measurement of metal emissions in the wastestreams of thermal treatment facilities. This effort led to the development of a prototype metals monitor based on an optical technique referred to as laser-induced breakdown spectroscopy (LIBS). The LIBS-based instrument enables *in situ* measurements that are both noninvasive and real-time. The metal emissions monitor was tested during September 1997 at the EPA Rotary Kiln Incinerator Simulator (RKIS) located in Research Triangle Park, North Carolina. This report describes the field test, including the monitor installation, test cycle, and overall instrument performance. Concentration data for the metals beryllium, cadmium, chromium, iron, and yttrium were recorded and are compared with independent Method 29 results.

LIBS Data Acquisition and Analysis

Conditional Analysis

To improve LIBS response at low concentration levels, a new conditional data analysis routine was incorporated into the Sandia metal emissions monitor in the Spring of 1997. For low particle loadings, separation of LIBS spectra containing the desired metal signals (i.e. hits) from the many spectra containing no information (i.e. misses) can greatly increase the signal-to-noise ratio for the selected metal emission lines. The conditional analysis approach implemented for the LIBS-based metals monitor is based on independent, fixed-rate sampling combined with the analysis of each single laser pulse in an overall sequence of pulses. Hits corresponding to targeted elements are identified using a threshold criteria applied to the characteristic atomic emission lines. With this approach, spectra are recorded and analyzed in real-time for a total number of desired shots, typically 600 to 1200 total pulses. An average spectrum is generated based on the ensemble average of the spectra recorded for all shots identified as hits (i.e., those exceeding the threshold). An equivalent metal concentration is then calculated from this average spectrum using the integrated line intensities and calibration curves as described below. The true or actual metal concentration is then calculated from the product of the equivalent concentration for hits only and the frequency of hits (i.e., number of hits/total number of pulses). When the frequency of identified hits equals 100%, the conditional analysis technique converges to a conventional ensemble-averaging scheme. This can be accomplished at any time by setting the hit threshold sufficiently low such that all shots are designated as hits. The current Sandia system can also operate simultaneously in both conditional analysis and ensemble-averaging modes.

Calibration

Using either the conditional analysis scheme or conventional ensemble-averaging, the resulting output spectrum contains a continuous background emission signal with superimposed discrete atomic emission line signals. For each targeted analyte emission line, a LIBS signal is calculated based on the integrated emission line peak divided by the surrounding continuous background intensity level. A concentration is calculated from a library of linear calibration curves entered for each target analyte atomic emission line, as determined in the laboratory using a calibration flow stream of known mass concentration, and with identical LIBS parameters (e.g. lens focal length, laser power) as utilized for the field measurements.

For the September 1997 field test at the RKIS facility, the Sandia LIBS-based metal emissions monitor was calibrated for the following elements:

Hardware and Data Acquisition

The current Sandia LIBS-based metals CEM utilizes a 1064-nm Nd:YAG laser as the excitation source, with a nominal pulse width of 10 ns and pulse energy of 500 mJ. The laser beam is expanded to 12 mm and then focused to create the plasma using a 75-mm focal length, 50-mm diameter UV-grade quartz lens. The 50-mm lens also functions to collect the plasma and atomic emission. A schematic of the LIBS monitor system is presented in Figure 1. LIBS spectra are collected at 5.0 Hz using a spectrometer and time-gated CCD array. The CCD intensifier gate width used for the RKIS field test was 3.5 μs, with a time delay of 18.0 μs from the laser pulse. The actual delay was different than the pre-calibrated delay of 6.0 μs, as discussed below, and resulted from a failed trigger circuit element. The complete system is controlled remotely by a PC-based computer. For the RKIS test, the computer was situated downstairs about 50 ft. from the duct, and was linked to the stack-mounted probe and instrument rack by a fiber optic communications cable.

External requirements for the LIBS monitor system include a 110 V, 5 amp power supply; a 220 V, single-phase, 10 amp power supply; and a 5 lpm supply of purge gas such as nitrogen or argon. The purge flow was blown across the outer surface of the 2 inch lens as a preventative measure to keep the optic clean.

Monitor Availability

The LIBS spectra are recorded with a 1/4 m spectrometer and CCD array detector. With the current configuration, the spectral bandwidth is 30 nm, with a spectral resolution of about 0.035 nm per detector array element (i.e. pixels). To cover all of the atomic emission lines listed in Table 1, four spectral windows were identified for the RKIS field test. The four spectral windows and targeted species are summarized in Table 2.

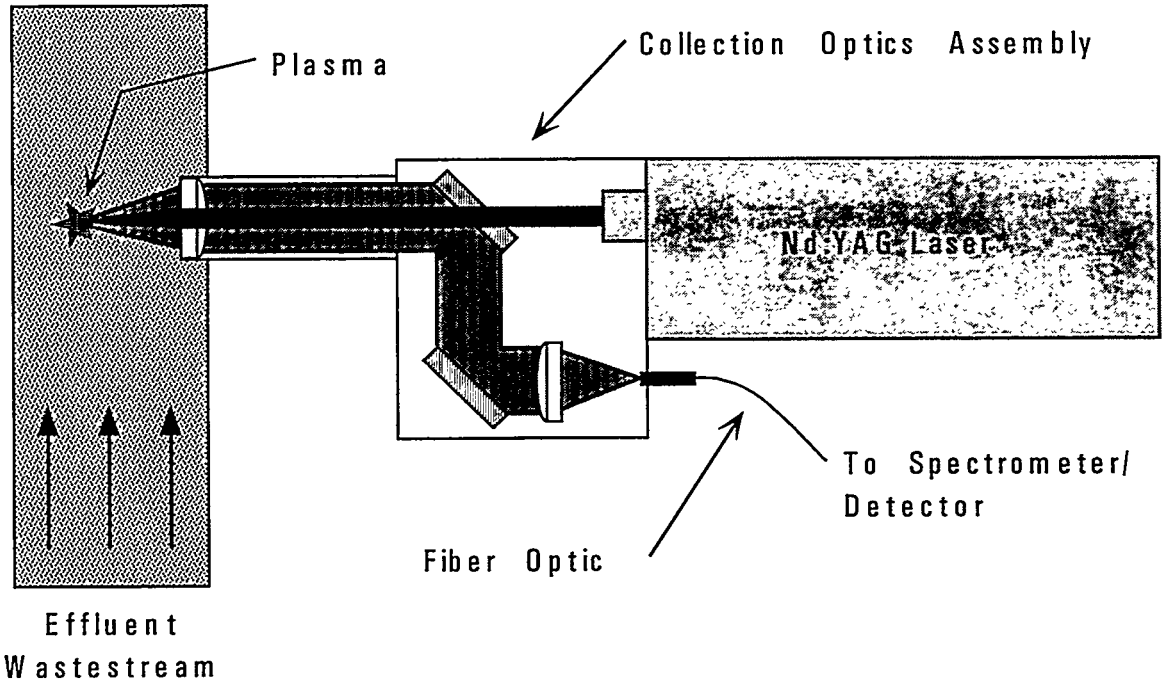

Figure 1. Schematic of LIBS monitor system probe.

Table 1. Calibrated atomic emission lines for the RKIS facility.

Element	Calibrated Atomic Line (nm)
Antimony (Sb)	252.9
Arsenic (As)	286.0
Beryllium (Be)	313.0
Cadmium (Cd)	228.8
Chromium (Cr)	283.6
Iron (Fe)	238.2
Mercury (Hg)	253.7
Lead (Pb)	220.4
Silicon (Si)	288.2
Yttrium (Y)	294.6

Table 2. Spectra Windows and corresponding species.

Window Center (nm)	Targeted Species
225	Cd, Pb,
250	Hg, Fe, Sb
277	As, Cr, Si
305	Be, Y

The Sandia monitor is controlled with a single LabVIEW based program that was designed and coded specifically for the LIBS system. A conditional data analysis interface allows the selection of up to six separate species for subsequent analysis in any given spectral window. In real-time, each spectrum is analyzed sequentially for each of the designated species using the corresponding hit thresholds. The specific windows and dedicated species are listed in Table 2.

For the RKIS test, the total number of laser pulses used for each data point was 600, corresponding to two minutes per data point, respectively, at the 5 Hz acquisition rate. At the end of each pulse sequence, the data are analyzed automatically using the calibration procedure outlined above, the concentration data are entered and stored on disk in a sequential log file, and the spectral data are stored on disk. The analysis and file writing process takes about two seconds for completion, at which time a new pulse sequence can be initiated immediately. For the individual one-hour test runs planned for this test, it was decided to cycle once through the four spectral windows listed in Table 2. Using either 800 or 1200 laser pulse sequences, 5 or 8 data points were generated for a given window, after which the spectrometer was rotated to the next window and the process repeated. The changing of spectral windows is also controlled remotely with the LabVIEW program and takes about 1 to 2 minutes to accomplish. With this procedure, concentration measurements comprised of 5 to 8 two-minute averages were recorded for each element during each one-hour test period. This corresponds to the monitor being on-line nearly

100% of the test period, with resulting data for any given targeted species covering about 25% of the test period.

Installation and Test Plan

Probe Installation

The field test was conducted at the RKIS facility located in RTP, North Carolina. The complete details of the RKIS system and of the placement of the LIBS monitor are described in the main body of this report. The Sandia LIBS monitor was placed upstairs in the horizontal test section of the duct. The LIBS laser assembly was inserted through a specially designed flange that functioned to anchor the probe and to seal the exhaust stack gases. The Sandia flange mounted to an existing standard 4-inch NPT pipe nipple. The entire laser probe module (see Figure 1) was mounted on a self-supporting table that enables the probe to easily slide into and out of the process stack. The entire laser probe module weighs about 75 lb. One supporting instrument rack (30" × 30" × 48", 300 lb.) was stationed nearby on the floor, and contained the laser power supply, the spectrometer, and the CCD detector and controller. It took approximately 6 hours to unload and install the equipment and to perform a system check.

System Check

The system check to ensure proper operation of the LIBS monitor is comprised of two primary tasks: spectral calibration of the spectrometer and CCD array, and a check of system response and calibration. Because the spectral data from the CCD array corresponds to light intensity as a function of detector element, or pixel number, all data analysis within LabVIEW is done in pixel-space rather than wavelength-space. Accordingly, each target analyte atomic emission line is assigned a pixel location number corresponding to a given spectral window. The pixel locations are entered into the software calibration file. However, the absolute pixel location of a given analyte line can shift by several pixels during instrument shipping or during extended instrument shutdown or wide temperature fluctuations. The carbon atomic emission line at 247.86 nm resulting from carbon species, mostly CO_2, present in the stack gases is used for instrument spectral calibration. During the nearly two-week test period, the pixel shift ranged from 1 to 2 pixels with respect to the laboratory calibration performed in California prior to shipment. The pixel offset from the spectral calibration was entered in the LabVIEW program for automatic correction of all atomic emission line locations.

The system response and calibration check is accomplished with a calibration cell of known gas composition. A helium gas cell at ambient pressure is used for the system check in the field. Helium has a strong atomic emission line at 388.86 nm. The concentration of helium gas within the calibration cell is calibrated in the laboratory prior to shipping and entered in the software calibration file. In the field, the concentration of helium within the cell is calculated and compared to the pre-shipment calibration value. The optical window of the helium calibration cell was broken at the previous field test at the K-25 Site TSCA Incinerator the week prior to the RKIS test. For this reason, no quantitative system response check was conducted at the RKIS test. The calibration cell has been demonstrated as a reliable diagnostic on previous field tests. If this diagnostic would have been available prior to the RKIS formal test period, a clear indication of the previously mentioned timing/calibration problems would have been provided.

Test Results

Correction for Temporal Gating

As noted above, the actual detector timing used during the RKIS test differed from the values used for laboratory calibration. Specifically, all laboratory data calibration was conducted with a detector gate-width of 3.5 μs and a delay time of 6.0 μs from the initial laser pulse. These same trigger parameters were specified for the RKIS field test. After the RKIS test, a system check was performed after the equipment had been shipped back to Sandia using the laboratory calibration source. The resulting signal intensity levels were still markedly low, as observed at the RKIS test, and the corresponding concentration values were high by factors ranging from 1.3 to 2.8. The problem was traced to a failed circuit element on the trigger level potentiometer of the CCD intensifier control unit that caused the detector gate to trigger on the positive-going trailing edge of the laser fixed-sync TTL output trigger, rather than on the negative-going leading edge. This resulted in a shift of 12 μs in the detector time delay, corresponding to a delay of 18 μs rather than the specified value of 6 μs. Due to the rapid and differing decay rates of the plasma continuum and the atomic emission lines, the instrument calibration was strongly affected.

No absolute correction can be introduced to account for the shift in detector delay times because the exact plasma characteristics realized in the RKIS duct can not be reproduced in the laboratory. However, a first order correction can be introduced by calculating the ratio of the instrument response for both delay times in the laboratory calibration apparatus. The correction factors are presented in Table 4 for all spectral calibration lines. All *corrected* data presented in this report have been corrected using the Table 4 values. The correction factors reveal a very linear dependence on wavelength. We note, however, that the Pb emission line at 220.4 nm exhibited atypical behavior. The 220.4 nm emission line decays in emission strength such that essentially no peak intensity remains at a delay time of 18 microseconds. This is consistent with our failure to detect any lead emissions throughout the test. The uncorrected data are presented in the main body of this report and summarized below, as documented during the RKIS test week. It is noted that the apparent low signal response and unusual plasma characteristics were reported to the test committee (namely Steve Priebe) during the test week, while the temporal gating problem was documented and reported prior to the release of the Method 29 reference data.

Data Collection Modes

The Sandia LIBS-based metals monitor was operated in a conventional ensemble-averaging mode for the species beryllium and iron due to the strong spectral responses recorded. Lead was also monitored using ensemble-averaging as well as conditional analysis. The two elements arsenic and antimony were

Table 4. Correction factors for temporal gating.

Species and Line (nm)	Correction Factor
Cd 228.8	2.61
Fe 259.9	2.15
Cr 283.6	1.80
Y 294.6	1.62
Be 313.0	1.32

not monitored during the actual test due to the presence of spectral interferences either recorded or expected on the most accessible atomic emission lines. The strongest arsenic emission lines at 228.81 and 234.98 nm have interferences with much stronger emission lines from cadmium at 228.80 nm and beryllium at 234.86 nm, respectively. A much weaker arsenic emission line at 286.0 nm was determined to lack sufficient sensitivity. Similarly, the strongest antimony emission lines at 252.85 and 259.81 nm have interferences with much stronger lines from silicon at 252.85 nm and iron at 259.94 nm, respectively. The very large spectral contribution from silicon and iron attributed to the fly ash made antimony analysis unfeasible with the available emission lines. The most suitable atomic emission lines for these two elements are 189.04 nm for arsenic, and 206.84 nm for antimony. Both of these lines are deeper into the ultraviolet wavelength region than can be accessed with the fiber-optic coupled detector system used in the current Sandia monitor. These short wavelengths require working with vacuum-UV spectrometers and purged or evacuated optical paths, which are not practical with a stack-mounted, *in situ* LIBS probe package.

The conditional data analysis scheme was used for cadmium, chromium, lead, and yttrium throughout the formal test period. The relatively low targeted concentration levels provided an excellent test of the conditional analysis mode as a means to enhance signal response.

Data Analysis

After each one-hour test period, the concentration values recorded for each targeted species were copied from the sequential data log file into a new spreadsheet file, and then correlated by time and species. When all formal test days were complete, all the individual test period data (R1 to R20) were incorporated into one master spreadsheet, where the data were all correlated by species, time, and test period. As noted above, all concentration values are generated in the units of micrograms per actual cubic meter (μg/acm) and were then converted to dry standard conditions, namely micrograms per dry standard cubic meter, (μg/dscm). The average conversion factor for the test period was a multiplication factor of 1.82 to convert from μg/acm to μg/dscm. Once the data were converted to dry standard conditions, the average and standard deviations were calculated for all species and test periods.

LIBS Data

The species measured at the RKIS facility were beryllium, cadmium, chromium, iron, and yttrium. The complete sets of data are reported in detail in the main body of this report, with a brief summary of the results presented here. The average LIBS concentrations are presented in Table 5 along with the average Method 29 results for each of the two feed conditions. The data presented in Table 5 include both the data as reported during the test period, and the data corrected for the timing problem using the factors presented in Table 4. The data reflect the average values for all 10 runs at each concentration feed rate.

As presented in Table 5, the overall agreement between the corrected LIBS CEM data and the Reference Method 29 data is rather good, with an average difference of 63% for all species, feed rates, and test periods. Excluding the beryllium data, which exhibited the largest differences, the average difference between the LIBS data and Method 29 data is 37%, which is excellent overall agreement when consideration is given to the detector timing problems. The corresponding average relative accuracy (RA) for cadmium and chromium is 72%. The Table 5 values represent the overall accuracy of the LIBS monitor as compared to the accepted standard reference method.

Table 5. Summary of LIBS CEM and Method 29 results.

Element	Method 29 (µg/dscm)	Low Feed (uncorrected) Conc. (µg/dscm)	Low Feed (uncorrected) RA (%)	Low Feed (corrected) Conc. (µg/dscm)	Low Feed (corrected) RA (%)
Be	20	85	367	65	253
Cd	21	77	290	29	55
Cr	27	70	196	39	66
Fe	2171	5450	166	2547	30
Y	182	124	46	76	70
		High Feed		High Feed	
Be	62	163	176	123	111
Cd	69	270	341	104	73
Cr	62	196	253	109	94
Fe	2176	4716	139	2193	18
Y	100	93	29	57	60

A few additional comments are noted with respect to the relative accuracy (RA) calculations. The RA values are normalized with respect to the reference method values for expression as a percentage. As a result, values measured higher than the reference method data result in higher RA values when compared to concentration data measured lower than the reference method results. As an example, if values were recorded for Be, Cd, and Cr on the order of 6 µg/dscm on the high feed rate day, the corresponding RA values are on the order of 90%. These RA values would be similar to the RA values presented in Table 5 for the Sandia LIBS system, yet the Sandia values for Be, Cd, and Cr for the high feed are on average a factor of 1.7 times too high, while the above example of 6 µg/dscm is on average a factor of *10 times* too low. It is further noted that measuring a constant value of zero results in a relative accuracy of 100%, which would be equal to the relative accuracy achieved for perfectly correlated data that was high by a consistent factor of two.

In addition to the average values presented in Table 5, it is useful to assess how well the LIBS CEM data tracked the individual Method 29 test results. The average LIBS data for each one-hour test period are presented along with the Method 29 results for cadmium and chromium in Figures 2 to 3, respectively. Overall, the data are observed to track rather well with the Method 29 data.

Conditional Analysis Results

The conditional analysis technique was successful in significantly enhancing the signal-to-noise ratios for cadmium, chromium, and yttrium. Non-detects would have been reported for cadmium, chromium on the low spiking days, while yttrium would not have been detected on any day, using a conventional ensemble-averaging scheme as currently configured. Examples of conditional analysis are presented in Figures 4 and 5 for the detection of cadmium and chromium, respectively. The ensemble-averaged spectrum for both figures corresponds to 600 laser pulses. In Figure 4, the conditionally analyzed cadmium spectrum corresponds to 24 laser pulses that triggered on cadmium, at hit frequency of 4%. The chromium spectrum in Figure 5 corresponds to 23 hits, a frequency of 3.83%. In both spectra,

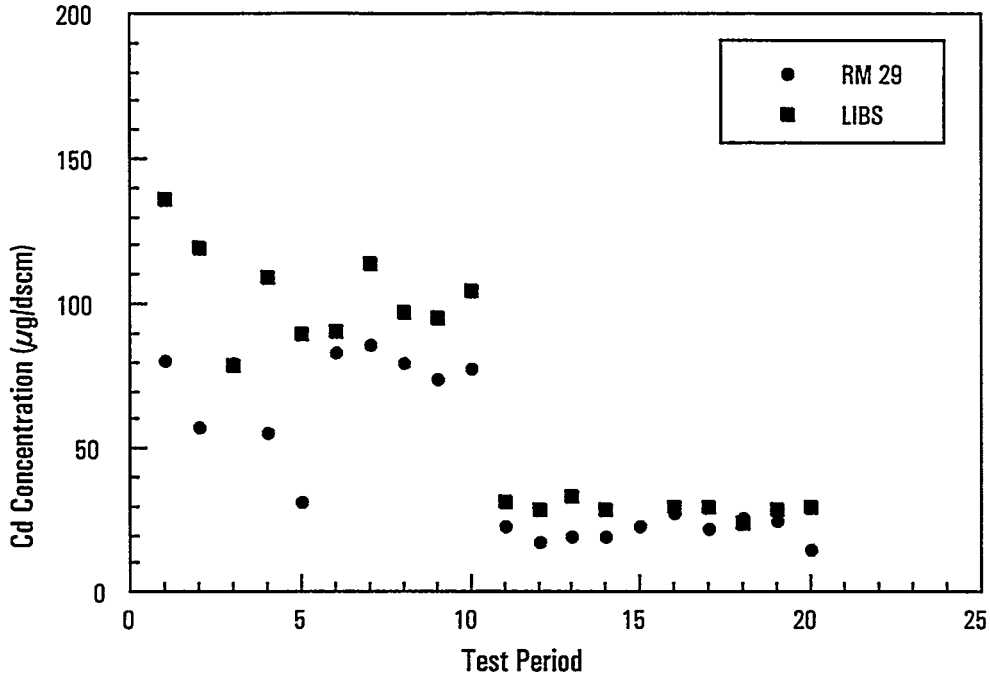

Figure 2. Comparison of Method 29 and corrected LIBS Cd concentration data.

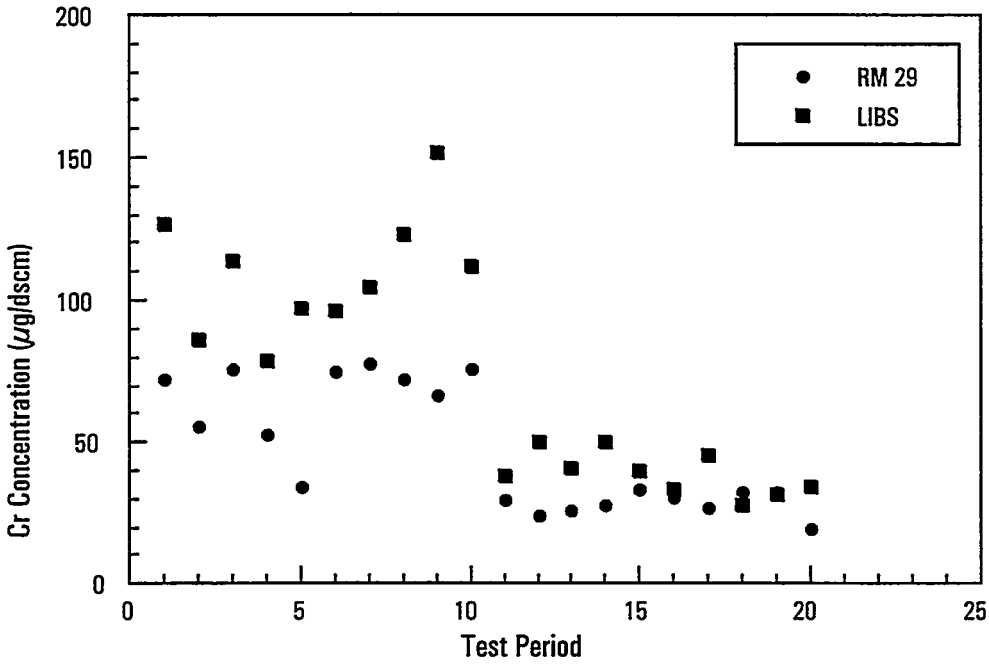

Figure 3. Comparison of Method 29 and corrected LIBS Cr concentration data.

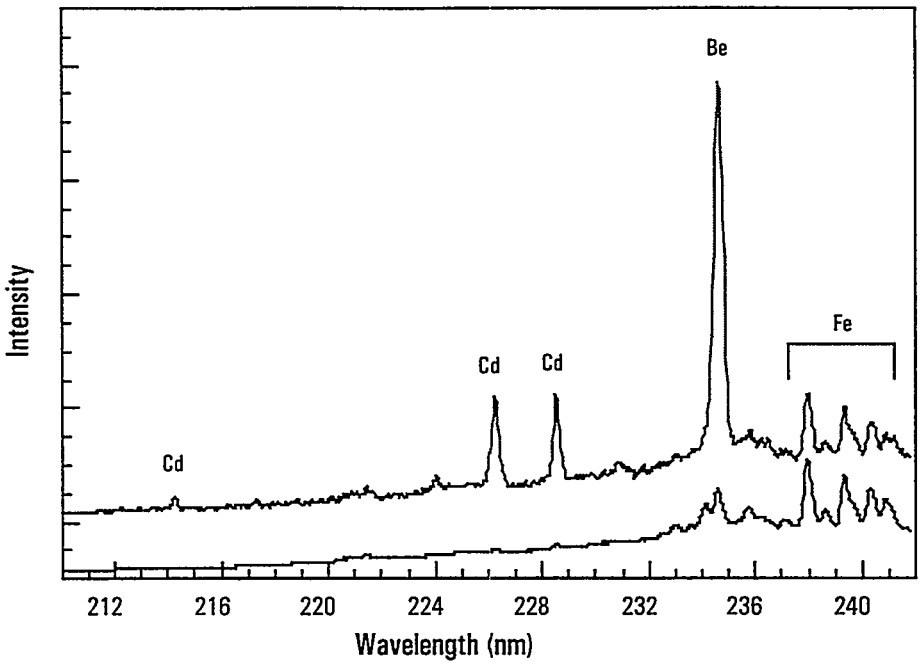

Figure 4. Spectrum of Cd hits (n=24) and corresponding ensemble-averaged spectrum (n=600). Spectra have same scale and are shifted for clarity.

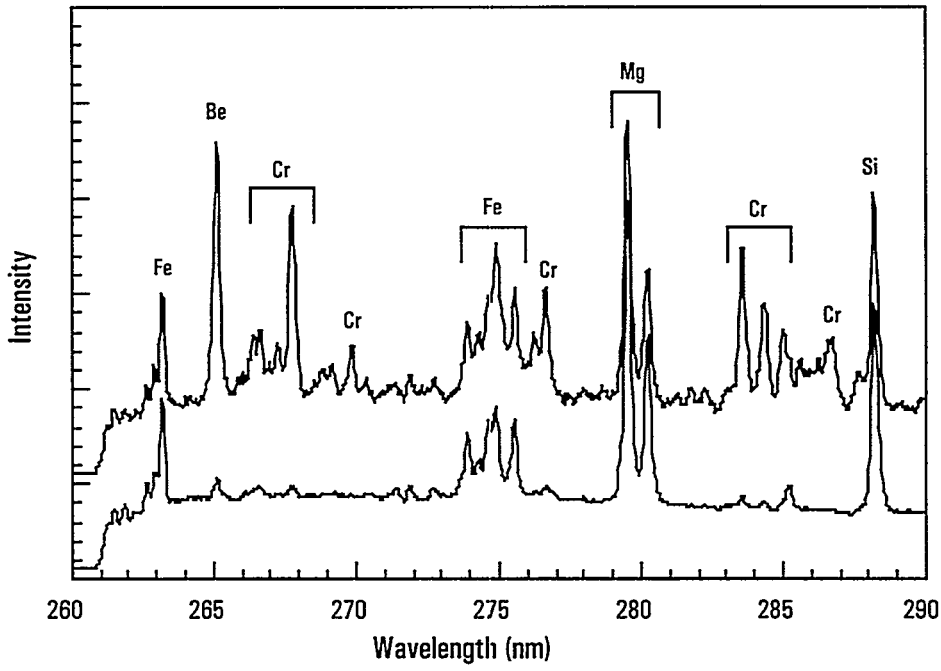

Figure 5. Spectrum of Cr hits (n=23) and corresponding ensemble-averaged spectrum (n=600). Spectra have same scale and are shifted for clarity.

the significant increase in signal-to-noise is apparent with conditional data analysis. Another interesting feature is noted with both figures. The spectral features attributed to iron, silicon, and magnesium (all constituents of fly ash) are present at comparable levels in both the ensemble-averaged spectra and in the conditional analysis spectrum. This suggests no correlation between the presence of fly ash and either cadmium or chromium. However, the beryllium emission lines are enhanced significantly with the presence of cadmium and chromium. This strong correlation was recorded consistently, and suggests that cadmium and chromium interact with beryllium during the nucleation process.

Availability

The Sandia LIBS monitor was on-line 100% of the time for all twenty of the 1-hour test periods. During the entire test, the Sandia monitor functioned normally, with no hardware or software problems noted. As discussed above, use of the calibration cell would have revealed the timing problem during the RKIS test. On average, concentration data were recorded corresponding to about 80% to 85% of each reference method test period. The additional time is attributed to the time required to change between spectral windows, and to enter the file names between runs. During the last test period on 9-24-97, the planned one-hour test was terminated approximately 15 minutes early by EPA personnel. As a result, no data had yet been recorded with the Sandia LIBS probe for the 225-nm cadmium window. Following the RKIS field test, the software package was revised to include an automatic data looping feature.

LIBS Sensitivity

Conditional Analysis

As discussed above, the conditional analysis method as a means to increase LIBS sensitivity was very successful during the EPA RKIS field test. The conditional analysis technique consistently detected discrete particle hits during the formal test period. On average, the hits rates were in the range of 2 to 5% throughout the test. To first order, this corresponds to an increase in signal-to-noise by a factor 25. This is apparent in Figures 4 and 5. Working with enhanced signal-to-noise ratios can extend the lower detection limits of a LIBS instrument and provide improved accuracy at near detection limits.

Signal Sensitivity and Detection Limits

The sensitivity of the LIBS technique to the targeted species under the RKIS stack conditions can be elucidated through comparison of LIBS spectral data and reported concentration values with the Method 29 reference data. A careful analysis was performed with regard to the targeted metals beryllium, cadmium, chromium, lead, and mercury.

A detailed examination of spectra recorded under high metals spiking, ash only, and zero metals spiking test conditions revealed no discernible emission line signal corresponding to the 220.4-nm lead emission line. The failure to record a significant lead response at the EPA test high concentration level of about 78 μg/dscm (43 μg/acm) is consistent with our pre-test estimated detection limit of approximately 250 μg/acm using the 220.4-nm lead line. More significantly, the lead response at 220.4 nm is greatly reduced at the increased delay time of 18 μs. An alternative lead emission line at 405.78 nm was also examined under various stack conditions. As with the 220.35-nm line, no discernible emission line signal was noted corresponding to the 405.78-nm lead line using the 18 μs delays. However, recent work completed at Sandia has revealed strong LIBS emission using the 405.8-nm lead line with delay times on the order of 50 μs, which significantly increases the sensitivity to lead.

No discernible atomic emission line intensities were observed for mercury under any of the test conditions at the EPA RKIS facility. The mercury line monitored was the 253.7-nm atomic emission line.

The use of this atomic emission line with the LIBS technique has historically not generated reliable detection results. Several reasons may exist, including the relatively weak emission strength of this line under laser-induced plasma conditions. Furthermore, the 253.7-nm emission line is an electronic transition that terminates in the ground state. This may result in the re-absorption of the emitted light by mercury between the plasma volume and the collection optics. In the current configuration of the Sandia monitor, this is a path length of about 7.5 cm. Re-absorption will depend on the concentration and speciation of mercury in the stack, and without *a priori* knowledge, it is not possible to make quantitative corrections.

A strong beryllium response was recorded at 313 nm using the LIBS technique. The signal-to-noise ratio of the 313-nm emission line remained very high even at the low spiking concentration levels of 20 μg/dscm, which corresponds to approximately 10 μg/acm. It is noted that beryllium has one of the strongest responses of all targeted metals to the LIBS technique.

Using the test data generated at the RKIS facility as described above, in combination with laboratory work and prior field experience, the lower detection limits for the Sandia LIBS monitor were determined for the RKIS facility and are summarized in Table 6. The values reflect a signal-to-noise ratio of 3-to-1 at the method detection limit (MDL). It is noted that the detection limits summarized in Table 6 are in the units of dry standard cubic meter, which reflect values approximately 1.8 times greater than those at actual stack conditions. In addition, the detection limits presented below are based on a combination of conventional ensemble-averaging and conditional analysis modes of operation. The lead detection limit reflects the recent results utilizing the 405.8-nm emission line.

Table 6 does not include detection limits for the elements antimony, arsenic, and mercury. Spectral interferences combined with relatively low emission signals were discussed above for these elements. Suitable atomic emissions lines are available at 206.83 nm for antimony, 189.04 and 197.20 for arsenic, and 184.95 and 194.23 nm for mercury. These lines are not accessible with the fiber-coupled configuration currently used for the *in situ* Sandia LIBS system. It is estimated that concentration levels greater than 1000 μg/dscm would be necessary for LIBS detection of these elements in stack conditions corresponding comparable to the RKIS facility. Such high detection limits make LIBS-based detection impractical for these three species under nominal stack operating conditions of 10's of μg/dscm or less.

Sandia is currently reevaluating the use of alternative emission lines in combination with very long delay times, as used with lead, as well as conditional analysis schemes, as a means to significantly enhance the detection limits.

Table 6. Estimated LIBS method detection limits for the EPA RKIS.

Element	Detection Limit (ug/dscm)
Antimony (Sb)	NA
Arsenic (As)	NA
Beryllium (Be)	2
Cadmium (Cd)	5
Chromium (Cr)	5
Mercury (Hg)	NA
Lead (Pb)	20

SUMMARY

The test of the LIBS-based continuous metal emissions monitor at the EPA RKIS facility was successful in demonstrating a real-time response to targeted metal species. However, a detector timing failure was noted after the test was complete, which significantly affected the absolute calibration of the LIBS system. All data analysis and data reporting procedures were fully automated and performed in real-time, with the instrument being on-line during 100% of all test periods. It is noted that the Sandia monitor utilizes an absolute pre-test calibration, that requires no on-site adjustment, post-processing, or post-test calibration. Overall, consistent stack concentration readings were recorded with the LIBS monitor that were in good agreement with independent Method 29 reference data after the data was corrected to first order for the detector timing gate problem. The Method 29 data enabled determination of overall accuracy and establishment of lower detection limits for the RKIS stack conditions.

The conditional data analysis approach was evaluated in the RKIS facility and concluded to be very useful in increasing the LIBS sensitivity through discrete particle detection. The conditional analysis approach was successful in detecting single particles under normal operating conditions, thereby yielding signals with significantly enhanced signal-to-noise ratios as compared to conventional ensemble averaging. The Sandia monitor also accurately tracked transient changes in metals feed rates as compared to a NO concentration measurements recorded with a commercial CEM. Overall, the RKIS field test has demonstrated that a LIBS-based continuous emissions monitor for metals can provide real-time response and concentration measurements in a pilot-scale treatment facility under ash-laden stack conditions.

RECOMMENDATIONS

As a result of the August/September 1997 field test at the EPA RKIS facility, the Sandia LIBS-based continuous emissions monitor project team has identified the following issues for improvement and incorporation into the current LIBS system:

1. Modification of the LIBS system software to allow scripting and automatic execution of a test plan. This was completed in November 1997. The goal is to extend the monitor data acquisition availability to near 100% by eliminating the operator requirement to control the software for spectral window changes. Furthermore, hardware changes are being evaluated to provide analysis of all metals simultaneously, eliminating the need to cycle between species.

2. Development of an *in situ* calibration technique to allow for correction of any plasma effects resulting from the stack environment. A concept has been identified and will be developed at Sandia during 1998.

3. Optimization of the LIBS emission signals (signal-to-noise) for ensemble-averaging and near-zero concentration levels with the goal of increasing the lower detection limits of targeted species. Modification of the LIBS system calibration scheme to better represent near-zero concentration levels consistent with both conditional analysis and ensemble-averaging.

4. Complete integration of the calibration cell and diagnostics into the LIBS hardware and testing protocol.

ACKNOWLEDGMENT

This work was sponsored in part by the U.S. Department of Energy, Office of Science and Technology, Characterization, Monitoring, and Sensors Technology Crosscutting Program (CMST-CP), and in part by a Memorandum of Understanding (MOU) between the U.S. Department of Defense, Office of Munitions, Joint Services Demil Technology Office, and the U.S. Department of Energy, Defense Programs Office.

Appendix G

Developer Report
Laser Diagnostics
Internal Calibration Procedure for LIBS

Internal Calibration Procedure for LIBS

Gary Loge, Ph.D.
Laser Diagnostics, LLC
35 Bonnie View Dr., Suite B
Los Alamos, NM 87544
(505)-672-3632
gloge@LaserD.com

CONTENTS

TABLES

Appendix G

INTERNAL CALIBRATION PROCEDURE FOR LIBS

Technology Description

Most toxic metal continuous emission monitor technologies are based on optical emission from a plasma source. The different plasma sources—inductively coupled plasma (ICP), electric discharge (or spark-induced plasma, SIP), microwave-induced plasma, and laser-induced breakdown (LIB), all require calibration of the atomic emission as a function of toxic metal concentration in the off-gas. This is usually performed using a metal aerosol source that generates aerosol containing gas of known metal concentration independent (external) to the actual off-gas. Unfortunately, using an external metal source for plasma emission calibration has several limitations, which include: (1) A skilled operator is required to perform the external calibration procedures; (2) Off-gas monitoring must be halted while an external calibration is performed; (3) Calibration error is possible if the off-gas and the external calibration source have different gas characteristics, such as water vapor and ash content; and (4) Gas and optical changes in the off-gas monitoring may occur between external calibrations causing calibration drift.

Laser Diagnostics is developing a plasma emission calibration procedure that avoids the limitations of external calibration. This is accomplished using an internal standard in the off-gas along with plasma temperature compensation that allows direct comparison of the internal standard emission strength to the metal emission strength (patent pending). For continuous monitoring of off-gases, nitrogen is the best choice for an internal standard, since its partial pressure is constant, and it has strong plasma emission. However, using atmospheric nitrogen as the internal standard is only useful for the LIB method, since it is the only method that generates a plasma hot enough to completely dissociate molecular nitrogen (>10,000 K).

This internal calibration method is applied to LIBS data obtained by Sandia National Laboratory at the CEM demonstration in a "blind" test. The results are reported and discussed.

Summary of Technology Development History and Sponsorship

The internal calibration procedure was first conceptualized in 1994, resulting from data obtained for Cd metal vapor and $CdNO_3$ wet aerosols, both in nitrogen carrier gas. The data were obtained as part of a Small Business Innovation Research Phase I project sponsored by the DOE (DE-FG02-94ER81671) to determine differences in LIBS characteristics for various gas conditions. Dramatically different emission spectra were observed for these two types of metal containing gases. The calibration concept was devised as a solution to this problem and is the basis of a patent application submitted on Oct. 24, 1995. Final patent issue is pending.

Full development and rigorous testing of the original concept began in 1996, sponsored by the DOE under contract DE-AC21-96MC32194. Additional testing and development is continuing, with new sponsorship being sought to complete development of a completely automated procedure.

A Small Business Technical Assistance Grant from Sandia National Laboratories supported their efforts in this collaborative test with Laser Diagnostics, LLC.

Equipment and Procedures

For a description of the LIBS equipment, see the Sandia National Laboratory report. Emission spectra obtained using their equipment was made available to Laser Diagnostics for testing of the internal calibration procedure. Additional data needed for the internal calibration procedure were also acquired by them. The additional data included a one-time spectral response calibration of their LIBS detection system before the test runs using calibrated spectral irradiance lamps and acquiring atomic nitrogen emission spectra during one of the reference method runs to be used as an internal calibration. This additional data allowed the internal calibration procedure to be performed as a reinterpretation of their metal emission spectra. Using the same data allows comparison of the internal calibration results and their external calibration results.

Instrument Spectral Calibration

A one-time calibration of the instrument's spectral response is a requirement of the internal calibration procedure. It allows the intensity of atomic emission lines at different wavelengths to be compared directly. This is especially important when comparing metal emission lines in the ultraviolet region to atomic nitrogen emission lines in the near infrared region, where the relative response of the detector can be significantly different. The overall spectral response of the detection system depends on spectral transmission and reflection, grating efficiency, and detector response (V/watt). In addition, another response factor for an array detector is how well the entrance slit image is focused onto the array detector across its entire width, the flat-field correction. Poorer focusing near the edges of the detector cause the effective sensitivity to decrease.

The combined effect of spectral response and flat-field correction of the SNL LIBS system was determined using spectral irradiance lamps, which have calibrated intensity as a function of wavelength. A spectrum of the lamp was taken at each center wavelength of the detection system used for each of the metals and for nitrogen. The lamp spectrum divided by the calibrated irradiance (W/cm^2) of the lamp on a pixel-by-pixel basis was used to obtain a calibrated spectral response. LIB spectra were divided by the calibrated spectral response to get spectra that are proportional to the emission strength (W/cm^2), independent of the instrument's spectral response.

This type of calibration needs to be performed only once unless the instrument's optical characteristics change. One possible uncorrected factor is if soot accumulation on the optical port causes the spectral response to change in addition to causing an overall decrease in response. For this test it was assumed that the spectral response was unaffected by clouding of the optical port. A further investigation of this is needed however.

When using the internal calibration procedure, no other external calibration is required.

Field Calibration

Since the internal calibration procedure is primarily based on the analysis of atomic nitrogen emission spectra, it is essentially a field calibration method. This calibration is performed by acquiring nitrogen spectra centered at 415 nm and 745 nm followed by data analysis to determine the intensity of individual emission lines after subtracting the plasma background emission intensity. The intensity of four nitrogen lines thus obtained, along with the known nitrogen number density in the gas stream, are used to determine a calibration factor, which can change as gas conditions or optical conditions change. This gives a continuous correction for calibration drift. This procedure can be performed as often as required, with the time required to take the two sets of nitrogen spectra being the only limitation.

For this test, internal calibration using atomic nitrogen emission was performed only once during the week, at the beginning of reference method #17 at 11:00 am on Thursday, Sept. 25. More internal calibration procedures were not performed largely because they would have had to been performed during a reference method run with the ash and metal feeds running to ensure the same gas conditions. However, during the reference method run as many metal emission spectra as possible were acquired to improve the data statistics. Since the feeds were stopped between reference method runs, internal calibration procedures could not be performed then.

Internal calibration was performed by dividing the observed line emission strength by the known line strength, which is proportional to the number of emitting atoms. The temperature was used to a number proportional to density of nitrogen atoms. This relative nitrogen density was divided by the actual nitrogen density in the gas sample to get the internal calibration factor. The actual nitrogen density in the gas sample at 11:00 am on Thursday, Sept. 25 was determined by subtracting the reported mole ratio of O_2, (16.9%), CO_2 (2.4%), and H_2O (6.0%) at the Sandia LIBS port to get 74.7% nitrogen in the gas. This mole fraction of N_2, along with an assumed total pressure of 0.97 atm and a gas temperature of 453 F, was used to get an atomic nitrogen number density of $2.1 \times 10^{19}/cm^3$.

Since only one internal calibration procedure was performed during the test week, calibration drift was monitored using the plasma background emission, as previously done by SNL. This method has the advantage of being acquired simultaneously with the metal atomic emission spectra. In addition to taking the ratio of line intensity to background to correct for calibration drift, a temperature correction was performed to adjust for the effect of a higher temperature plasma causes stronger emission. To obtain the plasma temperature during every RM measurement, Fe emission spectra centered at 250 nm were used. The effect of small variations in the plasma temperature on the background emission was assumed to be negligible.

Zero Check Procedure

Zero is defined by the broadband plasma emission intensity at the wavelength of the atomic emission line. This broadband plasma emission intensity is subtracted from the intensity of the atomic emission line for each LIB spectrum, so zero drift is continuously corrected.

Procedure for Determination of Metal Concentrations in the Gas Stream

The metal concentration was determined from the emission strength of one or more atomic emission lines after subtracting the broadband plasma emission. This was divided by the known emission strength of the line or lines used. The resulting quantity is proportional to the density of emitting atoms in the plasma. This number and the plasma temperature were used to obtain a number proportional to the density of all metal atoms in the plasma. This number was multiplied by the calibration factor obtained from the nitrogen emission (or the background emission intensity) to obtain the absolute (vs. relative) number density of metal atoms in the gas. The number density was converted to weight concentration using the molecular weight.

The metal emission spectra were acquired by SNL using "conditional averaging" to improve the signal-to-noise ratio. The conditional averaged spectra must be multiplied by the percentage of all single-pulse spectra used in the conditional average to get the true average. When analyzed using the internal calibration procedure, this percentage was not known, so the procedure was performed as a "blind" test. The resulting numbers for the "blind" test of the internal calibration procedure were then multiplied by the percentage of single-pulse spectra in the conditional average to get the final result.

Quality Assurance Procedures

Data quality was checked by obtaining several sets of spectra at each center wavelength to allow a standard deviation of the measured metal concentration to be determined. This standard deviation expressed as a percentage of the average measured concentration should be the same as SNL reports, since it is based on the same data. The only difference in the results should be in defining the baseline and peak areas from the emission spectra. The calibration method should not affect the standard deviation.

As an additional blind test of the internal calibration procedure, two sets of Cd data (RM#1 and RM#2) and two sets of Cr data (RM#1 and RM#5) were analyzed with and without conditional triggering, which should give similar results.

Typical Daily Test Sequence

SNL acquired several sets of averaged emission spectra at four wavelength regions centered at 225 nm, 250 nm, 277 nm, and 305 nm to detect Cd, Fe, Cr, and Be respectively. Conditional averaging was used for the Cd and Cr spectra. During each RM, several averaged spectra were obtained at each wavelength before changing to a new wavelength. In addition, spectra centered at 415 nm and 745 nm were acquired before one of the reference method runs to obtain nitrogen emission spectra, which was used for internal calibration of the instrument.

Results

Laser-Induced Plasma Temperature

The plasma temperature was obtained from each of three Fe spectra acquired during each reference method run. The average temperature and standard deviation from these three measurements are shown in Table 1. The observed plasma temperature variation between runs can cause the plasma emission intensity to vary a factor of two, which will affect calibration if not properly corrected. (The amount of atomic emission intensity change for a changing plasma temperature depends on the emitting atomic state).

Table 1. Laser-induced plasma temperatures.

RM Number	Plasma Temperature (K)
1	8232 ± 53
2	9428 ± 30
3	8258 ± 73
4	8586 ± 75
5	8645 ± 54
16	7739 ±123
17	7889 ± 55
18	8265 ± 54
19	8318 ±103
20	7624 ± 53

Nitrogen Internal Standard

The nitrogen spectra used for the internal calibration were acquired on Thursday, Sept. 25 at 11:15 am with ash and metal feeds. This was just before RM #17 started. Additional nitrogen spectra were obtained at 9:00 am with no feeds. Nitrogen signals were almost a factor of two lower with no feeds, which illustrates how gas conditions can affect calibration. The plasma temperature obtained using the N(I) emission was 8585 K, which is somewhat higher than using the Fe(II) spectra obtained during RM #17. This appears to be a systematic error, possibly resulting from imprecisely know line strengths.

Using the two sets of nitrogen emission spectra obtained at 11:15 am on Sept. 25 and the known nitrogen density in the off-gas, a calibration factor of 5.4×10^{-7} was obtained with an average N(I) temperature of 8585 K. When a third set of N(I) spectra taken on Sept. 26 was included in the average, a calibration factor of 1.11×10^{-6} was obtained.

Test Results

1. Blind Test

The SNL spectra were analyzed using the internal calibration procedure after correcting to constant spectral response. The original results were performed as a "blind" test, described previously. They are listed in Table 2. The calibration factor of 1.11×10^{-6}, obtained using the three N(I) sets of spectra, was used.

2. Revised

After the original results were reported, several corrections and modifications were made, with the revised results listed in Table 3. First, an error in the analysis routine for Cr spectra did not properly subtract the background except for the first three measurements, which gave artificially high Cr results, and was corrected. A modification to use the background at same wavelength as the emission line, rather than at some other wavelength was made and was found to not have a noticeable effect on the results. Another modification was to use the average temperature obtained from the three Fe(II) data sets during a RM. The original analysis was performed with the assumption that the spectra for each metal were obtained sequentially with the first Fe spectra corresponding to the first Be and Cr spectra, and so forth. Actually, all three Fe spectra were obtained in sequence, and then other metal spectra were obtained. This modification also did not have a noticeable effect on the results or the standard deviation of the results. A final correction was to use the average temperature from the N(I) spectra for the two sets of spectra taken on 11:15 am on Sept. 25 and exclude the N(I) spectra from Sept. 26 as described previously. Using only the two data sets gave a calibration factor of 5.4×10^{-7} and gave results that were about a factor of two higher than the original results.

The individual results are not reported here. They should be proportional to the Sandia measurement results, different by a constant factor.

Performance Figures of Merit

The standard deviation and standard error will be the same as the SNL report if expressed as a percentage of the mean value. This is because the same data was used with different calibration factors when the average temperature method is used. The estimated response time will remain unchanged.

Table 2. Average metal concentration (μg/acm) calibration results and standard deviation. (**Not** corrected for temperature, pressure, or O_2.) Italicized numbers are for the normal average of all data, rather than conditional averaged data.

RM Number, Date Time	Be Concentration	Cr Concentration	Cd Concentration
#1, 22 Sept. 0936–1037	5.0 ± 0.7	7.0 ± 6.6 *105.3 ± 5.9*	0.7 ± 0.2 *1.7 ± 0.2*
#2, 22 Sept. 1125–1225	3.8 ± 0.7	7.6 ± 2.8	0.5 ± 0.2
#3, 22 Sept. 1309–1409	3.6 ± 1.7	12.5 ± 2.5	0.5 ± 0.2
#4, 22 Sept. 1515–1615	2.9 ± 0.6	6.5 ± 1.7	0.4 ± 0.2 *1.2 ± 0.4*
#5, 22 Sept. 1702-1802	2.3 ± 0.3	4.6 ± 1.3 *67.1 ± 2.1*	0.3 ± 0.2
#16, 25 Sept. 0920-1050	3.1 ± 0.7	11.5 ± 2.2	0.3 ± 0.2
#17, 25 Sept. 1120-1250	3.1 ± 0.7	11.3 ± 3.8	0.2 ± 0.1
#18, 25 Sept. 1345-1515	2.9 ± 0.9	7.3 ± 1.3	0.1 ± 0.1
#19, 25 Sept. 1535-1705	2.8 ± 1.3	7.0 ± 1.4	0.1 ± 0.1
#20, 25 Sept. 1730-1900	3.7 ± 0.5	12.8 ± 2.1	0.5 ± 0.3

Table 3. Average metal concentration (μg/acm) calibration results. (Not corrected for temperature, pressure, or O_2.) Italicized numbers are for the normal average of all data, rather than conditional averaged data.

	Be Concentration	Cr Concentration	Cd Concentration
RM #1	11.1 ± 1.6	6.7 ± 1.8 13.7 ± 2.9	1.5 ± 0.4 *3.7 ± 0.3*
RM #2	4.5 ± 0.9	1.5 ± 0.7	0.4 ± 0.2
RM #3	6.9 ± 3.1	5.4 ± 1.3	0.9 ± 0.4
RM #4	6.6 ± 1.1	3.9 ± 1.5	0.8 ± 0.4 *2.5 ± 0.9*
RM #5	5.2 ± 0.7	2.5 ± 1.2 4.7 ± 1.0	0.7 ± 0.4
RM #16	6.5 ± 1.4	3.2 ± 2.8	0.7 ± 0.3
RM #17	6.1 ± 1.2	4.0 ± 5.2	0.4 ± 0.3
RM #18	5.4 ± 1.7	1.8 ± 1.3	0.3 ± 0.3
RM #19	5.6 ± 3.2	2.3 ± 1.3	0.3 ± 0.3
RM #20	7.1 ± 1.0	2.4 ± 1.1	1.1 ± 0.7

Discussion

The objective of this test was to determine the usefulness of an internal calibration procedure designed specifically for LIBS used as a CEM that avoids external calibration. The results were promising, considering it was the first test and that it was performed "blind." All results were low, with an apparent systematic error. The original Cd results was about 30 × low, Cr was about 15 × low, and Be was about 10 × low.

In the results presented, the spectral response calibration was performed assuming constant dispersion of the spectrograph over the range from 220 nm to 750 nm. In fact the dispersion was later found to be:

Spectra Wavelength	Dispersion
225 nm	0.0356 nm /pixel
250 nm	0.0351 nm/pixel
277 nm	0.0344 nm/pixel
305 nm	0.0336 nm/pixel
415 nm	0.0242 nm/pixel
745 nm	0.0100 nm/pixel

This affects the spectral calibration since the lamp calibration is in units of intensity/nm. Including the dispersion factor to get spectral calibration in units of intensity/pixel has the affect of decreasing the calibrated detector response in the UV and thus increasing the calculated metal concentrations by about a factor of three. This is likely a major reason why the reported results were low. This would give ca. 10×, 5×, and 3× error, respectively for Cd, Cr, and Be. However, when this factor is used to compare the 415 nm and 745 nm regions to measure N(I) emission intensities, a much higher temperature (ca. 14,000 K) is obtained, which is not consistent with the Fe(II) temperature measurements. So, additional details need to be understood before correcting for this effect.

Even if the dispersion of the spectrograph is included, additional error remains. This error could be due to changing spectral response between the time of spectral calibration(before the test began), and when the internal calibration using nitrogen emission was performed(Thursday), which could be possibly a result of optics transmission changing from accumulation of ash. However to change the spectral response, the transmission would have to decrease more at shorter wavelengths. When comparing the background emission from Monday's results to Thursday's results, a factor of ca. 2 to 3 decrease at 225 nm was seen, a factor of ca. 3 to 4 decrease at 277 nm was seen, and a factor of ca. 1.5 to 2 decrease at 305 nm was seen.

Another reason for the remaining error could be that the grating used was not very efficient at 750 nm, so a small error in calibration at 750 nm would give a larger error in the UV region, since the results are based on the ratio of calibrated nitrogen emission at 750 nm to calibrated metal emission in the UV region.

Using the background to correct for changing sensitivity was not particularly successful, with high and low concentration measurements not 3X different.

Nitrogen emission with and without ash and / or water vapor demonstrated that these gas conditions affect calibration. These same effects on LIBS emission have been seen in the laboratory for water aerosols and water vapor in the gas. These results show that a factor of two change in calibration can occur under typical operating conditions. This is a significant effect when the goal is an EPA certified CEM.

The CEM Test Program

More time should have been given between RM runs with full metal and ash feed to allow calibration under conditions identical to the conditions during the RM run.

Lessons Learned

When collaborating, a lot of small intricate details of how data is taken must be completely understood. A pre-test run using all the same procedures and equipment to be used during the test is a good way to identify problems or misunderstandings.

Recommendations

Tests should be performed "blind" with all developers turning in results before any indication of the estimated concentrations. After developers have turned in their measurement results feedback should be released.

Gas conditions should be varied so that different amounts of ash and water are present for different runs. This will be a good test of how different instruments and procedures can maintain calibration for changing conditions.

Acknowledgments

The collaborative efforts of Dr. David Hahn and the Small Business Initiative Program at Sandia National Laboratory are gratefully acknowledged.

Appendix H

Developer Report
Cooper Environmental Services
Hazardous Element Sampling Train with
X-ray Fluorescence

Evaluation of a Hazardous Elemental Sampling Train During EPA's Continuous Emission Monitoring Test

Draft Report

Prepared for

EPA/DOE Air Pollution Technology Branch
Research Triangle Park, North Carolina

Prepared by

Cooper Environmental Services
14657 S.W. Teal Blvd. 221
Beaverton, OR 97007

Eli Lilly Corporation
Lilly Corporate Center
Indianapolis, IN 46285

January 16, 1998

Evaluation of a Hazardous Elemental Sampling Train During EPA's Continuous Emission Monitoring Test

Prepared for

EPA/DOE Air Pollution Technology Branch

Research Triangle Park, North Carolina

Submitted to

Dr. Nina Bergan-French

Dr. Paul Lemieux

Submitted by

Cooper Environmental Services

J.A. Cooper, B.E. Johnsen, B. Richards

Eli Lilly Corporation

J.A. Owens, R.H. Lambert

Sunset Labs

R. Cary

January 16, 1998

CONTENTS

FIGURES

TABLES

TECHNOLOGY DESCRIPTION

Cooper Environmental Services (CES) tested a prototype Hazardous Elemental Sampling Train (HEST) during EPA's September 1997 CEM trial in Research Triangle Park, NC. The HEST system included two major components, the continuous sampling module and the continuous analysis module.

In the continuous sampling module a stack gas sample was extracted, diluted and allowed to pass through a rotating Resin Impregnated Filter (RIF) and a Carbon Impregnated Filter (CIF). After water removal, the sample volume penetrating a given filter area was determined (DSCM/cm^2). The post-experimental RIFs and CIFs, having collected particulate and gas phase elements respectively, were marked with a circular 1.1 cm wide filtrate smear. This filtrate was then analyzed in the continuous analysis module.

The continuous analysis module examined a series of spots along the midline of the circular filtrate smear using an Omicron energy dispersive x-ray fluorescence (XRF) analyzer. XRF is a nondestructive, multi-element analysis method that has been used to characterize air particulates on filters since the early 1970's. A sample is exposed to a high-energy electron beam, ejecting electrons from the K, L, and M shells. Higher energy electrons from outer shells "drop" to fill the vacancies and emit the excess energy as x-rays. Identification of individual elements is possible since each element emits x-rays at characteristic energy levels. A detector identifies the number of x-rays per second (x-ray intensity) emitted at each energy level and a plot is made of counts per second (cps) vs. energy. Ideally, these plots would occur as step functions; however, some random scattering due to electronic noise is inevitable. For this reason, gaussian peaks, centered on characteristic energy levels, appear on a typical XRF plot. The energy level at the center point of the peak identifies the element while the area under the peak is proportional to its concentration. Peaks are identified by the shell from which an electron was ejected and the number of shells through which the replacement electron passed. In naming the peaks, an α signifies a change of one shell by the replacement electron (e.g., L to the K shell) while a β signifies a drop of two shells. For example, the K_α for cadmium peaks at 23.172 keV and was created by the ejection of a K shell electron which was replaced using an electron originally in the L shell. An analysis for cadmium would include an integrated count of all x-ray intensity in the 22.89 to 23.45 keV range, subtraction of background intensity and a gaussian fit to determine net intensity. The product of XRF analysis is elemental mass per unit area (μg/cm^2) which, when divided by the associated volume per unit area, yields time-resolved concentrations.

TECHNOLOGY DEVELOPMENT HISTORY AND SPONSORSHIP

Interest in the use of charcoal and resin traps for the collection of hazardous elements has increased in recent years. Germani and Zoller (1990), for example, used activated charcoal to trap and analyze for Br, Se, As, I, Cl, and Hg in coal fired power plant emissions. However, previous efforts relied upon cold vapor atomic absorption for analysis. In 1992, Cooper et.al., demonstrated XRF's capability for testing mercury capture efficiency of carbon impregnated filters. Recently, a non-rotating version of the HEST was tested in Oak Ridge, TN. HEST development is being sponsored by Eli Lilly Corporation.

EQUIPMENT DESCRIPTION

Continuous Sampling Module

The continuous sampling module consists of a Stack-Sampler Interface (SSI), Rotating Disk Sampler (RDS), and a flow control unit. Figure 1 shows sampling components present during the CEM test.

Stack Sampler Interface

The SSI system is designed to extract and dilute a representative sample of stack gas. Using a 0.92 inch diameter probe, an isokinetic sample was taken from the stack. Flow then entered a 6.4 inch diameter stilling chamber, slowing velocity and allowing a small sub-sample to be extracted through a second probe 0.502 inches in diameter. The remaining stack gas was filtered, measured using a CS3 laminar flow element, and returned to the stack. Flow was controlled with a manual restriction valve located downstream of the laminar flow element.

The sub-sample passed through a ball valve and entered a dilution chamber where nitrogen was added to cool and dry the sample. All equipment in the SSI system was made from stainless steel. Components in contact with the sub-sample were teflon coated to minimize loss due to particulate impaction with the walls.

Rotating Disk Sampler

From the SSI system, the sub-sample entered two Delrin™ cassette boxes. Each cassette consisted of an inlet tube, photodetector, filter holder stand, outlet tube, and AMP stepper motor. The first cassette contained a resin impregnated filter (RIF), the second a carbon impregnated filter (CIF). Filters were glued to circular anodized aluminum filter holders, mounted within $1/8^{th}$ in. of the inlet tube, and positioned to remain in contact with the outlet tube during rotation.

Following the cassettes and a second ball valve, the sub-sample stack gas was cooled in an ice water bath and dried using Drierite™. It then passed through a Hastings mass flow meter which measured dry standard liters per minute. Sub-sample flow was electronically controlled using a Dwyer proportioning valve.

Continuous Analysis Module

Filter analysis was conducted on a Kevex Omicron XRF system. This system features a 100 watt, 50kV x-ray source capable of accurately determining spot sizes between 50 microns and 1.5 cm. CES used Kevex WinXRF software to remove background noise and apply gaussian fits for each elemental peak.

System Requirements

The HEST system requires 115 volt AC current and occupies a 5' by 2' footprint. It is controlled by a PC computer. For the EPA test, 0.8 l/min of nitrogen was added to cool the sample. CES used the nitrogen throughout the test and conducted a one-day experiment which added 40 ppm chlorine to this nitrogen.

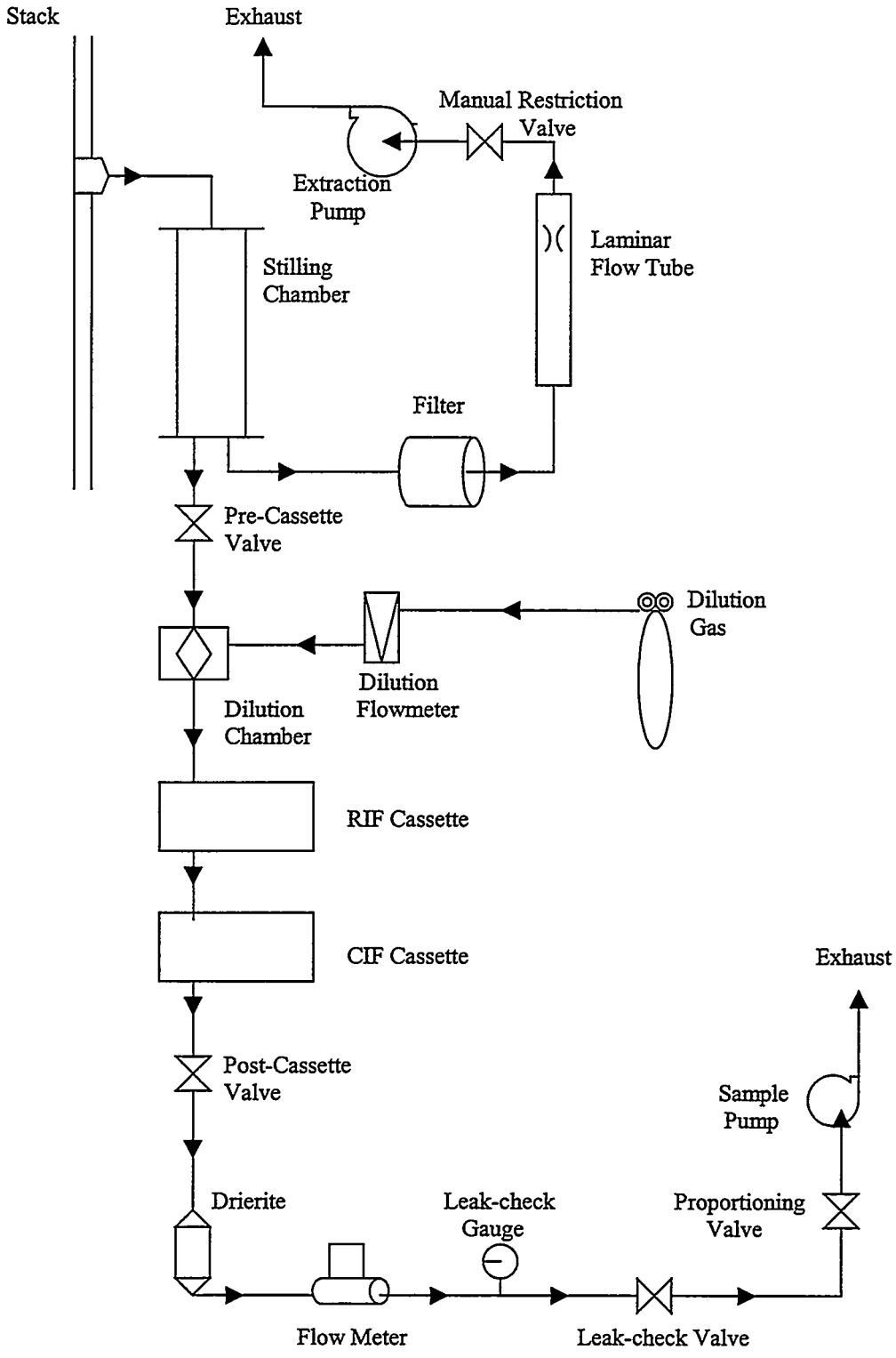

Figure 1. Test module flow diagram.

PROCEDURES

Sampling Procedures

Each sampling period was preceded by flow and leak checks on the cassettes and flow control unit. Nitrogen was then allowed to flow into the dilution chamber, and samples were pumped through the filter which remained in a calibration position until a pressure drop was noted. Pressure loss, caused by resistance of flow from the RIF, indicated contact between the filter and outlet tube. When flows stabilized and pressure loss was observed, the filters rapidly rotated 10 degrees and proceeded to collect stack samples.

Filter rotation rate was controlled with an AMP stepper motor and drive. In order to confirm rotation rate and filter position, notches were etched into the black circular filter holder at 30° intervals. An infrared photodetector, mounted on the cassette lid above the filter holder, verified the pre-determined rate by emitting a high intensity signal each time a notch rotated past its beam. The filter rotated at a constant rate while flow rate varied.

Both the larger flow extracted from the stack and the sub-sample were regulated for isokinetics. The large flow was determined using a Laminar Flow Element and manually controlled with a ball valve while the smaller flow was measured with a Hastings flowmeter and electronically controlled with a proportioning valve. Nitrogen, measured and controlled with a rotameter calibrated at Horizon Engineering (Portland, OR), was added to cool the sample. On Sept. 25th, chlorine gas was added to the nitrogen in order to test oxidation of elemental mercury. At the end of each sampling day, flows were stopped and the filters were removed for XRF analysis.

Analytical Procedures

Using an Omicron XRF analyzer, each filter was tested for five hazardous metals; As, Cd, Cr, Hg, and Pb; as well as Ag, Cu, Fe, Ni, Sb, Se, Sn, Sr, Ti, Y, and Zn. Results were calibrated using standards developed by Micromatter Inc. (Seattle, WA). These standards are produced by heating and flashing metal onto a nuclepore filter and result in a known mass per unit area ($\mu g/cm^2$). XRF analysis of the standards resulted in counts of x-rays per second (cps) for the elements of interest, and calibration/sensitivity factors ($cps/\mu g/cm^2$) were developed. Filters were measured in 9 mm^2 spots located every 2.5 degrees along the circular sample smear. At each spot, characteristic spectral peaks were generated for elements of interest and, after removal of background x-ray scattering, a gaussian fit was performed using Kevex WinXRF software. Typically, eight to nine spots were analyzed for each hour of the CEM test. In order to improve counting statistics, all spectra representing a given reference method run were summed and a gaussian fit was made of the sum peaks. All reported concentrations, except Pb and As, were identified using this method.

XRF Determination of Arsenic and Lead

The L_α line for Pb and the K_α line for As overlap at 10.5 keV. In order to adequately differentiate these two elements, the L_α/L_β intensity ratio for Pb was determined using Micromatter standards. This ratio, assumed to remain constant, was multiplied by the Pb L_β cps on each of the summed spectra to obtain lead's contribution to the 10.5 keV spectral intensity. Arsenic's cps was derived by subtracting Pb L_α cps from the total cps at 10.5 keV. When cps were converted to concentrations, the resulting Pb/(Pb + As) ratio for each reference run is 49 $\pm$ 5% (Appendix A). Since, according to reference method (RM29) results, As and Pb were at the same concentrations (52 $\pm$ 3) in the stack gas, this is supportive of precision in determining the relative ratio for these two elements.

Determination of Metal Concentrations in the Gas Stream

Metal concentrations were determined using the following equation

$$C = \frac{\left(\frac{I}{S}\right)}{V} \bullet F \bullet E \qquad (1)$$

where

C = concentration ($\mu g/m^3$)

I = net analyte peak intensity of the element (counts/sec)

S = sensitivity factor for the element ([counts/sec]/[$\mu g/cm^2$])

V = volumetric flux (m^3/cm^2)

F = x-ray absorption correction factor

E = filter collection efficiency.

Each of these terms and their associated uncertainty is discussed in the following subsections. A thorough mathematical discussion can be found in Appendix A.

Net X-Ray Intensity (I)

Net x-ray intensity measured in counts per second (cps) is equal to the gross analyte peak intensity minus peak intensity contributions from deposit scatter, blank filter scatter, and blank impurity contributions. Sources of uncertainty include instrument drift, Poisson counting statistics, and uncertainty in filter positions. Instrument drift and Poisson statistics typically contribute less than 1% uncertainty in net x-ray intensity. Comparison tests conducted on background scatter peaks indicate that variation in filter position contributed less than 5% to intensity uncertainty (Appendix B).

Sensitivity Factor (S)

The sensitivity factor relates net intensity to mass per unit area for XRF standards. Manufacturer specifications indicate uncertainties in mass on the standards to be less than 2.5%. This accuracy was confirmed by the smoothly varying curve derived when standard sensitivity factors versus atomic number were plotted (Appendix B).

Volumetric Flux (V)

In order to cool the stack sample, nitrogen was added to the stack sub-sample. Net sample volumes were calculated by subtracting nitrogen volumes from total volumes. Volumetric flux was determined by dividing this net flow of stack gas (m^3/sec) by the rotational rate of the exposed area (cm^2/sec). Although uncertainties in determining rotational rate and exposure area are believed to be relatively small, overall volumetric flux is highly dependent on nitrogen flow rates. Since flow rates of nitrogen and the stack gas were approximately equal, any uncertainty in nitrogen flow could contribute significantly to overall uncertainty in sample concentrations.

Absorption Correction Factor (F)

The measured x-ray intensity must be corrected for absorption of the incoming excitation x-rays and the out going characteristic analyte x-rays by the filter matrix and the deposit. A detailed mathematical explanation and listing of absorption factors can be found in Appendix B. Chromium, due to its low atomic number, has an F correction of 15% while all other hazardous metals had correction factors of about 1–3%. Since the Absorption Correction Factor has such a small impact on estimated metal concentrations, any uncertainty in this factor would not significantly affect overall estimates of uncertainty.

Filter Collection Efficiency (E)

The RIF trapping efficiency (E) is assumed to be 100% for all elements of interest except Hg. The validity of this assumption is supported by numerous previous studies as well as low metals' concentrations on the downstream back-up CIF (Appendix C). The trapping efficiency of the RIF was determined to be 35.6% for ionic Hg under the conditions encountered during these tests. On September 25th, CES added chlorine to the stack gas to increase oxidation of elemental Hg resulting in a higher RIF collection efficiency (71.2%). Uncertainty in Hg concentration, primarily due to mechanical difficulties with the CIF housing, is estimated at 10–20%.

RESULTS

Performance Figures of Merit

3 Sigma Limits of Detection

XRF detection limits are a function of uncertainties in background and gross intensity counts. As the detection limit is approached, gross intensity approximates background intensity and the 3 sigma limit is identified using the following equation:

$$3\sigma = 8.48 \bullet \sqrt{B} \qquad (2)$$

B = Background counts per time period

3σ = Detection limit

Dividing the 3 sigma limit by the sensitivity factor and volumetric flux, detection limits for each run were determined for each reference method time period. Table 1 presents the average detection limit for hazardous metals during each test day. A complete listing and explanation for the 3σ detection limits can be found in Appendix D.

Table 1. 3σ detection limits for HEST during CEM testing.

Test Date	Element	Detection Limit	Test Date	Element	Detection Limit
	As	0.37		As	0.37
	Cd	3.49		Cd	3.78
23-Sep-97	Cr	0.89	25-Sep-97	Cr	0.88
	Hg	0.66		Hg	0.64
	Pb	0.94		Pb	0.94
	As	0.17			
	Cd	1.70			
24-Sep-97	Cr	0.43	All detection limits are in µg/DSCM		
	Hg	0.30			
	Pb	0.43			

Estimated Response Time

Response time is not applicable to the HEST since it is an off-line analysis system requiring at least 24 hours to generate and process the XRF results. However, the HEST did retrospectively determine time averaged data for each 5 to 10 minute interval of the CEM test. Figure 2 presents HEST concentrations for September 23, 1997 reported in 6.75 minute intervals.

HEST resolving time was limited by the filter rotational rate. Rotational rate was limited, in turn, by available exposure area on the filter. CES is currently developing an improved system capable of increasing available exposure area with a resulting improvement in time resolution.

Metal Concentration vs. Time for Typical Test Period

Figures 3 presents HEST concentrations for the second test period on September 23, 1997. Data points were determined using a 9 mm^2 XRF spot every 2.5 degrees along the center circumference of the filter smear. These spots covered 82% of the sample circumference and 27% of its width. A radial transverse across the width of the smear was conducted to confirm that the spots were laterally representative.

Table 2 shows the average concentration and standard deviation for metals of interest in Figure 3. These values were derived by averaging the individual spectra for the nine spots examined during the hour long run.

Isokinetic Control

As a first run prototype, many of the flow control pieces had not been tested under field conditions. As such, flow control was maintained at ±55% of an isokinetic rate (Appendix E). This is a concern since unrepresentative samples could have been taken. However, since most of the hazardous elements under study were in the particulate phase, it is believed that the wide range in control did not significantly bias reported concentrations.

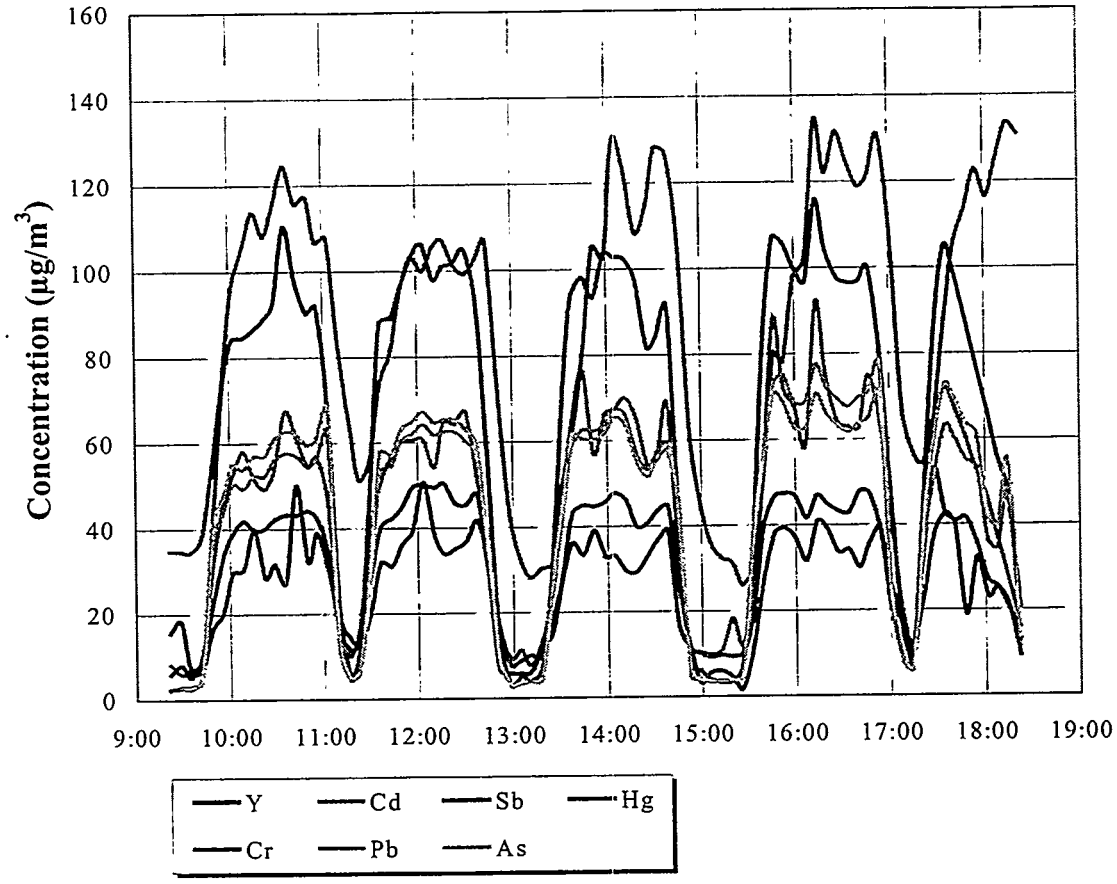

Figure 2. Concentration vs. time September 23, 1997.

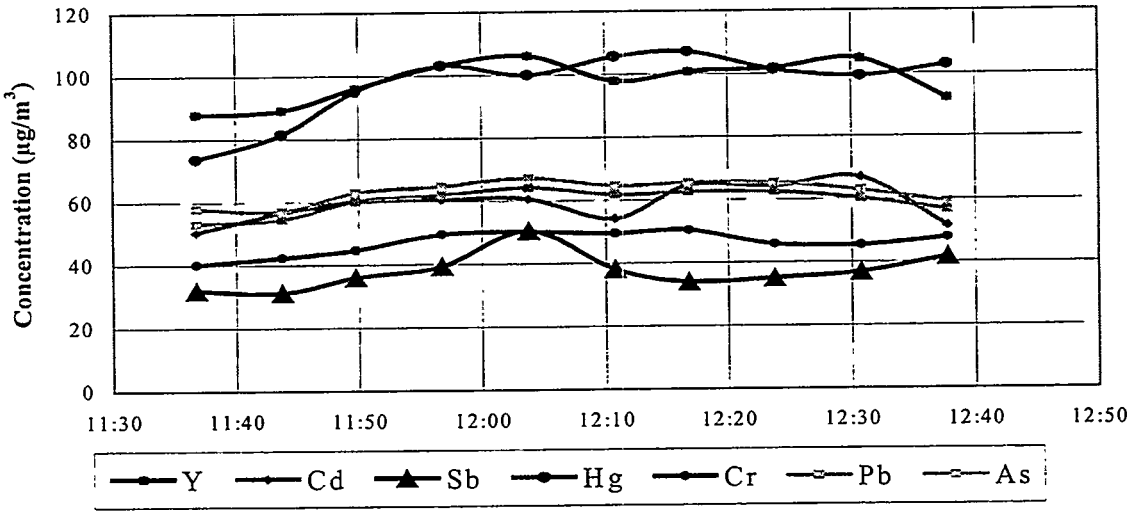

Figure 3. Concentration vs. time September 23, 1997 Run 2.

Table 2. CEM test September 23, 1997—Test Run 2.

Element	Average Conconcentration (µg/SDCM)	Standard Deviation	Element	Average Concentration (µg/SDCM)	Standard Deviation
Antimony	37.44	5.63	Lead	59.76	3.75
Arsenic	62.74	3.52	Mercury	96.98	10.92
Cadmium	58.99	5.66	Yttrium	97.96	6.51
Chromium	46.54	3.51			

a. Average concentrations determined from individual spectra.

Average Metal Concentrations for Reference Method Test Periods

Average HEST metal concentrations and Reference Method 29 values for CEM test periods are listed in Table 3. In addition to the five target hazardous metals tested by RM29, the HEST system also identified Ag, Cu, Fe, Ni, Sb, Se, Sn, Sr, Ti, Y, and Zn. Indeed, all metals with an atomic number greater than sodium are readily analyzed by this nondestructive method. Only the downstairs RM values were cited in Table 3 due to the proximity of the downstairs monitor to the HEST sample port and the fact that the downstairs concentrations were systematically lower than the upstairs concentrations.

In a comparison of upstairs RM results (RM-U) with downstairs RM results (RM-D), it was determined that a systematic difference in RM concentrations existed. When averages for each test day are compared, RM-U values were 6.4% higher than RM-D. Indeed, of the 24 potential averages (six elements for four days), 21 RM-U values were higher than RM-D and 3 values were equivalent (Table F1). Normalization of each RM to yttrium reveals a commendable correlation between RM-U and RM-D (Table F2) so the difference in actual concentrations is believed to be systematic and not random. HEST data normalized to Y also displays improved correlation with RM data (Table F3). Complete CES results and comparisons with RM29 and further discussion of the RM bias can be found in Appendix F (Table F4-F6).

DISCUSSION

Test Results

Except for cadmium, HEST determined concentrations for the five metals reported to the EPA were consistently lower than the RM29 values. Cadmium's relatively large concentration might be due to spectral interference with antimony. Antimony, projected to be at the same concentration as the other hazardous metals, was unusually low relative to the other HEST results. Antimony's K_α and cadmium's K_β share an intensity peak at 26.1 keV. The WinXRF program employs both K_α and K_β lines in its fitting routines. As such, a consistent low HEST bias of 30-50% is believed to exist.

This discrepancy can be seen in the best fit lines when RM29 vs. HEST results are plotted (Figure 4). In these charts, the change in HEST concentration, indicated by the slope, is between 54% and 75% of the RM29 value. Since the intercept of the best fit lines is close to zero (except for Cd) and the R^2 values indicate fairly good agreement between high and low days, the difference in measurements seems to be systematic.

Table 3a. Comparison of HEST and RM29 results at EPA's CEM test.

EPA Test Run		HEST Results (µg/DSCM)					Downstairs RM (µg/DSCM)[a]				
Date	RM Number	As	Cd	Cr	Hg	Pb	As	Cd	Cr	Hg	Pb
23-Sep-97	6	56.4	63.6	41.2	114.1	51.8	76.7	74.3	61.8	168.7	89.2
23-Sep-97	7	61.3	69.4	46.7	103.0	58.6	78.5	74.9	66.0	194.6	89.8
23-Sep-97	8	62.6	77.3	48.5	114.5	64.6	82.3	80.0	72.0	193.1	93.2
23-Sep-97	9	64.0	81.5	45.6	116.9	70.2	86.2	83.8	74.8	206.9	98.3
23-Sep-97	10	50.9	56.0	32.7	104.5	44.2	58.0	56.9	50.5	205.5	68.1
24-Sep-97	11	NA	NA	NA	NA	NA	26.7	22.4	28.0	37.3	27.5
24-Sep-97	12	15.2	24.4	14.4	21.9	14.1	23.3	19.1	25.4	40.8	23.5
24-Sep-97	13	19.0	32.1	18.2	23.3	18.4	15.8	13.3	18.7	35.7	15.1
24-Sep-97	14	19.9	27.2	18.6	16.8	16.3	26.2	20.6	27.5	28.6	26.6
24-Sep-97	15	18.0	31.4	19.4	21.8	21.1	25.6	20.3	29.4	37.6	26.1
25-Sep-97	16	14.4	15.5	12.4	10.2	14.8	23.8	20.2	22.1	32.8	26.6
25-Sep-97	17	19.4	29.2	15.7	14.6	15.9	29.3	24.7	29.5	40.2	30.9
25-Sep-97	18	21.4	28.9	18.5	15.0	20.8	28.0	23.7	27.5	36.1	30.7
25-Sep-97	19	20.0	24.6	18.1	19.8	17.4	26.1	21.2	26.4	41.8	27.0
25-Sep-97	20	20.0	33.5	19.6	17.6	16.8	28.4	23.0	29.1	39.3	29.5

a. Concentrations determined from summed spectra.

b. Since RM29 downstairs was lost, RM29 upstairs is used for run 8 on Sept. 23, 1997.

Table 3b. Comparison of HEST and RM29 results at EPA's CEM test.

EPA Test Run		Percent Difference					Relative Accuracy HEST vs. Avgerage RM				
Date	RM Number	As	Cd	Cr	Hg	Pb	As	Cd	Cr	Hg	Pb
23-Sep-97	6	26.4	14.4	33.3	32.4	41.9					
23-Sep-97	7	21.9	7.4	29.2	47.1	34.7					
23-Sep-97	8	24.0	3.4	32.7	40.7	30.7					
23-Sep-97	9	25.8	2.8	39.0	43.5	28.6		Average of RM 6-10			
23-Sep-97	10	12.1	1.6	35.3	49.1	35.1	31%	22%	43%	53%	47%
24-Sep-97	11	NA	NA	NA	NA	NA					
24-Sep-97	12	34.8	-27.4	43.4	46.3	39.8					
24-Sep-97	13	-20.3	-141.8	2.7	34.7	-21.8					
24-Sep-97	14	24.2	-32.0	32.4	41.4	38.7					
24-Sep-97	15	29.4	-54.7	34.1	42.0	19.3					
25-Sep-97	16	39.7	23.4	43.9	68.8	44.4					
25-Sep-97	17	33.9	-18.1	46.7	63.6	48.7					
25-Sep-97	18	23.5	-21.7	32.7	58.6	32.0					
25-Sep-97	19	23.5	-16.1	31.2	52.6	35.7		Average of RM 11-20			
25-Sep-97	20	29.5	-45.6	32.5	55.1	43.1	40%	55%	46%	66%	48%

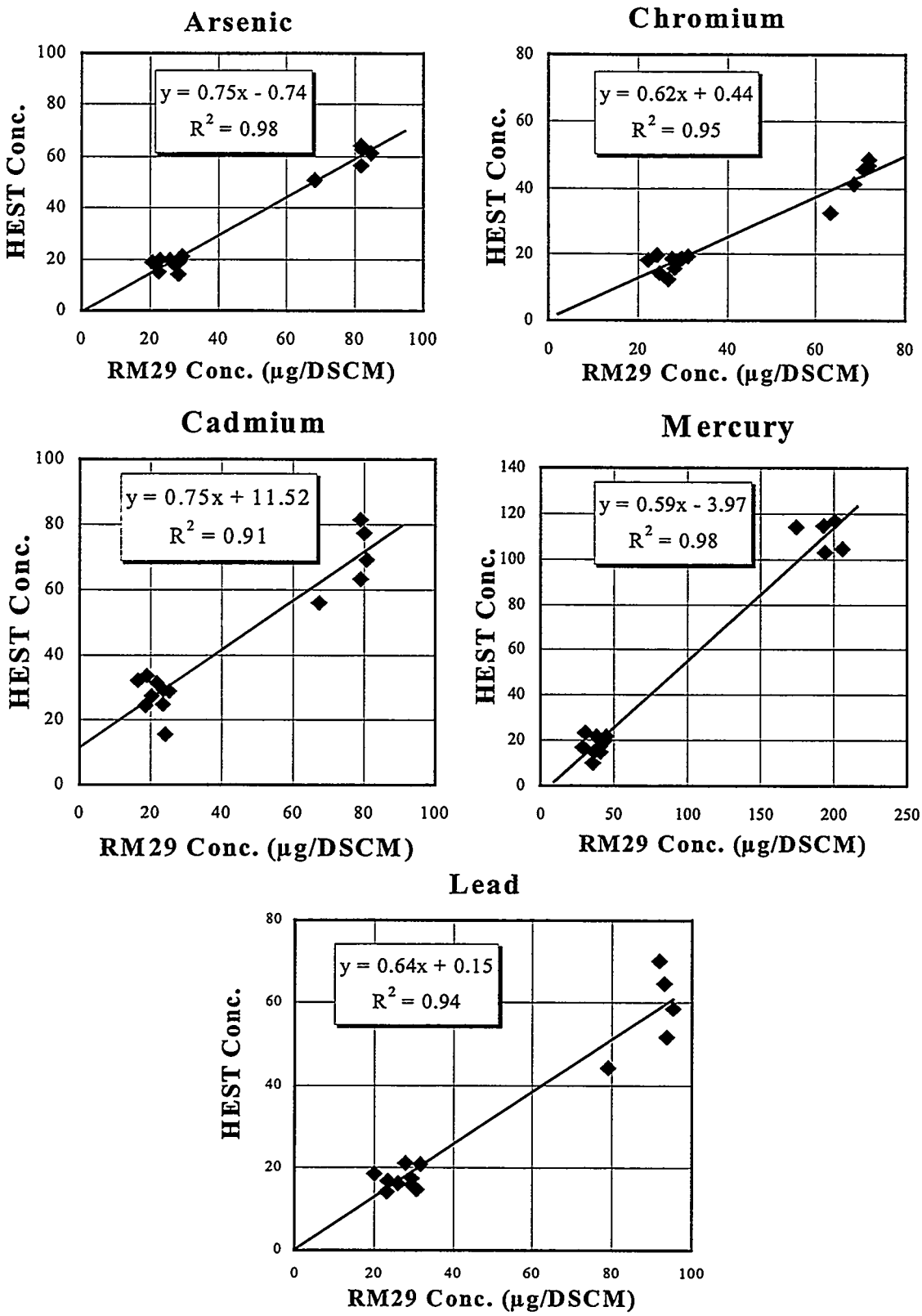

Figure 4. HEST vs. RM29 concentrations.

It is believed that the HEST's systematically low concentrations may be a result of a systematic problem with flow measurement. For example, if the nitrogen flow rate were 1.16 l/min instead of the reported value of 0.84 l/min, the daily average percent error between RM29 and the HEST is less than 20% for arsenic, chromium, mercury and lead. As a first-run prototype, no flowmeter, measurement system or sampling component had ever been tested under field conditions. Improvements in flow control and calibration are being developed to improve sampling accuracy and minimize measurement variability.

Given that metal feed rates and stack conditions were fairly constant during reference runs, differences in concentrations within the run are assumed to be a product of HEST measurement variability. As shown in Table 4, standard deviation of HEST measurements, indicative of this variability, ranges between 2 and 16 µg/DSCM. This translates to a variability of 5–12% of high day and 4–27% of low day concentrations.

The CEM Test Program (Optional)

In general, the CEM test program seemed to be efficiently and effectively run. Schedules were well-maintained and stack data was readily available. CES took advantage of the facility access to modify equipment after hours and appreciated this opportunity. The use of two RM29 sampling trains add credibility to the results and gave important insight into variation within the test stack. Improvements could be made by increased care in RM29 handling practices (e.g., open oven doors, covering of probes between exchanges, etc.), and longer reference runs on high concentrations days. We found the Accurex, EPA, and consulting staff, to be both helpful and professional and appreciated the opportunity that their work afforded us.

Table 4. Standard deviation of HEST concentrations during reference method runs[a] (µg/DSCM).

RM29 RUN	As	Cd	Cr	Hg	Pb
Run 6	3.3	5.6	1.9	8.4	3.0
Run 7	3.5	5.7	3.5	10.9	3.8
Run 8	4.5	7.4	2.5	16.3	4.6
Run 9	3.0	10.1	2.3	18.2	3.3
Run 10	12.6	15.4	8.6	27.7	10.9
Run 12	4.4	2.5	2.3	3.2	4.1
Run 13	6.8	4.0	2.5	0.4	6.6
Run 14	12.3	5.4	2.8	0.8	10.1
Run 15	7.0	5.9	2.8	1.5	8.2
Run 16	5.4	5.4	1.2	1.0	5.5
Run 17	7.8	3.5	1.1	1.2	6.4
Run 18	8.0	2.9	1.2	1.5	7.8
Run 19	6.7	3.7	1.5	2.4	5.8
Run 20	4.8	3.8	1.3	1.4	4.0
Average Low	5.4	8.8	3.7	16.3	5.1
Average High	7.0	4.1	1.9	1.5	6.5

a. Standard deviations were determined from individual spectra.

Technology Strengths and Limitations

HEST analysis using XRF allows for simultaneous determination of all elements with an atomic number greater than that of sodium. It is capable of very low detection limits, is relatively inexpensive to maintain, and is nondestructive, allowing for archiving or further chemical analysis of the filtrate. Once installed, the HEST system is easy to operate, requiring a filter change once per week; produces no toxic waste, and is readily adaptable to a variety of stack conditions. Other potential applications include: ambient sampling and source apportionment. Although its response time limitations do not allow it to qualify as a CEM, it does offer continuous feedback and gives the stack operator an assurance of compliance.

The HEST system is designed to give continuous assurance of compliance, but is currently limited in its time resolution, and flow control. Time resolution is limited by the length of time a single point on the HEST filter is exposed to sample gases. Slow moving filters, relatively large diameter inlet tubes (leading to cross-contamination), and limitations in XRF spot size analysis affected the prototype HEST time resolution. Engineering improvements to increase rotational rates and decrease filter exposure area are planned to overcome these problems. Kevex's Omicron is capable of accurate measurement of spot sizes $1/3600^{th}$ of that chosen by CES. Currently, however, a limit of 75 spots can be analyzed and recorded in one data file. A customized Omicron WinXRF program is being developed that will overcome this barrier to time resolution. Flow control will be improved by careful control of isokinetics and improved calibration of flow monitoring devices.

Although the HEST system is designed as an off-line analysis system, immediate access to an XRF analyzer will allow concentrations to be determined within 24 hours of sampling. In addition, the HEST system lends itself to installation of a beta gauge. This type of analysis is widely accepted as a method for determining total particulate matter. The combination of a rotating filter and a beta gauge would lead to time-resolved total particulate concentrations with a response time on the order of one-half hour.

Lessons Learned

The HEST instrument for the CEM tests was the first prototype ever put to use in the field. As such, these tests were viewed as an opportunity to examine the feasibility of the rotating disk concept. During the testing, important lessons in controlling water condensation, use of WinXRF software, and flow control were learned; but the most significant lesson was the demonstration that time resolved data can be obtained using the HEST system.

RECOMMENDATIONS

Although CEM test concentrations were systematically low, the successful demonstration of time-resolved measuring capabilities and the future potential of this sampler as an inexpensive, clean, and effective means of continuous assurance of compliance support the CES recommendation of continued research. Future research, focusing on flow control, increased filter exposure area, installation of a continuous particulate matter sampler, and improved engineering, will allow development of a more accurate sampling system with potential for stack, ambient, and source apportionment testing.

ACKNOWLEDGEMENTS

We would like to thank Rich Wong and Dave Weary of Kevex Instruments for their assistance in XRF analysis, and Alan Walters for his input into the HEST design. Logistical support from Accurex Environmental and employees of the EPA's Air Pollution Technology Branch is also appreciated.

This research has been sponsored in part by Eli Lilly Corporation.

Appendix I

Relative Accuracy Calculations

Appendix I

Relative Accuracy Calculations

Relative Accuracy Calculations

The relative accuracy compares average CEM data to RM data for the time period over which RM data is collected. The relative accuracy calculation is described in the EPA "Performance Specification 10 (PS 10) – Specifications and test procedures for multi-metals continuous monitoring systems in stationary sources" (61 FR 17499 – 17502, April 19, 1996). Note that this reference contains a typing error: the term d-bar should be an absolute value.

The RA was calculated using equation I-1.

$$RA = \frac{\left|\bar{d}\right| + \frac{t_{0.975}}{\sqrt{n}}(SD)}{R_{RM}} \qquad \text{(I-1)}$$

R_{RM}-bar is equal to either the average of the RM data set, calculated according to Equation (I-2), or the value of the emission standard, as applicable (see section 4.2 of PS 10.

$$\overline{RM} = \frac{1}{n}\sum_{i=1}^{n} RM_i \qquad \text{(I-2)}$$

In equation (I-1), $t_{0.975}$ is the t-value at 2.5 percent error confidence, as listed in Table I-3

Table I-3. t-values.

n	$t_{0.975}$
2	12.706
3	4.303
4	3.182
5	2.776
6	2.571
7	2.447
8	2.365
9	2.306
10	2.262
11	2.228
12	2.201

In equation (I-1), d-bar is equal to the arithmetic mean of the difference, d, of the i^{th} of n CEM and RM data set, calculated according to equations I-3 and I-4.

$$d_i = \overline{CEM}_i - RM_i \tag{I-3}$$

Note that the i^{th} CEM data set is the arithmetic average of m CEM data points taken in real-time or close to real-time:

$$\overline{CEM}_i = \frac{1}{m}\sum_{k=1}^{m} CEM_k \tag{I-4}$$

And then the arithmetic mean of the differences, d-bar is equal to:

$$\overline{d} = \frac{1}{n}\sum_{i=1}^{n} d_i \tag{I-5}$$

SD is the standard deviation calculated according to Equation (I-6)

$$SD = \sqrt{\frac{\sum_{i=1}^{n} d_i^2 - \left[\frac{1}{n}\left(\sum_{i=1}^{n} d_i\right)^2\right]}{n-1}} \tag{I-6}$$